Division of Biomedical Engineering

Department of Human Biology

University of Cape Town

Evaluation and Design of an Adapted Endobutton Fixation System to Be Used in Conjunction with Suture and Endobutton Techniques for The Treatment of Coronoid Process Fractures.

Full Research Dissertation

In fulfilment of the requirements for the degree:

MPhil in Biomedical Engineering

Nicola Mason (MSNNIC004)

Supervisor: Prof. Sudesh Sivarasu

Co-supervisor: Prof. Stephen Roche

December 2024

University of Cape Town

The copyright of this thesis vests in the author. No quotation from it or information derived from it is to be published without full acknowledgement of the source. The thesis is to be used for private study or non-commercial research purposes only.

Published by the University of Cape Town (UCT) in terms of the non-exclusive license granted to UCT by the author.

University of Cape Town

Declaration of Authorship

- Plagiarism is to use another's work and present it as one's own whether it be through copying the work (verbatim), paraphrasing, or not acknowledging the author. I have understood what plagiarism is, I am aware that is wrong. I have understood the University of Cape Town's policy in this regard.
- I have used the Harvard convention for citation and referencing. Each contribution to, and quotation present in this report has been attributed to the original author, cited, and referenced.
- I, **Nicola Mason**, hereby declare that the work on which this dissertation/thesis is based is my original work (except where acknowledgements indicate otherwise) and that neither the whole work nor any part of it has been, is being, or is to be submitted for another degree in this or any other university.
- I empower the university to reproduce for the purpose of research either the whole or any portion of the contents in any manner whatsoever.

Full name of student: Nicola Mason

Student number: MSNNIC004

Signature: Signed by candidate

Abstract

Introduction: The coronoid process is a critical anatomical structure of the elbow, playing a fundamental role in the joint's stability. Fractures of the coronoid, typically resulting from high-energy impact, can disrupt this stability and compromise the elbow joint posing a significant challenge to the Orthopaedic surgeon. 3D imaging and fracture mapping are becoming the standard practice for visualising the fractured area and a means of planning surgical treatment. Although there is an ongoing debate about the ideal method of treating coronoid fractures, there are several recommended surgical fixation options. One of the available fixation devices is the Endobutton. This dissertation's primary aim is to design an adapted Endobutton using fracture mapping and Q3DCT techniques. The secondary aim is to evaluate the existing Endobutton to establish criteria for comparison and assessment of the newly designed device.

Methods and Materials: Sixty-three upper limb computer tomography (CT) scans depicting coronoid fractures were acquired from Groote Schuur Hospital. Q3DCT techniques were used to generate fracture maps from multiple views. This involved editing CT scans to render 3D models of fractures and subsequent *in-silico* reduction and mapping. These were complimented by the generation of heat maps depicting the fracture line density. Templating and a qualitative assessment, performed by three Orthopaedic surgeons, evaluated the currently used Endobutton, leading to the establishment of evaluation criteria. This was followed by an iterative conceptual and detailed design process that was used to develop the adapted Endobutton. The designed device was verified through rapid prototyping, templating, and comparative qualitative assessment. Subsequent validation of the design was done using simulated surgeries in cadaver limbs, followed by the same comparative qualitative assessment.

Results & Discussion: The 3D fracture and heat maps enable comprehensive inspection of the coronoid fractures from multiple views, thus facilitating the identification of the recurring patterns on the anterior surface of the bone. Fracture type specific critical fracture patterns and weak points of the bone's structure are identified. These insights inform the design of an adapted Endobutton. The templating and assessment of the commercially available Endobutton underscore its inefficacy in addressing coronoid fractures, highlighting the limitations that the designed adapted Endobutton aims to mitigate. Verification results indicate that the adapted Endobutton design yields improved qualitative user data, which suggests its enhanced performance as a fixation method compared to the commercially available Endobutton. The validation results reinforce the improved qualitative outcomes for Type 2 and Type 3 coronoid fractures, however the outcomes for Type 1 favour the commercially available device. Overall observations note that a spiked and curved asymmetrical design

offer a more congruent fit to the bone, as well as effectively fitting over the majority of the fracture fragments.

Conclusion: The commercially available Endobutton leads to unfavourable reduction and fixation qualitative parameters when compared to the newly designed adapted Endobutton. The new design demonstrates promising potential as an effective approach to coronoid fracture fixation as evidence by its effective application to the 3D-printed fractures and cadaver specimens.

Acknowledgments

I would like to express my deepest gratitude to my supervisors, Professor Sudesh Sivarasu and Professor Stephen Roche, whose guidance, expertise, and encouragement have been instrumental throughout my Masters research journey. Professor Sivarasu's support and insightful feedback have been invaluable, and his dedication to advancing the field of Biomedical Engineering in South Africa is inspiring. Professor Roche's willingness to engage and his passion for the advancement of Orthopaedic surgery was influential in my design process. His dedication to the project motivated me to produce high-quality research.

My greatest appreciation also extends to Dr Roopam Dey, whose expertise in biomechanics, 3D imaging, and fracture mapping was instrumental in developing my research methodologies. Roopam's advice and support in all aspects of my Masters journey have been invaluable in helping me address research challenges and have guided me through this academic endeavour.

I am equally indebted to Dr Edmund Wessels. His constructive criticism and suggestions have help me structure and formulate my dissertation and address various challenges along the way.

My heartfelt thanks extends to the members of the Orthopaedic Biomechanics Lab, whose collaboration and camaraderie have been pivotal in completing this dissertation. Roopam, Leanne, Habtamu, Alexandra, Catherine, and Jonty, thank you for your support and friendship. I am particularly grateful to Habtamu Yimam, who helped guide me through various aspects of my research and the required software. Thank you to the Division of Biomedical Engineering and the University of Cape Town for the opportunity to pursue my Masters degree. And thank you to all the technical and administrative staff involved.

I would also like to thank Dr Robert Dachs and Dr Jean-Pierre du Plessis for their participation in the verification testing and their constructive feedback during the design process. Thank you to Dr Kim Tabeliao for her assistance in acquiring the DICOM images. My heartfelt thanks to Dr Jean-Pierre du Plessis, Dr Kim Tabeliao, Dr Barend Grey, Dr Rimon du Plessis, and Dr Ntambue Kauta for their participation in the validation testing, and their feedback on the designed device.

Last but not least, a special thanks to my friends and family for their unwavering support and encouragement throughout my relocation to Cape Town and my postgraduate academic career. Their love and belief in me has been a source of strength and motivation. I would particularly like to thank my mom, Debbie, and sister, Kelly, for their love that kept me going.

Table of Contents

Declaration of Authorship ii
Abstract iii
Acknowledgments v
List of Abbreviations x
List of Figures xi
List of Tables xiv
1. Chapter 1: Introduction to Study 1
1.1. Project Introduction 1
1.2. Dissertation Structure 2
1.2.1. Research Question 2
1.2.2. Aim and Objectives 2
1.2.3. Proposed Methodology Overview 2
1.2.4. Planned Data Scope 5
1.2.5. Ethical Considerations 5
1.2.6. Dissertation Overview 5
1.3. Background Information: Anatomy and Biomechanics of the Elbow 7
1.3.1. Normal Anatomy of the Elbow 7
1.3.2. The Biomechanical Role of the Coronoid Process in The Elbow 11
1.3.3. Coronoid Fractures and Their Maps 12
1.3.4. Open Reduction and Internal Fixation (ORIF) of Coronoid Process Fractures 13
1.3.5. Background Information Key Findings 14
2. Chapter 2: Coronoid Process Fracture Mapping 15
2.1. Chapter Introduction 15
2.2. Literature Review: Coronoid Fractures 15
2.2.1. Fractures of the Coronoid Process 15
2.2.2. Coronoid Process Fracture Classification 17
2.2.3. Fracture and Heat Mapping 20
2.2.4. Key Findings in Literature 22
2.2.5. Chapter Problem Identification and Research Question 23
2.3. Chapter Aims and Objectives 23
2.4. Materials and Methods 23
2.4.1. Patient Cohort 24
2.4.2. Data Collection 25
2.4.3. Fracture Mapping 26
2.4.4. Heat Mapping 31

2.5. Results.....33
2.5.1. Patient Cohort Demographic Data.....33
2.5.2. Patient Cohort Scan Data.....33
2.5.3. Fracture Classification and Subtypes.....34
2.5.4. All Patient Fractures (n=33).....35
2.5.5. Heat Maps.....38
2.6. Discussion.....42
2.6.1. Key Findings in Chapter.....43
2.6.2. Limitations.....44
2.7. Chapter Conclusion.....45
2.7.1. Chapter Outcomes.....45
3. Chapter 3: Qualitative Fit Analysis.....46
3.1. Chapter Introduction.....46
3.2. Literature Review: Coronoid Fracture Fixation, 3D Printing, and Templating of Fixation Devices 46
3.2.1. Coronoid Fracture Fixation.....46
3.2.2. Endobutton Fixation.....51
3.2.3. Use of 3D Printing in Orthopaedics.....53
3.2.4. Fitment Analysis and Templating of Coronoid Fixation Devices.....54
3.2.5. Key Findings in Literature.....54
3.2.6. Problem Identification and Research Question.....55
3.3. Chapter Aim and Objectives.....56
3.4. Materials and Method.....56
3.4.1. 3D Printing of Coronoid Fractures.....57
3.4.2. 3D Printing of Endobutton Imitation.....58
3.4.3. Templating & Qualitative Assessment.....59
3.4.4. Data Analysis and Statistical Methods.....61
3.5. Results.....61
3.6. Discussion.....63
3.6.1. Resultant Design Requirements.....65
3.6.2. Limitations.....66
3.6.3. Key Findings in Chapter.....66
3.7. Chapter Conclusion.....66
3.7.1. Chapter Outcomes.....67
4. Chapter 4: Design and Development of Adapted Endobutton.....68
4.1. Chapter Introduction.....68

4.2. Chapter Aims and Objectives 68
4.3. Design of Adapted Endobutton Device 68
4.3.1. Planning 68
4.3.2. Initial Design Concepts 69
4.3.3. Design Requirement 70
4.3.4. Testing and Evaluation Criteria 73
4.3.5. Design Methodology: Conceptual Design Stage 74
4.3.6. Design Methodology: Detailed Design Stage 82
4.4. Final Design Outcome 87
4.4.1. Limitations 88
4.5. Planned Testing 88
4.5.1. Verification Testing: Templating and Qualitative Assessment 88
4.5.2. Validation Testing: Cadaver Testing 88
4.6. Chapter Conclusion 89
4.6.1. Chapter Outcomes 89
5. Chapter 5: Design Verification & Validation 90
5.1. Chapter Introduction 90
5.2. Chapter Aims and Objectives 90
5.2.1. Verification and Validation Testing Objectives 91
5.3. Testing Methods and Procedures 91
5.3.1. Verification - Templating and Qualitative Assessment 92
5.3.2. Validation – Cadaver Studies 97
5.4. Discussion 103
5.4.1. Discussion of Verification Results 104
5.4.2. Discussion of Validation Results 104
5.4.3. Discussion of Results Comparison 105
5.4.4. Limitations 106
5.4.5. Key Findings in Chapter 107
5.5. Conclusion 107
5.5.1. Chapter Outcomes 108
6. Chapter 6: Project Conclusion 109
6.1. Overall Discussion 109
6.1.1. Key Findings in Overall Study 111
6.2. Limitations of Study 112
6.3. Overall Conclusions 112
6.3.1. Overall Study Outcomes 113

6.4. Recommendation for Future Studies....114
References....115
Appendix A - HREC Approval Letter.... A-1
Appendix B – Fracture Mapping Data Collection Sheet....B-4
Appendix C – Fracture Maps....C-30
Appendix D – Heat Mapping Code.... D-39
Appendix E – Heat Maps....E-40
Appendix F – Endobutton Drawing....F-49
Appendix G – Qualitative Assessment Questionnaire.... G-50
Appendix H - Detailed Design Drawing.... H-53
Appendix I – Design Prototype Images....I-54

List of Abbreviations

2D	Two dimensional
3D	Three dimensional
ABS	Acrylonitrile Butadiene Styrene
ACL	Anterior Cruciate Ligament
AMCL	Anterior bundle of the medial collateral ligament
CAD	Computer Aided Design
CT	Computer Tomography
DICOM	Digital Imaging and Communication in Medicine
GIMP	GNU Image Manipulation Program
HREC	Human Research Ethics Committee
HU	Hounsfield Unit
ICC	Intraclass Correlation Coefficient
IPA	Isopropyl Alcohol
K-Wire	Kirschner Wires
LCL	Lateral Collateral Ligament
LUCL	Lateral Ulnar Collateral Ligament
MCL	Medial Collateral Ligaments
mm	Millimetres
ORIF	Open Reduction and Internal Fixation
PACS	Picture Archiving and Communication System
PMCL	Posterior bundle of the Medial Collateral Ligament
Q3DCT	Quantitative 3D Computer Tomography
RCL	Radial Collateral Ligament
SD	Standard Deviation
SR	Professor Stephen Roche
STL	Stereolithography / Standard Triangular Language
UCL	Ulnar Collateral Ligaments
UV	Ultraviolet

List of Figures

Figure 1: Proposed overall methodology to be used throughout the project. 4
Figure 2: Bones of elbow joint (Netter, 2018). 8
Figure 3: Capsuloligamentous anatomy of the elbow (Netter, 2018). 9
Figure 4: Fall on an outstretched hand (FOOSH), with the forces and moments causing posterolateral rotatory instability (Adapted from Adams (2020)). 16
Figure 5: Regan and Morrey classification of coronoid process fractures with the Type 1, Type 2 and Type 3 fractures labelled accordingly (Adapted from (Doornberg et al., 2006)). 18
Figure 6: O'Driscoll classification system for coronoid process fractures. (A) Type 1 fracture of the tip. (B) Type 2 and the type 2 subtype fractures of the anteromedial facet. (C) Type 3 basal fracture of the coronoid process (6). 19
Figure 7: An example of a single fracture line shown on the superior view of the ulna articular surface (Mellema et al., 2014). 21
Figure 8: Fracture map (left) and resultant heat map (right) depicting a Terrible Triad fracture-dislocation pattern (Mellema et al., 2014) 22
Figure 9: Simplified version of methodology followed during the fracture mapping process. 24
Figure 10: Exclusion criteria used to evaluate the CT scans. 25
Figure 11: Initial digital mask showing the different orientations and 3D rendered model of the fractured elbow. 3D rendered model (bottom right corner) is shown in the reconstruction platform of Materialise Mimics® 26
Figure 12: Close up of the labelling system used for the individual digital masks and their associated 3D models. 27
Figure 13: Mimics 16.0 (Materialise, Leuven, Belgium) 3D model of the edited and separated bones and fragments. 28
Figure 14: Fragmented (original) fracture state of the coronoid. 29
Figure 15: Fracture with reduced fracture fragments. 29
Figure 16: Merged state of the fractured coronoid. 30
Figure 17: A resultant superior view heatmap showing the density of all 33 patients' fracture lines overlaid over the healthy template boundary line. 32
Figure 18: Superior view resultant heat map after undergoing editing in GIMP 2.10.32 (GIMP Development Team – Open Source). 33
Figure 19: Distribution of proportions of coronoid fracture Types and Subtypes present in this study. 35
Figure 20: (A) Fracture map showing the location, distribution, and frequency of all 33 patient fractures in the anterior view. (B) Fracture map showing the location, distribution, and frequency of 32 of the patient fractures along the superior view of the coronoid. 36
Figure 21: (A) Medial fracture map involving all the fracture lines from the 33 selected patients. (B) Lateral fracture map including 32 of the 33 fracture lines from the selected patients. 36
Figure 22: Anterior fracture maps depicting the location and distribution of all the Type 1 coronoid fractures. 37
Figure 23: Type 2 Coronoid fractures. (A) Anterior view of Type 2 Subtype 2 coronoid fractures showing the distribution of the fractures, and the common 'Africa pattern'. (B) Type 2 Subtype 3 coronoid fractures which encompass the anterior rime and the sublime tubercle 38
Figure 24: (A) Anterior heat map of the coronoid depicting the density of all patient fracture lines, with the presence of one evident weak point in the coronoid. (B) Superior heat map showing the density of all the patient fractures; as well as the weak points of the coronoid. 39

Figure 25: (A) Lateral heat map of all the patient fracture lines, (B) Medial heat map of the 33-patient fracture lines. 39
Figure 26: (A) Heat maps showing the density of Type 1 fractures. (B) Critical fracture pattern of O'Driscoll Type 1 coronoid process fractures. 40
Figure 27: (A) Heat maps depicting the density of the fracture patterns classified as O'Driscoll Type 2 Subtype 2 fractures. (B) Critical fracture pattern for O'Driscoll Type 2 Subtype 2 fractures. The critical fracture pattern follows the 'Africa pattern.' 41
Figure 28: (A) Heat maps showing the distribution of the fracture line density for Type 2 Subtype 3 O'Driscoll fractures. (B) Critical fracture pattern for O'Driscoll Type 2 Subtype 3 fractures. 42
Figure 29: Coronoid buttress fixation plate which makes use of rigid cortical screws and a buttress plate to secure the fragment (Kloen and Ring, 2018). 48
Figure 30: Non-biological (left) and biological (right) coronoid protheses (Bellato and O'Driscoll, 2019). 49
Figure 31: Suture lasso technique used for small fragment coronoid fractures (Kloen et al., 2018). 50
Figure 32: Suture anchors used in Orthopaedic ORIF surgeries (Kloen et al., 2018). 50
Figure 33: Endobutton used for ACL repair (Left – red box) and coronoid fixation (Right) (Altan et al., 2016). 51
Figure 34: Simplified flow diagram of the methodology followed during the Qualitative Fit Analysis of the Endobutton imitation 56
Figure 35: 3D Printed coronoid fractures from four different patients with the fragments attached using a temporary adhesive. Each fracture is notably different from the others. 58
Figure 36: Simplified 3D CAD image of the Endobutton imitation 59
Figure 37: 3D Printed Endobutton imitation. 59
Figure 38: 3D printed Endobutton imitation templated on the 3D printed fractured coronoids of four different patients, using the temporary adhesive 60
Figure 39: Overview of the design methodology to be used during the production of the adapted Endobutton device. 69
Figure 40: A) Anterior view of the coronoid showing the angulation (red arrow) and convexity (blue arrow) of the process. B) Superior view of the coronoid showing the convexity (blue arrow). 73
Figure 41: Drawing of the initial design 1 (Image drawn by author – N. Mason). 75
Figure 42: (A) Simple 3D CAD model of the T-shaped design shown from an oblique view to depict the curvature needed to match the convexity of the coronoid surface. (B) Physical prototype of design, printed in clear resin, to be used for testing. 76
Figure 43: Simplified 3D CAD model of the curved transverse bar of the design. 76
Figure 44: Physical prototype, printed in clear resin, to be used for testing. 76
Figure 45: (A) Simplified 3D CAD model of Design 3 which incorporates a curvature to mimic that of the facets and tip of the coronoid. (B) Physical prototype of design to be used during testing. 77
Figure 46: (A) Simplified 3D CAD mode of the symmetrical curved arrow design. (B) Rapidly produced prototype to be used for testing. 79
Figure 47: (A) Simplified 3D CAD model of the asymmetrical curved arrow design. (B) Rapidly produced prototype to be used for testing. 79
Figure 48: Symmetrical (Left) and Asymmetrical (Right) design of adapted Endobutton. 80
Figure 49: Simplified 3D CAD model of chosen design concept. 82
Figure 50: SolidWorks drawing showing the dimensions of the arms and suture holes of the designed Endobutton (Anterior/front view) 84
Figure 51: SolidWorks drawing showing the angles of the curvature of the spline and the location of the suture holes in relation to the edge of the device (Anterior/front view). 84

Figure 52: SolidWorks drawing showing the total top-to-bottom length and the thickness of the designed Endobutton (Medial/left view). 85
Figure 53: SolidWorks drawing showing the total width (medial/left to lateral/right) of the designed Endobutton (Superior/top view). 85
Figure 54: Left and right versions of design compared to the Endobutton imitation. 88
Figure 55: Simplified methodology depicting the rapid prototyping, templating, and cadaver studies. 92
Figure 56:Templating of design adapted Endobutton on a small number of the 3D printed bones, using a temporary adhesive. 93
Figure 57: Short (red), standard, and long (purple) versions of the adapted Endobutton. 97
Figure 58: Spiked versions of the adapted Endobutton compared to the original design. Devices had spikes of 2mm (black), 3mm (blue) and 4mm (green). 98
Figure 59: Colour coded left and right sided versions of adapted Endobutton design. Short (Red), Original (unmarked), Long (Purple), 2mm Spiked (Black), 3mm Spiked (Blue), and 4mm Spiked (Green). 98
Figure 60: Designed adapted Endobutton (Original) used in the fixation of a coronoid fracture in left cadaver limb. The device is roughly outlined in green, within the green box. 100

List of Tables

Table 1: Selected Patient Cohort Demographic Information 33
Table 2: Fracture Characteristics 34
Table 3: Additional characteristic frequencies 34
Table 4: Fracture type and subtype description and frequency 34
Table 5: Summary of coronoid fixation devices 52
Table 6: Qualitative ordinal scale used to evaluate the aspects of the imitated Endobutton. 61
Table 7: Table showing the overall percentages of the reported responses for each question. 62
Table 8: Limitation response rates (Type 1 n=11, Type 2 n=20). 63
Table 9: Interobserver reliability. 63
Table 10: Design specifications for the adapted Endobutton based on the functional and technical design requirements. 72
Table 11: Updated dimension requirements (red) of the adapted Endobutton design. 78
Table 12: Review of design against the technical requirements for adapted Endobutton. 80
Table 13: Revision of the criteria which establish the viability of the device design. 81
Table 14: Table showing the overall results from the questionnaire. 95
Table 15: Limitation report frequency. 96
Table 16: Interobserver reliability of the verification study. 96
Table 17: Interobserver reliability for the cadaver validation studies. 103

1. Chapter 1: Introduction to Study

1.1. Project Introduction

The elbow is a hinge joint of the upper limb that allows for a wide range of motion whilst maintaining the stability of the limb (Fornalski, Gupta *et al.*, 2003a). The coronoid process, a critical anatomical structure within the elbow, plays a fundamental role in preserving the joint's stability (Fornalski *et al.*, 2003a). It acts as a key attachment and anchor point for ligaments and tendons, offering resistance against valgus and varus stresses, and its integrity is vital for the overall function of the joint (Alcid, Ahmad *et al.*, 2004; Fornalski *et al.*, 2003a).

Coronoid fractures, often associated with high-energy trauma such as falls or automobile accidents, disrupt this balance, resulting in joint instability and impaired elbow function (Adams, 2020). Fractures of the coronoid process pose a significant challenge in Orthopaedic surgery. These fractures compromise elbow stability, leading to long-term functional limitations if not treated appropriately (Adams, 2020). Traditional approaches to coronoid fracture fixation typically rely on the use of screws, plates, and wires, which do not always provide optimal fixation and are associated with various complications (Chen, He *et al.*, 2018; Liu, Hu *et al.*, 2018).

This project aims to explore the design and development of an adapted coronoid fracture fixation device using interdisciplinary efforts. Collaborations with orthopaedic surgeons will help design and develop an adapted Endobutton fixation device for coronoid process fractures to offer a possible improvement in fracture reduction and stability, as well as reduced complications.

The development of the adapted device involves an approach that integrates the use of fracture pattern studies, anatomy, and biomechanics. 3-Dimensional (3D) rendered Computer Tomography (CT) scans and *in-silico* reduction of the fractures, provide the baseline for the critical fracture patterns of the coronoid process. The maps and critical fracture patterns, in conjunction with an in-depth anatomical knowledge of the ulna bone and coronoid, inform the design process. This device aims to restore the normal anatomy and biomechanics of the coronoid process, while providing the necessary stability for normal functioning.

Advanced manufacturing techniques such as 3D printing and computer-aided design (CAD) play a role in the design and development of this improved device. CAD software allowed for virtual prototyping and facilitated rapid prototype development. 3D printing enabled the production of these prototypes that could then be assessed through physical handling and templating.

1.2. Dissertation Structure

1.2.1. Research Question

"Can a redesigned adapted Endobutton fixation device be produced to provide improved reduction and fixation of coronoid fractures?"

1.2.2. Aim and Objectives

Aim

This study's primary aim is to design and develop an adapted Endobutton fixation method to treat coronoid process fractures. This design's purpose is to provide improved fracture reduction and fixation. A secondary aim is to establish 3D maps of coronoid process fractures which reflect the overall morphology of the coronoid fracture fragments.

Objectives

To achieve the aim, this study has the following objectives:

1) Establish reference fracture maps of O'Driscoll classified coronoid process fractures using Computer Tomography (CT) scans.
2) Establish the limitations of the currently used Endobutton fixation methods through physical device templating.
3) Design of an adapted version of the Endobutton fixation device.
    i. Verify the design using rapid prototyping, design templating, and qualitative assessment.
    ii. Validate the design through cadaver testing and qualitative design evaluation by surgeons.

Each objective is addressed separately in a project chapter.

1.2.3. Proposed Methodology Overview

The first step towards creating the adapted Endobutton will be establishing fracture maps that will guide the morphometric characteristics of the design. These maps will be created using CT scans of coronoid fractures acquired from Groote Schuur Hospital. Heat maps will be produced to reinforce the fracture maps. They will establish the coronoid's weakest points and provide fracture density information to determine the critical fracture patterns. These maps will allow for an understanding of the critical points and fracture pattern of the coronoid process which the adapted design will aim to address.

Secondly, an understanding of the strengths and limitations of the Endobutton currently used in coronoid fracture fixation needs to be established through templating and qualitative assessment by trained Orthopaedic surgeons. These insights will guide the design by identifying which elements of the current device should be included and excluded. In turn, this will help establish the device design requirements and inform the formation of the viability and efficacy criteria.

The third step will follow a set out design process which makes use of a two-step approach. The initial conceptual design phase includes the development of the design concepts into multiple possible solutions, from which the most suitable option will be selected. The detailed design phase involves further development through to prototype production. A thorough review process will be followed between each phase to ensure the specified design requirements are met and address any problems encountered.

The fourth step will be the design verification, which will be done through rapid prototyping using 3-Dimensional printed models. The 3D model will be created with accurate design specifications. This will allow for the physical inspection and assessment of the design. The verification process will also encompass the evaluation of the device's usability, its fit and its ability to fixate the coronoid fractures. This evaluation will be done using the criteria which will be established during the fracture fixation study phase.

The last step will focus on anatomical testing of the device using cadavers with simulated coronoid fracture patterns and performing fixation surgeries. The cadaver testing will allow for the evaluation of the device under conditions which are as close to real surgical procedures as possible, taking into consideration the presence of soft tissue. This testing will provide a practical assessment of the design's congruency with the bone structure, as well as its interactions with the related sutures and surgical instrumentation. To validate the design, a review process by six surgeons will be undertaken using a qualitative evaluation of the device's usability and fixation efficacy.

The proposed overall methodology is summarized in the following flow diagram (Figure 1).

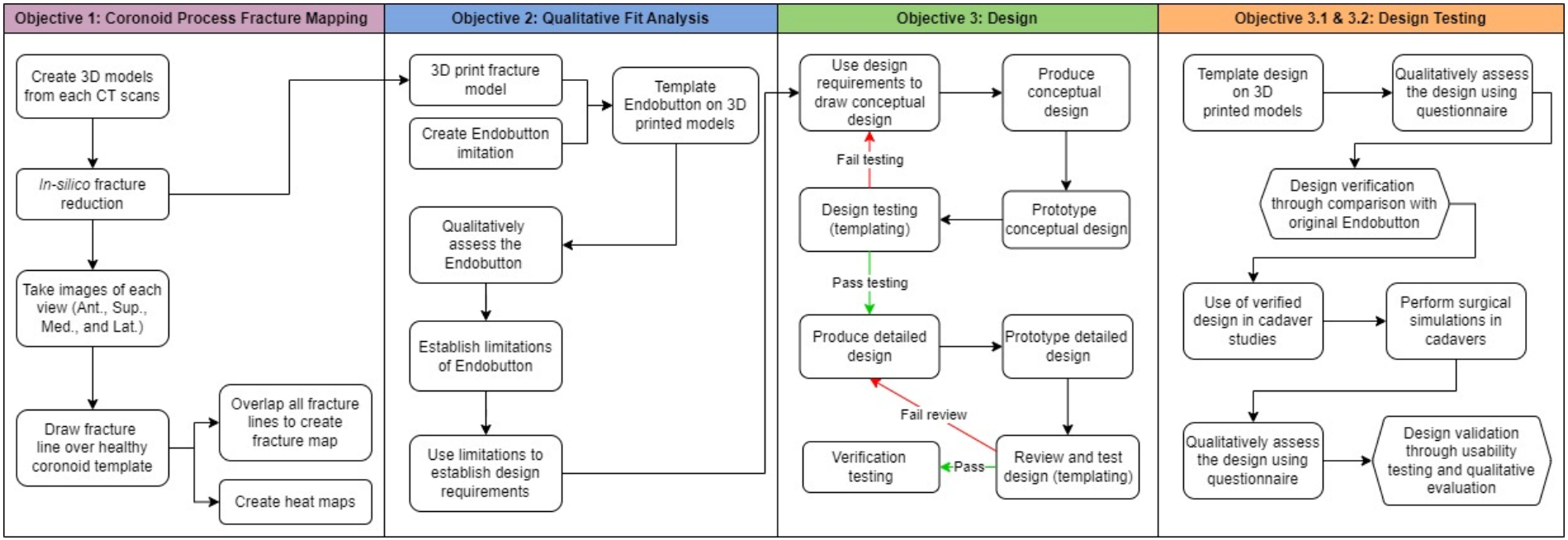

Figure 1: Proposed overall methodology to be used throughout the project.

1.2.4. Planned Data Scope

The fracture studies will make use of retrospective CT imaging data of patients with coronoid fractures. The use of the retrospective data is important due to the long timeline required for the collection of new scans.

The validation studies will make use of a small sample of cadaver material donated to the University of Cape Town. Exclusion criteria for the cadaver materials is the presence of previous surgeries to the elbow. The use of cadavers provide a safe and ethically monitored way in which to conduct testing in a real-world anatomical setting without any risks to patients, and minimal risks to the surgeons, University of Cape Town staff members or investigators on this study.

1.2.5. Ethical Considerations

Ethical approval was acquired from the University of Cape Town Human Research Ethics Committee (HREC) (HREC Ref Number: 588/2022) prior to the start of this study. The approval allows this study to be conducted in the Division of Biomedical Engineering at the Faculty of Health Sciences. Ethical approval was also granted to register on the Picture Archiving Communication System (PACS) in the Division of Orthopaedics at Groote Schuur Hospital, Cape Town.

Permission for the cadaver study was granted by the Cadaver Research Governance Committee, Department of Human Biology, Faculty of Health Sciences, University of Cape Town. Additional approval was obtained from the Human Research Ethics Committee (HREC) to perform the cadaver studies within the Department of Human Biology. The inclusion of the cadaver studies falls under an amendment of the aforementioned ethical clearance (HREC Ref Number: 588/2022) (Appendix A).

1.2.6. Dissertation Overview

This project is a study into the evaluation of the currently available Endobutton device used for coronoid process fracture fixation, and the design of an adapted Endobutton. This includes the creation of coronoid fracture maps, the evaluation of the limitations of the currently available Endobutton fixation device, and the development of the adapted device design. Also included is the verification of the adapted design through rapid prototyping (3D printing), and validation of the device's efficacy via cadaver-based testing.

Chapter One introduces the project and its structure. This is followed by a relevant discussion of the anatomy of the elbow joint and more in-depth investigation of the normal anatomy of the coronoid process. The biomechanical role of the coronoid process in the elbow is reviewed. The topics of coronoid fractures and their mapping as well as surgical fixation are introduced to provide an understanding for the project.

Chapter Two follows the creation of the coronoid fracture maps. The chapter begins by describing the causes of injuries to the coronoid process. To follow is the review of the Regan and Morrey, and O'Driscoll systems of coronoid fracture classification. The materials and methods section explain the information relevant to the patient cohort, and the steps followed, and programs used to create the fracture maps and heat maps. A results and discussion section for these maps follows. The results and discussion identify and explain the critical fracture patterns of the coronoid, which are a key element in the subsequent device design.

Chapter Three is the qualitative evaluation of the Endobutton currently used as a method of surgical fixation. The evaluation process adopts a physical templating approach. The chapter begins by reviewing the available fixation methods for coronoid fractures and their corresponding advantages and disadvantages. The use of 3D printing and fitment analysis of devices in Orthopaedic surgery is introduced. Physical templating is employed to assess the current Endobutton fixation method using 3D-printed models of the critical fracture patterns. A Qualitative Feedback questionnaire is used to evaluate the efficacy of the Endobutton-based fixation method and identified limitations are noted. The results of the qualitative assessment are presented and discussed, while noting how the identified limitations influence the development of the adapted device design. The chapter concludes with the reiteration of the limitations and the recommendations for the design requirements for the following chapters.

Chapter Four describes the initial design planning, concepts, and design requirements for the adapted Endobutton design. The test and evaluation criteria are established prior to the generation of multiple conceptual designs. The most suitable concept is determined using the selection criteria. The detailed version of the chosen design is elaborated upon, finalized, and reviewed before being rapidly prototyped (3D printed). The planned testing of the rapidly prototyped design is explained prior to the chapter's conclusion.

Chapter Five encompasses the verification and validation testing of the adapted Endobutton by means of rapid prototyping, testing and qualitative assessment. After stating the objectives specific to the verification and validation process, the testing methods and procedures that will be used to verify and validate the designed device are laid out. The verification framework includes functionality, usability, and safety testing, while the validation encompasses cadaver studies. The results are explained, and their relevance is discussed. The challenges and limitations of the testing and the methods used are described prior to the conclusion of the chapter.

Chapter Six addresses the overall content of this study. Predominant discussion points are highlighted, and limitations are considered. Chapter Six also posits the overall study conclusions, and recommendations for future studies.

1.3. Background Information: Anatomy and Biomechanics of the Elbow

1.3.1. Normal Anatomy of the Elbow

Bones of the Elbow

The elbow joint is comprised of three bones: the distal end of the humerus in the brachium (upper arm), and the proximal heads of the radius and ulna in the antebrachium (forearm) (Alcid *et al.*, 2004). The distal head of the humerus comprises of a medial and lateral column with their corresponding supracondylar surfaces, epicondyles, and articulation surfaces (Figure 2) (Fornalski, Gupta *et al.*, 2003b; Alcid *et al.*, 2004). The medial column plays host to the spool-like trochlear articular surface of the humerus which corresponds to the trochlear notch of the ulna (Alcid *et al.*, 2004). The lateral column of the humerus includes the lateral spherical capitulum which articulates with the most proximal part of the radial head (Alcid *et al.*, 2004).

The radius, located laterally in the forearm, has an acylindrically shaped head with a superior concave surface, which articulates with the capitulum of the distal humerus (Figure 2) (Fornalski *et al.*, 2003b; Alcid *et al.*, 2004). The peripheral edge of the head articulates with the radial notch on the lateral aspect of the ulna and with the radial fossa of the humerus when the arm is in full flexion (Fornalski *et al.*, 2003b; Alcid *et al.*, 2004).

The ulna is located medially in relation to the radius (White and Folkens, 2005). The most prominent feature of the ulna is the olecranon process and the trochlear notch which articulates with the trochlear of the distal humerus (Figure 2) (Fornalski *et al.*, 2003b; Alcid *et al.*, 2004). At the distal base of the trochlear notch is the coronoid process, a beak-shaped anterior projection (Fornalski *et al.*, 2003b; Alcid *et al.*, 2004; White *et al.*, 2005). On the lateral aspect of the coronoid process is the radial notch (Fornalski *et al.*, 2003b; Alcid *et al.*, 2004; White *et al.*, 2005).

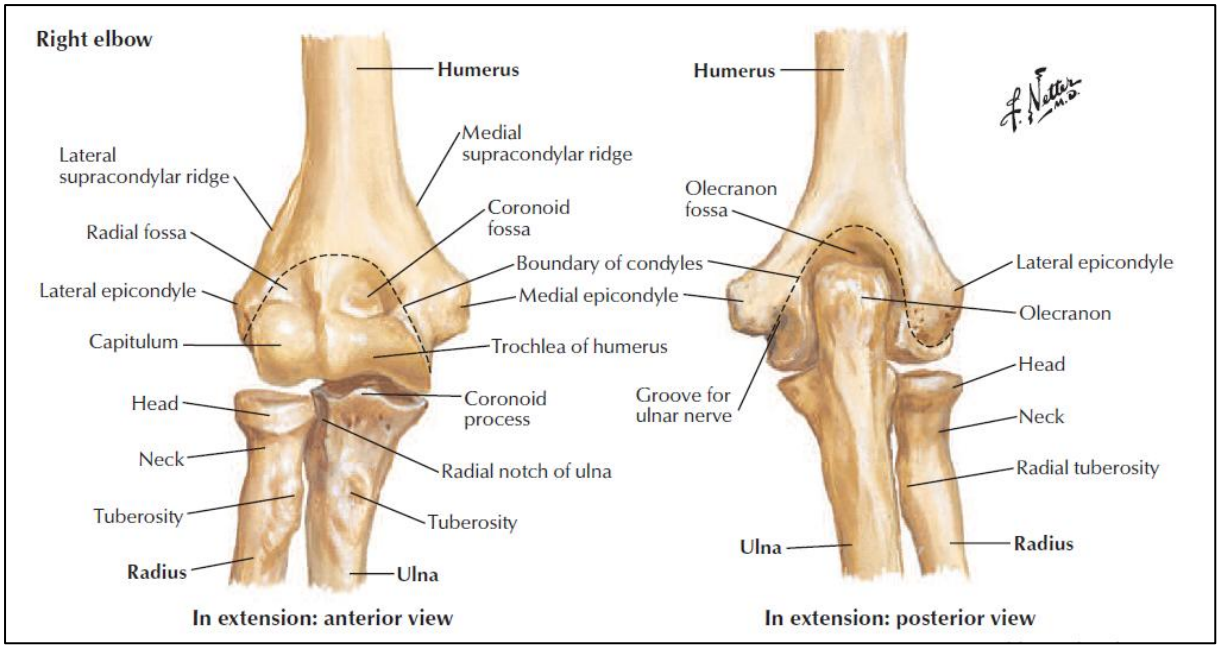

Figure 2: Bones of elbow joint (Netter, 2018).

Musculature of the Elbow

Muscle attachments around the elbow joint consists of the muscles of the brachium and antebrachium, which can be categorised into either primary or secondary flexors or extensors (Fornalski *et al.*, 2003b; Alcid *et al.*, 2004). The primary flexors are responsible for bending the elbow joint, decreasing the angle of the joint by applying a compressive load, while the secondary flexors only assist in this motion (Bryce and Armstrong, 2008a). Among providing the mechanism of flexion and extension of the elbow joint, these muscles also contribute to the supination, abduction and stabilisation of the joint (Fornalski *et al.*, 2003a).

The primary flexors of the elbow consist of the biceps brachii and the brachialis (Alcid *et al.*, 2004; Fornalski *et al.*, 2003a). The secondary flexors of the elbow include the brachioradialis, pronator teres, and the extensor carpi ulnaris; with their corresponding contribution to the flexing action decreasing respectively (Alcid *et al.*, 2004; Fornalski *et al.*, 2003a). Extensors, responsible for the straightening of the elbow joint, are the triceps brachii, anconaeus and flexor carpi ulnaris with the latter providing a secondary extensor contribution (Fornalski *et al.*, 2003a).

Ligaments of the Elbow (Capsuloligamentous Anatomy)

The elbow joint is enclosed by a complex network of ligaments and a joint capsule, which collectively maintain the joint's stability and allows for controlled movements. This network includes the Ulnar and Radial Collateral ligament groups, the joint capsule, and several additional reinforcing structures (Figure 3)(Lockard, 2006).

The Ulnar Collateral Ligament (UCL) is part of the medial and lateral capsular thickenings labelled the medial (MCL) and lateral collateral ligaments (LCL) respectively (Adams, 2020; Bryce *et al.*, 2008a). Both the MCL and the LCL consist of a posterior, transverse, and anterior bundle complex; each playing varying roles in the arm's range of flexion and extension movements (Lockard, 2006). The anterior bundle of the MCL is the most discrete of the group, whereas the posterior bundle presents as a thickening of the capsule rather than a distinct ligament (Bryce *et al.*, 2008a). The LCL complex includes the radial collateral ligament, the annular ligament, and the accessory ligament; each with varying attachment sites around the elbow joint (Figure 3)(Bryce *et al.*, 2008a). The lateral aspect of the coronoid process provides an attachment site for the lateral ulnar collateral ligament, while the medial aspect anchors the medial collateral ligament (Fornalski *et al.*, 2003a)

Radial collateral ligament (RCL) is a fan-shaped ligament which extends from the lateral epicondyle of the humerus to the annular ligament (Lockard, 2006). The RCL forms part of the LCL complex and acts in conjunction with the rest of the LCL group to restrain the elbow against varus forces (Figure 3)(Lockard, 2006). Closely related to the RCL is the annular ligament which is a fibrous band that encircles the radial head, and aids in the stabilisation of the radial head within the radial notch (Figure 3)(Lockard, 2006).

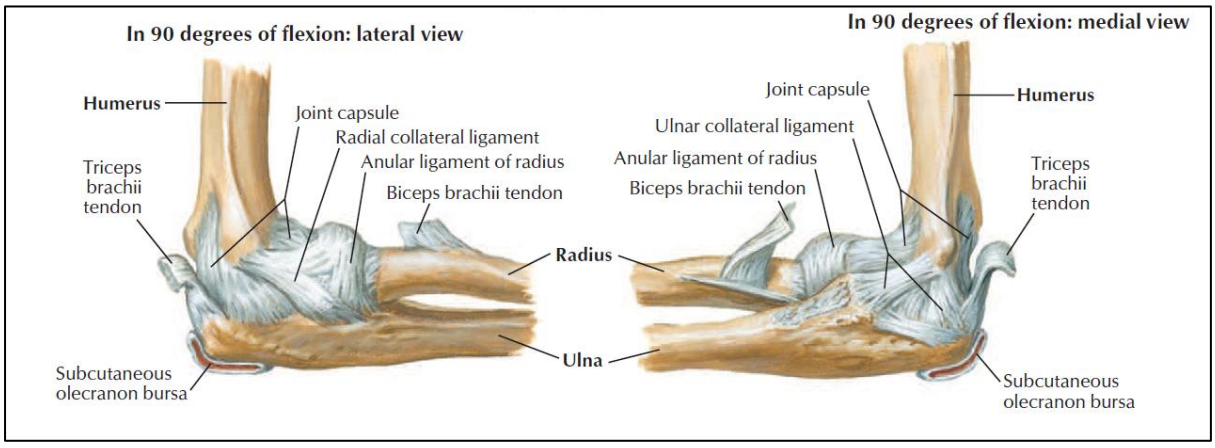

Figure 3: Capsuloligamentous anatomy of the elbow (Netter, 2018).

The joint capsule consists of an anterior and posterior part, with the anterior portion extending from above the coronoid and radial fossae to the distal edge of the coronoid process and laterally towards the annular ligament (Bryce *et al.*, 2008a). The posterior portion of the capsule attaches superior to the olecranon fossae of the humerus, and extends medially and laterally towards the articular margins of the sigmoid notch (Bryce *et al.*, 2008a). The capsule serves as a containment area for the synovial fluid whilst maintaining the integrity of the elbow joint (Lockard, 2006).

Additional structures in the capsuloligamentous network include the interosseous membrane, the quadrate ligament, the accessory collateral ligament, and the tendons of the extensor and flexor muscles. Notedly, the interosseous membrane connects the radius and the ulnar, and aids in supination/pronation movements, and in transmitting of forces through the length of the forearm (Lockard, 2006).

Neurovascular Structures of the Elbow

The upper limb's innervation is devised by four major nerves arising from the brachial plexus, which stems from the C5 to T1 spinal nerves (Alcid *et al.*, 2004). The radial nerve originates from the posterior cord and travels through the posterior brachial compartment, to supply the posterior brachial muscles (Alcid *et al.*, 2004; Latef, Bilal *et al.*, 2018). These include muscles that are crucial to the extension function of the elbow joint (Alcid *et al.*, 2004). From the lateral cord, the musculocutaneous nerve branches to provide innervation to the muscles of the anterior brachium (Alcid *et al.*, 2004).

The median nerve innervates the majority of the anterior compartment of the antebrachium (Alcid *et al.*, 2004). It branches to provide innervation to muscles like pronator teres, flexor carpi radialis, and palmaris longus (Fornalski *et al.*, 2003a). The median nerve travels through the anterior compartment of the antebrachium, innervating the wrist and digit flexors (Alcid *et al.*, 2004).

Derived from the medial cord, the ulnar nerve innervates the flexor carpi ulnaris muscles and travels through the anterior compartment of the antebrachium to the hand in order to provide the hand muscles' innervation through its deep branch (Drake, Vogl *et al.*, 2019).

1.3.1.1. Normal Anatomy of the Coronoid Process

The coronoid process is a beak-shaped anterior projection of the trochlear notch at the proximal ulna (White *et al.*, 2005; Drake *et al.*, 2019). The anterior surface of the process is triangular with the apex projecting distally (Drake *et al.*, 2019). This distal apex, or the tip of the coronoid process, projects more anteriorly or is higher than the anterior projection of the proximal olecranon process (Ring and Horst, 2015). In addition, the process is translated medially in relation to the ulnar metaphysis, which has biomechanical implementations for the bone (Ring *et al.*, 2015). The lateral and superolateral surfaces of the process are both articular and participate in the radial-ulnar and ulnar-humeral articulation respectively (White *et al.*, 2005; Matzon, Widmer *et al.*, 2006; Drake *et al.*, 2019). The anterior surface of the coronoid process contributes to the attachment of the fibrous joint capsule of the elbow, while also functioning as the attachment site for the anterior bundle of the medial collateral ligament (MCL)(Matzon *et al.*, 2006; Drake *et al.*, 2019). In addition, the medial edge of the coronoid

process has roughening which allows the projection to act as an attachment site for small linear regions of the pronator teres and flexor digitorum superficialis muscles (Drake *et al.*, 2019).

1.3.2. The Biomechanical Role of the Coronoid Process in The Elbow

This bony projection is translated medially in relation to the ulnar metaphysis, which provides the foundation of the biomechanical influence the coronoid has on the ulna and the elbow joint (Ring *et al.*, 2015). The biomechanical roles of the coronoid are focused around: function and movement, stability and dislocation prevention, and its clinical relevance. These roles are divided amongst the passive and active stabilisers of the elbow joint (Alcid *et al.*, 2004; Fornalski *et al.*, 2003a).

The elbow has two degrees of motion: flexion and extension, and supination and pronation, and acts in conjunction with the shoulder joint to position the hand in space (Alcid *et al.*, 2004; Bryce *et al.*, 2008a). During flexion/extension, the elbow has a range of motion from 0° to 140°, with 30° to 130° encompassing the movements of daily activities (Bryce *et al.*, 2008a). The maximal flexion is limited anteriorly by the muscle bulk, the impaction of the radial head and the coronoid process with their corresponding fossae, and the tightness of the triceps muscle (Alcid *et al.*, 2004).

The stability of the elbow joint relies on the balance between the anatomical structures and their roles in resisting several types of forces. Approximately 75-85% of the force exerted in a valgus stress direction is tolerated by the proximal half of the olecranon, while varus stress is countered primarily by the coronoid, specifically the distal portion of the sigmoid notch (Alcid *et al.*, 2004; An, Morrey *et al.*, 1986). The coronoid's significance extends beyond preventing posterior dislocation; it also plays a vital role in maintaining varus stability when the lateral collateral ligament (LCL) remains intact (Alcid *et al.*, 2004). Furthermore, the radial head acts as a secondary stabiliser against valgus stress and indirectly opposes varus stress (Alcid *et al.*, 2004). The biomechanical stability of the elbow joint depends on both passive and active stabilisers (Alcid *et al.*, 2004).

As part of the passive stabilisation category, the articular stability of the joint is inherently reliant on the interlocking and congruous surfaces of the bones involved; therefore fracture size and position may affect the stability of the joint (Alcid *et al.*, 2004). The coronoid process allows for flexion/extension movements as it articulates and interlocks with the coronoid fossa of the humerus; while preventing the posterior dislocation of the ulna during movement (Alcid *et al.*, 2004). The capsuloligamentous anatomy also plays a static and passive stabilisation role in the elbow joint. Therefore the anterior and posterior joint capsule, and the MCL and LCL complexes involvement of the ligament in the coronoid fracture may affect joint stability (Alcid *et al.*, 2004; Bryce *et al.*, 2008a). The MCL acts as the primary stabiliser against the valgus stress during 90° of flexion; whereas during extension, the MCL and the anterior capsule and the bony articulation are the resisters to the valgus

stress (Fornalski *et al.*, 2003a). The lateral ulnar collateral ligament (LUCL) stabilises the elbow joint against the varus stress through the elbow (Fornalski *et al.*, 2003a). The LCL and the other ligaments that form the complex originate around the axis of rotation; therefore, there is a constant tension throughout the ligamentous complex (Fornalski *et al.*, 2003a).

The active stabilisers of the elbow joint are comprised of the muscles which work primarily to move the joint; including but not limited to the muscles which have attachment sites along the structure of the coronoid (Alcid *et al.*, 2004). Collectively, the muscles which cross the elbow joint generate a reactive force which stabilises the joint by compressing the articular surfaces (Alcid *et al.*, 2004). The importance of the active stabilisers is underpinned by the dynamic support provided by the flexor/pronator muscles; specifically the flexor carpi ulnaris, and portions of the flexor digitorum superficialis (Alcid *et al.*, 2004). The extensor/supinator muscles contribute to the static and dynamic stability of the lateral side of the elbow joint (Alcid *et al.*, 2004).

The contributions of various anatomical structures to elbow joint stability vary as a function of displacement from the neutral position. In the neutral or mid-range position, the active dynamic stabilisers, primarily the surrounding musculature, play a more prominent role in maintaining joint stability through active contraction (Dunning, Zarzour *et al.*, 2001). As the joint moves toward the extremes of flexion or extension, the passive stabilisers, including the ligaments and the joint capsule, become increasingly engaged due to tension generated by stretching (Cohen and Hastings, 1997). This passive resistance provides critical stability particularly at the end of the ranges of motion. The bony congruency contributes to the joint stability, particularly during mid-flexion where joint surfaces are in close contact (Morrey and An, 1983).

Fractures of the coronoid process can have significant implications for elbow stability and function. A fracture that disrupts the coronoid's interlocking mechanism with the olecranon might lead to instability and increased risk of recurrent elbow dislocation (Feng, Zhang *et al.*, 2018). Fractures to the coronoid process are clinically relevant because if treated improperly can lead to chronic elbow instability, recurrent dislocation and progress loss of range of motion (Feng *et al.*, 2018). Over time, the instability can precipitate post-traumatic osteoarthritis, resulting in persistent pain and reduced functionality of the joint (Zhang, Lin *et al.*, 2020).

1.3.3. Coronoid Fractures and Their Maps

Fractures to the coronoid are a result of falls on an outstretched hand, or direct trauma or high energy injuries (such as sport or motor vehicle accidents) (Adams, 2020). Dislocations of the elbow are mostly commonly caused by an axial load to the elbow through the forearm which results in a rotational force

(Adams, 2020). Alternatively, posterolateral dislocations result from an axial load through the forearm during supination due to the sequential failure of the soft tissue stabilisers (Adams, 2020).

Fracture mapping involves the classification and categorisation of fractures based on specific characteristics, patterns, or anatomical locations (Ring, 2006). The mapping of fractures aids surgeons in diagnosis, understanding their severity, and determining the appropriate treatment (Mellema, Doornberg *et al.*, 2014). It provides a structured way to communicate and document fractures, with the aim of improving patient care and outcomes. Fracture mapping is dependent on the bone involved, how the bone is fractured, and the classification system used. Each type of fracture is classified using one or multiple methods of classification, which in-itself maybe vary depending on the location, size, or comminution of the fracture. Coronoid fractures can be classified using either the Regan and Morrey, or the O'Driscoll classification systems (Doornberg and Ring, 2006).

1.3.4. Open Reduction and Internal Fixation (ORIF) of Coronoid Process Fractures

Open Reduction and Internal Fixation (ORIF) is a surgical procedure employed in the treatment of bone fractures to restore optimal anatomical functionality. This process is used when treating coronoid process fractures to restore joint stability and function (Lowery and Massey, 2022). Coronoid process fractures can pose challenges due to their potential to disrupt elbow joint stability, and when left untreated or not properly managed, they can lead to chronic instability, rapid arthritis, and impaired joint function (Salwan, Saoji *et al.*, 2023).

ORIF is indicated under the following circumstances:

Joint Instability: When the fracture results in significant joint instability, ORIF becomes essential (Alcid *et al.*, 2004). The coronoid process is vital for maintaining the stability of the elbow joint, and its disruption can lead to dislocation or recurrent subluxation of the joint (Feng *et al.*, 2018).

Complex Elbow Injuries: Coronoid process fractures often occur in conjunction with other complex elbow injuries, such as elbow dislocations or radial head fractures. When multiple components of the elbow are affected, surgical intervention is frequently required to restore overall joint integrity (Adams, Hoskin *et al.*, 2009; Lowery *et al.*, 2022).

Fracture Severity: The decision to perform ORIF also considers the severity of the fracture. Fractures that involve large bone fragments or a substantial portion of the coronoid process may necessitate surgical treatment (Lowery *et al.*, 2022).

Early interventions using stable surgical fixation is the standard treatment protocol of displaced coronoid fractures (Feng *et al.*, 2018). Currently available surgical fixation methods include the

utilization of plate fixation, screw-based fixation, Kirschner wires (K-wires), suture-based fixation or suturing techniques, Endobuttons, or a combination thereof (Altan, Ozel *et al.*, 2016; Chen *et al.*, 2018; Liu *et al.*, 2018; Wang, Zhuang *et al.*, 2017).

1.3.5. Background Information Key Findings

1) **Anatomy and Function of the Elbow Joint:** The elbow joint is composed of the distal humerus, and proximal heads of the radius and ulna. The humerus features the trochlear and capitulum, which interact with the trochlear notch of the ulna and the head of the radius respectively (Fornalski *et al.*, 2003a). This joint allows for flexion, extension, supination, and pronation, with flexion/extension ranging from 0° to 140° (Bryce *et al.*, 2008a).
2) **Musculature and Ligamentous Support:** The primary and secondary flexors (e.g., biceps brachii, brachialis, brachioradialis) and extensors (e.g., triceps brachii, anconaeus) of the elbow are essential for movement and stabilisation (Alcid *et al.*, 2004; Fornalski *et al.*, 2003a). Ligaments, including the Ulnar Collateral Ligament (UCL) and Radial Collateral Ligament (RCL), along with the joint capsule, maintain joint stability against various stresses (Alcid *et al.*, 2004; Fornalski *et al.*, 2003a).
3) **Biomechanical Importance of the Coronoid Process:** The coronoid process of the ulna plays a critical role in elbow stability, particularly in preventing posterior dislocation and maintaining varus stability (Alcid *et al.*, 2004). It also serves as an attachment site for ligaments and muscles, contributing to both passive and active stabilisation of the joint (Alcid *et al.*, 2004; Fornalski *et al.*, 2003a).
4) **Clinical Significance of Coronoid Fractures:** Coronoid fractures are significant due to their impact on elbow stability and function. Coronoid fractures can lead to chronic instability and impaired joint function if not properly treated (Feng *et al.*, 2018).
5) **Treatment and Management:** Open Reduction and Internal Fixation (ORIF) is the preferred surgical treatment for severe coronoid fractures to restore joint stability and function (Adams *et al.*, 2009; Lowery *et al.*, 2022). The currently used surgical techniques include rigid plate or screw fixation, K-wires, suture-based methods, and Endobuttons, aiming to address the fracture effectively and prevent chronic instability (Altan *et al.*, 2016; Chen *et al.*, 2018; Liu *et al.*, 2018; Wang *et al.*, 2017).

2. Chapter 2: Coronoid Process Fracture Mapping

2.1. Chapter Introduction

The rationale for creating coronoid fracture maps is to establish a reference base to guide the design of coronoid fixation devices and improve surgical planning. Existing mapping for coronoid fractures is limited to only a 2D perspective from the superior view, which does not fully capture the complexity of the injuries. There is a need to develop more comprehensive maps to improve the understanding of the morphology and fracture patterns of the coronoid. The incorporation of heat mapping is a promising adjunctive technique, allowing for a more nuanced depiction of fracture density and distribution to address this limitation.

This dissertation chapter aims to add to the literature by establishing a set of reference fracture and heat maps depicting critical coronoid fracture patterns in various dimensions, allowing for the creation of a 3D map.

2.2. Literature Review: Coronoid Fractures

2.2.1. Fractures of the Coronoid Process

Coronoid fractures range from minor avulsion fractures to major basilar fractures, and account for approximately 10-15% of elbow fractures (Lowery *et al.*, 2022). The coronoid process assumes a critical role in buttressing against posterior dislocation of the elbow joint, as well as in the joint's overall stability. Consequentially, 2-15% of dislocations of the joint result in fractures to the coronoid process (Lowery *et al.*, 2022; Feng *et al.*, 2018). This integral role and the high energy impact required to fracture the coronoid and dislocate the humerus, are the main reasons that coronoid fractures rarely occur in isolation (Bryce *et al.*, 2008a; Lowery *et al.*, 2022). A frequently observed occurrence is the Terrible Triad which is characterised by the presence of a coronoid fracture, a radial head fracture, and ulnohumeral dislocation; with commonly associated soft tissue injuries to the ulnar collateral ligaments (Chan, MacDermid *et al.*, 2014; Bryce *et al.*, 2008a). While the Terrible Triad presents the most common occurrence, there are a host of other associated fractures to the ulna, including along the shaft, to the olecranon, and to the distal humerus; all of which have been evident in one or more patient scans in this study.

2.2.1.1. Causes of Coronoid Process Fractures

Various studies show that coronoid fractures are caused by high energy impacts directly to the elbow or transmitted to the joint through the other bones in the arm. A common example of force transmission through the arm is a fall on an outstretched hand (FOOSH)(Adams, 2020). These injuries subject the arm to forces such as supination valgus torque and an axial load during flexion (Figure 4)

(Adams, 2020). Specifically, the arm plants and becomes fixed while the body imparts a valgus and posterolateral rotatory force on the ulno-humeral joint (Figure 4)(Ring, 2006). The imposition of an external rotation moment on the joint leads to failure of the soft tissue structures, resulting in posterolateral dislocation, fracture to the coronoid, and other potential fractures to the surrounding structures (Adams, 2020; Ring, 2006).

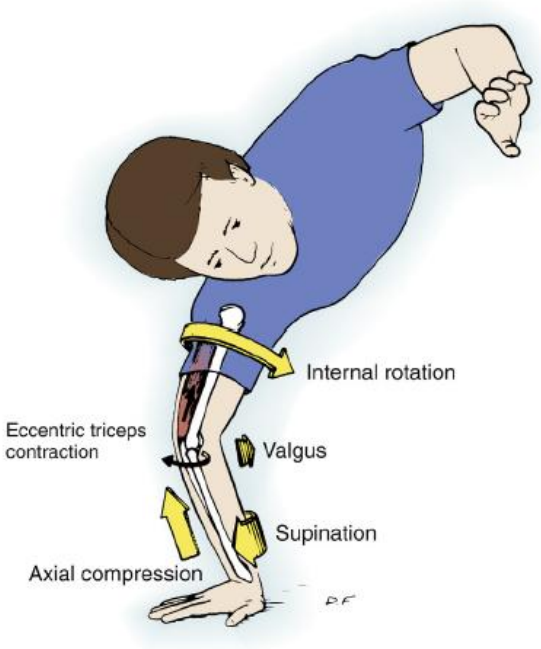

Figure 4: Fall on an outstretched hand (FOOSH), with the forces and moments causing posterolateral rotatory instability (Adapted from Adams (2020)).

Proximal ulna fractures, including coronoid fractures, are frequently attributed to motor vehicle accidents and accidents involving motorcycles or bicycles (Lowery *et al.*, 2022; Desouza, Jani *et al.*, 2020; Feng *et al.*, 2018). These collisions result in the transmission of substantial forces through the arm to the elbow joint (Desouza *et al.*, 2020). Additionally, high contact sports (football, rugby, and martial arts) involve collisions, hyperextension of the elbow, or direct blows to the elbow joint, thus increasing the risk of fracture (Lowery *et al.*, 2022; Feng *et al.*, 2018; Wells and Ablove, 2008). Instances of gunshots to the elbow joint are also a documented cause.

Coronoid fractures seldom occur in isolation, often presenting with additional complex fracture patterns beyond that of the Terrible Triad (Bryce *et al.*, 2008a). Frequently, coronoid fractures are also accompanied by complex olecranon dislocation, either anteriorly or more commonly, posteriorly (Doornberg *et al.*, 2006; Mellema *et al.*, 2014).

2.2.1.2. Clinical Presentation of Coronoid Fractures

The presentation of coronoid fractures varies depending on the presence of joint dislocation. Dislocation often occurs in patients with a history of hyperextension or hyperflexion, leading to the sensation of joint dislocation followed by spontaneous reduction (Lowery *et al.*, 2022; Wells *et al.*, 2008). Patients presenting with coronoid fractures and associated joint dislocation typically experience diffuse tenderness and swelling, often accompanied by an obvious deformity of the joint (Wells *et al.*, 2008).

Patient evaluation includes a thorough examination of medical histories and physical symptoms, with particular attention to joint deformity and restricted range of motion being significant indicators (Wells *et al.*, 2008). Assessments also encompass a range of motion evaluation, neurovascular testing, and assessment of light-touch and 2-point discrimination (Lowery *et al.*, 2022; Wells *et al.*, 2008). Plain radiographic imaging is used to detect fractures, although cases where radiographs fail to provide a conclusive diagnosis necessitate further evaluation using CT scans (Wells *et al.*, 2008).

2.2.2. Coronoid Process Fracture Classification

Coronoid process fractures are classified using different systems that rely on distinct identifying variables. The two most commonly used classifications are the Regan and Morrey, and the O'Driscoll classification systems (Doornberg *et al.*, 2006; Ring, 2006). An alternative approach involves categorising coronoid process fractures based on the determined treatment program (Ring, 2006).

2.2.2.1. Regan and Morrey Classification

The Regan and Morrey classification system provides a framework for categorising coronoid process fractures using the anterior-to-posterior size of the fracture fragment as the identifying variable (Ring, 2006). This works in conjunction with a modifier that differentiates absence (Type A) or presence (Type B) of dislocation of the elbow joint (Ring, 2006). According to Regan and Morrey, Type 1 includes an avulsion fracture to the tip of the process, while a Type 2 fractures encompass a fragment (single or comminuted) that affects less than 50% of the process (Figure 5)(Doornberg *et al.*, 2006; Ring, 2006). The key distinguishing factor between Type 1 and Type 2 fractures is the involvement of the capsular insertion, which typically attaches approximately 5mm distal to the coronoid tip (Doornberg *et al.*, 2006). Type 3 Reagan and Morrey fractures involve fragments (single or comminuted) that encompass more than 50% of the coronoid process (Figure 5)(Doornberg *et al.*, 2006; Ring, 2006).

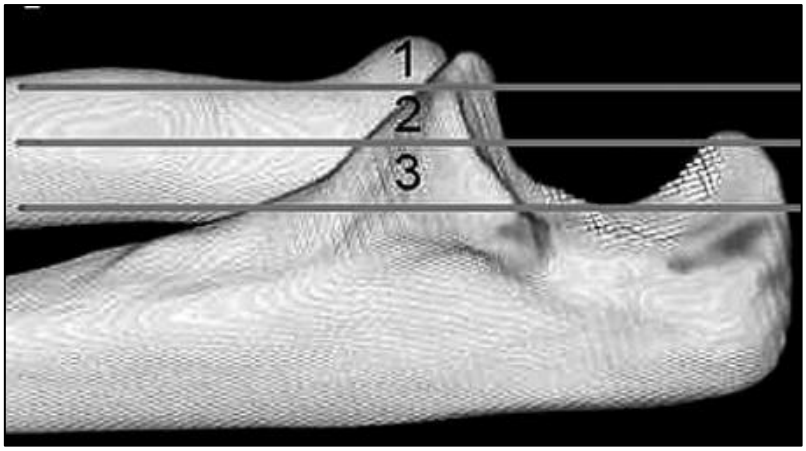

Figure 5: Regan and Morrey classification of coronoid process fractures with the Type 1, Type 2 and Type 3 fractures labelled accordingly (Adapted from (Doornberg et al., 2006)).

2.2.2.2. O' Driscoll Classification

The O'Driscoll classification system uses the anatomic location and the morphology of the fracture as the identifying variables (Ring, 2006; Chan, Faber *et al.*, 2016). The O'Driscoll system also takes the mechanism of injury, and the associated fractures and soft tissue injuries into account when assigning a classification (Ring, 2006). The inclusion of these injury characteristics provides a starting point for the dictation of treatment (Ring, 2006; Chan *et al.*, 2016). The O'Driscoll classification system makes use of 3 main categories with subdivisions based on the severity of the involvement of the coronoid process (Ring, 2006).

An O'Driscoll Type 1 fracture includes a transverse fracture of the tip of the process (Chan *et al.*, 2016; Feng *et al.*, 2018). The Type 1 fractures typically do not extend medially past the sublime tubercle or into the body of the process (Ring, 2006). Type 1 Subtype 1 involves fragments less than 2mm, and Subtype 2 involves more than 2mm (Figure 6)(Ring, 2006). In addition, the Subtype 2 fragments often contain the insertion point of the anterior capsule (Figure 6)(Ring, 2006).

Type 2 O'Driscoll coronoid fractures involve the anteromedial aspect and facet (Ring, 2006; Chan *et al.*, 2016; Feng *et al.*, 2018). Figure 6 shows that Type 2 Subtype 1 fractures include the area between the medial to the tip of the coronoid and the anterior half of the sublime tubercle (Ring, 2006). Subtype 2 fractures extend from the medial half of the sublime tubercle to the tip of the process (Ring, 2006; Chan *et al.*, 2016). Anteromedial fracture Subtype 3 involves the rim of the process and the entire sublime tubercle (with or without the involvement of the tip of the process) (Figure 6)(Ring, 2006; Chan *et al.*, 2016). O'Driscoll Type 2 Subtypes 1 and 2 are generally associated with concomitant injuries to the radial and the medial collateral ligament (MCL) (Ring, 2006; Chan *et al.*, 2016).

Type 3 or the basal fractures involve 50% or more of the coronoid process height (Ring, 2006). The third type includes two subtypes (Ring, 2006). Subtype 1 is limited to the tip of the coronoid; whereas, Subtype 2 involves associated fractures of the olecranon (Ring, 2006). O'Driscoll Type 3.2 have a lower involvement of the soft-tissue disruption than Type 3.1 (Ring, 2006).

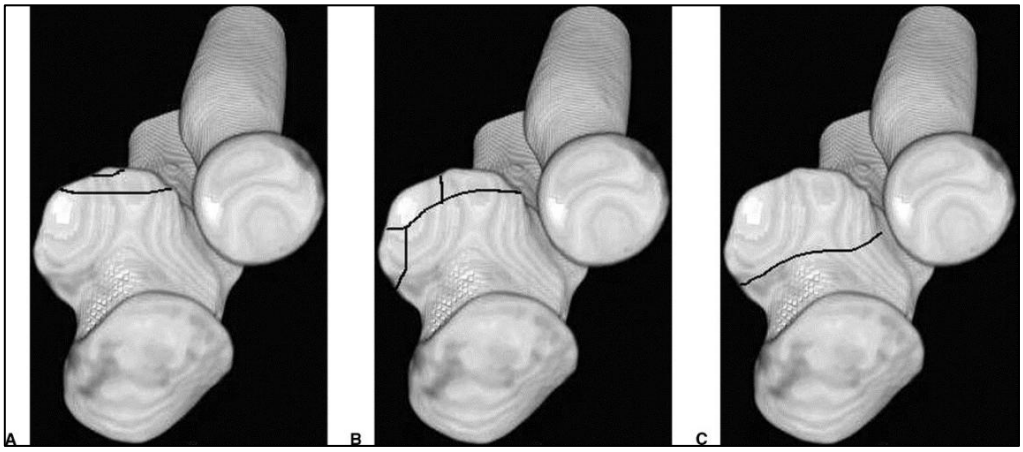

Figure 6: O'Driscoll classification system for coronoid process fractures. (A) Type 1 fracture of the tip. (B) Type 2 and the type 2 subtype fractures of the anteromedial facet. (C) Type 3 basal fracture of the coronoid process (6).

2.2.2.3. Alternative Coronoid Fracture Classification Systems

Another method of classifying coronoid process fractures is through the type of treatment (Ring, 2006). The system of classification takes into account the types of fracture, the mechanism of injury, and the determined method of treatment and surgical exposure of the coronoid (Ring, 2006). Using this system, coronoid fractures are classified as: transverse fractures, small anterior facet fractures, large anteromedial facet fractures, basilar fractures (that can be securely repaired), and complex or osteoporotic basilar fractures (Ring, 2006).

Adams, Sanchez-Sotelo *et al.* (2012) suggest an adapted alternative to the O'Driscoll system based on the anatomical location and morphology of the fragment. A Type 1 fracture involves the tip of the coronoid, thus following the convention Type 1 fracture defined by the Regan and Morrey, and O'Driscoll systems (Adams *et al.*, 2012). A Type 2 fracture is at the mid-transverse line, and a Type 3 is a basal fracture (Adams *et al.*, 2012). Type 4 and Type 5 are oblique fractures on the anteromedial or anterolateral sides, respectively (Adams *et al.*, 2012).

2.2.2.4. Usability of the Coronoid Fracture Classification Systems

A key issue in orthopaedics is that the usefulness of classification systems is dependent of the context of their use; as well as their accuracy and reliability being influenced by the available imaging modalities, observer experience, and anatomical visibility. The Regan and Morrey classification relies on lateral radiographs, which can sometimes obscure the true extent of the fracture, especially in

complex or comminuted fractures (Doornberg *et al.*, 2006; Ring, 2006). In contrast, O'Driscoll's classification, developed from CT imaging, allows for a more detailed view of fracture morphology, particularly in relation to the anteromedial facet and its contribution to joint stability (O'Driscoll, Jupiter *et al.*, 2003; Ring, 2006).

Despite these improvements, classification systems for coronoid fractures remain limited in their clinical application, as they often fail to capture the full complexity of associated soft tissue injuries or dynamic stability (Ring, 2006). Several authors have argued that while these systems offer useful frameworks for communication and academic discussion, their predictive value for treatment planning and outcomes remains modest (van Riet and Morrey, 2008).

2.2.3. Fracture and Heat Mapping

Fracture mapping is a widely explored area of orthopaedic research, with numerous studies dedicated to the classification and categorisation of fractures across the various bones of the body. The primary focus of such research is to establish the relationship between injury patterns and specific fracture types; as well as to assess the potential for complications arising pre- or post-surgical intervention. Moreover, fracture mapping is instrumental in visualising the areas of fracture propagation and the potential exit zones (Dey, 2023). This research highlights the usefulness of fracture mapping as a tool in determining the operative treatment plan and injury management. These maps guide the surgical exposure and fixation devices needed, and indicate any possible associated ligamentous injury (Mellema *et al.*, 2014).

Mapping of coronoid process fractures follows suit with the aim of identifying fracture-dislocation patterns associated with specific mechanisms of injury, building upon the foundation established by the Regan and Morrey, and O'Driscoll classification systems (Doornberg *et al.*, 2006; Mellema *et al.*, 2014). The classification systems, which are widely accepted in Orthopaedics, are instrumental in the understanding of their presence in relation to specific injury patterns, or the dislocation and subsequent instability of the elbow joint (Doornberg *et al.*, 2006; Mellema *et al.*, 2014; Ring, 2006). Traditionally, the mapping of coronoid fractures relies on 2D lateral radiographic images, but advancements in imaging technology and the increased access to and usage of axial imaging, particularly the use of CT scans, is enhancing the understanding of coronoid injuries (Adams *et al.*, 2012). The widespread adoption of CT scans as a pre-operative diagnostic tool enables the analysis of the more subtle fracture patterns, thus revealing the inadequacies of the plain film imaging-based classification systems (Adams *et al.*, 2012).

The implementation of quantitative 3D computer tomography (Q3DCT) techniques has led to a further refinement in the understanding of fracture morphology, and can aid in the accurate estimation of

articular surface involvement and degree of comminution (Janssen, ter Meulen *et al.*, 2015). Despite these advancements, a notable research gap remains, as most studies focus on the morphological characteristics of the fracture pattern rather than the resultant fragment morphology. Understanding the morphology of the fracture fragments may help to better inform Orthopaedic surgeons on the viability of different surgical treatment options and allow for the improved development of fixation devices.

Conventionally, fracture maps for the coronoid process are shown from the superior view (Figure 7), which for the purpose of this study has been defined as the view looking down at the ulna's articular surface from the perspective of the tip of the olecranon process. While this is a well-developed fracture visualisation tool, the limitation remains in the 2D nature of the image (Figure 7). Thus it makes it difficult to ascertain the exact location of the fracture site on different surfaces of the bone and the overall shape of the fragments (Dey, 2023).

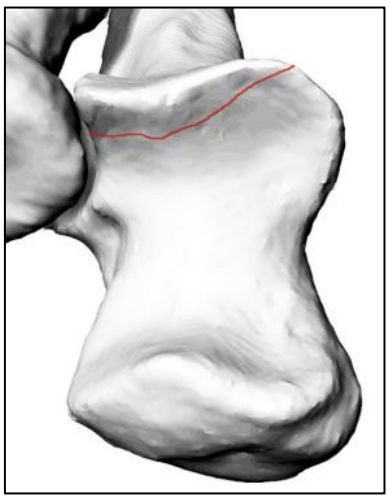

Figure 7: An example of a single fracture line shown on the superior view of the ulna articular surface (Mellema et al., 2014).

Heat mapping is an additional form of mapping that is effective in understanding fractures. Heat mapping is used to define the location, frequency, distribution and pattern of fractures through the use of colour to graphically depict the intensity of the fracture lines across the surfaces of the bone (Figure 8) (Mellema *et al.*, 2014). Additionally, the heat maps provide visual clues to weaker areas in the bone structure, and the critical regions of the bones in which the fracture is most likely to occur (Dey, 2023). Heat maps are a more helpful indicator in the design and development of orthopaedic fracture fixation devices (Dey, 2023). Although the use of this visual tool has been well established, the same issue arises as in the fracture maps, which are only shown from a superior perspective (Figure 8).

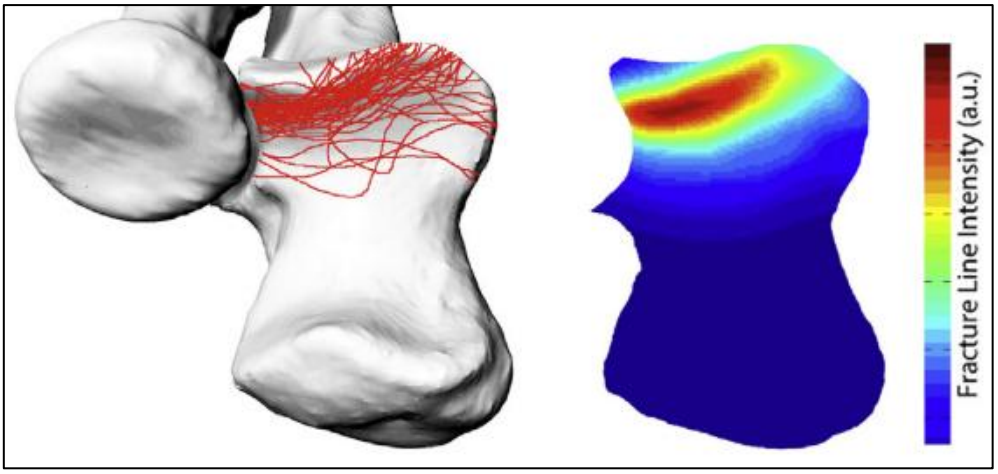

Figure 8: Fracture map (left) and resultant heat map (right) depicting a Terrible Triad fracture-dislocation pattern (Mellema et al., 2014).

2.2.4. Key Findings in Literature

1) **Incidence and Significance of Coronoid Fractures:** Coronoid fractures represent 10-15% of elbow fractures and play a crucial role in the causes of elbow instability (Lowery *et al.*, 2022).
2) **Common Mechanisms and Associated Injuries:** The most common mechanisms of injury are falls on an outstretched hand (FOOSH), high-energy impacts from motor vehicle accidents, high-contact sports, and direct trauma (Adams, 2020). These injuries often present in complex patterns and are frequently associated with joint dislocations and soft tissue injuries, exemplified by the Terrible Triad.
3) **Classification Systems:** Coronoid fractures are classified using various systems, with the Regan and Morrey, and the O'Driscoll classifications being the most widely used. Each system categorises fractures based on different criteria, such as fragment size and anatomic location, providing a framework for understanding fracture severity and guiding treatment planning.
4) **Advancements in Imaging and Fracture Mapping:** The implementation of advanced imaging technologies, particularly CT scans and Q3DCT techniques, have improved the understanding of coronoid fractures (Mellema *et al.*, 2014). These techniques offer detailed insights into fracture patterns, surpassing the limitations of traditional 2D radiographic images. However, these images are still limited to 2D planes and have not yet been used in an understanding of the fracture fragment morphology.
5) **Use of Fracture and Heat Maps:** Fracture and heat mapping techniques are valuable for visualising fracture propagation, identifying critical weak points, and informing surgical treatment plans (Dey, 2023). These maps provide essential data on fracture patterns, improving pre-operative planning and patient outcomes, and aiding in the development of more effective fixation devices.

2.2.5. Chapter Problem Identification and Research Question

Numerous studies explore the characteristics of coronoid fractures and their mechanisms of injuries, however, there remains a gap in understanding the morphology of the fracture fragment. In addition, while work has been done on mapping and categorisation of coronoid fractures on a single 2-dimensional plane, understanding of their 3-dimensional morphology can be improved. The limitation of the 2D maps is the difficulty in ascertaining the location of the fracture site beyond the superior viewpoint, and the overall shape of the fractured bone fragments. In order to address these limitations, the following research question is posed.

2.2.5.1. Research Question

"Can the analysis of 3D fracture and heat maps provide a better understanding of the morphology of O'Driscoll classified coronoid process fracture fragments?"

An additional question related to the use of the critical fracture patterns for the design of an adapted Endobutton can be inferred. This question is: "*Can the critical fracture patterns of the different coronoid fracture types provide the necessary understanding of the fragment morphology to inform the design of an adapted Endobutton fixation device?"*.

2.3. Chapter Aims and Objectives

Aim

The aim of this chapter is to establish a set of reference fracture and heat maps depicting the coronoid fracture patterns in multiple dimensions, to help determine the design of the adapted Endobutton device.

Objectives:

To achieve this aim, this chapter will address the following objectives:

1) Establish a reference base of O'Driscoll classified coronoid process fractures using Computer Tomography (CT) scans.
2) Produce fracture maps from the reduced coronoid fractures.
3) Produce heat maps based on the generated fracture maps.
4) Establish the critical fracture pattern of coronoid process fractures.

2.4. Materials and Methods

This chapter follows established Q3DCT (Quantitative 3D Computer Tomography), *in-silico* reduction, fracture mapping, and heat mapping methods. Q3DCT processing is widely used throughout literature and is a valuable tool in understanding fracture morphology (Janssen *et al.*, 2015). Q3DCT was the

foundation for the creation of the fracture and heat maps, which provided critical clues into the weak points of the bone structure (Dey, 2023). This process is simplified and shown in Figure 9.

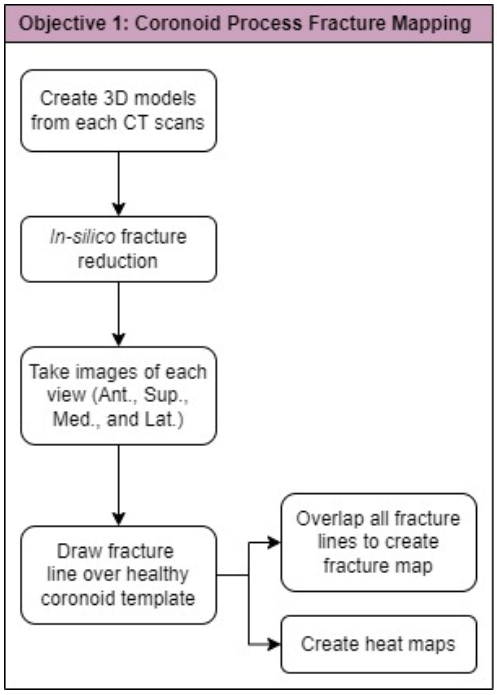

Figure 9: Simplified version of methodology followed during the fracture mapping process.

2.4.1. Patient Cohort

A retrospective study was conducted using radiographic data from the Picture Archiving and Communication System (PACS) within the Department of Orthopaedic Surgery at Groote Schuur Hospital, Cape Town. Access to the data was approved by the University of Cape Town Human Research Ethics Committee (HREC) (HREC number: 588/2022). All patients from the database who presented an elbow fracture with coronoid process fractures were included in the study. Each set of radiographic data was in the DICOM (Digital Imaging and Communications in Medicine) format. The patient cohort included in this study received treatment for the fractures at either Groote Schuur Hospital, Mitchells Plain Hospital, or the Victoria Hospital between August 2012 and September 2022. A total of 63 sets of radiographic data were collected, involving 42 male and 16 female patients, with an average age of 38.8 years (range: 14 to 78 years).

2.4.1.1. Exclusion Criteria

Each of the initial 63 sets of radiographic data were evaluated against predetermined exclusion criteria. Of these, 10 were excluded from the study due to poor scan quality, while an additional 5 sets were omitted due to incomplete or missing essential files (Figure 10). In 6 cases, the 3D models showed that

the fracture fragments were too small and were excluded (Figure 10). A further 4 scans were excluded from the study as their 3D models revealed the presence of additional compromising fractures to the proximal head of the ulna. These fractures would impact the surgical treatment of the coronoid fracture. Lastly, 5 scans were excluded for various reasons (Figure 10), such as the presence of scatter artefacts in the scans, difficulties in discerning the fracture, and the fracture being obscured due to the significant displacement of the distal head of the humerus. It is worth noting that numerous scans met more than one of these exclusion criteria.

After the evaluation of the initial scans, a total of 33 sets of radiographic data were included this study.

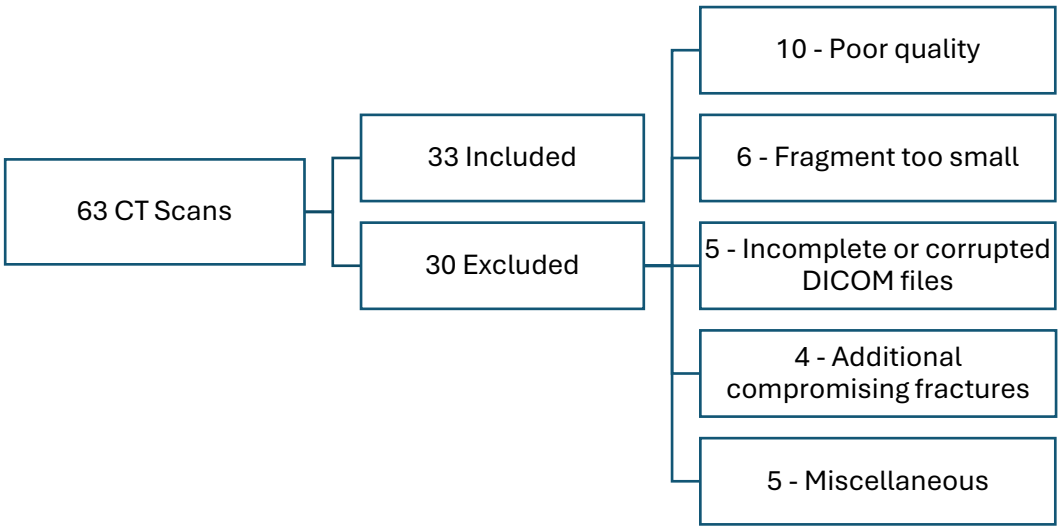

Figure 10: Exclusion criteria used to evaluate the CT scans.

2.4.2. Data Collection

During the fracture mapping phase of the study, all the relevant data was consolidated in a Microsoft Excel spreadsheet (Appendix B – Fracture Mapping Data Collection Sheet). This document encompasses the general information for each of the scans used. This general information includes the scan file name, the side of injury, patient age and sex, the presence of comminution, the additional fractures present, and whether the elbow joint was dislocated. The demographical information of the selected patients is separated, and the details of each patient's fracture. The scan information is also included in the data collection as a point of potential interest and has no influence on the study. This Excel document also contains images for each view of the reduced fracture, the merged state, and the resultant fracture pattern. For further reference, the completed data collection sheet is available in the appendices (Appendix B – Fracture Mapping Data Collection Sheet).

No data pertaining to the mechanisms of injury was collected for this study, as the aim is to establish reference set of fractures and determine critical fracture patterns.

2.4.3. Fracture Mapping

2.4.3.1. Importing and Editing the DICOM File

The raw DICOM CT scan files were processed using the Mimics 16.0 (Materialise, Leuven, Belgium) software. Once imported into the software, the raw CT scan images were converted to an editable Mimics Document. A digital mask was applied to the CT scan by identifying voxels above the pre-defined bone threshold value of 226 Hounsfield Units (HU); thus, creating the original mask of the structures present in the CT scan. This mask was edited and used to render a 3D model of the bones constituting the elbow joint (distal humerus, and proximal radius and ulna) (Figure 11).

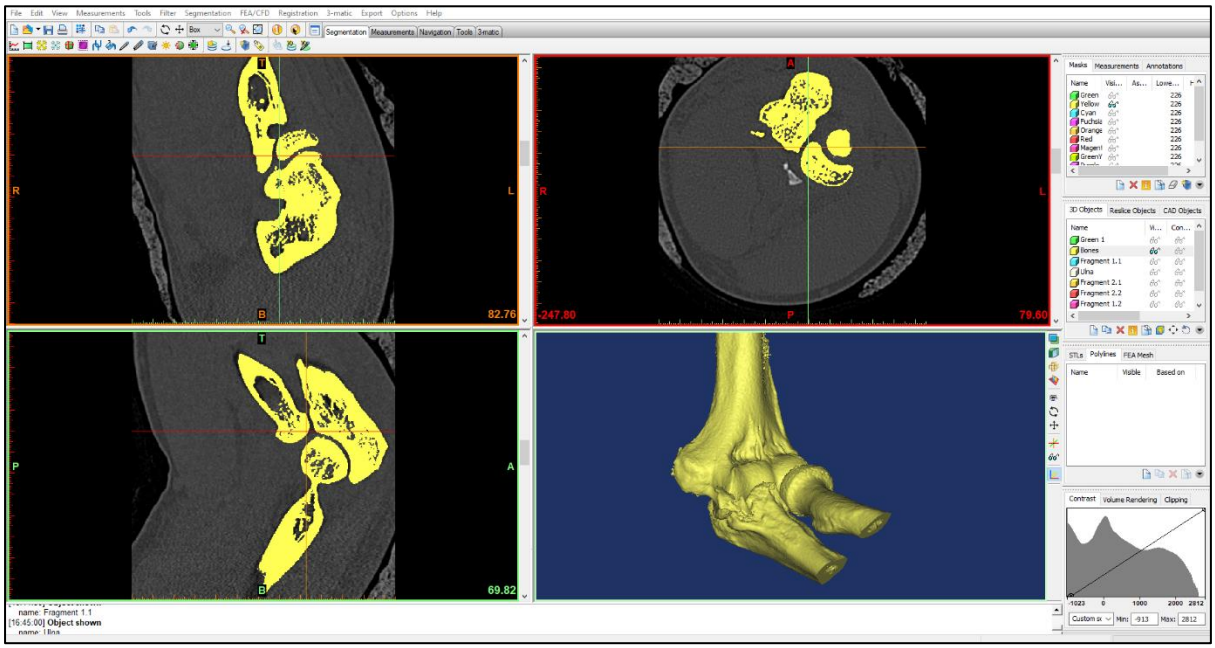

Figure 11: Initial digital mask showing the different orientations and 3D rendered model of the fractured elbow. 3D rendered model (bottom right corner) is shown in the reconstruction platform of Materialise Mimics®

This initial 3D model was used to evaluate the state of the coronoid fracture and determine specified factors related to the scan. These factors included: identifying the fracture side (right or left elbow), determining the presence of additional fractures, assessing the elbow joint dislocation, and evaluating the comminution state of the coronoid fracture. Simultaneously, the initial 3D model was subjected to an exclusion criteria evaluation in which the quality of the scan, the fragment size and the presence of compromising fractures were considered. Once all of these factors had been assessed, the fractures included in the study were classified using the O'Driscoll system. The type and subtype (described in the Coronoid Process Fracture Classification) were noted for use at a later stage of the study.

The primary (initial) 3D model of the scans included in the study were subsequently duplicated and the secondary models were edited. The fractured ulna was isolated from the coronoid fragments and the other bones comprising the joint. Using the initial 3D model of the entire joint, each coronoid process fracture fragment was observed, identified, and noted. The process used to separate the ulna was repeated for each individual coronoid fracture fragment. Separate digital masks were created for the ulna and each individual fragment. The individual masks for the ulna and each fragment were designated a name (i.e.: Ulna or Fragment 1) (Figure 12). All fracture fragments were labelled according to their decreasing size.

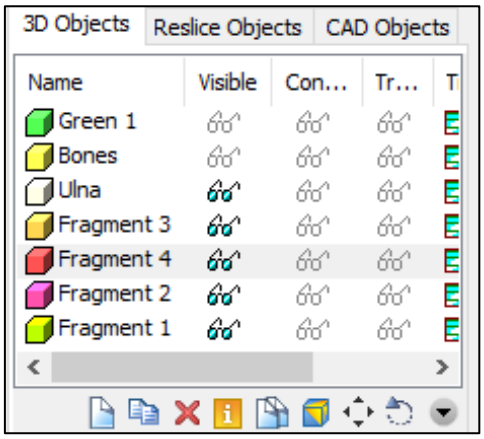

Figure 12: Close up of the labelling system used for the individual digital masks and their associated 3D models.

In instances where a distinct line of separation between the fragments or the fragments and the parent bone (ulna) was lacking, an interpreted line of separation was established based on a comprehensive analysis of the 3D structure, morphometry of the fragments, and their anatomical context. Knowledge of anatomy and an understanding of normal bone morphology was applied to ensure accurate fragment separation.

After successfully creating individual masks for the ulna and each fragment, discrete 3D models were generated from each of these masks (Figure 13). To ensure the accuracy of the editing process, the individual masks were compared to the original (primary) 3D model of the CT scan. Once the presence of all the fragments and all the required pieces of the fracture were confirmed, the 3D models were exported as Stereolithography/Standard Triangle Language (STL) files. These files were named according to their patient number and the labels assigned during the editing process (e.g., Patient 1_Fragment 1.stl), and subsequently saved in their designated parent patient folder.

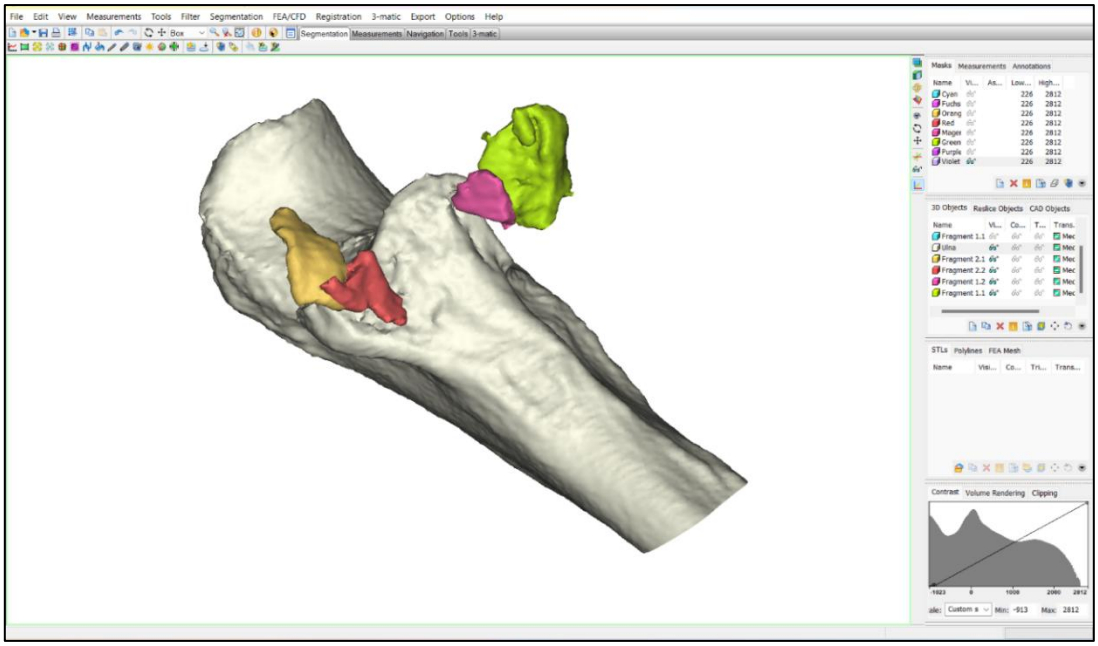

Figure 13: Mimics 16.0 (Materialise, Leuven, Belgium) 3D model of the edited and separated bones and fragments.

2.4.3.2. In-*Silico* Reduction of The Coronoid Fractures

The STL files were imported into the Materialise 3-Matic 8.0 (Leuven, Belgium) software. All imported STL parts maintained their dimensions (in mm) from the DICOM files obtained from the PACS. The resulting 3-Matic document was saved within the corresponding patient parent folder and was labelled with the respective patient number.

Each 3D model within the 3-Matic document was duplicated to maintain a reference of the original state, and location of the fracture. To prevent any unintentional alterations to the original models, they were hidden from view. The duplicated ulna model was colour-coded to mimic normal bone, while the fracture fragments were coloured with varying colours to distinguish the fragments from the parent bone and from each other. The largest of the fragments was identified, and the remaining fragments (if any) were hidden, leaving only the ulna and the largest fragment visible.

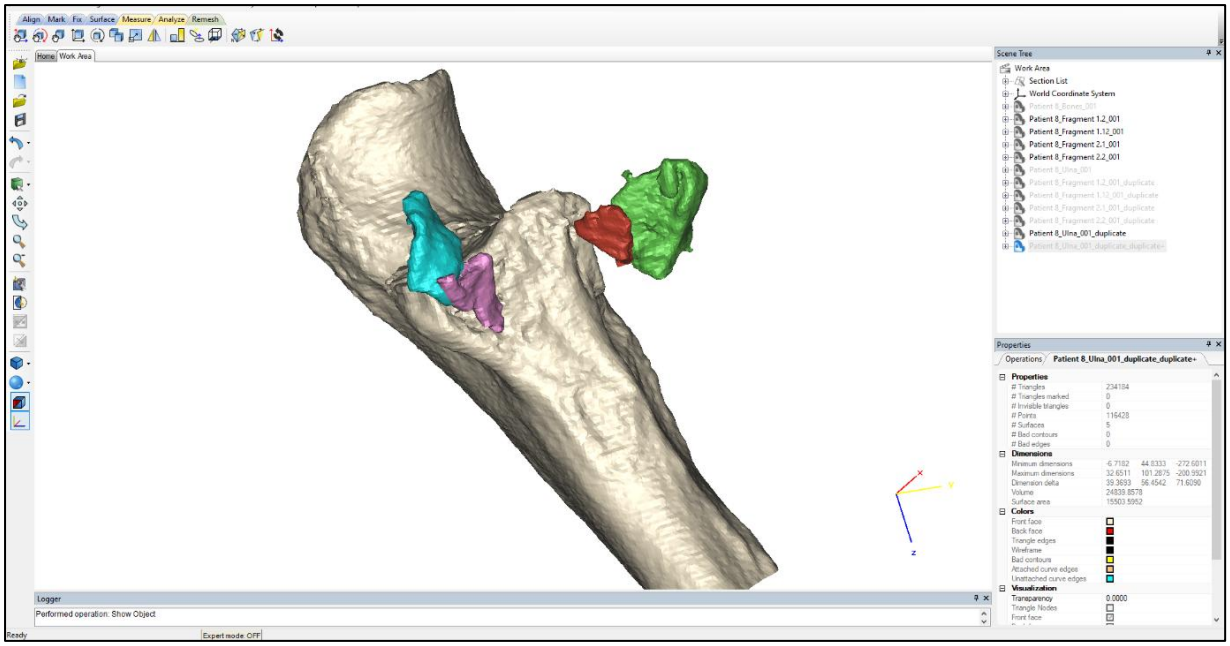

Figure 14: Fragmented (original) fracture state of the coronoid.

The fractured ulna served as the stationary point during the alignment process. Using the “Interactive Translate” and “Interactive Rotate” tools, the largest fragment was moved, rotated, and aligned to the ulna fracture site. The “Transparency” function was used to fine tune the placement of the fragment, ensuring that the fragment was correctly positioned without being virtually pushed through the ulna and creating a false impression of successful fracture reduction. This alignment process was iteratively applied to the smaller fragments, aligning them in decreasing size order (Figure 15). Alternatively, if specific placement for a fragment was clear, it was prioritized and aligned accordingly.

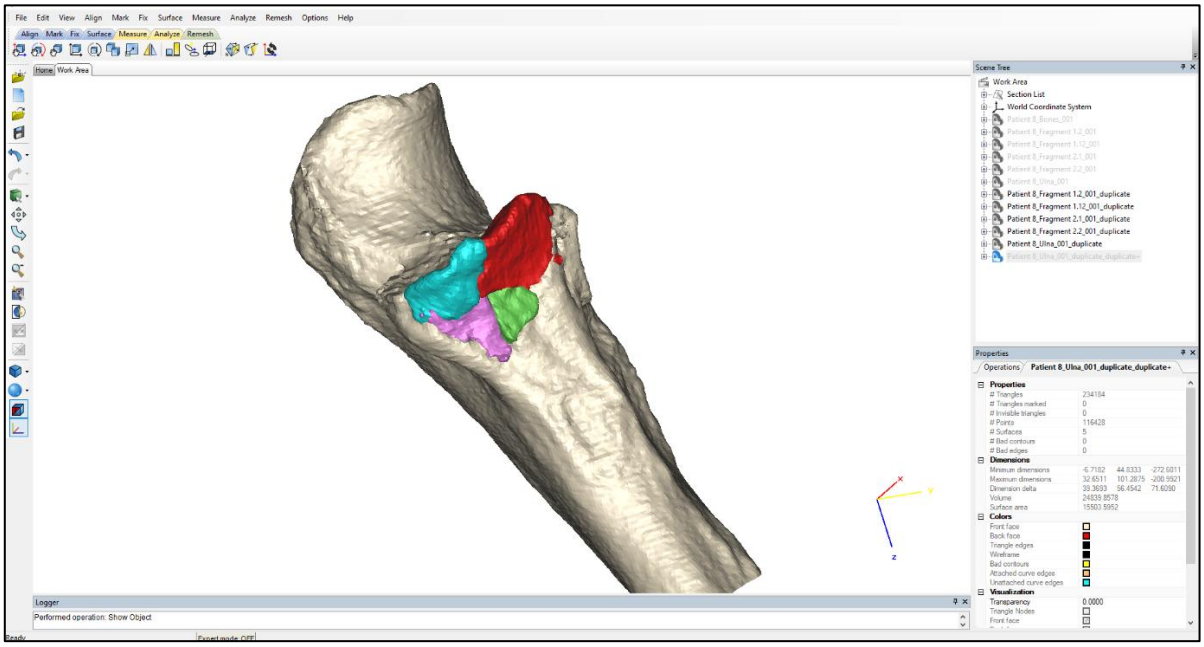

Figure 15: Fracture with reduced fracture fragments.

Once all fragments were successfully aligned, creating a restored representation of the normal anatomy of the ulna's coronoid process, the secondary models (duplicated and reduced) were duplicated once more and merged into a single model (Figure 16). This merged model was colour-coded to resemble bone. The use of multiple duplicates ensured the preservation of the original state, the reduced state, and the merged state for each of the patient's fracture reductions.

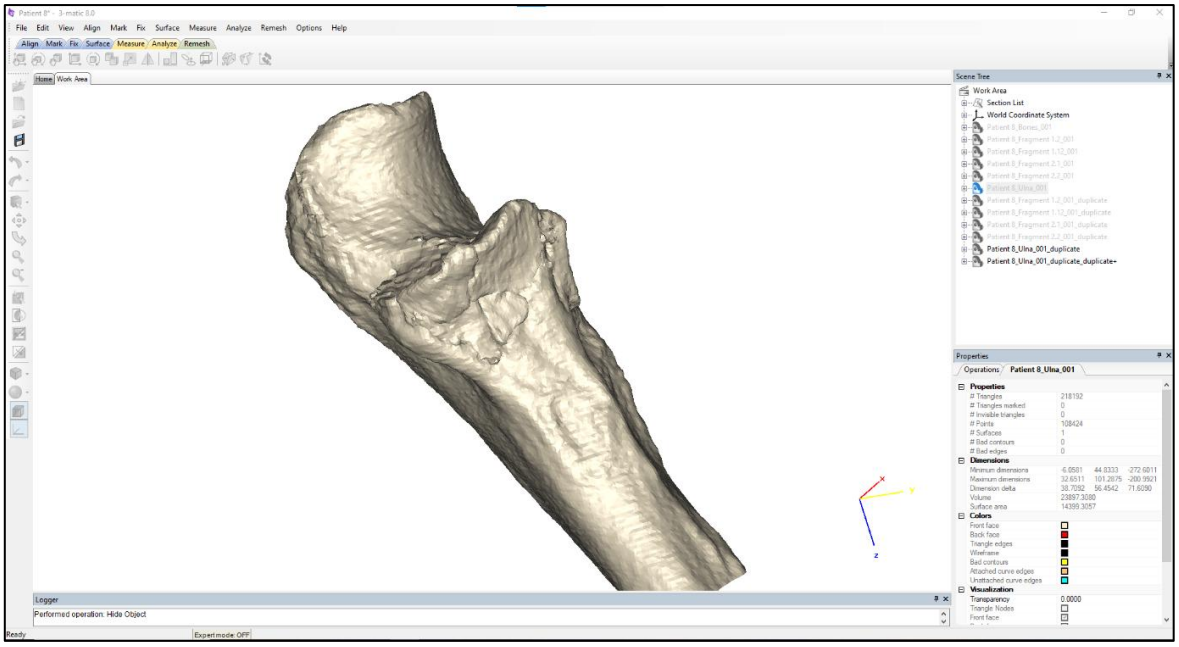

Figure 16: Merged state of the fractured coronoid.

With the reduced and merged states established, the merged model was hidden, and the reduced state was orientated to display the superior, anterior, lateral, and medial views of the bone. For the purposes of this study, the anterior view is defined as a frontal view of the ulna in which the coronoid can be viewed from the radial notch to the sublime tubercle. The superior view is defined as the view looking down on the ulna from the perspective of the tip of the olecranon process. The lateral and medial views follow the conventions of 2D radiographic images, with the radial notch being present in the lateral view, and the sublime tubercle being present in the medial view.

The Windows "Snipping Tool" is utilised to capture images of each orientation. This process was repeated for the merged model, and the images were saved in the patient folder with the labels stating the patient number, view, and an indication of whether the images pertained to the reduced or the merged model (E.g., P1 Anterior (M)).

2.4.3.3. Fracture Mapping and Overlapping of the Fracture Pattern

To create the fracture maps, a healthy coronoid model was used for the template. The images of each reduced fracture were imported as individual layers into the GNU Image Manipulation Program (GIMP) 2.10.32 (GIMP Development Team – Open Source) Image editing software.

Each individual fracture image was superimposed as a layer over the image of the healthy coronoid template. Crucial points on the healthy and the fractured bones were identified and aligned. During the alignment process, the imported layered image underwent adjustments, including scaling, rotation, and flipping if needed (for instance, when the image represented the right ulna while the healthy template depicted a left ulna). Once the image of the reduction and the healthy template were aligned, a blank layer was added on top of the reduced fracture image, and the healthy template was hidden. Within this blank layer, the pencil tool (equipped with a pixel brush at a size of 1.75) was utilised to trace a red line along the outline of the coloured fracture fragment. After outlining each fragment, the underlying layer showing the reduced fracture was hidden, and the healthy template image was made visible. Ultimately, leaving the outline layer superimposed over the healthy coronoid image. The eraser tool was used to remove any lines which went beyond the bounds of the healthy template.

This process was reiterated for each patient and each orientation (anterior, lateral, medial, and superior). 33 layers depicting the traced fracture patterns of each patient were superimposed over the healthy template, producing the fracture map. The anterior, lateral, medial, and superior fracture maps were saved using their corresponding names.

2.4.3.4. Fracture Subtypes

Using the classifications of the fractures provided during the initial phases of the data collection, the fracture maps were separated by fracture Type and subtype. The corresponding patient fracture lines (created for production of the overall fracture maps) were separated and layered over the healthy template, producing the subtype specific fracture maps. Each resultant subtype fracture map was saved into individual files.

2.4.4. Heat Mapping

To add further dimension to the fracture maps, heat maps were created to graphically represent the intensity of the fracture lines as colours. The initial steps involved drawing the boundary line for each view of the healthy coronoid templates. All the fracture lines from each patient for every view were saved individually without being layered over the template. Both the boundary and the fracture line images were saved with consistent dimensions, using their corresponding patient numbers, and organized into the view-specific folders (superior, anterior, lateral, or medial).

The PyCharm Community Edition 2022.3.3 (JetBrains, Prague, Czechia) program was used to execute a Python code acquired from prior studies conducted within the department (Appendix D – Heat Mapping Code). The images of the boundary line and the individual fracture lines were imported into the program. Within the code, the dimensions of the boundary and fracture line images were edited

accordingly. Each fracture line image was converted into digitised XY coordinates, and the resultant data was saved as a .csv file, within the view-specified folder. Once all data sets were imported and saved within the folder, the code merged the data and generated a density plot of the collected points.

The resultant heat map is an alternate version of the distribution of the fracture patterns with the red areas showing where there are frequent fracture zones (areas of highest fracture line intensity) (Figure 17). The changes in colour frequency helped determine the critical fracture patterns.

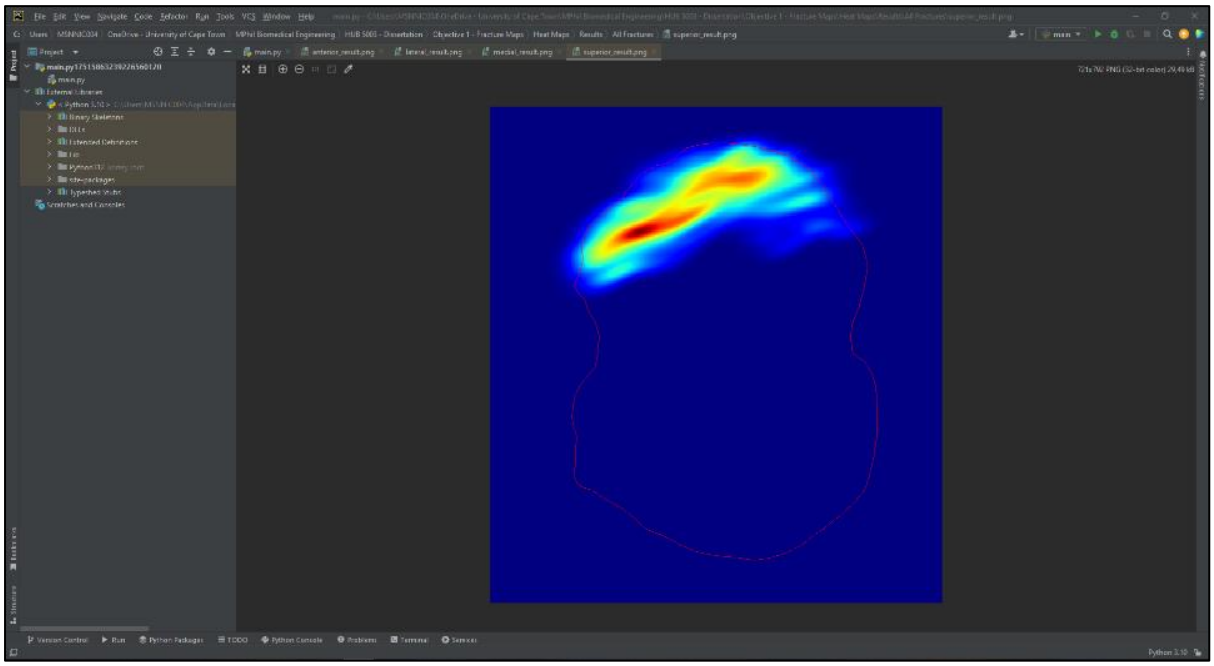

Figure 17: A resultant superior view heatmap showing the density of all 33 patients' fracture lines overlaid over the healthy template boundary line.

After generating the heat maps, they were saved as .png files in their respective view folders. Following this, the images were imported into GIMP 2.10.32 program for further editing and refinement. The editing process produced the final version of the heat map, displaying only the fracture density data within the view-specified boundary. The edited map was placed on a white background to emphasize the colour fracture line density distribution (Figure 18).

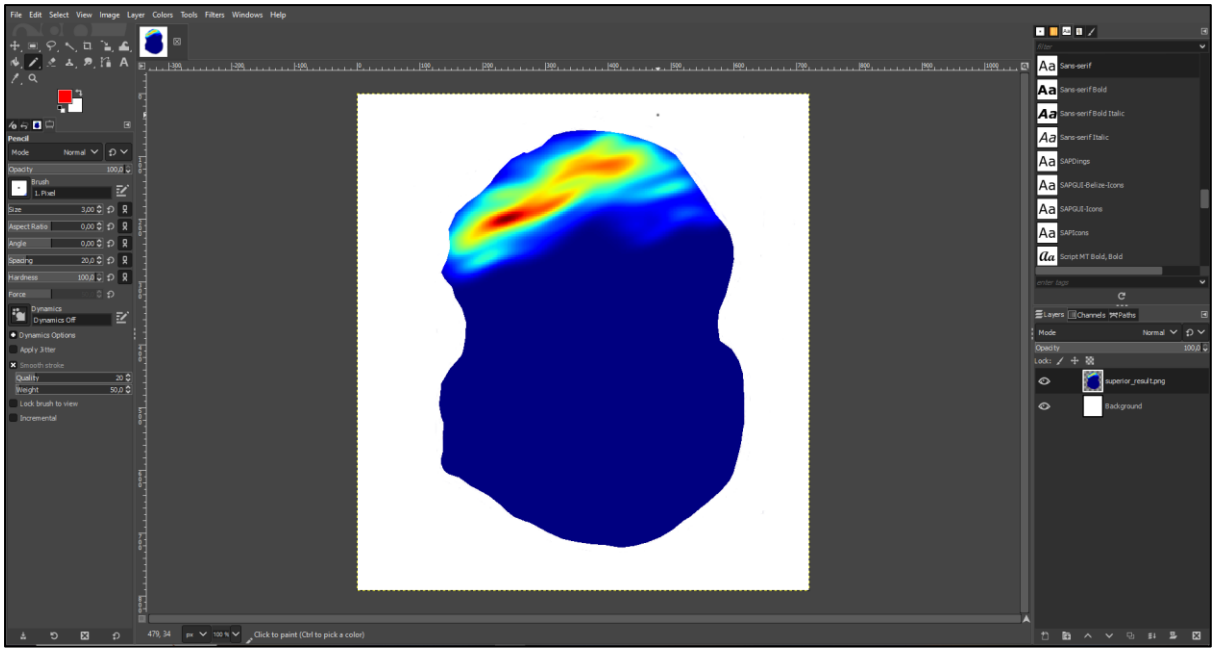

Figure 18: Superior view resultant heat map after undergoing editing in GIMP 2.10.32 (GIMP Development Team – Open Source).

2.5. Results

2.5.1. Patient Cohort Demographic Data

Of the included 33 unilateral scans, 25 were from male patients (n=25), and 8 from female patients (n=8); 21 were scans of the left elbow joint (n=21) and 12 were of the right elbow joint (n=12). Patients' age ranged between 14 to 78 years of age, averaging an age of 38.61 (SD $\pm$ 13.71) (Table 1).

Table 1: Selected Patient Cohort Demographic Information

Characteristic	Value (%)
Age, mean ± SD	38.61 $\pm$ 13.71
Sex, n (%)	
Male	25 (75.8)
Female	8 (24.2)
Side of Injury, n (%)	
Left	21 (63.6)
Right	12 (36.4)

*SD, standard deviation.

2.5.2. Patient Cohort Scan Data

Of the 33 scans used, 11 (33.3%) were of single fragment fractures, and the remaining 22 were of comminuted fractures. Overall, 23 (69.7%) of the chosen scans showed evidence of

additional/accompanying fractures present in and around the elbow joint (Table 2). 24.2% (n=8) of the selected scans also showed signs of potential or total elbow joint dislocation.

Table 2: Fracture Characteristics

Fracture Characteristic	Frequency, n (%)
Comminution	22 (66.7)
Additional Fractures Present	23 (69.7)
Dislocation	8 (24.2)

Amongst the scans, the comminution, the presence of additional fractures, and the dislocations of the joint often occurred simultaneously. The combination of a comminuted fracture, additional fractures, and the dislocation of the joint (all indicative of the terrible triad) was found in 4 of the 33 scans (12.1%) (Table 3). Other combinations of the comminution and additional fractures (no dislocation) made up 42.4% (n=14), and the combinations of comminuted fractures and dislocation, and dislocation and additional fractures made up 15.2% (n=5) and 18.2% (n=6) respectively (Table 3).

Table 3: Additional characteristic frequencies

Fracture Characteristic	Frequency, n (%)
Comminution + Additional Fractures	14 (42.4)
Comminution + Dislocation	5 (15.2)
Dislocation + Additional Fractures	6 (18.2)
Comminution + Additional Fractures + Dislocation	4 (12.1)

2.5.3. Fracture Classification and Subtypes

According to the O'Driscoll classification system, 12 of the 33 scans were Type 1 fractures (1 Subtypes 1 and 11 Subtype 2). The remaining 21 were of Type 2 fractures (involving different subtypes), and there were no Type 3 basal fractures present in this study (Table 4).

Table 4: Fracture type and subtype description and frequency

Type	Fracture Site Description	Frequency, n (%)
Type 1 Subtype 1	Tip (involves <2mm of tip)	1 (3.0)
Type 1 Subtype 2	Tip (involves >2mm of tip)	11 (33.3)
Type 2 Subtype 1	Medial to the tip to anterior half of sublime tubercle	0 (0)
Type 2 Subtype 2	Tip to medial half of sublime tubercle	15 (45.5)
Type 2 Subtype 3	Anteromedial rim and the entire sublime tubercle	6 (18.2)

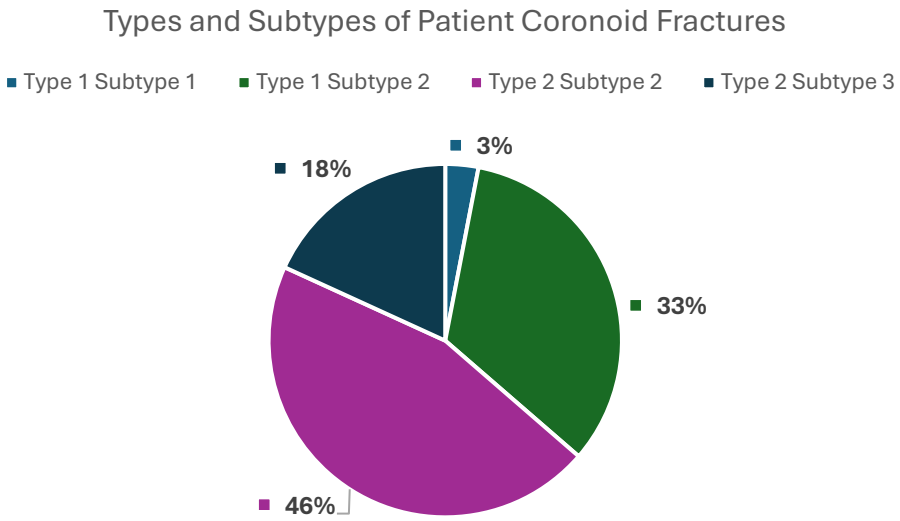

Figure 19: Distribution of proportions of coronoid fracture Types and Subtypes present in this study.

2.5.4. All Patient Fractures (n=33)

All 33 patient fracture lines were included in the anterior view (Figure 20A). For the superior view, only 32 patients had fracture lines which were included in the final fracture map (Figure 20B). The missing fracture line was due to a significant variation in the shape of the patient's ulna. This resulted in the fracture line falling outside the boundary of the healthy coronoid template after the reduced fracture was scaled and overlaid. In the lateral view of the ulna only 32 of the 33 fracture lines were included on the final fracture map (Figure 21B). This was due to the 33rd fracture being located on the medial aspect of the coronoid, and when viewed laterally, could not be seen. Lastly, for the medial view, all 33 fracture lines were present (Figure 21A).

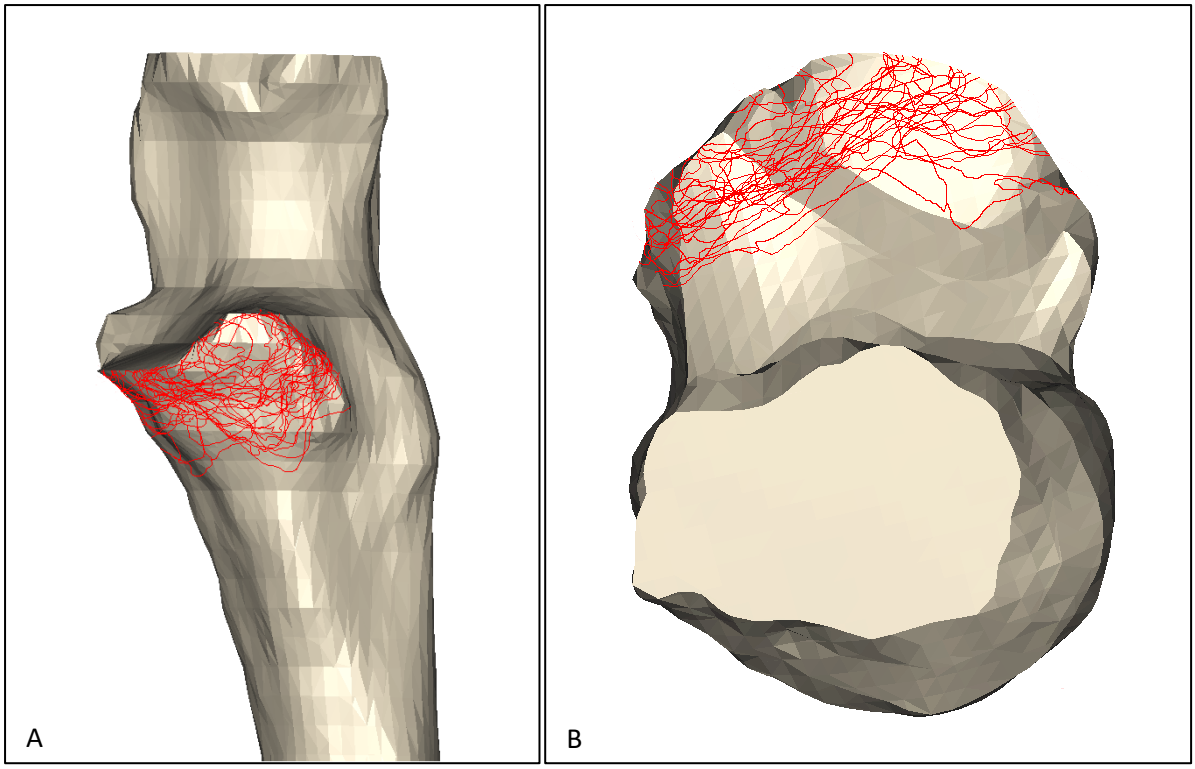

Figure 20: (A) Fracture map showing the location, distribution, and frequency of all 33 patient fractures in the anterior view. (B) Fracture map showing the location, distribution, and frequency of 32 of the patient fractures along the superior view of the coronoid.

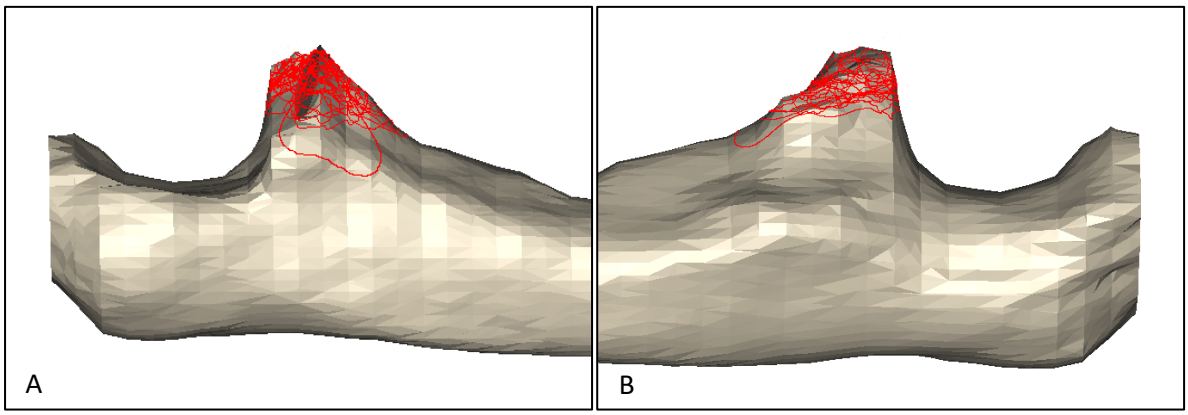

Figure 21: (A) Medial fracture map involving all the fracture lines from the 33 selected patients. (B) Lateral fracture map including 32 of the 33 fracture lines from the selected patients.

2.5.4.1. Type 1 & Type 1 Subtypes (n=12)

Type 1 fractures were grouped and shown together (Figure 22). Subtype 2, the larger of the Type 1 fractures, was more common (11 out of the 12 Type 1 fractures). There was no common pattern present among the Type 1 fractures.

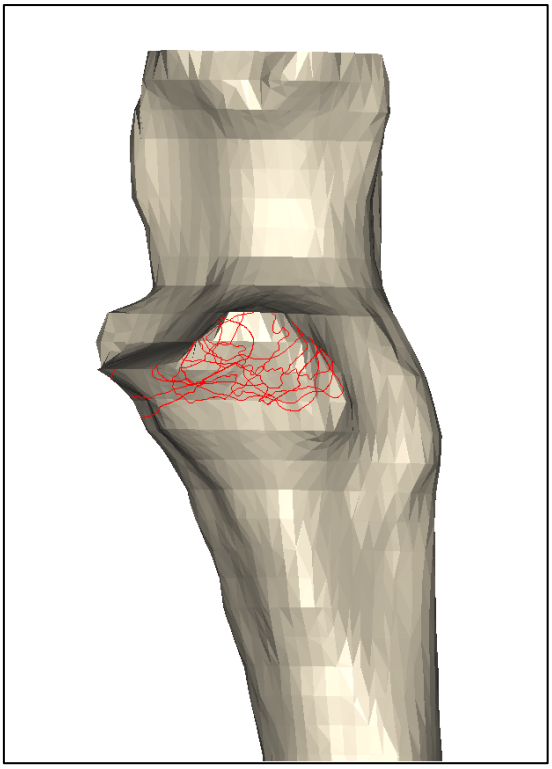

Figure 22: Anterior fracture maps depicting the location and distribution of all the Type 1 coronoid fractures.

2.5.4.2. Type 2 & Type 2 Subtype (n=21)

Subtype 1 - Tip To Anterior Half of Sublime Tubercle (n = 0)

A subtype 1 fracture was defined as reaching from just medial to the tip of the coronoid, to the anterior half of the sublime tubercle (Ring, 2006). As per this definition, no Subtype 1 fractures were present in the 33 included scans.

Subtype 2 - Tip To Medial Half of Sublime Tubercle (n = 15)

Of the twenty-one fractures, fifteen (45.5%) were categorised as Subtype 2 fractures, making up the largest proportion of the Type 2 category. Most of the fractures within this subtype presented in a similar pattern, informally dubbed as the 'Africa pattern,' as the fragments all resembled an oblong or elongated versions of the continent of Africa. This 'Africa pattern' was most seen in the anterior view of the coronoid in Figure 23A. Some of the fragments extended slightly more medially towards the sublime tubercle than others.

Subtype 3 - Anteromedial Rim and The Entire Sublime Tubercle (n = 6)

Type 2 Subtype 3 made up the smaller portion of the Type 2 fractures, with 6 (18.2%) of the 33 patients being included in this category (Figure 23B). The fragments of the Subtype 3 category did not follow a common pattern, although they were generally larger than those of the Subtype 2 category. All the fractures belonging to this category were comminuted (Table 1).

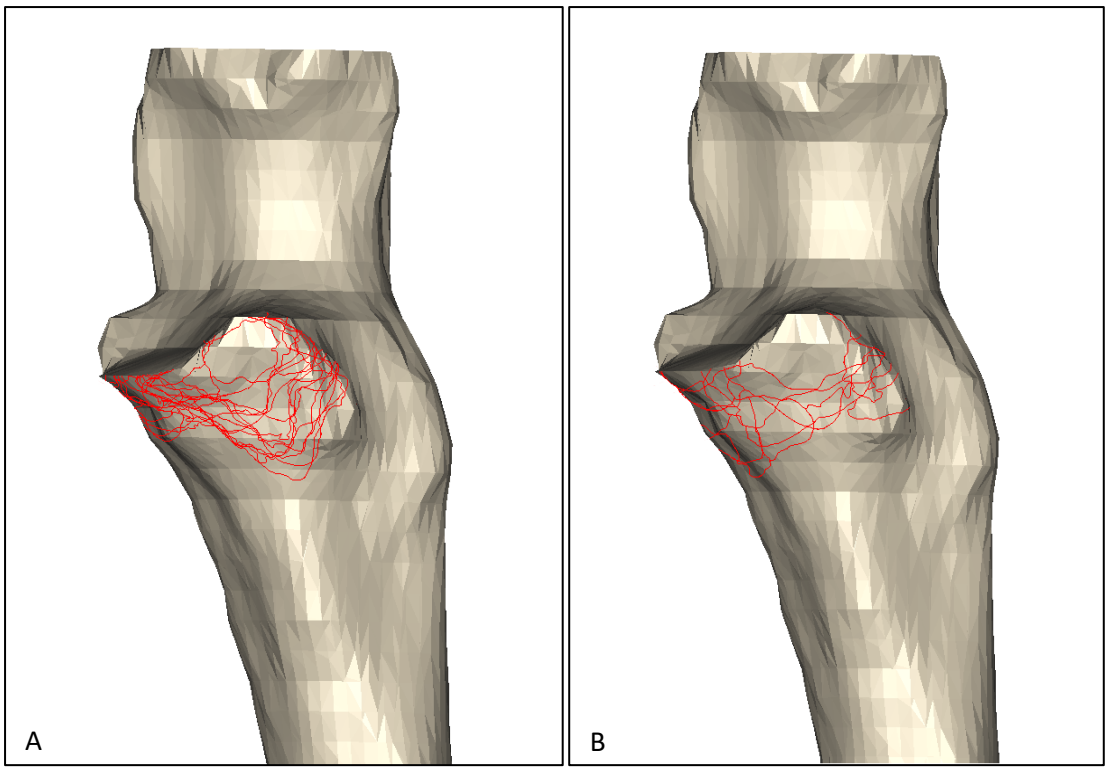

Figure 23: Type 2 Coronoid fractures. (A) Anterior view of Type 2 Subtype 2 coronoid fractures showing the distribution of the fractures, and the common 'Africa pattern'. (B) Type 2 Subtype 3 coronoid fractures which encompass the anterior rime and the sublime tubercle.

2.5.5. Heat Maps

The heat maps produced followed the same results methods as the fracture maps. The overall maps showing all 33 fracture lines (in each view) were produced; as well as the 4 views of each fracture Type and Subtype. These Subtype maps helped determine the critical patterns for their corresponding classifications. The heat maps depicting all the fractures showed the weak points of the coronoid where the majority of the fracture lines passed through. One weak point was prominent in the anterior view (Figure 24A); whereas more weak points were present when looking at the superior view (Figure 24B)

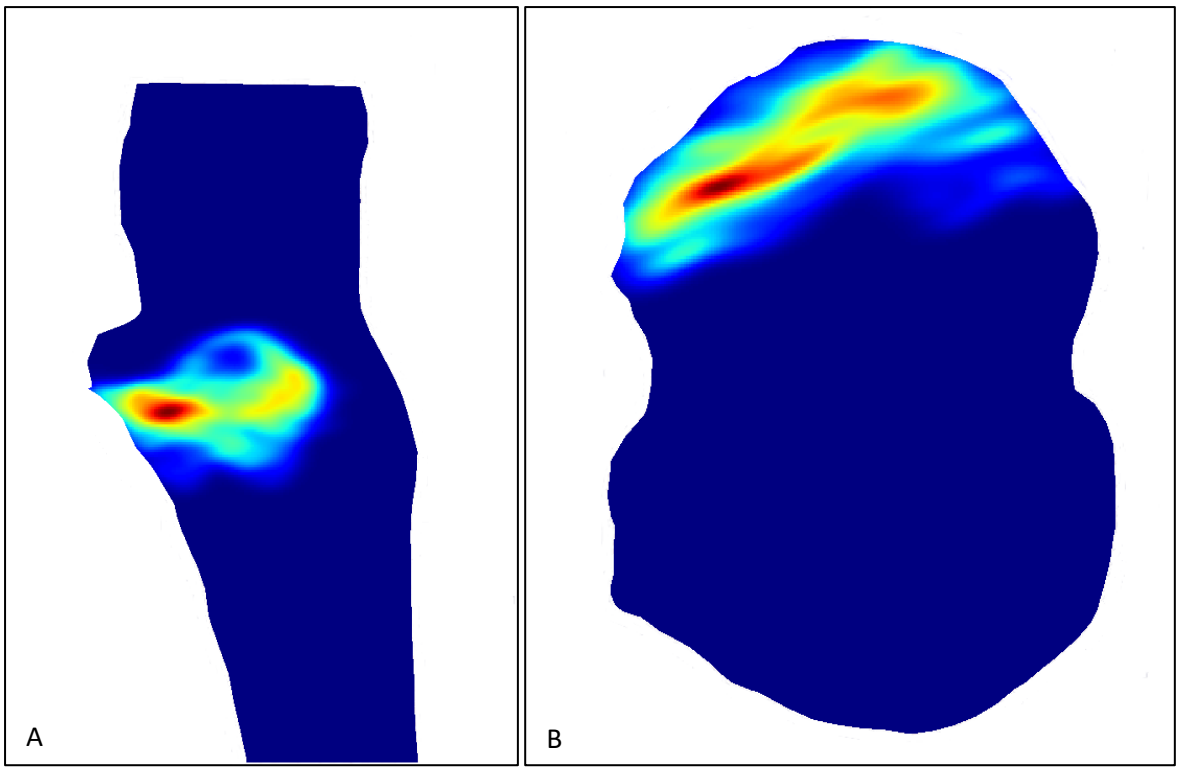

Figure 24: (A) Anterior heat map of the coronoid depicting the density of all patient fracture lines, with the presence of one evident weak point in the coronoid. (B) Superior heat map showing the density of all the patient fractures; as well as the weak points of the coronoid.

The lateral and medial heat maps also revealed weak points present on the coronoid. The lateral view (Figure 25A) showed that the coronoid was weakest along a line at approximately halfway of its height. The medial map (Figure 25B) showed one extended weak point of the coronoid as the fracture line travelled downwards from the trochlear articular surface to the anterior aspect of the coronoid.

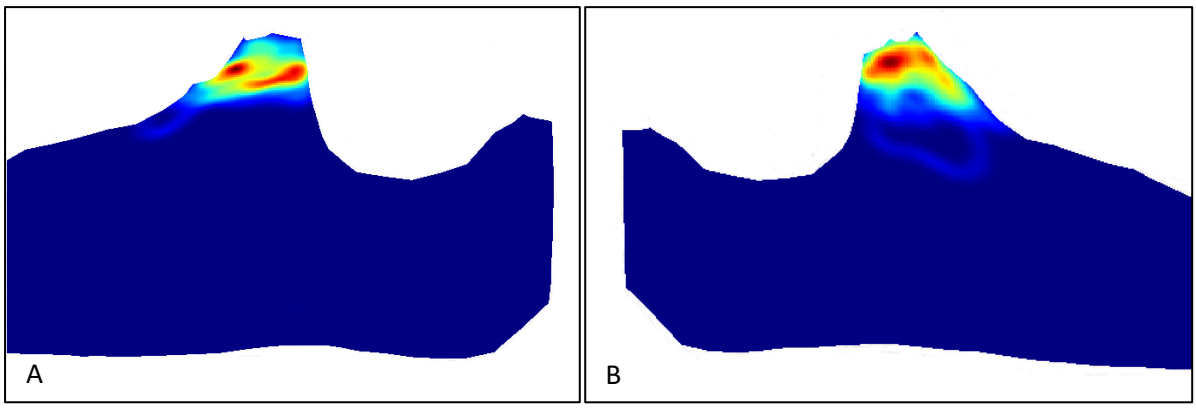

Figure 25: (A) Lateral heat map of all the patient fracture lines, (B) Medial heat map of the 33-patient fracture lines.

2.5.5.1. Type 1

The density distribution of the Type 1 fractures was contained to the tip of the coronoid, as per the type's definition. The anterior view showed a side-ways 'Y' shaped area in which the density of the fractures was highest, indicating a weak point in the coronoid (Figure 26A).

From these heat maps, the critical pattern for Type 1 coronoid fractures was inferred. The critical pattern was most clearly seen in the anterior view, showing the size and shape of the fragment (Figure 26B).

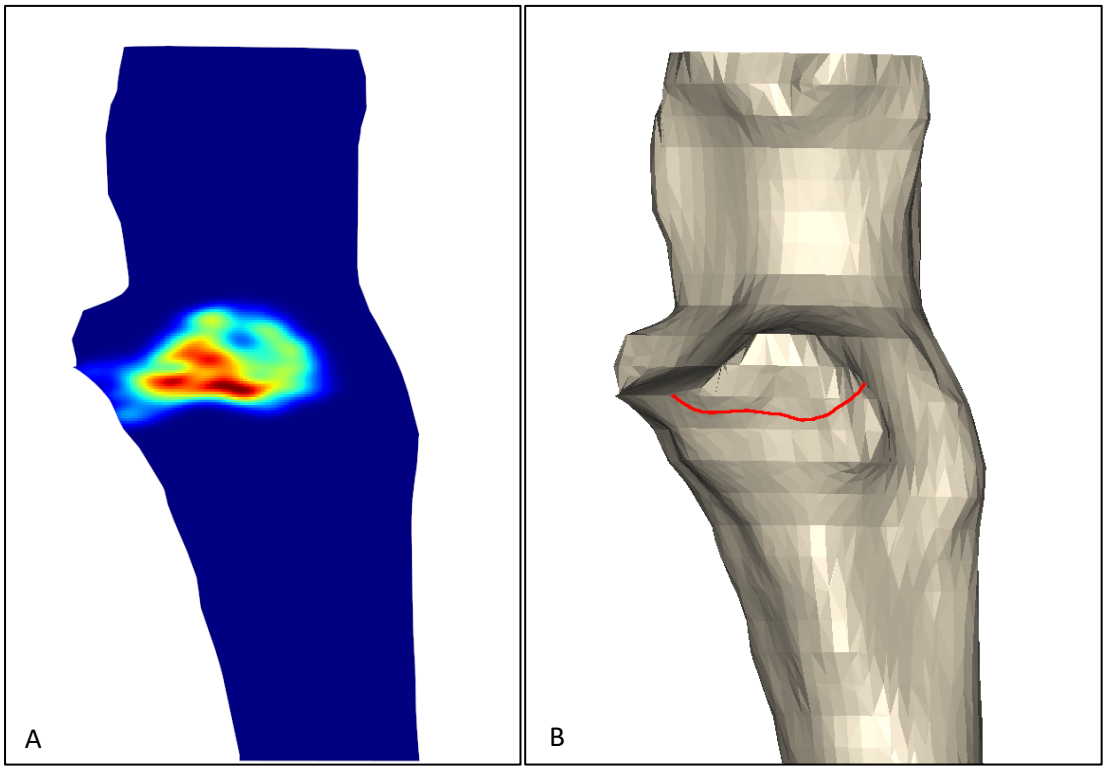

Figure 26: (A) Heat maps showing the density of Type 1 fractures. (B) Critical fracture pattern of O'Driscoll Type 1 coronoid process fractures.

2.5.5.2. Type 2 Subtype 2

The Type 2 Subtype 2 classified fracture lines were grouped and used to create the resultant heat maps, which reiterated the 'Africa pattern' on the anterior surface (Figure 27A). The density distribution of the fracture lines was concentrated around this pattern, with the slight variations in shape causing the distribution spread. The anterior heat map showed a weak point at a similar location to the one found for Type 1 fractures. This point sat medial (to the left) of the tip, towards the middle of the anteromedial rim. This point was shown in the deep red which signified the highest density of fracture lines.

The critical fracture pattern inferred from the Subtype 2 heat maps once again followed the 'Africa pattern' as it extended through the anteromedial rim towards the sublime tubercle (Figure 27B).

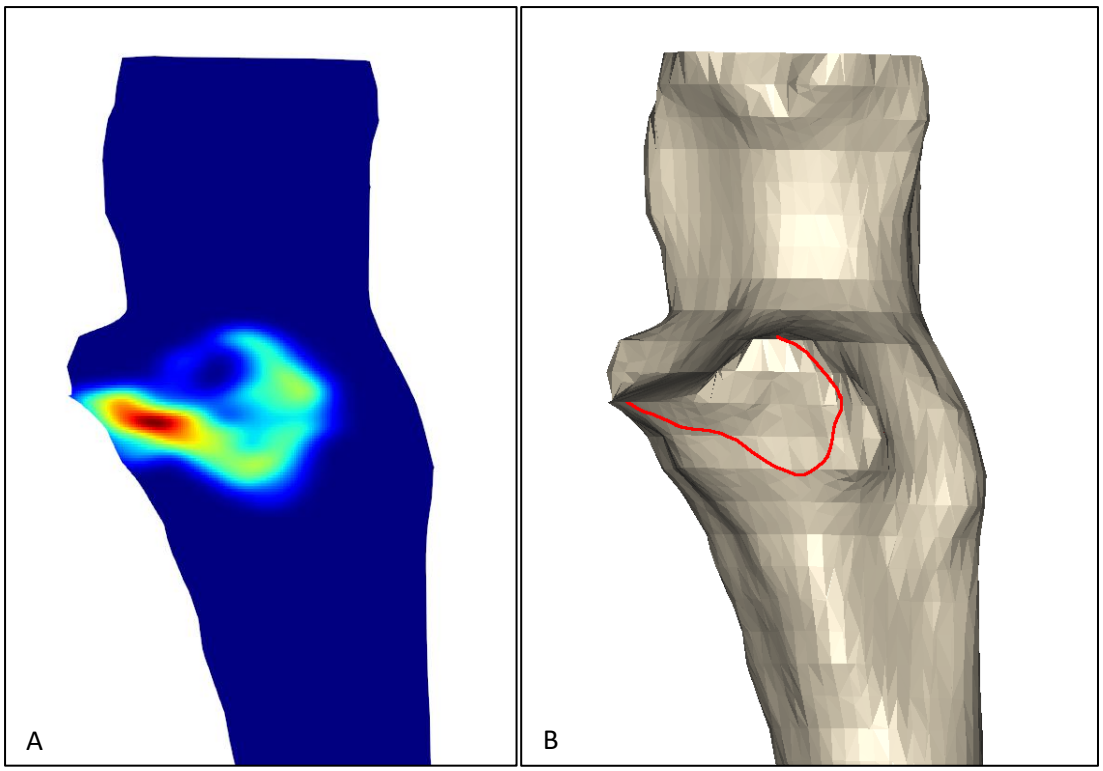

Figure 27: (A) Heat maps depicting the density of the fracture patterns classified as O'Driscoll Type 2 Subtype 2 fractures. (B) Critical fracture pattern for O'Driscoll Type 2 Subtype 2 fractures. The critical fracture pattern follows the 'Africa pattern.'

2.5.5.3. Type 2 Subtype 3

The density of the Subtype 3 fractures was widespread in comparison to those of the Type 1 and Type 2 Subtype 2. This was due to the fragments being larger and comminuted. There were areas of high fracture line density, signifying weak points in the coronoid structure (Figure 28A). The weak points on the anterior surface were at similar locations to those found in both Type 1 and Type 2 Subtype 2 fractures; specifically, the point medial (left) to the coronoid tip.

The resultant critical pattern for the Subtype 3 showed these fractures tended to be comminuted, larger and more elongated than those of Subtype 2 (Figure 28B).

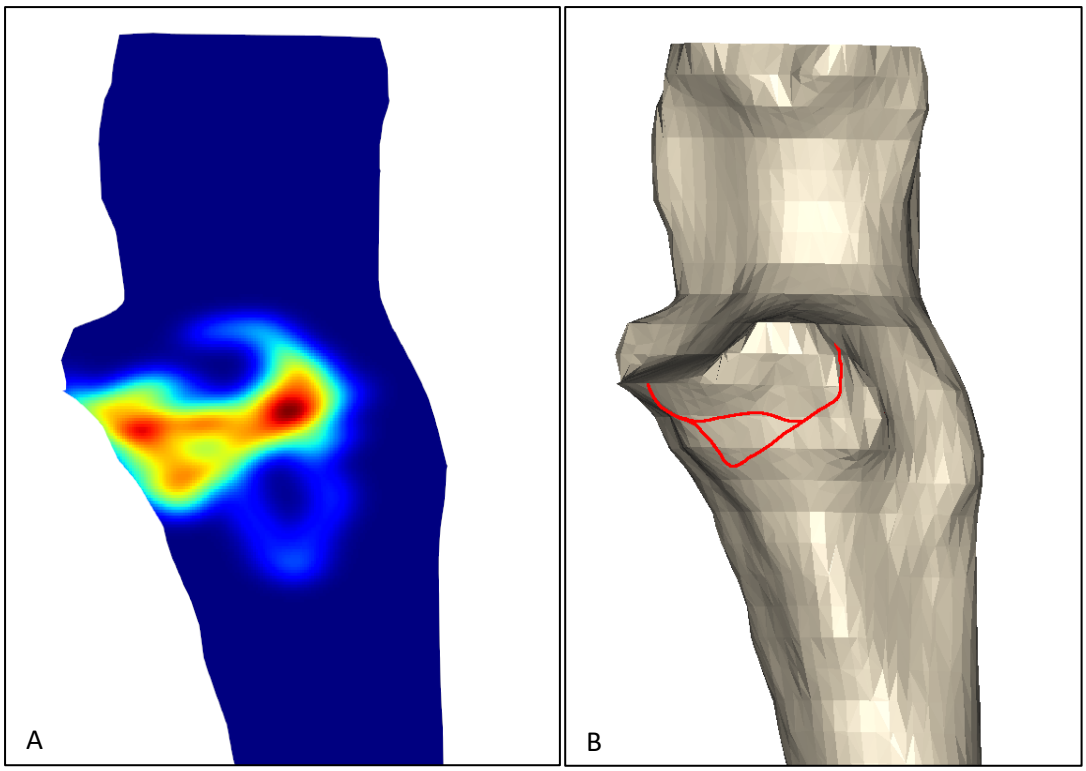

Figure 28: (A) Heat maps showing the distribution of the fracture line density for Type 2 Subtype 3 O'Driscoll fractures. (B) Critical fracture pattern for O'Driscoll Type 2 Subtype 3 fractures.

2.6. Discussion

The patient cohort information aligns with the existing research on the presentation and prevalence of coronoid fractures. Type 2 O'Driscoll fractures are the most common fracture with 21 cases (63.6%), while the remaining 12 cases are O'Driscoll Type 1. The majority of the Type 2 fracture highlights the clinical significance of the fracture type and the need to address them surgically. However, the findings of this study contradict those of Doornberg *et al.* (2006) when they observed anteromedial fractures with associated radial head fractures as an uncommon occurrence. This study has 14 of the 21 anteromedial Type 2 fractures with associated radial head fractures.

This study shares similarities in the methodology and programs used to perform the *in-silico* fracture reduction and Q3DCT analysis. Mellema *et al.* (2014), Doornberg *et al.* (2006) and Adams *et al.* (2012) all produced coronoid fracture maps using the same fracture line imposition over a 2D template technique, with all authors noting 3D mapping would be a beneficial clinical tool. These studies also focused on understanding the links between the mechanisms of injury and the fracture patterns. This study distinguishes itself by incorporating 3-dimensional views which allows for a comprehensive examination of the coronoid fragments.

The fracture and heat maps display the critical fracture patterns, providing insight into the fragment morphology and weak points within the ulna bone structure for which fixation devices would need to

accommodate. These maps, constructed from four different views (anterior, superior, medial, and lateral) for each fracture type and subtype, give a comprehensive 3D analysis of the fracture fragments.

Weak areas, indicated by the deep red spots, signify the highest density of the fracture lines. A single weak point can be identified in the superior view, while the anterior view reveals a significant primary and secondary weak point. Two weak points, forming a line halfway down the height of the coronoid, is noted on the lateral view. The medial map reveals a single weak point extending from the articular surface over the rim of the coronoid.

Further examination exposes distinct patterns for the different fracture types and subtypes. For Type 1, the critical pattern extends in an almost straight transverse line from the radial notch to the anteromedial rim, with the resultant fragments taking the shape of an abstract trapezium. The fragment is longer in length than in height, with the tip of the coronoid resembling the apex of the trapezium. In contrast the Type 2 Subtype 2 fractures exhibit a characteristic oblong 'Africa'-shaped pattern, with the fracture density distribution concentrated around this pattern. This pattern extends from the tip down the coronoid before curving up to the anteromedial facet. The resultant fragments following the 'Africa pattern' are often flat at the fracture site and were easily reduced during the In-*Silico* Reduction of The Coronoid Fractures. Similarly to Subtype 2, the Subtype 3 fractures display a critical pattern extending from the radial notch adjacent to the tip, to the anteromedial rim. However, the Subtype 3 fractures did not adhere to a common pattern. All of these fractures are comminuted, which is reflected in the multiple lines present in the critical fracture pattern. This highlights the difficulty of currently available devices to adequately address this variable fragment shape.

The critical fracture patterns provide an indication of the areas that need to be taken into consideration when designing a coronoid fixation device. The device should aim to cross over these lines to provide the necessary coverage for effective fracture reduction. The fracture and heat mapping from various viewpoints allows for a full understanding of the fragment morphology in a 3D manner and reveals common shapes of fragments associated with each O'Driscoll type and subtypes. These shapes add to the understanding required to improve the design by informing the size, shape and features needed to provide more targeted and efficient fixation.

2.6.1. Key Findings in Chapter

1) **Prevalence of Fracture Types:** Type 2 O'Driscoll fractures are the most common, accounting for 63.6% of cases in the study. This is in contrast to previous research conducted by Doornberg *et al.* (2006).

2) **Consistency with Existing Research:** The methodologies used in this study are consistent with those in previous research by Mellema (Mellema, Janssen *et al.*, 2015), Doornberg (Doornberg *et al.*, 2006), and Adams (Adams *et al.*, 2012).
3) **Fragment Morphology:** Different fracture types and subtypes exhibited distinct patterns and fragment shapes. Type 1 fractures had a transverse line pattern resulting in trapezium-shaped fragments, while Type 2 Subtype 2 fractures showed an oblong 'Africa'-shaped pattern. Type 2 Subtype 3 fractures are characterised by multiple lines and comminuted fractures.
4) **Heat Map Analysis:** Critical fracture patterns can be identified through fracture and heat maps from multiple viewpoints, revealing significant weak points in the coronoid.
5) **3D Analysis Benefits:** The 3D analysis of coronoid fractures provide a deeper understanding of fragment morphology, that aids in the design of targeted fixation devices and improves surgical decision-making.

2.6.2. Limitations

Variations in the quality of the acquired scans posed challenges in accurately identifying, segmenting, and analysing some of the fractures. Some scans exhibited fractures with multiple fragments which were displaced from the ulna but with minimal or no displacement between the fragments, therefore complicating the *in-silico* reductions. To address this limitation, the CT scans were re-sliced to produce more focused scans with thinner slices. In addition, consultations with an experienced Shoulder and Elbow Surgeon (Professor Roche) helped ensure the accuracy of reducing the displaced fragments and the incorporation of missing fragments into the fracture maps.

Perfect reduction of some of the fractures proved difficult due to the fracture's nature, size, and number of fracture fragments. The fracture reconstructions relied on osteometric and anatomical knowledge, with informed interpretations made where normal bone anatomy could not be deduced. In these instances of concern regarding fragment location, orientation or arrangement, consultations with Professor Roche were conducted to ensure correct fracture reconstruction.

This study was also constrained to the use of O'Driscoll Type 1 and Type 2 fractures, as the Type 3 fractures were excluded due to the presence of additional fractures to the elbow which would alter the type of fixation of the coronoid. Challenges also arose in classifying the fractures according to the O'Driscoll system as the classified subtypes lacked explicit clarity. Fragment variability from differing orientations made classification difficult as the fracture morphology and classification often shifted during changes in orientation. This prompted careful consideration and interpretation.

This dataset was restricted to local patients, therefore offering a limited view of the overall anatomical standing of the South African population. In addition, sexual dimorphism may play a role in this male-

dominant patient sample, due to noted instances of variations in the anatomy of the coronoid between sexes. This study had a left-side dominant dataset; however, previous research suggests minimal to no significant differences in the morphometry of the left and right side ulna (Zhang *et al.*, 2020).

2.7. Chapter Conclusion

Coronoid process fractures display repeated patterns and fragment shapes for each of the corresponding fracture types and subtypes described by O'Driscoll. This study also introduces additional methods of 3D visualization techniques for these coronoid fractures, by generating fracture and heap maps from multiple orientations. These methods enable improved identification and understanding of both the fractures and their resultant fragments.

2.7.1. Chapter Outcomes

The goal of this chapter is to establish a set of reference coronoid fracture and heat maps depicting critical fracture patterns in multiple views. This aim was achieved by fulfilling the four objectives:

Creation of a Reference Base of Fractures: The first objective was creating a reference base of O'Driscoll classified coronoid fractures. This was done by using established Q3DCT techniques to perform in-silico reductions of the fractures present in the acquired CT scans. These reduced fractures will serve as a reference against which fixation methods will be measured in future chapters.

Generation of Fracture Maps: The second objective of generating fracture maps was facilitated by the Q3DCT techniques used on the reference base of classified coronoid fractures. These maps, created from 4 orthogonal views: anterior, superior, lateral, and medial, enable a comprehensive 3D analysis of coronoid fracture patterns and the fracture fragments

Generation of Heat Maps: The third objective followed the generation of heat maps, which was accomplished using an established Python code. These heat maps highlight areas of structural weakness, which should be considered when designing effective fixation devices.

Establishing the Critical Fracture Pattern: The last objective built on the information provided by the heat maps. The critical fracture patterns were identified and described. The heat maps also offer insights into the shape of the resultant fragments for each fracture type which need to be taken into consideration in the design of the adapted Endobutton.

Identifying critical fracture patterns through fracture maps, and heat maps provide the groundwork for the design and evaluation of coronoid fixation devices.

3. Chapter 3: Qualitative Fit Analysis

3.1. Chapter Introduction

Coronoid fractures pose a challenge to surgeons due to their potential to disrupt the stability and anatomical functioning of the elbow joint; necessitating Open Reduction and Internal Fixation (ORIF) (Lowery *et al.*, 2022; Salwan *et al.*, 2023). There remains a considerable amount of uncertainty about the optimal method of coronoid fracture fixation (Altan *et al.*, 2016; Liu *et al.*, 2018; Salwan *et al.*, 2023). The rationale behind investigating coronoid fracture fixation methods is to understand the limitations of the currently used methods, in particular the Endobutton. The Endobutton has anecdotally proven effective in treating small and multi-fragmented coronoid fractures, but literature reports there is room for improvement (Altan *et al.*, 2016; Salwan *et al.*, 2023)

This chapter aims to qualitatively assess the Endobutton as a method of coronoid fracture fixation to understand its advantages, disadvantages, and limitations. These findings will be used to formulate design recommendations for an adapted Endobutton.

3.2. Literature Review: Coronoid Fracture Fixation, 3D Printing, and Templating of Fixation Devices

3.2.1. Coronoid Fracture Fixation

It is well established that early intervention using stable surgical fixation is the recommended standard treatment protocol for all displaced coronoid fractures, as conservative treatment is ineffective and often leads to recurrent instability of the ulno-humeral joint (Feng *et al.*, 2018; Ring, Jupiter *et al.*, 2002; Salwan *et al.*, 2023). The justification for the fixation of Type 2 and Type 3 fractures is well supported; however, a case can be made that all coronoid fractures are clinically relevant (Neill Cage, Abrams *et al.*, 1995). Therefore, it is proposed that all coronoid fractures, regardless of their size or shape, should be fixed; however, the method of fixation is still highly debated (Budoff, 2012). It is still particularly unclear how to treat comminuted fractures (Salwan *et al.*, 2023).

The indication for operative treatment of coronoid fractures is based on morphology, orientation of the fragment and accompanying injuries (O'Driscoll *et al.*, 2003; Rausch, Jettkant *et al.*, 2021). As the elbow's stability depends on the bony integrity and the state of the soft tissue constraints, the fixation of even small fragments provides better stability of the elbow and reduces the possibility of chronic joint instability (Salwan *et al.*, 2023). Therefore, it is standard to treat all the coronoid fracture types, especially Type 2 as they may contain pieces of the anteromedial facet and the anterior joint capsule (Salwan *et al.*, 2023). Fixation of the smaller type fractures also mitigate the chance of coronoid

insufficiency as a complication of the fracture, this is significant as insufficiency may result in posterolateral instability (Salwan *et al.*, 2023).

Traditionally, Type 1 and Type 2 fractures are treated with varying and often suture-based devices whereas ORIF using plates is preferred for the larger Type 3 basal fractures (Pai and Pai, 2009). Type 2 and Type 3 should be managed surgically because they are linked with an increased likelihood of instability and coronoid insufficiency, which may lead to posterolateral instability (Regan and Morrey, 1989; Salwan *et al.*, 2023). It is well established that the larger the fragment, the greater the resultant instability, and they're more likely to require surgical stabilisation, therefore reiterating the use of plates for the large Type 3 fractures to restore stability and minimise stiffness (Adams *et al.*, 2009; Feng *et al.*, 2018; Pai *et al.*, 2009).

Coronoid fractures can be treated conservatively (non-surgically) or surgically. Surgical outcomes involving coronoid fractures are extensively reported on, with wide ranging methods (Chen *et al.*, 2018; Mallard, Hubert *et al.*, 2015; Pai *et al.*, 2009; Rausch *et al.*, 2021; Salwan *et al.*, 2023). Operative methods range from sutures and plates to K-wire fixation, and the extreme of coronoid replacement using a prosthesis.

Conservative (non-surgical) treatment of coronoid process fractures has been studied extensively, with evidence suggesting that it is not ideal for achieving optimal outcomes for all patients. Studies, such as those performed by Ring *et al.* (2002), show that the conservative approach is often ineffective and leads to recurrent instability of the ulno-humeral joint. Moreover, if left untreated, coronoid process fractures and resultant persistent instability, result in potential loss of daily functioning (Zhang *et al.*, 2020). The complications of non-operative treatment add support to the favouring of ORIF procedures to treat coronoid fractures.

Plate-based ORIF is a commonly used technique for treating larger coronoid fractures. This technique's use is necessitated by the premise that the larger the fragment, the greater the instability of the elbow joint and therefore the greater the need for surgical stabilisation (Feng *et al.*, 2018). Fixation plates allow for accurate reduction of the fractured fragment and provide a more rigid internal fixation (Feng *et al.*, 2018). The use of plate-based fixation offers several additional advantages, such as providing a stable platform for early functional exercise and joint movement; as well as mitigating damage to the joint, ultimately promoting better post-operative rehabilitation outcomes (Chen *et al.*, 2018; Feng *et al.*, 2018). The two main types of fixation plates used for coronoid fractures are pre-contoured coronoid plates and buttress plates. Although both have benefits, a noted advantage of buttress plates is their use for the reliable and accurate reduction of small coronoid fragments (Feng *et al.*, 2018). Despite the numerous benefits provided by plate-based fixation, the use of these devices

is limited owing to some fractures being too small to accommodate the plate and the anatomical complexity of the fracture (Garrigues, Wray *et al.*, 2011; Jo and Shin, 2023).

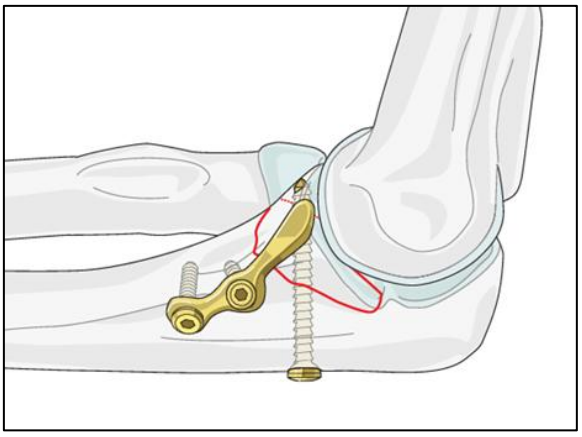

Figure 29: Coronoid buttress fixation plate which makes use of rigid cortical screws and a buttress plate to secure the fragment (Kloen and Ring, 2018).

Kirschner wires (K-wires) are occasionally used in the surgical fixation of coronoid process fractures; however, they are not highly favoured due to their associated complications and suboptimal post-operative outcomes when used as the primary fixation device (Chen *et al.*, 2018). Therefore, K-wires are frequently used as a method of temporary fixation, prior to the use of a screw or plate (Feng *et al.*, 2018; Lin, Kohli *et al.*, 2007; Park, Lee *et al.*, 2015). Numerous studies document the use of K-wires as provisional stabilisers to maintain the fracture reduction, until the definitive fixation method can be implemented (Feng *et al.*, 2018; Lin *et al.*, 2007; Park *et al.*, 2015).

Steel wire-based surgical fixation is occasionally used in the treatment of coronoid fractures by passing the steel wire sutures through a tunnel in the bone and around the fracture fragment. The wire sutures are then looped to provide stability and compression across the fracture site (Mallard *et al.*, 2015). Steel wire fixation offers advantages, including the relative ease of their use with any surgical approach in a minimally invasive capacity (Mallard *et al.*, 2015). This tension banding technique is straightforward and cost-effective without the need for sophisticated hardware (Mallard *et al.*, 2015). Despite these benefits, research shows that steel wire fixation is associated with greater rates of complications when compared to mini-plate, hollow screw and K-wire fixation and thus makes this method highly unfavourable (Chen *et al.*, 2018).

The design and use of both **biological and non-biological coronoid prostheses** are explored as potential solutions for cases where ORIF is not feasible (Gray, Alolabi *et al.*, 2013; Zhang *et al.*, 2020). Biological reconstruction methods involve the use of tissues or bony structures from donor sites such as the olecranon tip, iliac crest, radial head or the ribs (Zhang *et al.*, 2020). However, these replacements pose challenges such as donor site comorbidities and the lack of anatomical similarity

to the original shape of the coronoid (Zhang *et al.*, 2020). Non-biological alternatives such as stainless steel prostheses have been developed but have the similar challenge of lack of anatomical similarity, which compromises the efficacy and longevity of the implant (Zhang *et al.*, 2020).As a result of these limitations, the idea of prosthetic replacements has not gained popularity as a surgical approach in the treatment of coronoid process fractures.

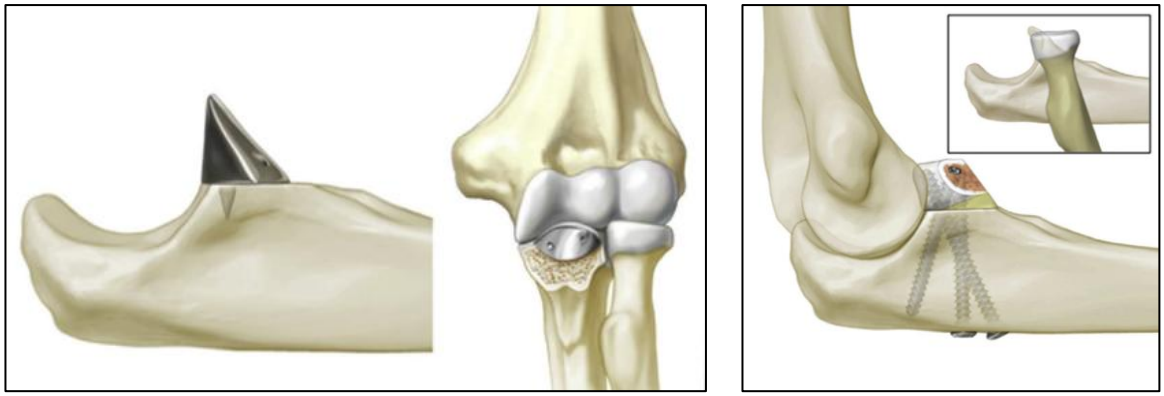

Figure 30: Non-biological (left) and biological (right) coronoid protheses (Bellato and O'Driscoll, 2019).

3.2.1.1. Use of Suture-Based Techniques for Coronoid Fracture Fixation

A significant category of the coronoid fracture fixation methods is those which rely on suturing techniques or suture-based devices. The rationale for these techniques and devices is the often-small size of the coronoid fracture, which are unable to accommodate screw and plate fixation methods. Commonly used suture-based methods includes suture anchors and the suture lasso technique; as well as the use of a novel designs such as the lasso plate. However, the most significant method within the context of this research is the Endobutton.

Suture Lasso Technique as a method of coronoid fracture fixation offers both advantages and disadvantages. On the positive side, this is proven to be an effective method, and Garrigues and Salwan agree that the suture lasso should be considered superior to suture anchors for non-comminuted fractures (Garrigues *et al.*, 2011; Salwan *et al.*, 2023). The drawbacks of this fixation technique are its inability to sufficiently cover the fracture fragment, which leads to compromised stability of the elbow joint. Additionally, the suture lasso is associated with risks of knot slippage and ultimately fixation failure (Salwan *et al.*, 2023). Further investigation shows that the lasso technique is particularly ineffective when treating comminuted fractures involving the anterior capsule, as it fails to hold the small fragments together (Garrigues *et al.*, 2011; Salwan *et al.*, 2023). Consequently, the suture lasso is only rarely indicated in cases where the fractures are too small to accommodate rigid fixation, such as Type 1 fractures. While these fractures do not significantly impact the elbow stability, their association with capsular rupture is significant (Morrey, Sotelo *et al.*, 2017). The repair of the capsule

becomes a critical goal especially in complex injuries when the tip is a component of the terrible triad, and there is persistent instability despite ligament and radial head stabilisation (Morrey *et al.*, 2017).

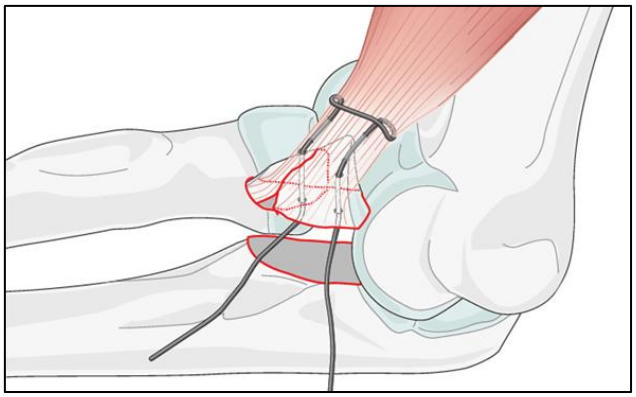

Figure 31: Suture lasso technique used for small fragment coronoid fractures (Kloen et al., 2018).

Suture anchors act as an alternative suture-based fixation mechanism which focuses on the reattachment of soft tissues by being implanted into the bone. This provides a secure anchor point through which the suture can be threaded. Fixation using suture anchors is thought to be simpler than methods requiring trans-ulnar drilling, and allows for better resistance of suture materials which minimises the stress along the fracture line (Pai *et al.*, 2009). This facilitates better stability and early range of motion (Pai *et al.*, 2009). Despite these outcomes, suture anchors have limitations and are prone to difficulties including being less effective for treating comminuted fractures, higher rates of malunion, are more expensive, and have higher infection rates (Garrigues *et al.*, 2011; Pai *et al.*, 2009). Anecdotal evidence shows that the suture lasso provides improved stability with fewer complications compared to suture anchors (Garrigues *et al.*, 2011). The favouring of the suture lasso has led to limited current research on the use of suture anchors for coronoid fracture fixation (Garrigues *et al.*, 2011).

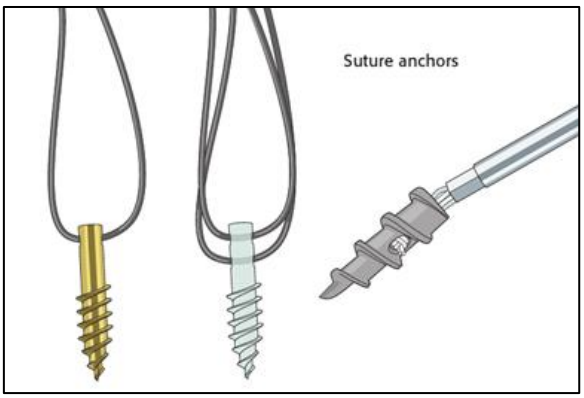

Figure 32: Suture anchors used in Orthopaedic ORIF surgeries (Kloen et al., 2018).

The **Lasso Plate** is a novel device designed by Wang *et al.* (2017), which combines wire suturing techniques with a pre-contoured plate to concentrically reduce and provide stable fixation for coronoid process fractures. The Lasso plate allows for increased contact area between the soft tissue and

implant, providing improved stability by pressing on the coronoid and insertion of the anterior capsule (Wang *et al.*, 2017). By using suture wires to fix a pre-contoured plate, the lasso plate addresses the challenge of fixing small coronoid fractures. This novel device attempts to address the increasing requirement for a anatomically pre-contoured device for coronoid fixation, and led to promising results and ultimately a potential solution to the statement posed by Salwan *et al.* (2023).

3.2.2. Endobutton Fixation

Previous research is unclear about the optimal method of fixation for small comminuted coronoid fractures (Altan *et al.*, 2016; Liu *et al.*, 2018; Salwan *et al.*, 2023). The Endobutton is typically used as a secondary device for securing larger sutures intended to replace the ligamentous structures of the knee (Figure 33 - Left) (Ayati Firoozabadi, Dehghaniashkezari *et al.*, 2024; Eguchi, Ochi *et al.*, 2014). Although the Endobutton is intended for use elsewhere in the body, it is often used as an alternative to traditional rigid fixation or the suture-lasso for coronoid process fractures (Figure 33 – Right). Research surrounding the use of Endobuttons for coronoid fractures focuses on an assessment of their efficacy as a method of suspensory fixation, demonstrating the techniques required for their use, and comparisons between the Endobutton and other methods of fixation (Altan *et al.*, 2016).

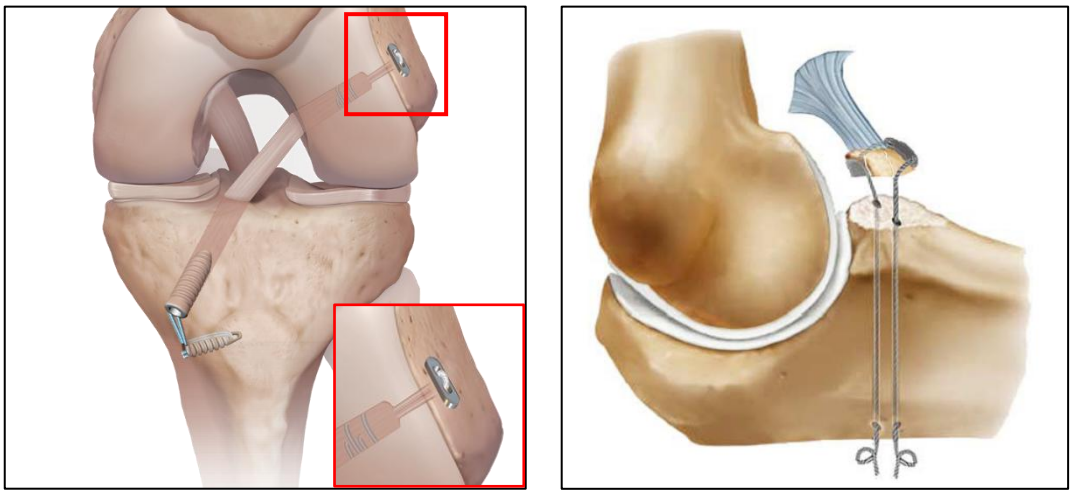

Figure 33: Endobutton used for ACL repair (Left – red box) and coronoid fixation (Right) (Altan et al., 2016).

The Endobutton is recommended for Type 1 and Type 2 coronoid fractures, particularly where there was minimal capsule attachment, or where the fragments are too small for rigid screw fixation (Salwan *et al.*, 2023; Wang *et al.*, 2017). This recommendation is based on the device's ability to enable good suspensory fixation while providing the anterior buttress force necessary to hold down the fragments (Altan *et al.*, 2016; Salwan *et al.*, 2023). The inclusion of the sutures through the joint capsule provides an additional anchor effect and affords a more accurate and stable anatomical reduction (Altan *et al.*, 2016; Salwan *et al.*, 2023).

Discussions with Orthopaedic surgeons associated with this study revealed that the small size of the Endobutton leads to difficulty in manipulation in the tissues, and its flat, rigid design does not conform well to the curved anatomy of the coronoid, potentially slipping during the procedure.

Several studies report on the use of the Endobutton of a fixation method, either in independent case reports or in small studies in which patient outcomes are compared to others who received alternative methods of fixation. Most of these studies provide positive anecdotal evaluations of the device through satisfactory post-operative outcomes and low complication rates. Although there is a consensus that combining sutures with plates provides promising results, there is no coronoid-specific Endobutton papers. These independent studies which report good results suggested that a pre-contoured button made from materials resembling a plate could offer better stabilisation and coverage, addressing many of these issues with the Endobutton (Altan *et al.*, 2016; Salwan *et al.*, 2023). Work done by Wang *et al.* (2017) on the development of a novel lasso-plate, emphasises the benefits of creating an anatomically pre-contoured plate.

However, there is a gap in the literature regarding the performance of the Endobutton. Studies that conduct fitment analysis and qualitative assessment could potentially emphasize the efficacy or lack thereof of the Endobutton device. In addition, they can provide a more comprehensive evaluation of its potential as an optimal method for small multi-fragmented coronoid fractures.

Table 5: Summary of coronoid fixation devices

Fixation Methods	**Advantages**	**Disadvantages**
Conservative	• Cost and no surgery	• May lead to chronic instability
Plate-Base ORIF	• Allow for accurate reduction • Provide rigid fixation • Allow early exercise and joint movement	• Contra-indicated for small fragments
Kirschner Wires (K-Wires)	• Effective temporary method of fixation	• High complication incidence rates
Steel-Wire	• Ease of use • Minimally invasive • No need for sophisticate hardware • Cost effective	• High complication incidence rates
Protheses	• Complete replacement of coronoid	Biological • Donor site co-morbidities • Lack of anatomical similarity Non-biological • Lack of anatomical similarity

Suture Lasso	• Effective • Superior to suture anchors	• Insufficient cover of fragment • Risk of knot slippage • Ineffective for comminuted
Suture Anchors	• Better resistance of suture materials • Minimises stress along the fracture line	• Less effective for comminuted fractures • High rates of malunion • Expensive • High rate of infection
Lasso Plate	• Increased contact area • Improved stability	
Endobutton	• Hold small fragments • Inclusion of sutures through capsule	• Small • Flat and rigid • Lack of conformity to anatomy

In summary, conservative treatment is not advisable for certain small, comminuted fractures, and most existing surgical fixation methods have a range of disadvantages, which may distract from their benefits. Although the Endobutton shows considerable potential, there is still room for improvement with studies calling for the development of an anatomically pre-contoured device.

3.2.3. Use of 3D Printing in Orthopaedics

The use of 3D printing in healthcare, particularly in the Orthopaedic field, is well established in literature as a process that addresses the requirements of personalisation, availability and affordability (Marinescu, Popescu *et al.*, 2020). These requirements offer significant benefits for surgical planning, fixation device analysis, and development (Charilaou, Dey *et al.*, 2021; Marinescu *et al.*, 2020).

By enabling the creation of accurate, tangible and reproducible models, 3D printing allows surgeons to examine the anatomy in more concrete ways, enhancing the visualisation and analysis of complex fracture patterns (Bryce, Pennypacker *et al.*, 2008b; Eltorai, Nguyen *et al.*, 2015; Marinescu *et al.*, 2020). Studies, such as Bizzotto, Sandri *et al.* (2015), show that using physical anatomically accurate models, as opposed to traditional 2-dimensional radiological images and 3D reconstructions on screens, leads to significant improvements in a surgeon's understanding of complex fracture patterns (Bizzotto *et al.*, 2015; Eltorai *et al.*, 2015).

Extensive literature reports additional benefits beyond fracture analysis and surgical planning. Applications of 3D printing ranges from using titanium 3D printing for patient-specific implants or replacements, such as vertebrae and skulls, to gaining a better understanding of previously misunderstood paediatric orthopaedic disorders (Eltorai *et al.*, 2015). Furthermore, 3D printing is used to evaluate the fit and efficacy of fixation devices through the method of device templating (Charilaou *et al.*, 2021). The use of anatomically accurate models helps reveal that commercially available devices

frequently used in surgeries do not always fit the bones as well as they should, nor do they address the fracture patterns encountered (Charilaou *et al.*, 2021). This indicates the need for redesigning of these devices to improve the effectiveness (Charilaou *et al.*, 2021).

3.2.4. Fitment Analysis and Templating of Coronoid Fixation Devices

Various plates, screws, wires, and other fixation devices have been designed for the fixation of the coronoid process in an attempt to identify an optimal method of fixation (Altan *et al.*, 2016; Chen *et al.*, 2018; Rausch *et al.*, 2021; Wang, Zhang *et al.*, 2023). As far as this author is aware, there are no studies which qualitatively or quantitatively measure the overall fit of the currently available coronoid fixation devices. A small number of case studies address the ability of the device to fixate a single or small number of coronoid fractures. The evaluations of the effectiveness of these fixation methods is done using the post-surgical elbow scoring systems that assess the range of motion of the joint and the strength of the muscles in the area, but do not lend themselves to an evaluation of the device beyond the resultant fixation (Altan *et al.*, 2016).

Numerous studies assesses the fitment, fixation, and efficacy of the Endobutton in its intended use in ACL repairs; however, there are no fitment analysis studies focused on the use of the Endobutton in coronoid process fracture treatment (Ayati Firoozabadi *et al.*, 2024; Eguchi *et al.*, 2014; Rylander, Brunelli *et al.*, 2014). Because the Endobutton is suture-based, it cannot be assessed by the same standards as screw-based fixation methods. This might provide a reason as to why there is a gap in the literature.

Moreover, there appears to be no studies that look at templating of coronoid fixation devices. Templating fixation devices on either 3D-printed bones or human specimens is an effective tool for evaluating the device and allowing for pre-operative planning. In a comprehensive systematic literature review by Marinescu et al. (2020), there was no evidence of any 3D printing-based studies done for coronoid process fractures.

3.2.5. Key Findings in Literature

1) **Challenges in Treating Small Comminuted Coronoid Fractures:** Traditional rigid fixation methods, such as plates and screws, are often unsuitable for small comminuted coronoid fractures (Wang *et al.*, 2017). There is a notable uncertainty regarding the optimal method of fixation for small comminuted coronoid fractures (Altan *et al.*, 2016; Liu *et al.*, 2018; Salwan *et al.*, 2023).
2) **Lack of Fitment Studies for Coronoid Process Fracture Devices:** Numerous studies exist on the fitment and efficacy of the Endobutton for its intended use in ACL repairs (Ayati Firoozabadi *et al.*, 2024; Eguchi *et al.*, 2014). However, there is an absence of fitment studies focused on the

use of the Endobutton in coronoid fracture treatment. This gap is significant given the complexity of coronoid fractures and the current reliance on anecdotal evidence of the fit and subsequent efficacy of the Endobutton.

3) **3D Printing as a Tool for Surgical Planning and Device Templating:** The application of 3D printing in healthcare, particularly in Orthopaedics, is recognised for creating accurate, tangible models (Bryce *et al.*, 2008b; Eltorai *et al.*, 2015; Marinescu *et al.*, 2020). These models enhance visualisation and analysis of complex fracture patterns, allowing for improved pre-operative planning, as well as device templating and fitment evaluation (Bryce *et al.*, 2008b; Eltorai *et al.*, 2015; Marinescu *et al.*, 2020). However, there is no evidence of 3D printing-based studies which evaluate the fixation methods for coronoid fractures.
4) **Potential of Anatomically Pre-Contoured Devices:** The development of an anatomically pre-contoured fixation device, like the novel lasso plate, shows promise in addressing the challenges posed in coronoid fracture treatment (Wang *et al.*, 2023; Wang *et al.*, 2017).

3.2.6. Problem Identification and Research Question

Current research establishes a clear challenge in effectively fixating coronoid fractures that are too small for rigid fixation, with suture-based techniques being recommended in these cases. The need to fix these small fractures is deemed critical, as Type 1 fractures often accompany instability and damage to the LUCL, MCL, and anterior capsule (Chamseddine, Zein *et al.*, 2010; Wang *et al.*, 2017). The Endobutton is suggested as a potential method, but anecdotal evaluations in small patient populations with little follow-up show limited insight into the device's efficacy. There is a notable lack of research on the fit and fixation performance of the Endobutton, with no large-scale studies having been conducted. This gap in the literature highlights the need for research to address questions such as: How well does the Endobutton fit the coronoid process? What is its effectiveness in providing stable fixation in a larger patient population? Would a pre-contoured plate offer better potential outcomes for small coronoid fractures compared to the Endobutton?

3.2.6.1. Research Questions

The main research question posed is: "*Is an Endobutton a viable fixation method for coronoid process fractures, and what are the device's limitations when fixing these fractures?"* A secondary question can be posed: "*Can a set of criteria which effectively evaluate the functionality of an Endobutton be created?".*

3.3. Chapter Aim and Objectives

Aim

The aim of this chapter is to qualitatively analyse and evaluate the Endobutton's ability to fix coronoid process fractures. A secondary aim of this chapter is to establish a set of criteria against which the Endobutton will be assessed; as well as the formation of design requirements for the design of the adapted Endobutton device.

Objectives

To achieve this aim, this chapter addresses the following objectives:

1) Produce 3D-printed models of coronoid fractures to use in the qualitative assessment of the Endobutton.
2) Establish a set of criteria that evaluate the fit of the Endobutton, using a 3D-printed imitation and a templating process.
3) Establish a set of conclusions that describe the limitations of the Endobutton as a fixation method through device templating.
4) Establish a set of design requirements to be used in the design of the adapted Endobutton device.

3.4. Materials and Method

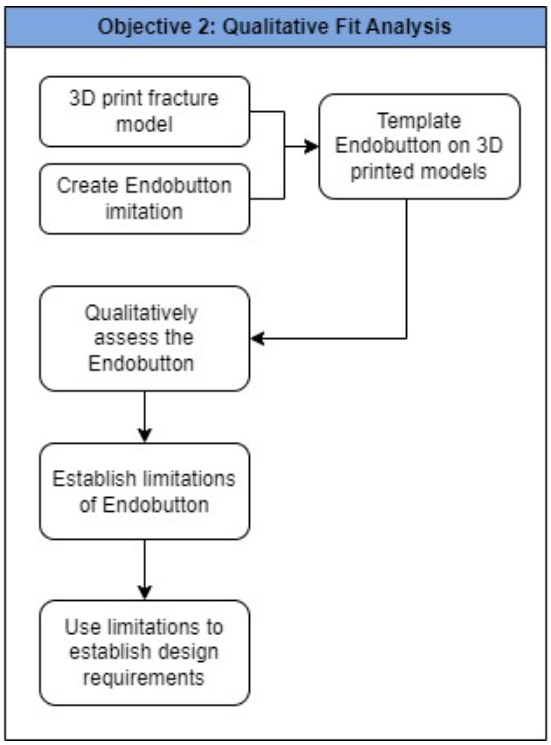

Figure 34: Simplified flow diagram of the methodology followed during the Qualitative Fit Analysis of the Endobutton imitation.

This chapter follows a templating and qualitative evaluation methodology. Templating of orthopaedic devices on 3D printed bones is a well-established and inexpensive method of assessing the fit of the devices (Charilaou *et al.*, 2021; Marinescu *et al.*, 2020). 3D-printed bones serve as anatomical replicas, which facilitate more accurate intervention planning (Marinescu *et al.*, 2020). This method also mitigates the need for additional clearances required to perform osteometric or cadaver-based analyses of the devices, while allowing for continuous use and multiple templating sessions to be conducted. This analysis will be used as a basis for comparison of the adapted design for the Endobutton.

Ethics Clearance

Ethical approval is unnecessary for this aspect of the study as it does not involve live participants or other elements requiring ethical clearance. However, ethical approval was obtained for the CT scans used to create 3D prints of the fractures (HREC: 558/2022), and no identifying or compromising data was used during the printing of the fractures.

3.4.1. 3D Printing of Coronoid Fractures

3.4.1.1. Patient Selection

The selected printed fractures depicted the typical fracture pattern associated with each O'Driscoll type. This resulted in the use of five fractures from the pool of thirty-three patients (specifically patients: 6, 8, 12, 40, and 52). These initial five scans showed the variations (size, shape, or comminution) associated with their respective fracture classifications.

During the later stages of the project, the scope of the printed fractures was expanded to include a total of fifteen patient fractures for a comparative and qualitative fixation analysis. The ten additional patient fractures were selected using a random number generator. The randomness of the selection removed any bias from the selection process. The patient numbers of those who were excluded from this study were disregarded if they were an output from the random number generator. There was no identifying information associated with any of the printed fractures.

3.4.1.2. 3D Printing Process

The STL files of the bones and individual fragments, created during the "Importing and Editing the DICOM File" phase of the fracture mapping, were used for the 3D printing of the models. All bones and fragments were 3D printed using the Zortrax M200 Plus additive manufacturing device (3D printer). They were printed in "Pure White" Zortrax Z-Acrylonitrile Butadiene Styrene (ABS) material.

The STL file of the ulna was imported from the patient file into the Z-Suite 2.32.0.0 software (Zortrax S.A., Olsztyn, Poland). The ulna was orientated on the printer bed so that the articular surface of the

bone faced away from the print raft. This positioning of the ulna was done to ensure that the maximum support was provided between the raft and the bone, while minimising the supports required along the articular or fractured surface.

During the print, a nozzle diameter of 0.4mm and a layer thickness of 0.09mm were used. The print quality was set to high, and the infill density was set at a standard of 30%. The Z-Suite document was exported in a format readable by the printer (Zortrax Printing Code). The code was transferred via USB to the printer and used to print the ulna bone. This process was reiterated for each of the individual fracture fragments, and again for the other patient fractures (Figure 35).

Figure 35: 3D Printed coronoid fractures from four different patients with the fragments attached using a temporary adhesive. Each fracture is notably different from the others.

3.4.2. 3D Printing of Endobutton Imitation

Dimensions for the Endobutton imitation were obtained from a study by Rylander *et al.* (2014). Using the derived dimensions, an imitation of the Endobutton (Appendix F – Endobutton Drawing) was made within the Dassault Systems SolidWorks Computer Aided Design (CAD) program (Velizy-Villacoublay, France) (Figure 36). The recreated Endobutton was uploaded, and 3D printed using a Formlabs Form 2 Resin printer (Somerville, Massachusetts USA). The device was printed using the Formlabs Clear V4 resin with a layer thickness of 0.100mm. Once the Endobutton was successfully printed, it underwent a standardised curing process. This included an Isopropyl Alcohol (IPA) wash cycle of 15 minutes and timed exposure to an ultraviolet (UV) light for 10 minutes to allow for final curing (Figure 37).

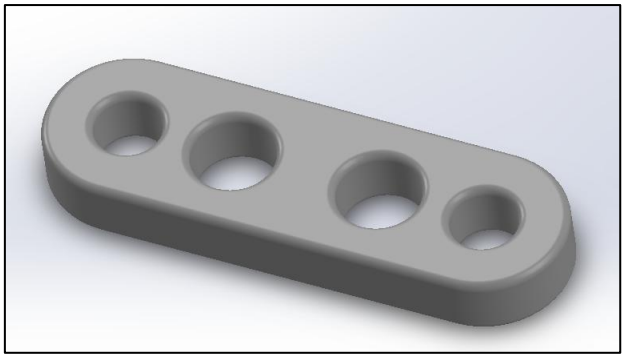

Figure 36: Simplified 3D CAD image of the Endobutton imitation.

Figure 37: 3D Printed Endobutton imitation.

3.4.3. Templating & Qualitative Assessment

3.4.3.1. 3D Printed Endobutton Imitation Assessment

The aim of templating the 3D-printed Endobutton imitation is to establish the device's limitations and to determine potential criteria which would be used to evaluate future device designs.

Using a readily available temporary adhesive, the 3D printed fracture fragments were attached to their respective bones in the correct anatomical position. Three Shoulder and Elbow Fellowship trained Orthopaedic surgeons, each with more than 10 years of upper limb surgical experience, were asked to place/template the Endobutton on the reduced 3D printed fractures in accordance with how the device would be placed during surgical fixation. Using the same temporary adhesive, each surgeon placed the Endobutton over each of the fifteen printed fracture-fragment combinations (Figure 38) and qualitatively evaluated specific factors pertaining to the functionality of the device.

Figure 38: 3D printed Endobutton imitation templated on the 3D printed fractured coronoids of four different patients, using the temporary adhesive.

The 3D printed Endobutton imitation device's performance was evaluated according to the following criteria:

- Ease of device use.
- Ease of attachment to the bone in a surgical setting.
- Fit of the device over the fracture.
- Patient specific suitability and use of the device.
- Stability of the resultant fixation provided by the device.
- Reduction of the fracture.

3.4.3.1.1. Method of Recording Data – Feedback Questionnaire

The functionality of the 3D printed Endobutton imitation was assessed through the conversion of the criteria into a series of qualitative questions. These were compiled into a feedback questionnaire (Appendix G – Qualitative Assessment Questionnaire) which consisted of a total of six questions:

1) Do you think this fixation device is easy to use?
2) This device is easily attached to the bone.
3) This fixation device fits on the fracture.
4) This fixation device would be used in the fixation of the fracture.
5) This fixation device would result in stable fixation of the fracture.
6) The use of this fixation device would result in adequate reduction of the fracture.

Questions one, two, four, five and six made use of a predetermined qualitative assessment scale to evaluate the factors (Table 6). The device's ease of use and ease of attachment to the bone was evaluated using a 1-5 ordinal scale, in which 1 represented a very poor evaluation, 2 was a poor evaluation, and 3 indicated an adequate evaluation. 4 and 5 were deemed as good and very good evaluations respectively (Table 6). Whether the device fit over the respective fractures was assessed using a "Yes or No" answer. The stability and reduction of the fracture was assessed using the same 1-5 scale (Table 6).

Table 6: Qualitative ordinal scale used to evaluate the aspects of the imitated Endobutton.

1 – Very Poor	2 - Poor	3 – Adequate	4 - Good	5 – Very Good

During the initial evaluation three significant limitations were noted: lack of coverage, overhang and incongruency. Lack of coverage refers to the device's inability to sufficiently cover the coronoid fragment. Overhang is defined as the Endobutton extending beyond the fragment or bone, and incongruency indicates that the Endobutton does not conform to the anatomical shape of the coronoid. These limitations were reported when reviewing the fit of the device on the bone (Question 3).

The feedback questionnaire's completion marked the end of the formalised evaluation process, however, a brief and informal discussion of the Endobutton followed. Important points from the discussion were noted and reported on. The Qualitative Assessment feedback forms were collected, and the results were transcribed into a Microsoft Excel spreadsheet for data collection and analysis.

3.4.4. Data Analysis and Statistical Methods

All responses to the Quantitative Assessment Questionnaire were collected and transcribed into a Microsoft Excel Spreadsheet. This ordinal data was exported to IBM SPSS Statistics v.28 (Armonk, NY: IBM Corp) for statistical data processing. To evaluate the performance of the 3D printed Endobutton (control) device, the mode of responses for each question was calculated. Since we were interested in the most frequently occurring response from the surgeons, the mode was chosen as the central tendency of the dataset.

3.5. Results

According to the surgeons, the 3D printed Endobutton imitation was rated "Good" (mode = 4) for ease of use, and "Poor" (mode = 2) for its attachment to a bone.

The imitated Endobutton only fit 33% of the 3D printed fractured coronoids, with the most common response to the question regarding fit being "No" (mode = 2). The Endobutton imitation was deemed

an “Adequate” (mode = 3) fixation option for the fractures assessed. It was also indicated that it would result in “Poor” (mode = 2) post-fracture stability and “Poor” (mode = 2) fracture reduction. The overall responses are presented in Table 7.

Table 7: Table showing the overall percentages of the reported responses for each question.

Questions	Options	Responses (%)
Q1: Do you think this fixation device is easy to use?	Very Poor	0%
	Poor	0%
	Adequate	0%
	Good	67%
	Excellent	33%
Q2: This device is easily attached to the bone?	Very Poor	33%
	Poor	33%
	Adequate	33%
	Good	0%
	Excellent	0%
Q3: This fixation device fits on the following fractures?	Yes	33%
	No	67%
Q4: This fixation device would be used in the fixation of the following fractures?	Very Poor	26%
	Poor	16%
	Adequate	29%
	Good	20%
	Excellent	9%
Q5: This fixation device would result in stable fixation of the fracture?	Very Poor	29%
	Poor	31%
	Adequate	18%
	Good	20%
	Excellent	2%
Q6: The use of this fixation device would result in adequate reduction of the following fractures?	Very Poor	27%
	Poor	38%
	Adequate	22%
	Good	11%
	Excellent	2%

For Type 1 fractures, there were eleven reported instances of limitations, and the Type 2 fractures had twenty instances. The most frequently reported limitation was incongruency at 55% for Type 1 and 50% for Type 2. The second most prominent limitation for Type 1 fractures was overhang, whereas for the Type 2 fractures it was insufficient coverage. The reported rates of lack of coverage, overhang and incongruency are elaborated on in Table 8.

Table 8: Limitation response rates (Type 1 n=11, Type 2 n=20).

Fracture Type	Limitation	Responses, n (%)
Type 1	Lack of Coverage	1 (9.1)
	Overhang	4 (36.4)
	Incongruency	6 (54.5)
Type 2	Lack of Coverage	7 (35.0)
	Overhang	3 (15.0)
	Incongruency	10 (50.0)

During the informal discussions, the surgeons noted that the commercially available Endobutton device is small and easily lost in the surgical field. It was also noted that the device does not have 'railroad' sutures which could be used to guide the device into place during surgery.

Interobserver Reliability

There were too few data points to determine the interobserver reliability for Questions 1 and 2. The ICC was calculated for the ordinal data for Questions 3 to 6. Question 3 yielded a value of 0.45 (95% CI: -0.34 - 0.80), reflecting poor reliability between the device ratings. Questions 4 to 6 yielded moderate reliability results with their ICC values equalling 0.71, 0.70 and 0.55 respectively (Table 9). Question 4 to 6 all had statistically significant p values <0.05.

Table 9: Interobserver reliability.

	Intraclass Correlation	95% Confidence Interval		F Test With True Value 0			
		Lower Bound	Upper Bound	Value	*df*1	*df*2	Sig
Question 3	0.45	-0.34	0.80	1.80	14	28	0.091
Question 4	0.71	0.31	0.90	4.69	13	26	<0.001
Question 5	0.70	0.31	0.88	3.50	14	28	0.002
Question 6	0.55	0.03	0.82	3.26	14	28	0.004

3.6. Discussion

To address the primary research question this chapter aimed to produce 3-dimensional models of various coronoid fractures that could be used in the qualitative assessment of the currently used Endobutton. The secondary research question of *"Can a set of criteria which effectively evaluate the functionality of an Endobutton be created?"* was indirectly addressed as part of the assessment process.

The templating and assessment study shows that while the Endobutton receives a “Good” rating for the ease of use, it has “Poor” ratings for its attachment to the bone and only fits 33% of the fractures in the cohort. Despite being rated “Adequate” for fixation, the Endobutton is predicted to result in “Poor” fracture reduction and post-surgical stability. The Endobutton device is frequently considered incongruent with the anatomy of the coronoid. Notably, the Endobutton’s small size is an issue as it may lead to difficulty in handling during surgical procedures, with the device possibly getting lost in the surgical field. These findings indicate that the commercially available Endobutton, as imitated in this study, is not an ideal method of fixation for comminuted coronoid fractures. These results underscore the notion that the Endobutton requires improvements to optimize its role in coronoid fracture fixation.

In a retrospective review by Altan *et al.* (2016) they acknowledge that the Endobutton allows for the maintenance of concentric anatomical reduction without major complications such as the device migrating or slipping. Similarly Arrigoni, D’Ambrosi *et al.* (2016) reported anecdotal evidence that the Endobutton prevents clinical instability due to varus and valgus stress. These retrospective reviews used the post-operative functional score outcomes to judge the efficacy of the fixation method. However, to the best of this author’s knowledge, there were no existing papers wherein the Endobutton itself was the focus of a quantitative or qualitative evaluation as a viable method of coronoid fracture fixation prior to its clinical use. Therefore, this gap in the literature meant that there are no studies directly comparable to the findings of this research, complicating efforts to align these findings with previous research.

Despite the lack of comprehensive evaluations, the anecdotal reviews of the Endobutton can be contrasted with the findings of this study. Unlike the outcomes reported by Altan *et al.* (2016), this study found that “Poor” stability results are anticipated from the use of the Endobutton. Similar contrasts can be drawn between the predicted poor stability outcome, with the recommended use in Type 1 fracture treatment by Salwan *et al.* (2023). Potential reasons for these contrasts include the joint immobilisation during the first few weeks of post-operative care and how this influences the healing of the joint not being considered during the evaluation. An alternative reason might be Altan *et al.* (2016) use of a small patient population, which did not accurately represent the device’s efficacy and associated complications.

A secondary comparison can be drawn between the methodology employed in this study and those used in broader studies, particularly those unrelated to fixation methods specific to the coronoid process. Marinescu *et al.* (2020) demonstrates through an extensive literature review, that the use of 3D printing has significant advantages in Orthopaedics. They highlight how 3D-printed templates are

extensively used for evaluating pre-contouring fixation devices. This widespread adoption of 3D-printed models emphasizes the validity of the methodology used in this study., which relied heavily on 3D-printed bone templates for evaluating coronoid fixation methods.

Additionally, Charilaou *et al.* (2021) show that 3D printed bones can be an effective tool in assessing the fit of available fixation methods. Their study provides insights into the use of 3D printing in determining the appropriateness of fixation devices, which forms the foundation of the methodology of this research. By adopting the techniques outlined by Charilaou *et al.* (2021), and the extensive research and favourable outcomes reported by Marinescu *et al.* (2020), emphasize the significant potential of 3D printing technology in the development of orthopaedic fixation devices.

In conclusion, while there is only anecdotal evidence that suggests that the Endobutton is effective in maintaining anatomical reduction and preventing instability, this study's findings highlight significant qualitative design concerns associated with the commercially available Endobutton. These differences underscore the need for more comprehensive, quantitative, and qualitative evaluations of this fixation method, prior to its use in a clinical setting, to better understand its potential, limitations and potential measures which can be implemented to mitigate these challenges.

3.6.1. Resultant Design Requirements

There remains a considerable amount of uncertainty regarding the optimal method of coronoid fracture fixation (Altan *et al.*, 2016; Liu *et al.*, 2018; Salwan *et al.*, 2023). And the various downsides of the currently available methods (such as lack of anatomical similarity and unsuitability, high cost, lack of coverage and high post-operative complication rates) only fuel this uncertainty (Chen *et al.*, 2018; Gray *et al.*, 2013; Pai *et al.*, 2009; Zhang *et al.*, 2020). The Endobutton, which is suggested as an alternative fixation device, has shown to be capable of holding the small multi-fragmented bones together (Salwan *et al.*, 2023). Nonetheless, there is still room for improvement, as noted by this study, and Altan *et al.* (2016) and Salwan *et al.* (2023) who both call for an anatomically pre-contoured plate

An objective of this study was to establish requirements which would be used to drive the design of a fixation device which would resemble an anatomically pre-contoured endobutton in attempt to mitigate the found limitations. To address these issues, potential design requirements for an alternative fixation device could include the resemblance of an anatomically pre contoured endobutton that does not require screws, ensuring better suitability for small fragments. Anatomical similarity is important, therefore necessitating a pre-contoured design which fits more appropriately over the bone for maximum anatomical restoration and stability. The pre-contoured shape and anatomical similarity requirement would aim to resolve the high incidence of incongruency and overhang between the device and the bone. Finally, increasing the size to help maintain its ability to

hold multiple small bone fragments together effectively, while enabling easier use and visibility of the device.

3.6.2. Limitations

The lack of comparable literature specifically addressing the Endobutton's efficacy in treating coronoid fractures limits the comparisons which can be drawn in this study. Another limitation is the use of a 3D-printed imitation of the fixation device, which introduces a level of inaccuracy due to printer tolerances and post-printing processes. Furthermore, the absence of established standards for evaluating the Endobutton makes it challenging to identify and assess the critical factors required for the device's optimal performance.

3.6.3. Key Findings in Chapter

1) **Effectiveness of the Endobutton:** The Endobutton is rated "Good" for ease of use but received "Poor" ratings for attachment to the bone and overall fit of the device, covering only 33% of the fracture models. It is considered to be "Adequate" for fixation and "Poor" fracture reduction and post-surgical stability.
2) **Anatomical Incompatibility:** A significant limitation of the Endobutton is the high reported rate of incongruency with the anatomy of the coronoid. The device's small size leads to possible handling difficulties.
3) **Literature Gap:** There is a lack of comprehensive quantitative or qualitative assessments of the Endobutton's efficacy in coronoid fracture treatment, making it difficult to compare this study's findings with those of existing studies. The available research is anecdotal, retrospective and focuses on the post-operative functional score as the measure of effectiveness.
4) **Validity of 3D Printing:** This study's methodology is validated by extensive literature which highlights the numerous advantages of 3D printing in Orthopaedics.
5) **Design Requirements of Adapted Endobutton:** Potential design requirements include creating a small anatomically pre-contoured endobutton that does not require screws. The device should incorporate the suture lasso technique and an increase in size to effectively hold the multiple bone fragments.

3.7. Chapter Conclusion

The qualitative assessment of the Endobutton as a method of coronoid fracture fixation reveals aspects of the device that require improvement. Through the production of accurate 3D models, it is possible to evaluate the Endobutton's fit and efficacy. While the Endobutton is relatively easy to use, it falls short in key aspects, including attachment to the bone, fracture reduction and post-surgical stability.

The device demonstrates poor anatomical congruency and fails to provide adequate coverage of the fracture fragments. Discussions with surgeons also reveal significant size issues.

The establishment of the set of evaluation criteria and subsequent qualitative assessment underscore the necessity for substantial design changes. By addressing these design recommendations, the forthcoming adaptation of the Endobutton will aim to provide a possible solution to these limitations.

3.7.1. Chapter Outcomes

The aim of this chapter was to qualitatively evaluate and analyse an Endobutton's ability to fixate coronoid process fractures. This aim was addressed through four objectives:

Production of 3D Models: The first objective was to produce 3D models to use for the qualitative assessment. This was done using established 3D additive printing techniques to create models rendered from the acquired CT scans.

Establishment of Evaluation Criteria: The second objective encompassed the establishment of a set of criteria for evaluating the Endobutton and future potential designs. This was achieved through discussions with 3 Fellowship Elbow Surgeons and a thorough review of literature. These criteria were used to create the Qualitative Assessment Questionnaire.

Set of Limitation Conclusions: The third objective addressed the main aim of the chapter by identifying the limitations of the commercially available Endobutton. These conclusions were drawn from responses to the Qualitative Assessment Questionnaire which was completed after templating the 3D printed imitation on the 3D coronoid fracture models. Additionally, discussions amongst the participating surgeons informed these conclusions.

Set of Design Requirements: The final objective was to create a set of requirements to guide the design of the adapted Endobutton. This objective was successfully achieved by reviewing the complications noted in literature, the ratings in the Qualitative Assessment Questionnaire, and the discussions among the surgeons involved in the study. These identified limitations were then translated into requirements which aimed to mitigate their predecessor limitations.

4. Chapter 4: Design and Development of Adapted Endobutton

4.1. Chapter Introduction

This chapter describes the iterative design process used for the development of an adapted Endobutton fixation device. It aims to develop a fixation device that addresses the need for a pre-contoured adapted Endobutton which is suitable for the treatment of smaller coronoid fracture types. This design's purpose is to provide improved reduction and fixation, while mitigating the limitations of the currently used Endobutton. The scope of this chapter encompasses the design journey, from initial design inputs following fracture mapping, to concept generation and the final refined design.

This chapter also discusses the rapid prototyping process, including the selection of materials and the 3D printing techniques used. Additionally, the proposed verification and validation testing procedures are outlined, aiming to ensure the viability of the device.

4.2. Chapter Aims and Objectives

Aim

The aim of this chapter is to design and develop an adapted Endobutton coronoid fracture fixation device.

Objectives

The chapter objectives are:

1) Establish the requirements and specifications of the adapted Endobutton design.
2) Produce conceptual and detailed design of an adapted Endobutton coronoid fracture fixation system.
3) Review the design using the design requirements to confirm the fit and viability.

4.3. Design of Adapted Endobutton Device

4.3.1. Planning

The design process for the adapted Endobutton follows the standardised methodology, beginning with creating conceptual designs and progressing a selected design through to the detailed phase. Initially, multiple possible solutions are generated to meet the requirements determined during the Templating & Qualitative Assessment. This is done using simple sketches and CAD models. The range of generated designs undergo review to determine the most viable option.

The fracture maps and heat maps produced in Chapter 2: Coronoid Process Fracture Mapping serve as a reference in the initial stages of the process. They aid in the design by providing insights into the

dimensions of the fractures and the resultant fragments that the device would need to accommodate; as well as if the device addresses the critical fracture patterns. Additionally, the reference fractures helped identify and determine the limitations of the currently used Endobutton (Chapter 3: Qualitative Fit Analysis). By understanding these limitations, design requirements were established to effectively address and potentially mitigate the limitations in the new design.

Upon the confirmation of the conceptual design's compliance with the requirements, the detailed design phase commences. This stage involves the refinement of the chosen conceptual design until a finalised versions is achieved. This entails the generation of a detailed CAD model, and a review of adherence to the requirements to ensure the implant fits and operates as intended.

A flow diagram (Figure 39) summarises and lays out the overall design methodology, including the establishment of the limitations of the currently used Endobutton.

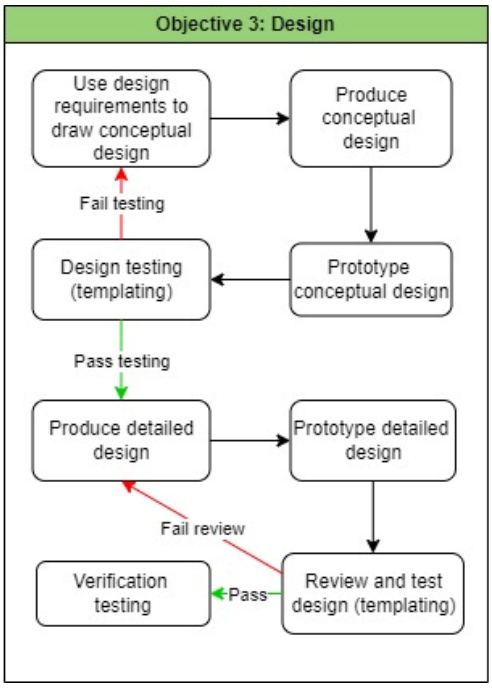

Figure 39: Overview of the design methodology to be used during the production of the adapted Endobutton device.

4.3.2. Initial Design Concepts

The initial design ideas were conceived through a series of discussions with Professor Stephen Roche before the commencement of the project. Once the project was underway, further design refinements were added through the continued discussions with Professor Roche.

4.3.3. Design Requirement

4.3.3.1. Functional Requirement

The functional requirements serve as the primary motivator during the design process. These requirements outline the desired optimal outcomes for the adapted Endobutton.

Primary Function

The primary functional requirement of the designed device is to effectively reduce the coronoid process fracture. The incorporation of suture-techniques will allow the device to provide adequate tension to the reduced fracture. An effective reduction would restore the normal anatomy.

Secondary Function

As a secondary function, the device needs to provide reattachment of the joint capsule and musculotendinous tissue (Brachialis muscle) via a whip suture. This is intended to enhance the comprehensiveness of the device.

Performance Benchmarks

The performance benchmarks revolve around the device's ease of use, efficacy and compatibility; and are addressed in Chapter 5: Design Verification & Validation. The device aims to provide adequate tension to the reduced fracture, promoting stability and functionality of the joint. The compatibility requirements prioritise the compatibility of the device with existing surgical equipment. This is intended to enable an easy integration of the device into established surgical procedures, therefore ensuring smooth and efficient placement. The performance benchmarks also include the flexibility and bendability of the device, which ensure the device is adaptable to varying anatomical structures and surgical scenarios.

The device's performance and efficacy is evaluated based on its ability to effectively reduce the fracture (therefore achieving anatomical restoration), and to produce reliable fixation and perceived overall procedural outcomes.

4.3.3.2. Technical Requirements

The device needs to have dimensions of 5mm to 30mm in total length (top to bottom), with an optimal range of approximately 10-20mm. The width of the device (right to left) should range from 15mm to 40mm, with the desired width being between 20-25mm, as derived from the fracture mapping. It requires a shape that matches the coronoid anatomy. It also needs three points of fixation – one central, one lateral, and one medial – for stabilisation of the fracture, and to accommodate an additional attachment hole for a whip suture (No.2 non-absorbable) for joint capsule attachment. Additionally, it requires a spiked surface to grip the bone, capsule, and soft tissue. Initial considerations

include a with or without buttress feature, with the final design including this feature. The device is intended to make use of No.2 non-absorbable fibre-wire sutures. The final appearance should have a spiked surface with a T-shape and include some elements of the Endobutton CL Ultra Fixation System (Smith & Nephew).

Potential Manufacturing Material

Titanium would be the preferred material for the construction of the adapted Endobutton device due to its established efficacy and compatibility in fracture fixation and, is used already with the existing Endobutton. High-molecular-weight polyethylene, while a good potential alternative due to its biocompatibility and compatibility with post-operative MR scans (unlike titanium), would necessitate extensive additional testing to ensure the device's safety and efficacy. An argument could be made to produce the device in a bio-absorbable material which would avoid the need for it to be removed. However, the use of bio-absorbable materials would require a significant amount of material studies, biocompatibility, and biomechanical testing. Titanium, therefore, offers the most reliable choice, as it aligns with established standards and minimises the need for additional validation.

This study aims to verify and validate the design itself, and not the materials. Therefore, this study used hard plastic as the material during the rapid prototyping process as it is the easiest and readily available. This was done through additive manufacturing using Formlabs (Somerville, Massachusetts USA) Clear V4 resin-based 3D printing.

4.3.3.3. Additional Requirements

Several additional requirements need to be considered when designing the adapted Endobutton, as discussed below. Although these requirements are considered, they do not serve as primary influences on the design and its verification and validation.

User Requirements

In the design phase of the adapted Endobutton, specific user requirements are not identified. However, considering the intended application of the final product as an Orthopaedic device, the users of this device are expected to be doctors qualified in Orthopaedics. Ideally, users should have prior surgical experience with Endobuttons as fixation methods for coronoid fractures; however, an indirect objective of this design is simplicity, which would allow for widespread use without the need of prior experience.

Regulatory Requirements

During this initial design, evaluation and verification, regulatory requirements are not a primary concern as the design is being assessed, rather than the device itself as an end product. Once the

overall design is verified and validated, the regulatory requirements are considered as part of the potential methods of manufacturing.

The titanium manufacturing process that would be used would have to comply with the same requirements as those established for the manufacturing of orthopaedic implants. Such a standard would include ISO 5832, which addresses the use of metallic materials for surgical implants. During the manufacturing process, ISO standard 9585 which is related to the bending strength and stiffness of bone plates, would be considered.

Safety and Reliability Requirements

Similarly to the regulatory requirements, the safety and reliability requirements are considered during the manufacturing of the device. Measures should be taken to eliminate sharp edges unless they are explicitly required, thus taking into consideration the safety of the surgeon and the patient. These considerations ensure that the design minimises any potential damage to the patient. The reliability of the design is judged during the review process, and the reliability of the functional implant would be reassessed once again after manufacturing.

4.3.3.4. Resultant Design Specifications

The requirements set out above lead to the following design specifications:

Table 10: Design specifications for the adapted Endobutton based on the functional and technical design requirements.

Specification	Description	
Dimensions	Length	5mm(±1mm) < y < 30mm(±1mm)
	Width	15mm(±1mm) < x < 40mm(±1mm)
	Thickness	1mm(±0.5mm) < z < 3mm(±0.5mm)
Shape	Curved shape – follows the curvature of the coronoid.	
	Convex shape – follows convexity of ulna bone.	
Features	Suture holes	2 or more
	3 points of fixation	
	Hole for whip suture	
Additional Characteristics	Bendable/flexible	

Each design iteration features a single Endobutton which incorporates all the specified design requirements. When referring to the shape of the device, the curvature of the coronoid refers to the angulation (downwards and upward slopes) from the anteromedial facet to the tip on the anterior view of the coronoid (shown by the red arrow in Figure 40A). The convexity of the device corresponds

to the convex shape of the anterior surface of the coronoid as it becomes part of the most proximal part of the ulnar shaft (shown by the blue arrow in Figure 40A & B).

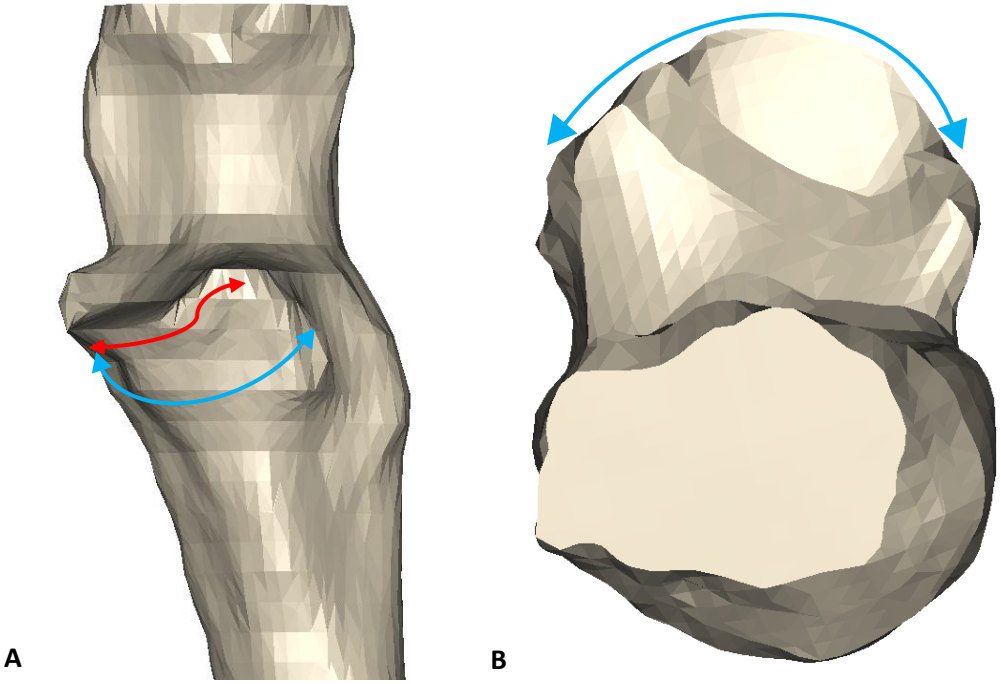

Figure 40: A) Anterior view of the coronoid showing the angulation (red arrow) and convexity (blue arrow) of the process. B) Superior view of the coronoid showing the convexity (blue arrow).

This device is designed to be used with readily available stock components such as sutures, drills, and all other surgical equipment. The goal of component compatibility is to mitigate the need for the design and development of additional components and streamline the manufacturing process.

4.3.4. Testing and Evaluation Criteria

3D printed fractures, rapid prototyping, and templating are used to test the size, shape and impingement of the device. This is done after placing the device prototype on the 3D printed fracture used to evaluate the fitment of the Endobutton imitation as in Chapter 3. During the initial design phases, the technical requirements as above of size and shape became the primary focus prior to the design being rapidly prototyped using 3D printing. Finally the functional requirements will be assessed following the same format as that used to assess the Endobutton imitation, with the qualitative fitment analysis questions being asked in an informal discussion.

The evaluation criteria mainly focus on the technical requirements which dictate the overall shape, size and features of the design; as well as determine the suitability of the design before being tested for functionality. These criteria include:

- If the design is an appropriate length.
- If the design is an appropriate width.
- If the design is an appropriate thickness.
- If the design is an appropriate shape
- If the design has 2 or more suture holes.
- If the design has 3 points of fixation.
- If the design has a hole for a whip suture.

The viability of the design is based on criteria which assess the physical nature of the design in relation to the fractured coronoid and the respective fragments. These criteria include:

- If the design is an appropriate size relative to the surgical site.
- If the design is an appropriate size relative to the coronoid
- If the design fits over the fracture site and fragment.
- If the design agrees with the curvature of the bone.
- If the design protrudes into the radial notch space.
- If the design protrudes past the coronoid tip.

4.3.5. Design Methodology: Conceptual Design Stage

4.3.5.1. Introduction of Conceptual Design

The conceptual design purpose was to provide a vast number of designs that could potentially address the challenges with the currently used Endobutton. The rationale for producing various designs was to increase the possibility of finding a successful solution. The conceptual design was the first step in creating a device that met the requirements outlined above and to mitigate the limitations established in Chapter 3.

4.3.5.2. Problem Statement and Design Objectives

"An adapted Endobutton can be designed to be used in the treatment of coronoid process fractures."

This problem statement led to the following design objectives:

1) Produce numerous potential designs.
2) Confirm the most suitable design using a through revision of the design requirements and evaluation of design criteria.

4.3.5.3. Generation of Design Concept

The initial conceptual designs were generated through discussions with Professor Roche, basic sketches, and simplified CAD models. All CAD models were created using the Dassault Systems

SolidWorks CAD program (Velizy-Villacoublay, France), and saved in STL (Stereolithography) format to streamline rapid production using 3D printing techniques.

Design 1:

The first design of the adapted Endobutton mimicked the Y-shaped plates that are currently commercially available, with the alteration of a mesh or net-like aspect between the arms of the Y (Figure 41). The mesh/net was thought to be able to catch and hold all the fragments of the coronoid process fracture, regardless of the sized of the fragments. However, the design was not feasible as it would interfere with the attachment of the ligaments and muscular anatomy of the area. This was the outset design during the initial stages of the project before any in-depth research was conducted and design inputs were discussed.

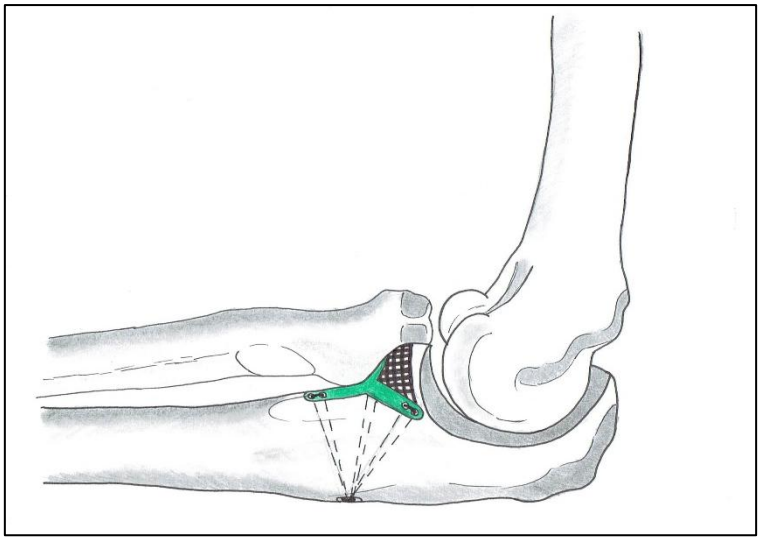

Figure 41: Drawing of the initial design 1 (Image drawn by author – N. Mason).

Design 2:

This design resembled a "T", featuring a long horizontal bar which would be positioned transversely across the lateral-to-medial aspect of the coronoid. A secondary bar was placed at the midpoint of the horizontal bar, which extended vertically downwards along the ulnar shaft (Figure 42). While retaining the initial 3-pronged element, this design differed significantly in shape. The transverse bar of the device was curved to accommodate the convexity of the coronoid. The overall size was increased to encircle most of the lateral-to-medial width of the coronoid and to allow for this device's application in the fixation of larger fragments.

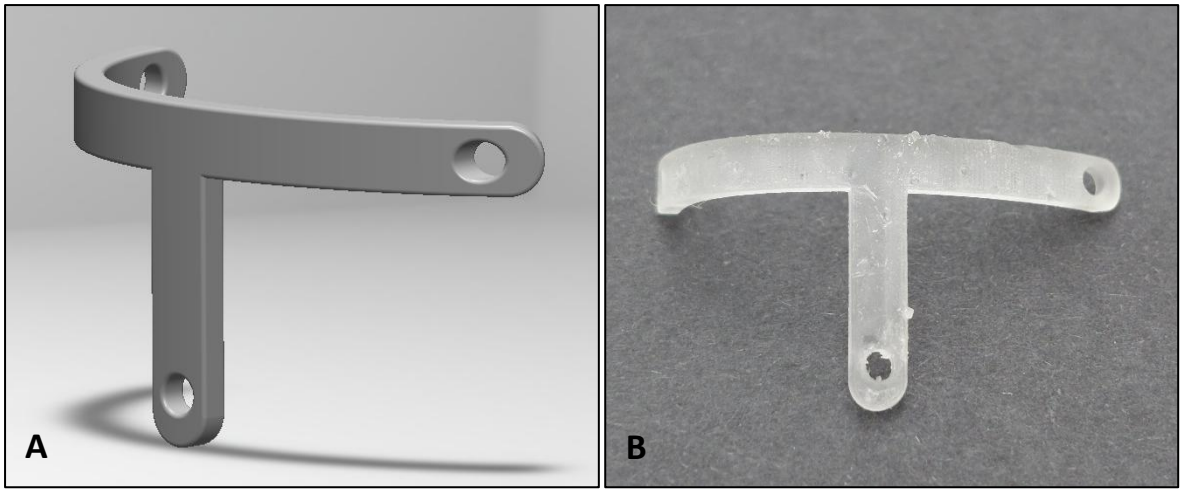

Figure 42: (A) Simple 3D CAD model of the T-shaped design shown from an oblique view to depict the curvature needed to match the convexity of the coronoid surface. (B) Physical prototype of design, printed in clear resin, to be used for testing.

During the development of this design, a secondary version was also created. This variant consisted solely of the straight transverse bar of the design (Figure 43). The idea behind this version aimed towards substituting the small and flat Endobutton with a larger curved version that would cover the coronoid while taking the shape of the bone into account.

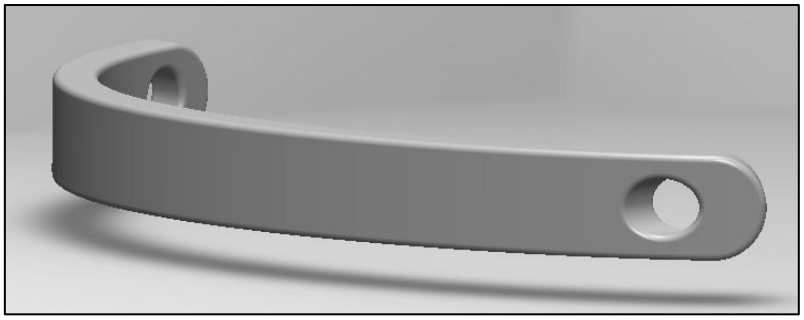

Figure 43: Simplified 3D CAD model of the curved transverse bar of the design.

Figure 44: Physical prototype, printed in clear resin, to be used for testing.

After being reviewed, it was determined that certain aspects of the design held merit while others required adjustment. The downwards buttressing bar was deemed advantageous as it would allow for improved resultant stability and offered an additional point of attachment. The straight transverse bar

was seen as less beneficial as it did not allow for the buttressing of the smaller tip fragments. Therefore, it was suggested that some curvature be introduced to better accommodate the shape of the coronoid tip.

Design 3:

The third design iteration maintained a "T" shape concept while incorporating a splined curvature to match and accommodate the shape of the facets and tip of the coronoid (Figure 45). By integrating the curvature, the adapted Endobutton aimed to provide a better anatomical fit, allowing for better fracture fixation. Additionally, this design also maintained the vertical arm/bar that would lie along the vertical (superior-inferior) axis of the coronoid shaft.

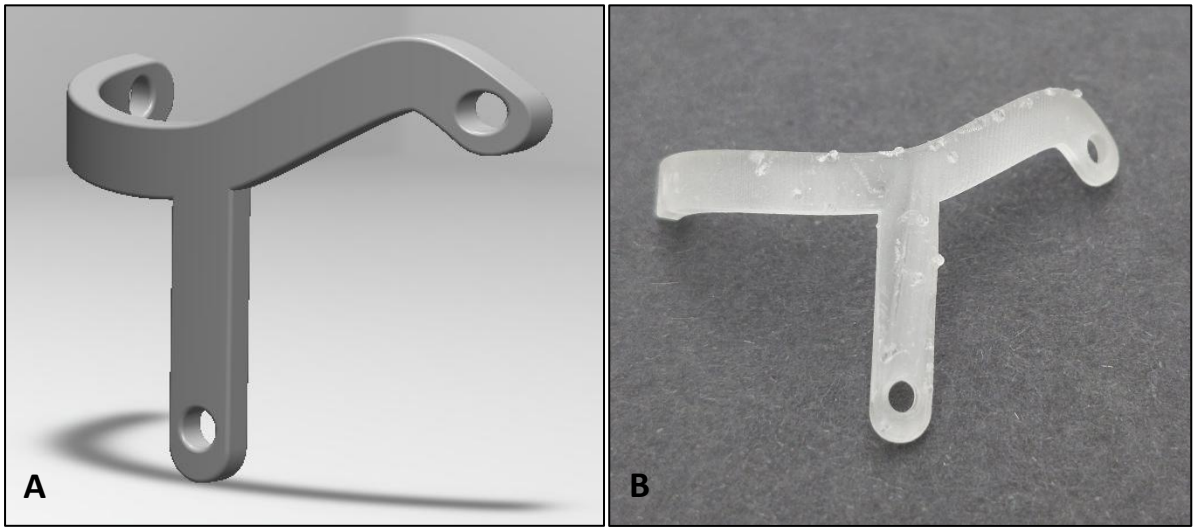

Figure 45: (A) Simplified 3D CAD model of Design 3 which incorporates a curvature to mimic that of the facets and tip of the coronoid. (B) Physical prototype of design to be used during testing.

This design showed potential and underwent 3D printing using the same techniques used to print the imitated Endobutton. This rapid prototyping provided the opportunity for a physical evaluation of the design to take place. The physical evaluation revealed the design was too big and the convexity of the device only matched the larger anatomical variations of the ulna. Despite the large size, Professor Roche approved of the spline curvature incorporated to accommodate the coronoid tip's anatomy. The suggestion was made that the lateral (radial notch side) (right side in Figure 45) of the spline be elongated, and the anteromedial side be shortened.

The production of a physical prototype of the design also enabled the refinement of the dimensions (Table 11). After considering the suggested changes, the device aimed for a total length of approximately 20-25mm. Professor Roche expressed a preference for the vertical buttressing arm, but this element needed to be central to the peak of the spline. Additionally, an extra hole at the peak of the spline was deemed necessary in order to accommodate a whip suture. Ultimately, the envisioned

design resembled a triangular shape, rather than an anatomical shaped spline. To fulfil these specifications, a new design was developed.

Table 11: Updated dimension requirements (red) of the adapted Endobutton design.

Dimension	Value
Length	5mm < y < 25mm
Width	15mm < x < 25mm
Thickness	1mm < z < 2.5mm

Design 4.1 & 4.2:

The fourth concept incorporated all the advantageous aspects of the previous designs into a smaller, curved arrow (↑) shaped device (Figure 46). The arrow shaped curvature accommodated the anatomy of the tip while fitting over a large portion of the coronoid, without the device being an excessive size. Retaining the downwards bar aspect ensured the provision of an additional buttress. This design also included the additional hole at the apex of the arrow which could accommodate a whip suture for soft tissue attachment. Alternatively, the hole at the peak could also serve as a potential additional point of fixation using a vertically placed suture. The convexity remained to accommodate the shape of the coronoid; however, the angles were adjusted to less acute and more generalized, allowing the device to fit a larger range of anatomical variations.

Two iterations of the design were developed: one was symmetrical (Figure 46) and one asymmetrical (Figure 47). Both of these designs were rapidly produced and subjected to a physical evaluation.

Design 4.1 - Symmetrical

The arms of the symmetrical version were the same length, and were intended to provide uniform forces across the coronoid to help improve fixation results (Figure 46).

The symmetrical design underwent a formalised templating and evaluation. Although the design initially seemed suitable, the templating results showed that the symmetrical version presented an issue: the laterally positioned arm protruded into the radial notch. As a consequence, the drill holes required for the sutures would be made too far laterally, risking interference with the radial notch. This could also result in impingement of the device, radial articulation issues, lead to device failure, and potentially risk the healthy functioning of the elbow joint.

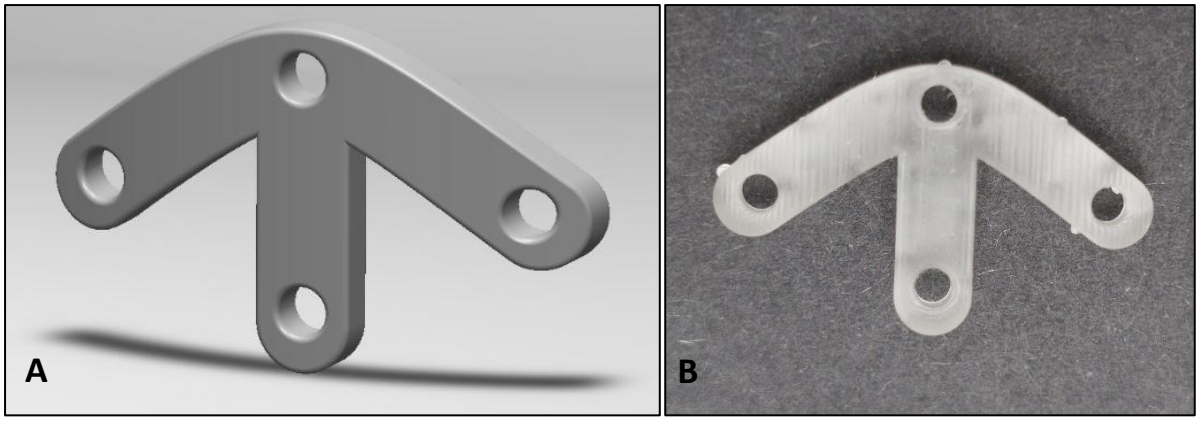

Figure 46: (A) Simplified 3D CAD mode of the symmetrical curved arrow design. (B) Rapidly produced prototype to be used for testing.

Desing 4.2 - Asymmetrical

The asymmetrical design was produced in response to the unfavourable results of the symmetrical design. The right arm of the asymmetrical design (which would be positioned laterally towards the radial notch) was shortened. The creation of the asymmetrical variant was aimed at accommodating the shorter distance between the tip and the radial notch and avoid the possibility of impingement of the device.

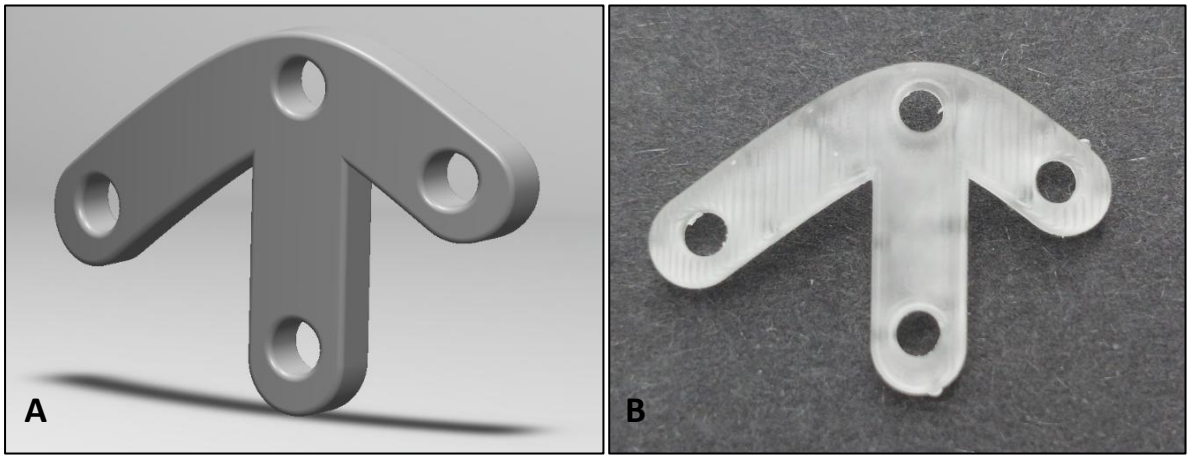

Figure 47: (A) Simplified 3D CAD model of the asymmetrical curved arrow design. (B) Rapidly produced prototype to be used for testing.

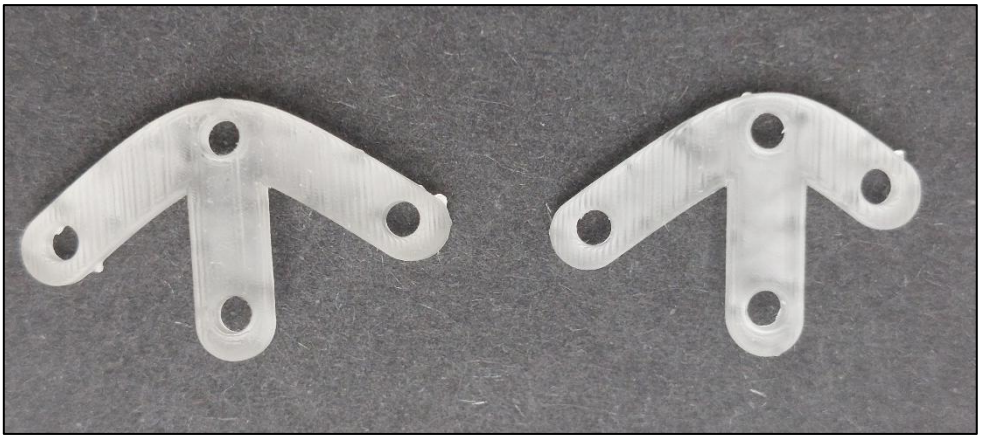

Figure 48: Symmetrical (Left) and Asymmetrical (Right) design of adapted Endobutton.

4.3.5.4. Evaluation Criteria and Selection Process

As previously mentioned (Testing and Evaluation Criteria), the evaluation criteria were primarily focused on the technical requirements of the design (Table 12). These requirements dictated the overall shape, size, and features of the design. They included:

- If the design was an appropriate length.
- If the design was an appropriate width.
- If the design was an appropriate thickness.
- If the design was an appropriate shape
- If the design had 2 or more suture holes.
- If the design had 3 points of fixation.
- If the design had a hole for a whip suture.

Table 12: Review of design against the technical requirements for adapted Endobutton.

	Length	**Width**	**Thickness**	**Shape**	**2 or more suture holes**	**3 points of fixation**	**Hole for whip suture**
Design 1	No	No	No	No	Yes	Yes	No
Design 2	No	No	Yes	No	Yes	Yes	No
Design 3	No	No	Yes	No	Yes	Yes	No
Design 4.1	Yes	Yes	Yes	Yes	Yes	Yes	Yes
Design 4.2	Yes	Yes	Yes	Yes	Yes	Yes	Yes

Selection Process

The most promising designs underwent rapid prototyping using 3D printing techniques. The designed devices were produced in the Division of Biomedical Engineering laboratory spaces using a Formlabs (Somerville, Massachusetts USA) Form 2 resin printer, and were printed in the Clear V4 Formlabs resin.

Once printed, each of the designed devices were informally templated on the 3D printed fractures using a temporary adhesive. An evaluation of the device was carried out using the criteria which determined the viability of the design (Table 13). These criteria, which assessed the physical nature of the device in relation to the fractured coronoid and fragments, included:

- If the design was an appropriate size relative to the surgical site.
- If the design was an appropriate size relative to the coronoid
- If the design fit over the fracture site and fragment
- If the design agreed with the curvature of the bone
- If the design protruded into the radial notch space
- If the design protruded past the coronoid tip

Where designs did not meet the criteria, suggestions were made to improve them. The protrusions of the device past the boundaries of the anatomy of the coronoid proved crucial in determining the length of device aspects. Despite meeting all the technical requirements, several designs failed to satisfy the criteria which established the viability of the design as an effective method of fixation.

Table 13: Revision of the criteria which establish the viability of the device design.

	App*. Size (Surgical Site)	App*. Size (Coronoid)	Length	Width	Shape	Fit	Curvature	Protrusion
Design 1	Unknown	No	Yes	Yes	No	No	No	Unknown
Design 2	No	No	Yes	Yes	No	Yes	No	No
Design 3	No	No	No	No	Yes	Yes	No	No
Design 4.1**	Yes	Yes	Yes	Yes	Yes	Yes	Yes	Yes
Design 4.2**	Yes	Yes	Yes	Yes	Yes	Yes	Yes	No

*App. = appropriate
**Design 4.1 = Symmetrical, Design 4.2 = Asymmetrical

4.3.5.5. Chosen Concept

The fourth design, which featured the asymmetrical arrow shape, was the chosen concept (Figure 47). This design met all the technical requirements and showed the most potential as a viable fixation method that would address the functional requirements. It had the most promising feedback during the informal templating. When roughly evaluated, this design averaged “Good” outcomes, compared to the averaged “Poor” outcomes from the imitated Endobutton.

Rational and Benefits

The asymmetrical design allowed for all the technical requirements to be met. This device featured an increased size which would ensure the device was easier to manage. The increased size of the design

also allowed the majority of the fractured coronoid to be covered, without being too large to result in an impingement with other structures. This design was also advantageous by having multiple points of fixation and an additional hole for the inclusion of a whip suture for soft tissue attachment.

4.3.6. Design Methodology: Detailed Design Stage

The detailed design stage focused on refining the details and features of the chosen design concept. The iterative process aimed to enhance the device's viability and ensure it met all the functional requirements.

4.3.6.1. Detailed Design Overview

The chosen design was the asymmetrical arrow-shaped device, which featured 3 fixation points and an additional point to incorporate a whip suture. Figure 49 depicts a simplified CAD model of the chosen design.

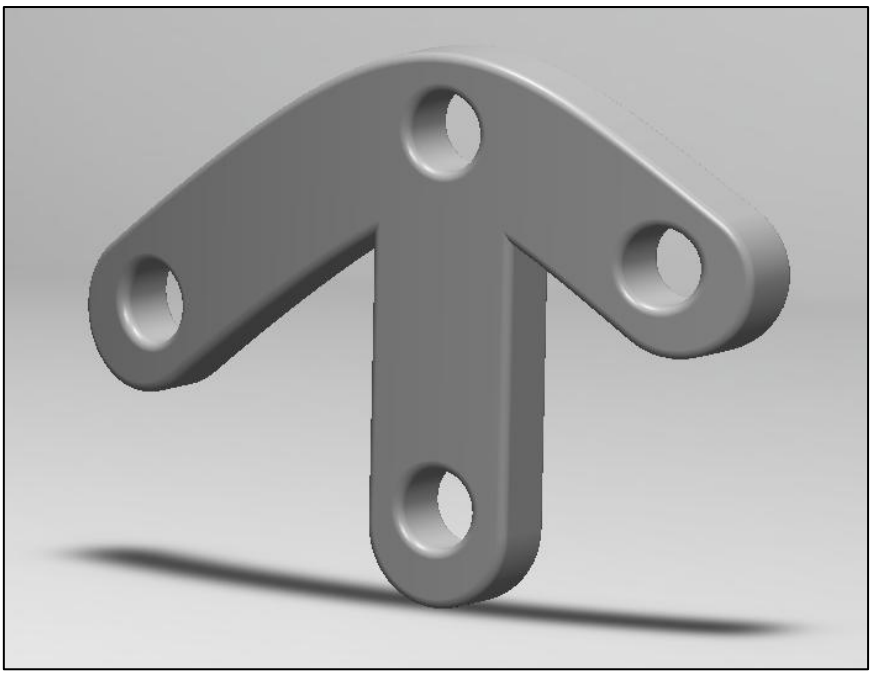

Figure 49: Simplified 3D CAD model of chosen design concept.

Dimensions

The total width of the device (from left to right) was 19.85mm (Figure 53), which fell within the optimal range of the required width of the device. The length of the shorter lateral arm, which extends towards the radial notch, was 10mm and that of the longer arm was 14mm (Figure 50).

The total length of the device (from top to bottom) was 14mm (Figure 52), falling within the desired range. The width of all three arms was no more than 4mm, and the thickness (front to back) of the device was 2mm, which matches the thickness of the current Endobutton.

The suture holes on the lateral, medial, and downward vertical arms were 2.5mm from the circumferential edge of the arm and 2mm from the straightened edges (Figure 51). The suture holes were 2mm in diameter (Figure 50).

Shape

As previously discussed, the spline shape (depicted in Figure 50 and Figure 51) served to accommodate the anatomical nuances of the tip of the coronoid while using a generalised shape to allow easy fit and adaptability of the device across most anatomical variations. The convexity of the design, highlighted in Figure 53, was aimed at conforming to the coronoid's anatomy. Similar to the curvatures, the convexity employed common angles to enable the device fit across a large range of coronoid variations.

Minor adjustments were made to the angle of curvature of the spline. The angle was increased from 104° to 105° (Figure 51), thus enabling the device to match the curvature of the coronoid. The angles used to for the convexity of the design remained unchanged at 150°.

Features

The detailed design phase saw no significant changes to the design features, as they were addressed as part of the initial technical design requirements. However, the dimensions for the whip suture hole were defined with a diameter of 2mm. By standardising the dimensions of the suture holes throughout the device, the additional hole could serve as a secondary point of fixation, should the surgeon opt to pass a vertical loop through the device.

4.3.6.2. Technical Drawings and CAD Models

During the detailed design phase, comprehensive 3D CAD models were produced using Dassault SolidWorks (Velizy-Villacoublay, France), with accompanying technical drawings (Refer to Appendix H-Detailed Design Drawing).

These technical drawings provide precise dimensions of the various aspects of the detailed design. In Figure 50, the dimensions used for both the lateral (left) and medial (right) arms of the device were illustrated, along with the dimensions for the width of each arm and the diameter of the suture holes. The location of the suture holes in relation to the edges of the arms, and the refined angles of the spline have been illustrated in Figure 51. Figure 52 shows the design from the medial/left view, which allowed for the depiction of the overall length and the device thickness. Lastly, the overall width of the design device has been shown in Figure 53.

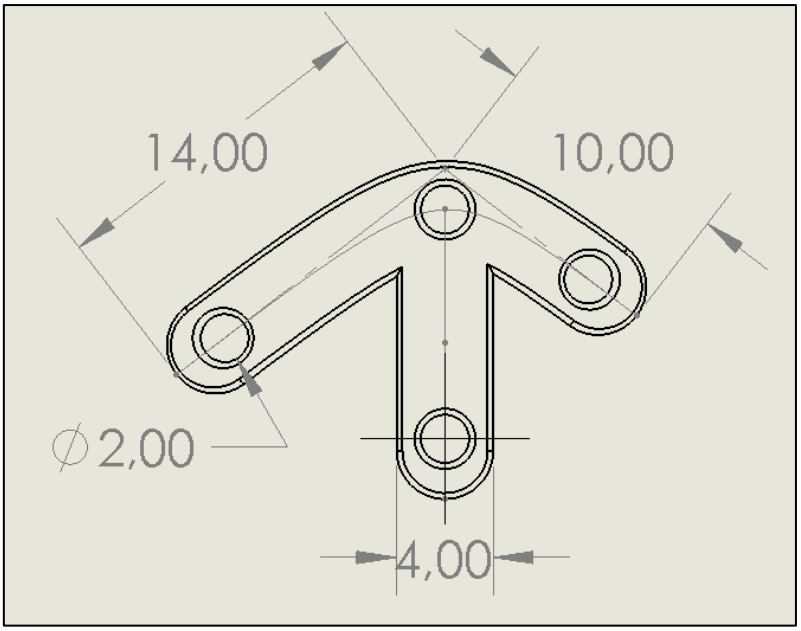

Figure 50: SolidWorks drawing showing the dimensions of the arms and suture holes of the designed Endobutton (Anterior/front view).

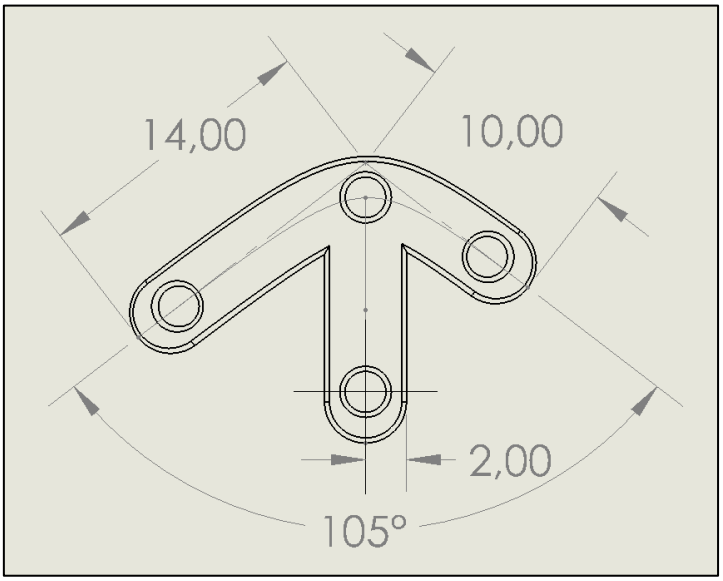

Figure 51: SolidWorks drawing showing the angles of the curvature of the spline and the location of the suture holes in relation to the edge of the device (Anterior/front view).

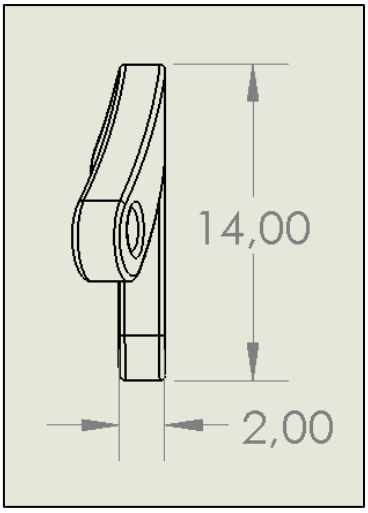

Figure 52: SolidWorks drawing showing the total top-to-bottom length and the thickness of the designed Endobutton (Medial/left view).

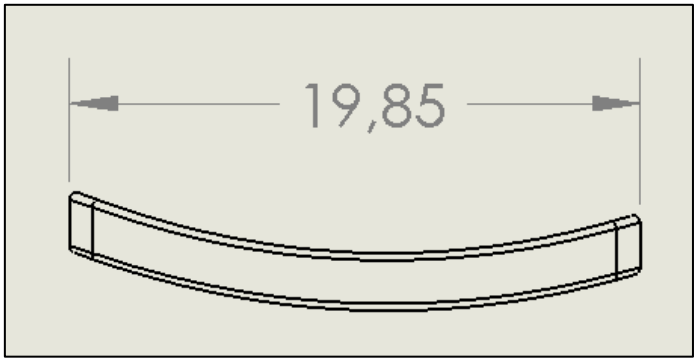

Figure 53: SolidWorks drawing showing the total width (medial/left to lateral/right) of the designed Endobutton (Superior/top view).

4.3.6.3. Prototyping

The detailed design underwent rapid prototyping and an informal templating process as part of the iterative design review cycle. The designs were rapidly prototyped using additive manufacturing practices such as 3D printing. Every iteration of the device was 3D printed using the Clear V4 resin on a Formlabs (Somerville, Massachusetts USA) Form 2 resin printer.

4.3.6.4. Prototype Production Process

Materials and Components

Prior to verification and validation testing, the devices were 3D printed on a Formlabs Form 2 using Clear V4 resin. No additional components required manufacturing; however, the stock standard No.2 Non-Absorbable Fiber Wire sutures needed to be sourced to be incorporated in the device.

Assembly and Integration

There was no assembly necessary as it was a single part fixation device. However, the device needed to integrate with the No.2 Non-Absorbable Fiber Wire sutures which would be used to secure the device.

Interfaces and connections

The only interfaces existed between the sutures and the fixation holes of the device. This interface was not expected to pose problems as it mimicked the interface which would occur with the currently used Endobutton. Any potential issues may arise from a difference in suture type. Further research conducted on the interface between sutures and fixation devices may offer solutions should the interface prove to be problematic.

Safety Features and Compliance

There were no required built in safety features for this device beyond the smoothing of sharp edges. The safety features for the device were to be considered at a later stage.

Possible Future Titanium Manufacturing Process

Once verified and validated, the design would have undergone a titanium manufacturing process. Surgical grade titanium alloys would be used for this device as it mimics the material used for the current Endobutton. The rationale behind the use of the titanium was the established biocompatibility, and the mechanical and biomechanical capabilities of the material, which would reduce the need for additional material testing.

The titanium implant would be manufactured using a CNC milling machine. This process would be outsourced to a certified company in order to make sure the material was of the correct surgical grade material, and that the device was accurately manufactured. The outsourcing to a certified surgical implant manufacturer would have ensured that the respective ISO standards were met.

The compliance of the device would also only come into play once the detailed design was being manufactured in the titanium. The manufacturing process used would have to complied with the same requirements as those established for the manufacturing of orthopaedic implants. Such as standard would include ISO 5832 which address the use metallic materials for surgical implants. During the manufacturing process, ISO standard 9585 which is related to the bending strength and stiffness of bone plates, would also need to be considered. The safety and biocompatibility of surgical grade titanium alloys is well established; however, safety and biocompatibility would form part of the assessment of the manufactured device.

4.4. Final Design Outcome

The final design outcome is a curved arrow shaped adapted Endobutton intended for use in conjunction with sutures for the fixation of coronoid process fractures, with dimensions of approximately 20mm by 14mm with a thickness of 2mm. This device features 3 fixation points and an extra hole for the inclusion of a whip suture. By meeting all functional and technical requirements, this adapted device presents a viable method of fixation for coronoid factures. A detailed design drawing is available in Appendix H- Detailed Design Drawing.

The images below show the designed device from a variety of angles:

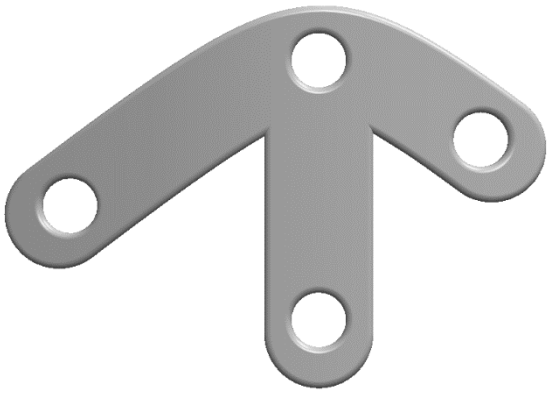

Anterior/front view

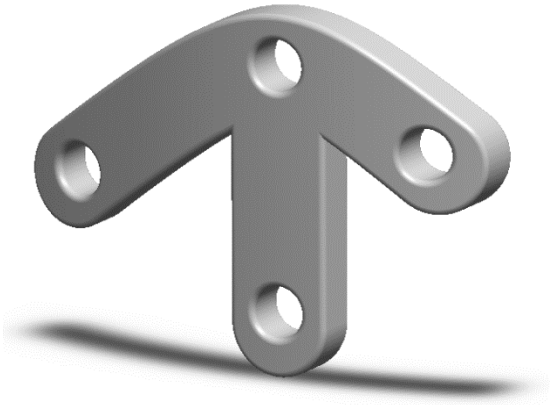

Oblique anterior/front view

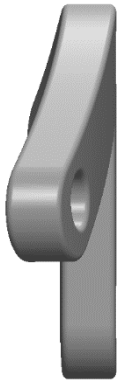

Medial/left view

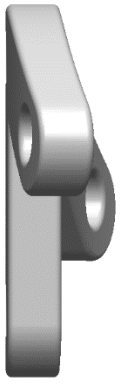

Lateral/right view

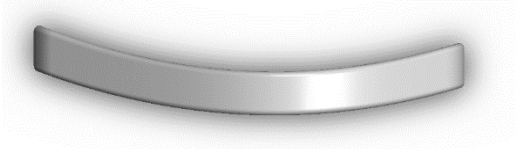

Superior/top view

Inferior/bottom view

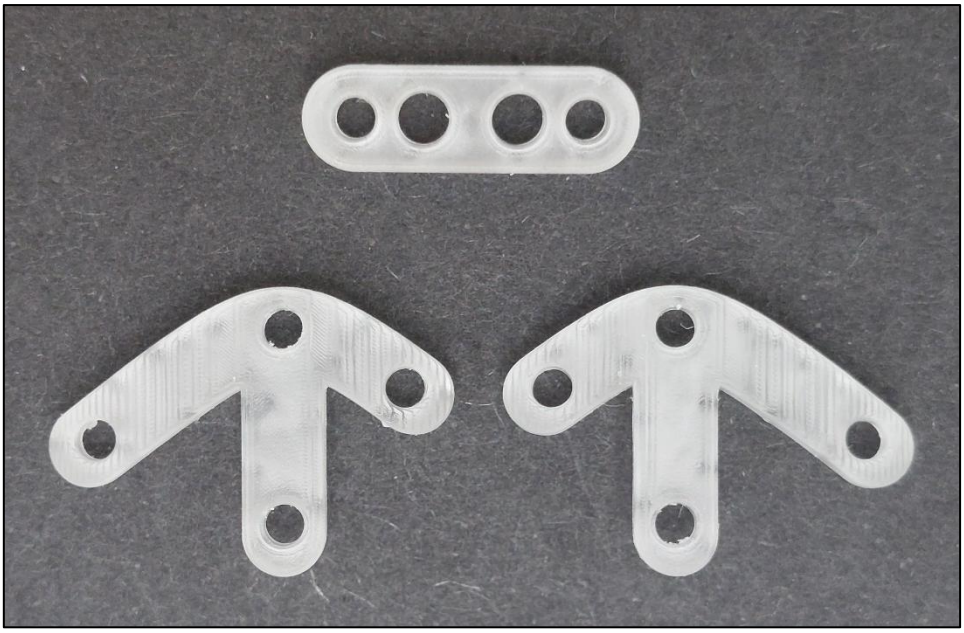

Figure 54: Left and right versions of design compared to the Endobutton imitation.

4.4.1. Limitations

Due to the constraints of time and scope within this project, manufacturing the device in titanium was not feasible. This decision was primarily based on the fact that titanium manufacturing is both expensive and time-consuming. As a result, the following verification and validation testing will focus solely on assessing, verifying, and validating the design and its potential as a method of coronoid fracture fixation.

4.5. Planned Testing

4.5.1. Verification Testing: Templating and Qualitative Assessment

The planned verification testing intends to follow the same methodology used in the evaluation of the imitated Endobutton (Chapter 3). This includes the device being formally templated on the 3D printed bones using a temporary adhesive and being evaluated through a Qualitative Assessment. During this evaluation, a set of questions will be answered by trained Orthopaedic surgeons which address the criteria required of the device.

4.5.2. Validation Testing: Cadaver Testing

The planned validation testing will involve simulated surgical fixation of coronoid fractures using the designed device in cadavers. The use of cadaver materials offer the advantage of evaluating the designed device in simulated surgical situations, as well as evaluating how the device interacts with the sutures and surgical instruments. Qualitative user questioning assessing the same criteria as those assessed during the verification testing will be conducted. Additionally, the incorporation of sutures

during the cadaver testing will also enable the authors to assess the devices' ability to provide adequate fixative tension on the coronoid.

4.6. Chapter Conclusion

The iterative design process undertaken aimed to address the requirements and criteria established for a coronoid fixation device. Through the successive iterations, a curved asymmetrical arrow-shaped adapted Endobutton device was produced. This adaptation aims to provide a viable method of suture-based coronoid fracture fixation, particularly in cases where the fragment is too small to accommodate screws. By considering the anatomical variations, the final design endeavours to offer improved stability and anatomical reduction for coronoid fractures, as well as ease of use and attachment.

4.6.1. Chapter Outcomes

The primary aim of this chapter was to design and develop an adapted Endobutton fixation plate by fulfilling the following three main objectives:

Establishing Design Requirements and Specifications: The first objective was establishing the requirements and specifications for the design. This was met through extensive discussions between those involved in the study. The use of the heat maps helped identify the shape, size and pattern of the fragments which the designed device would have to address.

Production of Conceptual and Detailed Design: Creating the conceptual and detailed design encompassed the bulk of the work, with multiple reviews and redesigns to meet the design requirements being covered in this chapter. The final design was an arrow-shaped Endobutton.

Design Review and Approval: The third objective focused on the final review of the designed device. Professor Roche inspected the prototyped device. The design was approved prior to proceeding to the Verification Testing: Templating and Qualitative Assessment stage.

5. Chapter 5: Design Verification & Validation

5.1. Chapter Introduction

This chapter aims to verify and validate the adapted Endobutton design through qualitative assessment. Verification and validation testing are essential phases in the development of the adapted Endobutton, ensuring that the design meets the specified requirements and performs effectively. The verification involves qualitative assessments by templating the device on the previously printed 3D models of the coronoid fractures. Validation furthers this testing through simulated surgical fixation using cadaver limbs to assess practical functionality and usability.

5.2. Chapter Aims and Objectives

Aim

This chapter aims to verify and validate the design of the coronoid adapted Endobutton and its potential for improved fixation, using rapid prototyping (3D printing) and qualitative assessment.

The verification assesses the design of the device through templating and the qualitative assessment, prior to the use of the device in simulated surgeries in cadavers. Cadaver testing is used to validate the design of the adapted Endobutton as a proof of concept. The comparison of the designed device with the imitation of the currently used Endobutton establishes if the adapted Endobutton provides improved fixation for coronoid fractures. The verification and validation of the adapted Endobutton also indicate whether the device should be put through the manufacturing process to produce a titanium version of the design for further testing.

Objectives

The objects necessary for the aim to be achieved are:

1) Rapidly prototype the detailed design of the adapted Endobutton using resin-based 3D printing.
2) Perform simulated coronoid fracture fixation using a templating methodology and conduct a qualitative assessment and revision of the design.
3) Establish a set of conclusions which verify the design of the device.
4) Perform mock surgical fixation of induced fractures in cadaver specimens using the designed adapted Endobutton, allowing for qualitative assessment of the design.
5) Establish a set of conclusions which validated the design of the adapted Endobutton.
6) Form a comparison between the designed device with the 3D printed Endobutton imitation.

5.2.1. Verification and Validation Testing Objectives

Functional Testing

The functional testing aims to verify that the rapidly prototyped design meets the functional requirements. This includes effective reduction of the coronoid fracture by restoring the normal anatomy.

The verification of the design is done through the qualitative evaluation of the device after being templated on the 3D printed bones. The validation follows by testing the functionality of the device in simulated surgical scenarios using cadavers, which includes another round of qualitative assessment. The cadaver testing offers a more accurate assessment of the functional requirements of the designed device. The involvement of the suture techniques during the cadaver studies provide a better understanding of the device's functionality and integration.

The device's technical requirements were discussed and confirmed in the Design Methodology: Detailed Design Stage.

Usability and User Testing

The usability and user testing aims to judge, verify and validate whether the design of the adapted Endobutton meets the usability criteria and addresses coronoid process fractures effectively. Objective evaluation of the design's ease of use, ease of attachment and appropriate for use inform the usability of the designed device.

Using cadavers for the validation testing facilitate a better assessment of the device's usability within the surgical space. By performing a fixation of an induced fracture, surgeons are better able to determine how easy it is to use the designed device.

5.3. Testing Methods and Procedures

The testing used to verify and validate the design of the adapted Endobutton followed a rapid prototyping, testing and Qualitative Assessment format. The verification consisted of templating, and the validation consisted of cadaver testing.

These methods allowed for a physical assessment of the designed device while combining the functionality and user testing. The rapid prototyping and templating process used to verify the device were the same as those used to assess the imitated Endobutton during the Templating & Qualitative Assessment.

The cadaver studies allowed for further physical assessment of the device while providing valuable functionality information when used in a simulated surgical setting. This enabled a comprehensive evaluation of the device and its fixation potential.

The iterative design process, the verification, and the validation processes were simplified and shown in Figure 55.

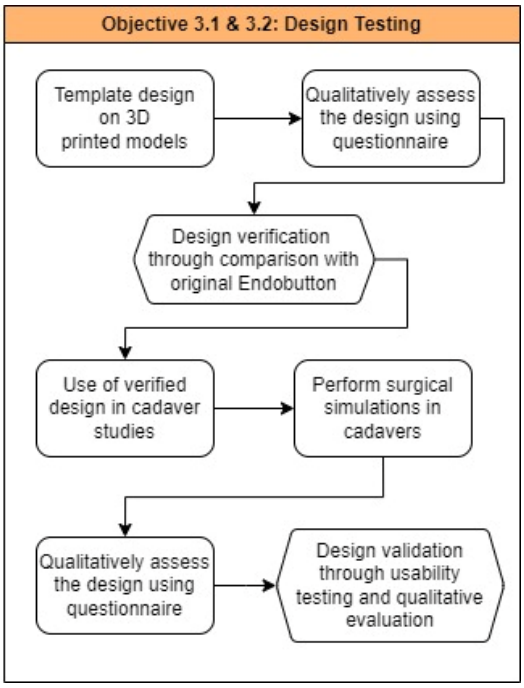

Figure 55: Simplified methodology depicting the rapid prototyping, templating, and cadaver studies.

5.3.1. Verification - Templating and Qualitative Assessment

The designed adapted Endobutton was formally templated on the 3D printed bones used to evaluate the imitated Endobutton in Chapter 3: Qualitative Fit Analysis (Figure 38). The evaluation of the designed device was conducted by the same three Orthopaedic surgeons who had evaluated the imitated Endobutton.

5.3.1.1. Functional Testing

Once templated on the 3D printed bones, the designed device was physically assessed, and the feedback questionnaire was answered (Figure 56). Specific questions within the questionnaire assessed the performance of the device's primary function of fracture reduction and restoration of the normal anatomy.

The physical prototyping and the templating of the device provided an accurate representation of the device's potential functionality. Informal discussions were conducted after the templating of the

device. The points discussed were noted and used as indicators of how well the device performed its intended function.

5.3.1.2. Usability and User Testing

Rapid prototyping and production of a physical device allowed for its usability to be assessed by the three Orthopaedic surgeons (the same three surgeons who participated in Chapter 3: Qualitative Fit Analysis). Usability was contingent on the intended users being trained Orthopaedic surgeons, which was sufficiently met. The usability requirements consisted of the same criteria used to evaluate the Endobutton imitation:

- Ease of device use.
- Ease of attachment to the bone in a surgical setting.
- Patient specific suitability and use of the device.

These usability criteria were integrated into the Qualitative Assessment questionnaire (Appendix G), mirroring the assessment of the imitated Endobutton. Although the device could not be surgically attached to the 3D printed bones, the educated assessment of the physical prototype and discussion of the design allowed the verification of the device's usability.

5.3.1.3. Safety Testing

No safety testing was required during the verification stage; however, the device was rapidly produced using an inert and safe plastic material which posed no harm to the users. All edges of the design were filleted (smoothed/curved) to avoid sharp edges which would potentially compromise the surrounding soft tissue, should this device be used in an anatomical setting.

Figure 56:Templating of design adapted Endobutton on a small number of the 3D printed bones, using a temporary adhesive.

5.3.1.4. Method of Recording Data - Qualitative Assessment Questionnaire

The same Qualitative Assessment questionnaire (Appendix G) used to evaluate the imitated Endobutton was used in order to ensure reliability and comparability of the results. This questionnaire consisted of the same 6 questions:

1) Do you think this fixation device is easy to use?
2) This device is easily attached to the bone.
3) This fixation device fits on the fracture.
4) This fixation device would be used in the fixation of the fracture.
5) This fixation device would result in stable fixation of the fracture.
6) The use of this fixation device would result in adequate reduction of the fracture.

The same 3 limitations of lack of coverage, overhang and incongruency were evaluated when templating the designed adapted Endobutton. These limitations were reported when answering the question regarding the fit of the device.

The completion of the questionnaires marked the end of the templating and formalised evaluation process; however, informal discussions of the designed adapted Endobutton followed. Important points from the discussion were noted and reported. The Qualitative Assessment feedback forms were collected, and the results were transcribed into a Microsoft Excel spreadsheet for data collection and analysis.

5.3.1.5. Data Analysis and Statistical Methods

The elbows were categorised based on the O'Driscoll fracture types (Type 1 and Type 2). Each participants' responses were recorded, and coded. The Mode for each question was calculated from the coded ordinal values to determine the most common response to each question. This was calculated using the SPSS statistical package v.29 (SPSS Inc, Chicago, IL) based on the independent samples Mann-Whitney test. The cut-off for statistical significance was $p<0.05$. The responses obtained for each type of fracture were compared between the control (Endobutton imitation) and designed adapted Endobutton.

Interobserver reliability was also assessed to evaluate the consistency of the device ratings between the surgeons for each question. Intraclass Correlation Coefficient (ICC) estimates and their corresponding 95% confident intervals were calculated based on mean-ratings (k=3), absolute-agreement, 2-way mixed-effects model.

5.3.1.6. Verification Results

The surgeons rated the designed adapted Endobutton as "Good" (mode = 4) for ease of use and "Adequate" (mode = 3) attachment to the bone. The designed device fit most of the fractures, with the most frequent response to the question regarding fit as "Yes" (mode = 1). The surgeons also evaluated the adapted Endobutton as an "Excellent" (mode = 5) fixation option for the fractures tested. Additionally, they ranked it as "Excellent" (mode = 5) for post-fracture stability and "Excellent" (mode = 5) in fracture reduction. Further details of the observations are presented in Table 14.

Table 14: Table showing the overall results from the questionnaire.

Questions	Options	Responses (%)
Q1: Do you think this fixation device is easy to use?	Very Poor	0%
	Poor	0%
	Adequate	0%
	Good	67%
	Excellent	33%
Q2: This device is easily attached to the bone?	Very Poor	0%
	Poor	0%
	Adequate	67%
	Good	33%
	Excellent	0%
Q3: This fixation device fits on the following fractures?	Yes	76%
	No	24%
Q4: This fixation device would be used in the fixation of the following fractures?	Very Poor	7%
	Poor	2%
	Adequate	18%
	Good	33%
	Excellent	40%
Q5: This fixation device would result in stable fixation of the fracture?	Very Poor	4%
	Poor	9%
	Adequate	16%
	Good	27%
	Excellent	44%
Q6: The use of this fixation device would result in adequate reduction of the following fractures?	Very Poor	4%
	Poor	9%
	Adequate	22%
	Good	18%
	Excellent	47%

A total of 11 reports were noted for the 3 limitations, with 4 reports for Type 1 fractures, and 7 were for Type 2 fractures (Table 15). This marks a 66.7% reduction in the report rates of the noted limitations. In both fracture types, incongruency remained the main limitation. However, the overall report rate decreased from 16 instances for the control to 9 for the adapted Endobutton, therefore

indicating an improvement in the device congruency. The report rate of overhang was 1 instance per fracture type, showing a decrease compared to the control Endobutton. There were no reports of the adapted Endobutton insufficiently covering the fragment.

Table 15: Limitation report frequency.

Fracture Type	Limitation	Response Frequency, n (%)
Type 1	Lack of Coverage	0 (0.0)
	Overhang	1 (25.0)
	Incongruency	3 (75.0)
Type 2	Lack of Coverage	0 (0.0)
	Overhang	1 (14.3)
	Incongruency	6 (85.7)

Interobserver Reliability

There were too few data points to determine the interobserver reliability for Questions 1 and 2. The ICC was calculated for the ordinal data for Questions 3 to 6. Question 3 yielded a value of -0.11 (95% CI: -1.36 - 0.58). The negative ICC indicates inconsistency among the observers and poor agreement between the ratings. Questions 4 to 6 yielded moderate reliability results with their ICC values equalling 0. 60, 0.70 and 0.68 respectively (Table 16). Question 4 to 6 all had statistically significant p values <0.05.

Table 16: Interobserver reliability of the verification study.

	Intraclass Correlation	95% Confidence Interval		F Test With True Value 0			
		Lower Bound	Upper Bound	Value	*df*1	*df*2	Sig
Question 3	-0.11	-1.36	0.58	0.897	14	28	0.57
Question 4	0.60	0.10	0.85	2.62	14	28	0.02
Question 5	0.70	0.33	0.89	3.93	14	28	0.001
Question 6	0.68	0.26	0.89	3.16	14	28	0.005

Comparative Usability Outcomes

When the control plate (imitated Endobutton) was templated on the 3D printed bones, surgeons rated its ease of use as “Good” but found its ease of the attachment to bone as “Poor”. When the designed adapted Endobutton was templated on the same 3D printed bones, the ease-of-use rating remained “Good”, and there was a noted improvement (Adequate) in the attachment to the bones.

During the informal discussions, it was noted that the increased size of the device compared to the control Endobutton was advantageous. The larger size also made the device easier to handle and manipulate, while still being small enough to fit within the required surgical space.

Comparative Functional Outcomes

There was no significant difference between the control and designed Endobuttons in the process of fixation for the Type I fractures. Whereas, for the Type II fractures, the adapted Endobutton demonstrated a significantly better fixation process ($p<0.001$).

5.3.2. Validation – Cadaver Studies

5.3.2.1. Ethical Clearance

Permission for the cadaver studies was granted by the Cadaver Research Governance Committee, Department of Human Biology, Faculty of Health Sciences, University of Cape Town. Approval was granted by the Human Research Ethics Committee (HREC) at the University of Cape Town to include the cadaver studies within the ethics clearance scope with reference number 588/2022 (Appendix A).

5.3.2.2. Further Prototype Development

Prior to the start of validation testing, additional versions of the verified design were developed in order to incorporate a range of sizes. This involved adjusting the length of the downwards buttress arm to create shorter and longer alternatives (Figure 57). In the short version, the arm's length was reduced by 2mm, bringing the total length to 12mm. Conversely, in the long version, the length of the arm was increased by 2mm, resulting in a total length of 16mm. All other dimensions remain consistent across the versions.

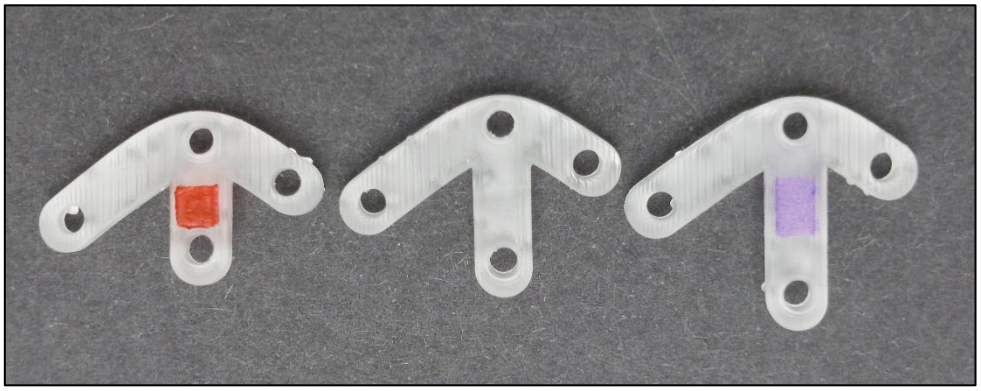

Figure 57: Short (red), standard, and long (purple) versions of the adapted Endobutton.

Iterations featuring a spiked downwards arm were also created based on the original design, with the intention of enhancing the devices grip on the surrounding soft tissue (Figure 58). Three versions were produced, incorporating spikes of 2mm, 3mm, and 4mm in height; therefore increasing sharpness corresponding to the spike height. The length of the downwards arm remained the same as the original

version of the design, and all the other dimensions were unchanged across the spiked versions. Unlike the original, the spiked versions did not include a hole for an additional point of fixation on the downwards arm.

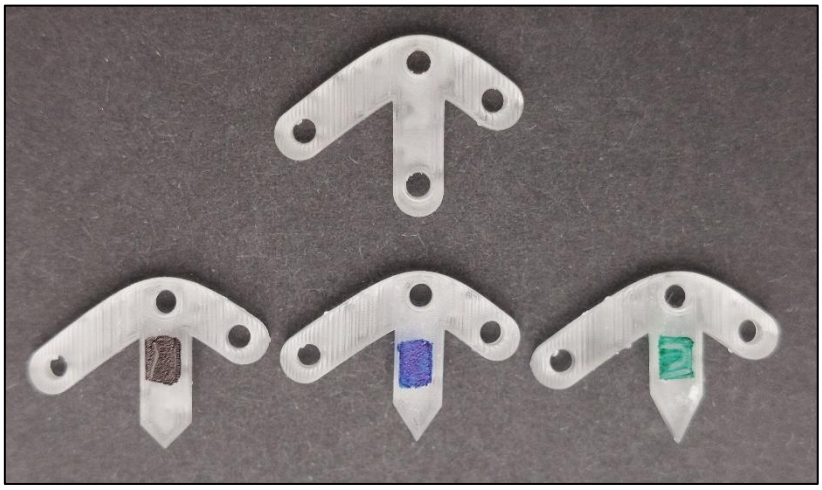

Figure 58: Spiked versions of the adapted Endobutton compared to the original design. Devices had spikes of 2mm (black), 3mm (blue) and 4mm (green).

For the purposes of the cadaver testing, all the designs (originally designed for a left elbow) were mirrored to create a right-side version, which were then 3D printed using the same processes described in the Prototyping section of Chapter 4: Design and Development of Adapted Endobutton. To ensure there was an adequate supply, ten left- and ten right-sided prints of each of the six designs were printed (Original, long, short, spiked – 2mm, spiked – 3mm and spiked – 4mm) to avoid a shortage of available devices in the event of breakage during testing.

The devices were marked, and colour coded to make identification of the devices easier during testing and assessment (Figure 59).

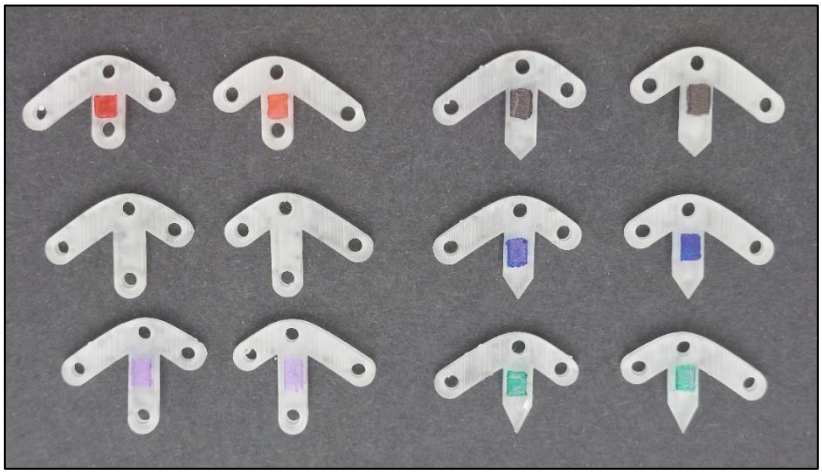

Figure 59: Colour coded left and right sided versions of adapted Endobutton design. Short (Red), Original (unmarked), Long (Purple), 2mm Spiked (Black), 3mm Spiked (Blue), and 4mm Spiked (Green).

5.3.2.3. Cadaver Testing Methodology

Three fresh cadaver upper limb specimens - two right arms and one left – were prepared. The cadaver specimens were disarticulated single arms, therefore there was no need to position the entire body. Instead, the arms were orientated to expose the medial (inside) aspect to perform the surgical incisions required to gain access to the elbow joint. Using the medial approach, a surgical incision was made to expose the superficial structures surrounding the elbow joint. Deeper incisions followed which allowed access to the bones of the elbow and the associated ligamentous capsular structures.

Prior to inducing the fractures, the Endobuttons were placed externally on the capsule to assess their fit. The joint capsule was then opened to access the coronoid. Using a surgical osteotome and mallet, the fractures were induced, creating Type 1, Type 2, and Type 3 fractures, each in separate elbows. Each fragment was displaced from the parent bone to simulate the presentation of the fractures in real patients.

Once the fragment was displaced, two drill holes were made from the posterior aspect of the ulna towards the fracture bed; one laterally located towards the radial notch and the other more medially located. The drill holes were slightly offset from the fracture site to correspond with the holes on the designed device and to avoid interference with the fragment reduction. Sutures were passed through the adapted Endobutton device, and the device was placed over the fragment. The fragment and device were reduced restoring to the anatomical position.

The sutures attached to the device were passed through the drill holes using suture passers and then tightened to achieve sufficient tension for stable fixation. Once satisfied with the fragment's position and the device's tension, the reduction sutures were tied on the posterior aspect of the ulna. The final position of the device and reduction of the fracture is evident in Figure 60.

The device was then evaluated using the Qualitative Assessment Questionnaire. Six trained Orthopaedic surgeons participated in the evaluation of the device's usability, and functionality. Each surgeon completed the questionnaire and participated in an informal discussion of the device.

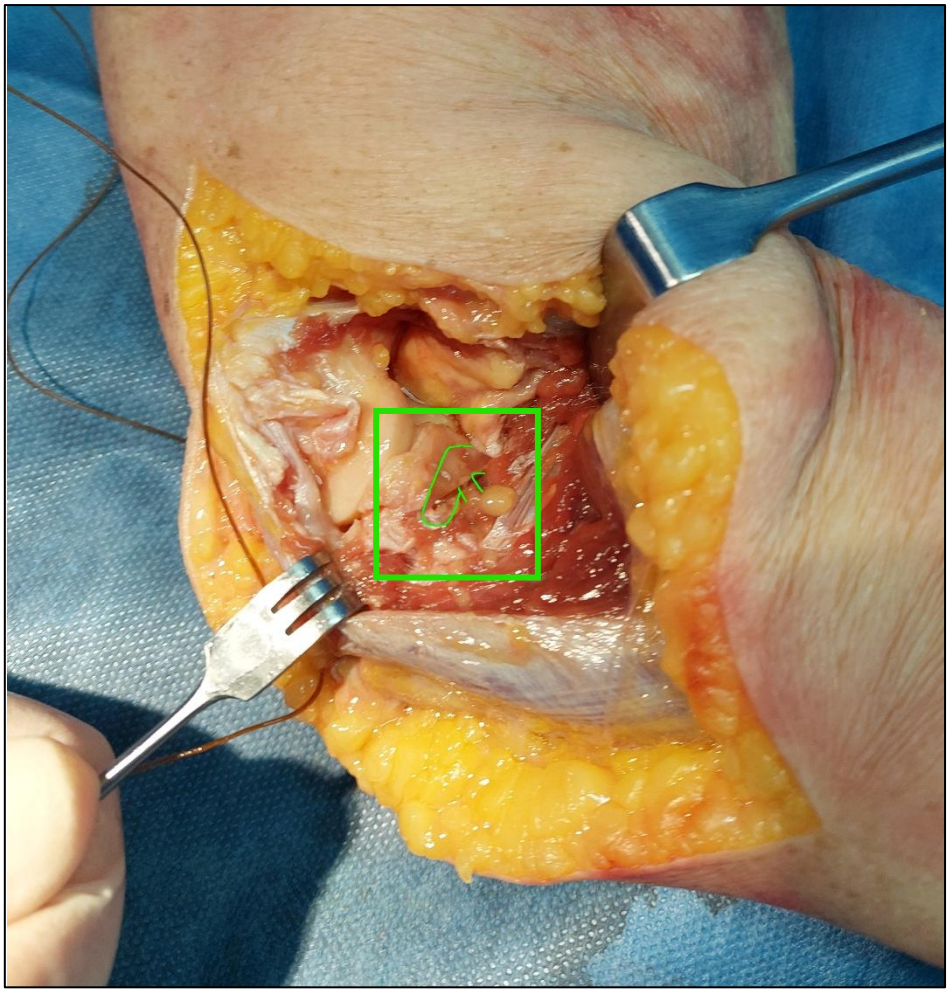

Figure 60: Designed adapted Endobutton (Original) used in the fixation of a coronoid fracture in left cadaver limb. The device is roughly outlined in green, within the green box.

5.3.2.4. Method of Recording Data - Qualitative Assessment Questionnaire

A change to the questionnaire occurred prior to the cadaver testing, to allow for a better evaluation of the designed device. An additional question was included to help evaluate the tension under which the sutures would place the device and the coronoid. The cadaver testing questionnaire consisted of the following questions:

1) Would you use this device?
2) Is this device appropriate for coronoid fixation?
3) Do you think this fixation device is easy to use?
4) This fixation device fits on the following fractures.
5) This fixation device would be used in the fixation of the following fractures.
6) This fixation device would result in stable fixation of the fracture.
7) The use of this fixation device would result in adequate reduction of the following fractures.
8) This device allows for adequate tension to be placed on the coronoid.

Similar to the data collection process followed during the verification testing, the Qualitative Assessment Questionnaire answers were collected and transcribed into a Microsoft Excel spreadsheet. For each completed questionnaire, the frequency of the responses to each question and the reported limitations were recorded.

5.3.2.5. Data Analysis and Statistical Methods

The fractures were classified following the O'Driscoll classification system. The responses for the validation cadaver testing were coded. The Modes for each question were identified from the ordinal datasets, and the intra-type responses were compared. Responses from the 3D printed bone templating were compared with those from the cadaver studies.

Statistical analysis was performed using the independent samples Mann-Whitney test, with a significance threshold of $p<0.05$. To compare the responses obtained for the six different coronoid plates, a Kruskal Wallis test was performed, with the statistical significance being at <0.05. Both tests were performed using the SPSS statistical package v.29 (SPSS Inc, Chicago, IL).

As was done with the verification results, interobserver reliability was also assessed to evaluate the consistency of the device ratings between the surgeons for each question. Intraclass Correlation Coefficient (ICC) estimates and their corresponding 95% confident intervals were calculated based on mean-ratings (k=6), absolute-agreement, 2-way mixed-effects model.

5.3.2.6. Validation Results

Usability Outcomes

All the participant surgeons indicated that they would use the original adapted Endobutton device. They found the device appropriate for coronoid fixation and reported that it was adequately easy-to-use.

The different adapted Endobutton versions did not have significantly different usability outcomes. Overall, the surgeons reported that they would "Yes" use the device (mode = 1), "Yes" (mode = 1) to the appropriateness for coronoid fractures, and "Good" (mode = 4) for the device's ease of use.

Functional Outcomes

Among the six different versions, there were no significant differences in the functional outcomes for each type of fracture. For Type I fracture, the responses were as follows: the response to the device's fit on the fracture was "No" (mode = 2); and its use in treating Type 1 fractures was reported as "No" (mode = 2). The resultant stability of fixation was rated as "Very Poor" (mode = 1); the adequacy of the resultant reduction was "Very Poor" (mode = 1); and "No" (mode = 2) was the response for whether the device allows adequate tension.

For Type II fracture, the responses were “Yes” (mode = 1) for the device’s fit on the fractures, and “Yes” (mode = 1) was the modal response for the use of the device in Type 2 fracture treatment. “Good” (mode = 4) was the outcome for the resultant stability of the fixation; “Good” (mode = 4) for adequate reduction of the fracture; and “Yes” (mode = 1) for adequate tension on the coronoid

Lastly, regarding the Type 3 fracture, the ratings were: the device’s fit on the fractures was “Yes” (mode = 1), and its use in the treatment of the Type 3 fractures was “Yes” (mode = 1). “Very Good” (mode = 5) for the resultant stability of the fixation; the adequacy of the fracture reduction was “Very Good” (mode = 5), and it was noted that, “Yes” (mode = 1), adequate tension was placed on the coronoid by the sutures.

Interobserver Reliability

There was no variation between the data points for Question 1 and 2, which evaluate the device’s usability. Question 3 demonstrated excellent reliability between Observer 2 and 6 (ICC=1.00), with no variation between the other observers (1, 3, 4, and 5).

For the Type 1 fractures, moderate interobserver reliability (ICC = 0.64) was seen between Observers 2,4 and 6 for Question 7, which assesses the device’s ability to provide adequate reduction. The reliability was statistically significant (p = 0.006). There was no variation between the remaining data points for the Type 1 fracture.

For the Type 2 fractures, there was excellent reliability (ICC = 1.00) between Observer 1 and 4 for Question 5. Significant moderate reliability (ICC = 0.74, p <0.001) was noted between Observers 1, 2 and 6 in Question 6. Additionally, there was excellent reliability (ICC = 1.00) recorded between Observers 1 and 4 for Question 8. There was no variation observed between the rest of the data points for the Type 2 fracture.

For the Type 3 fracture, moderate reliability (ICC = 0.73, p = 0.16) was seen between Observer 2 and 6 for Question 4. There was excellent reliability (ICC = 1.00) between Observer 1 and 4 for Question 5. There was significant excellent reliability (ICC = 0.76, p value = 0.02) between Observers 1, 2 and 4 for Question 6. There was no variation recorded in the remaining data points for the Type 3 fracture.

Table 17: Interobserver reliability for the cadaver validation studies.

		Intraclass Correlation	95% Confidence Interval		F Test With True Value 0			
			Lower Bound	Upper Bound	Value	*df*1	*df*2	Sig
Type 1	Q7	0.64	-0.04	0.94	6.65	5	10	0.006
	Q5	1.00	-	-	-	5	-	-
Type 2	Q6	0.74	0.04	0.96	25.00	5	10	<0.001
	Q8	1.00	-	-	-	5	-	-
	Q4	0.73	-1.81	0.98	3.67	3	3	0.16
Type 3	Q5	1.00	-	-	-	5	-	-
	Q6	0.76	0.15	0.96	4.83	5	10	0.02

Comparative Usability Outcomes

The control (imitated Endobutton), when templated on the 3D printed bones, elicited a "Good" rating for the ease of use. This rating remained consistent throughout the use of the adapted Endobutton on the 3D printed models and in the cadaver limbs. Although changes were made in the questionnaire regarding the ease of attachment to the bone, the device was deemed "Appropriate" for its intended use in fixing coronoid fractures and still had positive usability outcomes.

Comparative Functional Outcomes

For Type I fractures assessed on the cadavers, the surgeons felt that the novel device was significantly inferior in creating a stable fixation compared to the control device ($p<0.05$). For the Type II fractures in cadavers the surgeons found that the novel device performed significantly better to fit the fractures ($p<0.05$), they also found that the novel device was significantly inferior ($p<0.05$) in creating a stable fixation but be superior in creating adequate reduction for the fractures ($p<0.001$).

5.4. Discussion

The adapted Endobutton was designed to address the lack of an effective method of fixation for small coronoid fractures. This chapter aimed at verifying and validating the device's design to show its potential as a method of coronoid fixation.

For the usability and user-based testing, the objective was to verify and validate whether the adapted Endobutton met the usability criteria while effectively addressing the coronoid fractures. The functional testing was conducted to ensure the prototyped design met the pre-established requirements. The primary goal being the achievement of fracture reduction, while restoring the natural anatomy of the bone.

The verification process involved a qualitative evaluation of the design after templating it on 3D printed fractures, while validation involved testing the designed device in simulated surgical scenarios using cadaver limbs. The use of cadaver material allowed for a realistic assessment of the device's functionality and usability in a practical setting, enabling the surgeons to accurately determine its practical effectiveness.

5.4.1. Discussion of Verification Results

The primary aim of the verification process was to assess the design of the adapted Endobutton using templating techniques before proceeding with cadaver testing. Rapid prototyping the detailed design of the adapted Endobutton, combined with templating, facilitated the physical qualitative evaluation. This led to the establishment of a set of conclusions which verifies the design.

The templating and assessment indicated that the adapted Endobutton had a "Good" rating for ease of use and "Adequate" for attachment to bone. It demonstrated a 76% fit on the 3D printed fracture models and was rated "Excellent" as a fixation option, providing "Excellent" reduction and post-fixation stability. The overall report rates of limitations were reduced by 66.7%, with incongruency remaining the most reported issue. Additionally, the increase in the size of the adapted Endobutton proved advantageous, as it made the device easier to handle and manipulate.

The outcomes of the Qualitative Assessment indicate that the device meets all the pre-determined (Design Requirements) functional and user requirements, showing a better fit to the anatomy of the coronoid. This suggests the designed adapted Endobutton is well-suited for its intended purpose. Therefore, these improved ratings imply that this device offers a better option for coronoid fracture fixation when compared to the existing methods. This implication aligns with the suggestions made separately by Salwan *et al.* (2023) and Altan *et al.* (2016) that an anatomically pre-contoured plate would be a viable fixation option, and indicate that the adapted Endobutton could fulfil this need.

The verification process demonstrated that the adapted Endobutton meets the necessary criteria for effective coronoid process fracture fixation and provides a robust foundation for subsequent validation and potential clinical use. The positive results from the verification process indicated that the design was ready to undergo validation testing including evaluating the functionality and usability in cadaver limbs through simulated ORIF procedures.

5.4.2. Discussion of Validation Results

The validation process for the adapted Endobutton aimed to confirm the device's efficacy as a proof of concept through cadaver testing. This phase of testing involved performing simulated surgical fixation of induced fractures in cadaver limbs using the designed device, followed by a thorough

Qualitative Assessment. The primary objective was to establish a set of conclusions that validate the design. By evaluating the adapted Endobutton in a real anatomical setting, the validation tests were crucial in determining the device's practical functionality and usability.

The validation of the adapted Endobutton provided clinical setting-based results regarding the device's usability. Overall, the device was deemed appropriate for its intended use and received a "Good" rating for ease of use. There were no significant differences in the usability outcomes between the different adapted Endobutton designs tested. The positive feedback from participating surgeons emphasised the potential clinical applicability.

Functionality outcomes of the adapted Endobutton showed a mixed performance of the device based on the coronoid fracture type. For Type 1 O'Driscoll fractures, the device received poor ratings. Surgeons reported that the device did not fit well and would result in "Very Poor" reduction and post-fixation stability. Additionally, the device did not provide adequate tension on the coronoid. In contrast, the functionality outcomes were positive for Type 2 fractures, with surgeons affirming that they would use the device. The surgeons noted the device fits well over the fracture and would result in "Good" stability and reduction while providing adequate tension. For Type 3 fractures, the device was highly rated. The surgeons agreed it fit well over the fragment and the anatomy of the bone, while resulting in "Very Good" reduction and stability after providing adequate tension on the fracture.

The findings from the validation testing in the cadaver studies indicate that the adapted Endobutton is not an ideal fixation option for Type 1 fractures; however, it is aptly suited for Type 2 and Type 3 fractures. Despite the unfavourable outcomes, the device in its current form was still deemed appropriate for Type 1 fractures. This suggested that with improvements, it could potentially address the needs of the Type 1 fractures more effectively.

The discrepancies in the ratings across the fracture types suggest that the current design is not optimal for all fracture types, particularly Type 1. This poses an issue as the device's intended purpose was to treat these fracture types; and therefore necessitates a refinement of the design to better fix Type 1 fractures. Moving forward, design modifications to improve the fit and functionality for Type 1 fractures are crucial to ensure the device's effectiveness across all types of coronoid process fractures.

5.4.3. Discussion of Results Comparison

The results from the comparative analysis of the adapted Endobutton and the imitated commercially available Endobutton (control) highlight several key findings and implications for the device's future development and clinical applicability.

The adapted Endobutton consistently received “Good” rating for ease of use, corresponding to the usability outcomes of the commercially available Endobutton. This showed that the adapted Endobutton did not compromise on the usability that was crucial for surgical procedures. The increased size of the adapted Endobutton was seen as beneficial as it made it easier to handle and manipulate. The attachment to the bone improved from “Poor” in the control device to “Adequate” in the adapted Endobutton, demonstrating a tangible improvement in the fixation potential of the device

The adapted Endobutton performed better in the functionality testing for the Type 2 fractures compared to the control device. This superiority was evident in both the verification and validation testing, where the adapted Endobutton provided improved reduction and post-fixation stability. The participating surgeons indicated a higher likelihood of using the adapted Endobutton for the fixation of Type 2 fractures, reinforcing its potential to be a preferred fixation method for coronoid fractures.

A direct comparison could not be made for the Type 3 fractures due to the absence of Type 3 fractures among the 3D-printed fracture models. The cadaver testing alone showed promising results, as the surgeons rated the adapted Endobutton as “Very Good” for the reduction and post-surgical fixation.

A noted area was the discrepancies in the outcomes of the Qualitative Assessment, particularly for the Type 1 fractures. The findings showed the performance of the designed device for Type 1 fractures was less than favourable. Although during verification there was no significant difference observed between the adapted Endobutton compared to the control, the validation testing indicated the control Endobutton was superior to the adapted Endobutton. These differences suggest that the adapted Endobutton might face challenges in treating Type 1 fractures in an anatomical setting due to potential differences between the morphology of the induced fractures and the 3D printed Type 1 fractures. An alternative cause might be unforeseen issues during the cadaver testing. These findings advocate for further refinement and optimisation of the design to ensure it can effectively address Type 1.

The consistent usability outcomes and improved functionality scores support the design concept and potential clinical viability of the adapted Endobutton. The results justify potential further steps including manufacturing the device in an approved surgical-grade titanium, which will allow for more robust verification and validation testing. Additionally, addressing the challenges identified regarding the treatment of the Type 1 fractures will be crucial for making the adapted Endobutton a comprehensive solution for all coronoid process fractures.

5.4.4. Limitations

The verification testing was limited by the absence of Type 3 fractures in the original patient cohort. As previously explained, scans with Type 3 fractures were excluded from the cohort due to the

presence of compromising fractures. An expansion of the data set to include more scans with Type 3 fractures would allow the verification testing to be performed to determine the device's suitability for all fracture types. Additionally, the validation testing was limited to three cadaver specimens. Expanding the cadaver sample size would be beneficial in confirming the positive outcomes and ensuring the robustness of the findings.

5.4.5. Key Findings in Chapter

1) **Usability and Handling:** The adapted Endobutton received consistent ratings for ease of use across all testing phases, and the increased size of the adapted Endobutton proved advantageous.
2) **Improved Fixation Potential:** The attachment to the bone improved over the commercially available Endobutton (control).
3) **Functionality Across Fracture Types:** The adapted Endobutton showed mixed performance based on the type of coronoid fracture:
    a. For Type 1 O'Driscoll fractures, the device received poor ratings for fit, reduction, stability, and tension.
    b. For Type 2 fractures, the device received positive ratings for fit, stability, reduction, and tension.
    c. For Type 3 fractures, the device received high ratings for fit, reduction, and stability.

    These findings indicate that the adapted Endobutton is not ideal for Type 1 fractures but is well-suited for Type 2 and Type 3 fractures.

4) **Comparison with Control Device:** The adapted Endobutton performed better than the control device in functionality testing for Type 2 fractures. However, during validation testing, the control was found to be superior for Type 1 fractures.
5) **Implications for Clinical Viability and Future Development:** The consistent usability outcomes and improved functionality scores support the design concept and potential clinical viability.

5.5. Conclusion

The verification and validation testing of the adapted Endobutton demonstrates its potential as an effective method for coronoid fracture fixation. Usability assessments remain consistent and show a significant improvement in bone attachment compared to the commercially available Endobutton. Functionality testing reveal mixed results: the device performs poorly for Type 1 O'Driscoll fractures but excels in Type 2 and Type 3 fractures, providing superior reduction and post-fixation stability

The comparative analysis highlights the adapted Endobutton's enhanced performance over the control for Type 2 fractures, while validation testing confirms its viability for Type 3 fractures. Despite challenges with Type 1 fractures, the device's consistent usability and improved functionality support its design concept. Future potential steps include manufacturing in surgical-grade titanium and addressing identified challenges to ensure efficacy. Expanding the data set and increasing the sample size for validation testing is crucial to confirm these positive outcomes and ensure robustness. Overall, the adapted Endobutton shows promise as an option for coronoid fracture fixation, warranting further development and optimisation.

5.5.1. Chapter Outcomes

The aim of this chapter was to verify and validate the design of the adapted coronoid Endobutton, and it potential to provide improved fixation. This was completed by fulfilling the following objectives:

Rapid Prototype of Adapted Endobutton: The first objective was to create a prototype of the adapted Endobutton. This was accomplished throughout several stages in the methodology. Using resin-based 3D printing techniques allowed for rapid production of the device and testing to be conducted in a timely manner.

Qualitative Assessment and Verification Conclusions: The second and third objectives encompassed evaluating the adapted Endobutton and drawing conclusions from the Qualitative Assessment results. These objectives were achieved by templating the device on the same 3D-printed coronoid fracture models and rating the device against the established criteria.

Mock Surgical Fixation Validation Conclusions: The fourth and fifth objectives involved performing mock surgical fixation using the adapted Endobutton and evaluating the device using the Qualitative Assessment Questionnaire. These objectives were completed by following standard surgical procedures, fixing induced coronoid fractures with the adapted Endobutton and assessing its fit and efficacy. Conclusions validating the designed device were drawn based on the questionnaire results and discussions among participating surgeons.

Comparison of the Endobutton and Adapted Endobutton: The final objective involved comparing the commercially available Endobutton and the adapted Endobutton. This objective was achieved through the statistical analysis and comparison of the Qualitative Assessment results. A final evaluation supporting the design of the adapted Endobutton, and its potentially superior fixation ability was produced.

6. Chapter 6: Project Conclusion

6.1. Overall Discussion

The functional anatomy of the elbow joint significantly depends on the integrity of the coronoid process of the ulnar (Alcid *et al.*, 2004). This bony projection, muscles and ligamentous structures are crucial for elbow stability (Alcid *et al.*, 2004). Numerous literature sources have emphasized the biomechanical role of the coronoid process in maintaining varus stability and preventing posterior dislocation during everyday ranges of motion (Alcid *et al.*, 2004; Fornalski *et al.*, 2003a). However, failure to perform these functions as a result of a fracture may lead to chronic instability, recurrent dislocation and ultimately a loss in daily functioning (Zhang *et al.*, 2020; Salwan *et al.*, 2023). Open Reduction and Internal Fixation (ORIF) has become the standard treatment for coronoid process fractures, as it has been well established that even some of the smallest fractures warrant fixation to ensure proper elbow function (Regan *et al.*, 1989; Salwan *et al.*, 2023).

The reported prevalence of coronoid fractures is low, at around 10-15% of reported elbow fractures, and these fractures rarely occur in isolation (Lowery *et al.*, 2022). The most common coronoid fracture is Type 1, which typically occur in association with the Terrible triad, while Type 2 is reported less frequently (Doornberg *et al.*, 2006). The findings of this study correspond with the association of the Type 1 fractures but contradict existing research with a notably high ratio (63.6%) of Type 2 fracture within the patient cohort.

Although present in the original set of collected CT scans, the Type 3 fractures were excluded from the study due to the presence of additional compromising fractures. The fracture mapping revealed repeated patterns within the specified Types of coronoid fractures. Type 1 often results in a trapezium shaped fragment of the tip of the coronoid, while Type 2 Subtype 2 created a distinctive oblong ‘Africa’ shaped pattern. The production of the fracture type and subtype heat maps which depicted the critical fracture pattern, further emphasized these repeated patterns. Although the repetition of fracture patterns was less prominent in the Type 2 Subtype 3 fractures, the critical fracture pattern shown in the heat maps allowed for the conclusion to be drawn that this specific fracture type is often complex and comminuted in nature.

Qualitative 3D Computer Tomography (Q3DCT) techniques and coronoid process fracture maps are commonplace in the literature. However, these maps are often limited to a two-dimensional plane making it difficult to understand the overall morphology of the fracture and the resultant fragment. This limitation forces surgeons to rely on 2D radiographic images and CT scans to understand these fractures. Mellema (Mellema *et al.*, 2014), Doornberg (Doornberg *et al.*, 2006) and Adams (Adams *et*

al., 2012) all produced two-dimensional coronoid fracture maps in their respective studies, and each of these studies noted that three-dimensional mapping would prove to be a beneficial clinical tool. This study aimed to address that need and found that three-dimensional mapping allowed for an advancement in the understanding of the overall and often recurrent morphology of the fracture fragments. Understanding these characteristics has numerous practical implications, including informing surgical decisions, refining fracture management protocols, and informing the designs of targeted and efficient fixation devices.

The varying fracture morphology among the types and subtypes of coronoid fractures has led to a notable uncertainty in the ideal treatment method (Altan *et al.*, 2016; Liu *et al.*, 2018; Salwan *et al.*, 2023). It is well established that ORIF is the standard for coronoid fracture treatment. Regardless of if the resultant fragments are small, they are still clinically significant due to the coronoid's fundamental role in the elbow's stability (Regan *et al.*, 1989; Salwan *et al.*, 2023; Alcid *et al.*, 2004; Neill Cage *et al.*, 1995). Among the various options for coronoid fracture fixation, the Endobutton emerged as a potentially effective method for suspensory fixation of the coronoid (Altan *et al.*, 2016). However, there is a significant lack of a comprehensive assessment of this fixation device and its effectiveness in treating coronoid fractures. This study aimed to partially address this gap by identifying and understanding the limitations associated with the Endobutton. The results contradicted the positive anecdotal evaluations in existing literature by suggesting this device had a limited efficacy and was anatomically incongruent with the coronoid (Altan *et al.*, 2016; Arrigoni *et al.*, 2016; Salwan *et al.*, 2023). This incompatibility was highlighted by the high report rates of limitations such as incongruency with the bone and a lack of coverage of the fracture fragment. These findings underpinned the call made by Altan *et al.* (2016) and Salwan *et al.* (2023) for an anatomically pre-contoured fixation device.

In order to achieve a better fixation device, the limitations identified during the analysis of the Endobutton were converted into design requirements for an anatomically pre-contoured adapted Endobutton device. Through an elaboration of these design requirements, design specifications were formulated and used to drive a device intended as a potential option for non-rigid suspensory fixation. Through an iterative conceptual and detailed design process, the adapted Endobutton was developed and tested through Qualitative Assessment. The device showed consistent usability results when tested on 3D printed fractures as well as cadavers with simulated fractures. There was a noted improvement in the functional outcomes of the new design for the treatment of Type 2 coronoid fractures compared to the control device (imitated Endobutton). However, the control Endobutton performed better for the fixation of Type 1 fractures. Despite the unfavourable outcomes related to the Type 1 fractures, the adapted Endobutton demonstrated potential as the optimal anatomically pre-contoured device for coronoid fixation.

The idea behind the design and development of the adapted Endobutton was further underscored by the study performed by Wang *et al.* (2017), in which they designed a novel Lasso-plate aimed at the treatment of Type 1 and Type 2 coronoid fractures. Similarly, this study employed an anatomically pre-contoured design through which the lasso-technique sutures were passed. With a relatively large patient population, their study demonstrated that the lasso-plate was able to provide concentric reduction and stable fixation. The promising results and shared motivation for the development of an anatomically pre-contoured plate for treating the small and comminuted coronoid fractures enhanced the robustness of this study.

The clinical implications of the anatomically pre-contoured device are significant. Although some modifications are needed regarding the device's efficacy in treating Type 1 fractures, this device offers itself as a potential option for improved non-rigid suspensory coronoid fracture fixation.

6.1.1. Key Findings in Overall Study

1) **Fundamental Role of the Coronoid Process:** The coronoid process is essential for the varus stability of the elbow joint, and prevents posterior dislocation (Alcid *et al.*, 2004). Fractures of the coronoid can lead to chronic instability and functional loss, emphasizing the importance of effective treatment methods (Alcid *et al.*, 2004; Fornalski *et al.*, 2003a).
2) **Advantages of Three-Dimensional Mapping:** The use of Q3DCT techniques and three-dimensional fracture mapping allow for an advancement in the understanding of the morphology of coronoid fractures. Unlike traditional 2D mapping, 3D mapping offers multiple views of the fracture patterns, which facilitate better surgical planning and management.
3) **Efficacy of the Adapted Endobutton:** Compared to the commercially available Endobutton, the adapted Endobutton showed improved functional outcomes for Type 2 and Type 3 coronoid fractures. However, it performed poorly for Type 1 fractures, indicating a need for further refinement.
4) **Design and Development Insights:** The study underscores the importance of anatomically pre-contoured fixation devices. The adapted Endobutton, developed through iterative design processes, shows potential as a method for coronoid fracture fixation.
5) **Clinical Implications and Future Directions:** The adapted Endobutton holds promise as an improved option for non-rigid suspensory coronoid fracture fixation. However, further modifications are needed to enhance its efficacy for Type 1 fractures. This study highlights the necessity of ongoing research and development to optimise fixation devices for effective clinical application.

6.2. Limitations of Study

Although this study had varying limitations, the noted and most prominent ones included issues with the quality of some of the collected scans, the lack of literature that have comprehensive evaluations of the Endobutton and its usage relative to the coronoid process, and the limited number of available cadaver specimens for validation testing.

The challenges with the quality of the collected scans stemmed from the scans being of poor quality, missing files, and having dropout sections. The variations in the scan quality created downstream effects as the scan quality complicated the identification, segmentation, and analysis of fracture fragments.

The study was limited to O'Driscoll Type 1 and Type 2 fractures, excluding Type 3 fractures as they had additional compromising which would require more robust plate fixation. However, the final number of usable scans was sufficient to produce a well-populated fracture map.

A significant limitation was the lack of evaluation methods for coronoid fracture fixation other than anecdotal evaluations in small patient groups using post-surgical functional scores. The lack of comparable literature addressing the Endobutton's efficacy for treating coronoid fractures and the noted absence of established standards for device evaluation made it challenging to identify and assess critical factors for the device's optimal performance.

The validation testing was limited to three cadaver specimens and although this still provided a representative sample of all the coronoid fracture types, it constrained the study's robustness.

6.3. Overall Conclusions

Coronoid fractures, their complexity and subsequent surgical treatment remain a point of interest in the Orthopaedic field, and the optimal method for the fixation of these fractures remain a point of contention.

This dissertation aimed to design and develop an alternative fixation option in an attempt to mitigate the limitations associated with currently available devices. During the process of achieving this aim, this study provided insight into the morphology of coronoid fractures and their resultant fragments, depicted the critical fracture patterns and determined the limitations of the commercially available Endobutton. The use of fracture and heat maps; as well as understanding the limitations of the commercially available fixation devices, provided a foundation for the design of the adapted Endobutton device.

The produced design of the adapted Endobutton showed substantial promise in addressing this study's research question: *Can a redesigned adapted Endobutton fixation device be produced to provide improved reduction and fixation of coronoid fractures?*" This answer lent itself to the overall conclusion of this study that an anatomically pre-contoured Endobutton shows significant potential as an optimal method of fixation for coronoid process fractures.

6.3.1. Overall Study Outcomes

The overall study outcomes matched the set-out study objectives and addressed the aim of designing and developing an adapted Endobutton fixation method for treating coronoid process fractures.

Set of Reference Fracture Maps: This objective of creating a set of fracture maps to use as a reference and guide for the design of an adapted Endobutton device was successfully completed. Using Q3DCT techniques, 3D models of each scan were created, and images of the fractures were two-dimensionally layered. These layered images from various viewpoints formed a three-dimensional fracture map. Heat maps were used to further elaborate on the 3D mapping of the coronoid and provided an understanding of the critical fracture patterns, as well as identifying weak points within the bone's structure. The use of fracture and heat maps enhanced the understanding of the morphology of coronoid fractures and their resultant fragments.

Endobutton Limitations: The second objective included a comprehensive evaluation of the commercially available Endobutton to determine the device's limitations. This was effectively achieved by templating the imitated device on accurate 3D-printed coronoid fracture models and performing a Qualitative Assessment. This facilitated a comprehensive understanding of the device's usability, functionality, and the limitations of most consequence. As a result, these limitations formed the foundation of the initial design requirements for the adapted Endobutton.

Design and Development of The Adapted Endobutton: The third and most prominent objective encompassed the design and development of the adapted Endobutton device. The objective was successfully met through an iterative conceptual and detailed design process. This process was based on the foundation of the limitations of the commercially available Endobutton.

Verification and Validation of Adapted Endobutton: The verification and validation of the designed device fulfilled the fourth and final main objective of the study. Verification was acquired through templating the device on the 3D printed bone models and performing a

Qualitative Assessment. Validation of the design came through simulated surgical fixation procedures performed using the adapted Endobutton in cadaver limbs. The adapted Endobutton showed promising results in treating Type 2 and Type 3 coronoid fractures; however, design modifications are required to improve the device's efficacy in treating Type 1 fractures.

6.4. Recommendation for Future Studies

The fracture and heat mapping studies proved fruitful in providing insight into the 3-dimensional view of the fractures of the coronoid; however, there were only a handful of Type 1 fractures and a notable lack of Type 3 fractures in the maps. This research could be furthered by doing more extensive fracture maps with a larger CT sample number. Additional fracture studies using an alternative source of CT scans (i.e.: different hospitals in Cape Town or from hospitals throughout South Africa) would prove beneficial in gaining a widespread understanding of coronoid fractures and their prevalence in the South African population.

This study aimed to design and develop an initial proof of concept for the adapted Endobutton. Therefore, there is a lot of potential for further testing to be conducted. The design showed promising results, suggesting that the next step in the design's evolution would be to manufacture the device using an approved orthopaedic titanium alloy. The manufacturing of this device would allow more comprehensive testing to be conducted. To ensure the device is manufactures using the correct materials and methods, compliance testing would be involved in the manufacturing process.

More in-depth verification testing could be done using a finite element model (FEM) analysis. This could be done prior to, during or after the manufacturing process has taken place.

After manufacturing the device, tests used during the verification and validation can be repeated using the titanium device. The repetition and comparison would allow us to establish whether the design is actually suitable for addressing the problematic coronoid fracture fixation methods, and if the material used has any effect on the functionality and usability of the device. The repetition of the functionality and user testing would help ascertain if the promising results from the pre-manufacturing process can be repeated or improved upon. Essential post-manufacturing testing would include safety, durability and reliability, performance metrics testing, biocompatibility, and sterilisation testing.

Overall, the designed device shows significant potential as a solution to the lack of an optimal fixation method for small, multi-fragment coronoid fractures. However, substantial work remains before this device is ready for clinical application.

References

Adams, J.E. 2020. Elbow instability: evaluation and treatment. Hand Clinics. 36(4):485-94.

Adams, J.E., Hoskin, T.L., Morrey, B.F., Steinmann, S.P. 2009. Management and outcome of 103 acute fractures of the coronoid process of the ulna. The Journal of Bone & Joint Surgery British Volume. 91-B(5):632-5.

Adams, J.E., Sanchez-Sotelo, J., Kallina, C.F., Morrey, B.F., Steinmann, S.P. 2012. Fractures of the coronoid: morphology based upon computer tomography scanning. Journal of Shoulder and Elbow Surgery. 21(6):782-8.

Alcid, J.G., Ahmad, C.S., Lee, T.Q. 2004. Elbow anatomy and structural biomechanics. Clinics in Sports Medicine. 23(4):503-17.

Altan, E., Ozel, O., Ozbaydar, M.U., Bekmezci, T. 2016. Endobutton Fixation Technique for Multifragmented Coronoid Fractures. Techniques in Hand & Upper Extremity Surgery. 20(4):137-40.

An, K., Morrey, B.F., Chao, E.Y. 1986. The effect of partial removal of proximal ulna on elbow constraint. Clinical orthopaedics and related research. (209):270-9.

Arrigoni, P., D'ambrosi, R., Cucchi, D., Nicoletti, S., Guerra, E. 2016. Arthroscopic fixation of coronoid process fractures through coronoid tunnelling and capsular plication. Joints. 04(03):153-8.

Ayati Firoozabadi, M., Dehghaniashkezari, D., Seyedtabaei, S.M.M., Tabatabaei Irani, P., Khaledian, H., Bozorgi Savodji, P., et al. 2024. Arthroscopic ACL Avulsion Fixation With Adjustable Loop Length Cortical Endobutton. Arthroscopy Techniques. 13(1):102815.

Bellato, E., O'driscoll, S.W. 2019. Management of the Posttraumatic Coronoid-Deficient Elbow. Journal of Hand Surgery. 44(5):400-10.

Bizzotto, N., Sandri, A., Regis, D., Romani, D., Tami, I., Magnan, B. 2015. Three-Dimensional Printing of Bone Fractures: A New Tangible Realistic Way for Preoperative Planning and Education. Surgical Innovation. 22(5):548-51.

Bryce, C.D., Armstrong, A.D. 2008a. Anatomy and biomechanics of the elbow. Orthopedic Clinics of North America. 39(2):141-54.

Bryce, C.D., Pennypacker, J.L., Kulkarni, N., Paul, E.M., Hollenbeak, C.S., Mosher, T.J., et al. 2008b. Validation of three-dimensional models of in situ scapulae. Journal of Shoulder and Elbow Surgery. 17(5):825-32.

Budoff, J.E. 2012. Coronoid Fractures. The Journal of Hand Surgery. 37(11):2418-23.

Chamseddine, A.H., Zein, H.K., Hamdan, H.R., Khalil, B.N., Obeid, B.M. 2010. Unstable elbow dislocation with coronoid process fracture associated with distal radius fracture: a case report and review of the literature. European Journal of Orthopaedic Surgery & Traumatology. 20(2):157-63.

Chan, K., Faber, K.J., King, G.J.W., Athwal, G.S. 2016. Selected anteromedial coronoid fractures can be treated nonoperatively. Journal of Shoulder and Elbow Surgery. 25(8):1251-7.

Chan, K., Macdermid, J.C., Faber, K.J., King, G.J.W., Athwal, G.S. 2014. Can We Treat Select Terrible Triad Injuries Nonoperatively? Clinical Orthopaedics and Related Research®. 472(7).

Charilaou, J., Dey, R., Burger, M., Sivarasu, S., Van Staden, R., Roche, S. 2021. Quantitative fit analysis of acromion fracture plating systems using three-dimensional reconstructed scapula fractures - A multi-observer study. Sicot j. 736.

Chen, H.-W., He, H.-H., Gao, B.-L. 2018. Efficacy of internal fixation with mini plate and internal fixation with hollow screw for Regan-Morrey type II and III ulna coronoid fractures. BMC Musculoskeletal Disorders. 19(1):194.

Cohen, M.S., Hastings, H., Ii. 1997. Rotatory Instability of the Elbow. The Anatomy and Role of the Lateral Stabilizers*. JBJS. 79(2).

Desouza, C., Jani, C., Kale, A. 2020. Elbow dislocation with coronoid and ipsilateral distal radius fracture. International Journal of Case Reports in Orthopaedics. 272-4.

Dey, R. 2023. Mapping of Orthopaedic Fractures for Optimal Surgical Guidance. In: Shapiro, L.Rea, P. M. (eds.) Biomedical Visualisation : Volume 13 – The Art, Philosophy and Science of Observation and Imaging. Cham: Springer International Publishing.

Doornberg, J.N., Ring, D. 2006. Coronoid Fracture Patterns. Journal of Hand Surgery. 31(1):45-52.

Drake, R., Vogl, A.W., Mitchell, A.W.M. 2019. Gray's Anatomy for Students E-Book. 4 edn.: Elsevier Health Sciences.
Dunning, C.E., Zarzour, Z.D.S., Patterson, S.D., Johnson, J.A., King, G.J.W. 2001. Muscle Forces and Pronation Stabilize the Lateral Ligament Deficient Elbow. Clinical Orthopaedics and Related Research (1976-2007). 388.
Eguchi, A., Ochi, M., Adachi, N., Deie, M., Nakamae, A., Usman, M.A. 2014. Mechanical properties of suspensory fixation devices for anterior cruciate ligament reconstruction: Comparison of the fixed-length loop device versus the adjustable-length loop device. The Knee. 21(3):743-8.
Eltorai, A.E.M., Nguyen, E., Daniels, A.H. 2015. Three-Dimensional Printing in Orthopedic Surgery. Orthopedics. 38(11):684-7.
Feng, D., Zhang, X., Jiang, Y., Zhu, Y., Wang, H., Wu, S., et al. 2018. Plate fixation through an anterior approach for coronoid process fractures: A retrospective case series and a literature review. Medicine. 97(36):e12041-e.
Fornalski, S., Gupta, R., Lee, T.Q. 2003a. Anatomy and biomechanics of the elbow joint. Sports Medicine and Arthroscopy Review. 11(1):1-9.
Fornalski, S., Gupta, R., Lee, T.Q. 2003b. Anatomy and Biomechanics of the Elbow Joint. Sports Medicine and Arthroscopy Review. 11(1).
Garrigues, G.E., Wray, W.H., Lindenhovius, A.L.C., Ring, D., Ruch, D.S. 2011. Fixation of the coronoid process in elbow fracture-dislocations. The Journal of bone and joint surgery. American volume. 93 201873-81.
Gray, A.B., Alolabi, B., Ferreira, L.M., Athwal, G.S., King, G.J.W., Johnson, J.A. 2013. The Effect of a Coronoid Prosthesis on Restoring Stability to the Coronoid-Deficient Elbow: A Biomechanical Study. The Journal of Hand Surgery. 38(9):1753-61.
Janssen, S.J., Ter Meulen, D.P., Hageman, M.G.J.S., Earp, B.E., Ring, D. 2015. Quantitative 3-Dimensional CT Analyses of Fractures of the Middle Phalanx Base. HAND. 10(2):210-4.
Jo, S.W., Shin, D.J. 2023. The Novel Hooked Kirschner Wire Technique for Ulna Coronoid Process Fractures. Clin Orthop Surg. 15(1):127-34.
Kloen, P., Ring, D./AO Surgery Reference[Internet]. AO Surgery Reference - Repair of coronoid fracture. AO Surgery Reference. Available from: https://surgeryreference.aofoundation.org/orthopedic-trauma/adult-trauma/proximal-forearm/ulna-articular-coronoid/repair-of-coronoid-fracture.

Latef, T.J., Bilal, M., Vetter, M., Iwanaga, J., Oskouian, R.J., Tubbs, R.S. 2018. Injury of the radial nerve in the arm: a review. Cureus. 10(2).
Lin, F., Kohli, N., Perlmutter, S., Lim, D., Nuber, G.W., Makhsous, M. 2007. Muscle contribution to elbow joint valgus stability. Journal of Shoulder and Elbow Surgery. 16(6):795-802.
Liu, G., Hu, J., Ma, W., Li, M., Xu, R., Pan, Z. 2018. Surgical treatment for terrible triad injury of the elbow with anteromedial coronoid fracture through a combined surgical approach. Journal of International Medical Research. 46(8):3053-64.
Lockard, M. 2006. Clinical Biomechanics of the Elbow. Journal of Hand Therapy. 19(2):72-81.
Lowery, M., Massey, P. 2022. Coronoid Fractures. Statpearls [internet]. StatPearls Publishing.
Mallard, F., Hubert, L., Steiger, V., Cronier, P. 2015. An original internal fixation technique by tension band wiring with steel wire in fractures of the coronoid process. Orthopaedics & Traumatology: Surgery & Research. 101(4, Supplement):S211-S5.
Marinescu, R., Popescu, D., Laptoiu, D. 2020. A Review on 3D-Printed Templates for Precontouring Fixation Plates in Orthopedic Surgery. Journal of Clinical Medicine. 9(9):2908.
Matzon, J.L., Widmer, B.J., Draganich, L.F., Mass, D.P., Phillips, C.S. 2006. Anatomy of the Coronoid Process. The Journal of Hand Surgery. 31(8):1272-8.
Mellema, J.J., Doornberg, J.N., Dyer, G.S.M., Ring, D. 2014. Distribution of Coronoid Fracture Lines by Specific Patterns of Traumatic Elbow Instability. The Journal of Hand Surgery. 39(10):2041-6.
Mellema, J.J., Janssen, S.J., Guitton, T.G., Ring, D. 2015. Quantitative 3-Dimensional Computed Tomography Measurements of Coronoid Fractures. The Journal of Hand Surgery. 40(3):526-33.

Morrey, B.F., An, K.-N. 1983. Articular and ligamentous contributions to the stability of the elbow joint. The American Journal of Sports Medicine. 11(5):315-9.
Morrey, B.F., Sotelo, J.S., Morrey, M.E. 2017. Morrey's The Elbow and Its Disorders E-Book. Fifth Edition edn.: Elsevier Health Sciences.
Neill Cage, D.J., Abrams, R.A., Callahan, J.J., Botte, M.J. 1995. Soft Tissue Attachments of the Ulnar Coronoid Process: An Anatomic Study With Radiographic Correlation. Clinical Orthopaedics and Related Research®. 320.
Netter, F.H. 2018. Atlas of Human Anatomy. 7 edn.: Elsevier.
O'driscoll, S.W., Jupiter, J.B., Cohen, M.S., Ring, D., Mckee, M.D. 2003. Difficult elbow fractures: pearls and pitfalls. Instructional Course Lectures. 52113-34.
Pai, V., Pai, V. 2009. Use of Suture Anchors for Coronoid Fractures in the Terrible Triad of the Elbow. Journal of Orthopaedic Surgery. 17(1):31-5.
Park, S.-M., Lee, J.S., Jung, J.Y., Kim, J.Y., Song, K.-S. 2015. How should anteromedial coronoid facet fracture be managed? A surgical strategy based on O'Driscoll classification and ligament injury. Journal of Shoulder and Elbow Surgery. 24(1):74-82.
Rausch, V., Jettkant, B., Lotzien, S., Rosteius, T., Mempel, E., Schildhauer, T.A., et al. 2021. Biomechanical comparison of screw osteosyntheses and anatomical plating for coronoid shear fractures of the ulna. Archives of Orthopaedic and Trauma Surgery. 141(9):1509-15.
Regan, W., Morrey, B. 1989. Fractures of the coronoid process of the ulna. JBJS. 71(9):1348-54.
Ring, D. 2006. Fractures of the Coronoid Process of the Ulna. The Journal of Hand Surgery. 31(10):1679-89.
Ring, D., Horst, T.A. 2015. Coronoid Fractures. Journal of Orthopaedic Trauma. 29(10).
Ring, D., Jupiter, J.B., Zilberfarb, J. 2002. Posterior Dislocation of the Elbow with Fractures of the Radial Head and Coronoid. JBJS. 84(4):547-51.
Rylander, L., Brunelli, J., Taylor, M., Baldini, T., Ellis, B., Hawkins, M., et al. 2014. A biomechanical comparison of anterior cruciate ligament suspensory fixation devices in a porcine cadaver model. Clinical Biomechanics. 29(2):230-4.
Salwan, A., Saoji, A., Pisulkar, G., Awasthi, A.A., Taywade, S. 2023. Use of Endobutton for Small Avulsion Fracture of Coronoid in the Terrible Triad of the Elbow: A Case Report. Cureus. 15(4).
Van Riet, R.P., Morrey, B.F. 2008. Documentation of associated injuries occurring with radial head fracture. (0009-921X (Print)).
Wang, C., Zhang, C., Zhou, D., Lu, D., Li, Z., Duan, N., et al. 2023. A novel and superior Lasso-plate technique in treatment for coronoid process fracture in the terrible triad of elbow. Scientific Reports. 13(1):11656.
Wang, P., Zhuang, Y., Li, Z., Wei, W., Fu, Y., Wei, X., et al. 2017. Lasso plate – An original implant for fixation of type I and II Regan-Morrey coronoid fractures. Orthopaedics & Traumatology: Surgery & Research. 103(3):447-51.
Wells, J., Ablove, R.H. 2008. Coronoid fractures of the elbow. Clinical medicine & research. 6(1):40-4.
White, T.D., Folkens, P.A. 2005. The Human Bone Manual. Elsevier Science.
Zhang, H.-L., Lin, K.-J., Lu, Y. 2020. Prediction of the Size of the Fragment in Comminuted Coronoid Fracture Using the Contralateral Side: An Analysis of Similarity of Bilateral Ulnar Coronoid Morphology. Orthopaedic Surgery. 12(5):1495-502.

Appendix A - HREC Approval Letter

UNIVERSITY OF CAPE TOWN
Faculty of Health Sciences
Human Research Ethics Committee

Room 45 E-52-E-Floor- Old Main Building
Groote Schuur Hospital
Observatory 7925
Telephone [021] 406 6492
Email: hrec-submissions@uct.ac.za
Website: www.health.uct.ac.za/fhs/research/humanethics/forms

20 September 2022

HREC REF: 588/2022

Prof S Sivarasu
Division of Biomedical Engineering
Office 7.17, Floor 7- Anatomy Building
Email: Sudesh.sivarasu@uct.ac.za
Student: MSNNIC004@myuct.ac.za

Dear Prof Sivarasu

PROJECT TITLE: EVALUATION AND DESIGN OF AN IMPROVED PLATE FIXATION SYSTEM USED IN CONJUNCTION WITH SUTURE AND ENDOBUTTON TECHNIQUES FOR THE TREATMENT OF CORONOID PROCESS FRACTURES-
(MPHIL CANDIDATE-MISS NICOLA MASON)

Thank you for submitting your study to the Faculty of Health Sciences Human Research Ethics Committee (HREC) for review.

It is a pleasure to inform you that the HREC has **formally approved** the above-mentioned study.

Approval is granted for one year until the 30 September 2023.

Please submit a progress form, using the standardised Annual Report Form if the study continues beyond the approval period. Please submit a Standard Closure form if the study is completed within the approval period.
(Forms can be found on our website: www.health.uct.ac.za/fhs/research/humanethics/forms)

The HREC acknowledge that the student: -Miss Nicola Mason will also be involved in this study.

Please quote the HREC REF 588/2022 in all your correspondence.

Please note that the ongoing ethical conduct of the study remains the responsibility of the principal investigator.

Please note that for all studies approved by the HREC, the principal investigator **must** obtain appropriate institutional approval, where necessary, before the research may occur.

Yours sincerely

PROFESSOR M BLOCKMAN
CHAIRPERSON, FACULTY OF HEALTH SCIENCES HUMAN RESEARCH ETHICS COMMITTEE

HREC.REF 588.2022

UNIVERSITY OF CAPE TOWN

FACULTY OF HEALTH SCIENCES
Human Research Ethics Committee

FHS016: Annual Progress Report / Renewal

HREC office use only (FWA00001637; IRB00001938) **This serves as notification of annual approval, including any documentation described below.**			
☑ Approved	Annual progress report	Approved until/next renewal date	28.02.2025
☐ Not approved	See attached comments		
Signature Chairperson of the HREC/ Designee		Date Signed	7/2/2024

Note: Please email this form and supporting documents (if applicable) in a combined pdf-file to hrec-enquiries@uct.ac.za.
Please clarify your plan for research-related activities during COVID-19 lockdown.
Please use the latest form found on our website:
http://www.health.uct.ac.za/fhs/research/humanethics/forms

HUMAN RESEARCH ETHICS COMMITTEE
- 7 FEB 2024
HEALTH SCIENCES FACULTY
UNIVERSITY OF CAPE TOWN

Comments to PI from the HREC
Thank you for the deviation document

Principal Investigator to complete the following:

1. Protocol information

Date (when submitting this form)	06 February 2024		
HREC REF Number	588/2022	Current Ethics Approval was granted until	30 Sept 2023
Protocol title	Evaluation and Design of an Improved Plate Fixation System Used in Conjunction with Suture and Endobutton Techniques for The Treatment of Coronoid Process Fractures.		
Protocol number (if applicable)			
Are there any sub-studies linked to this study?		☐ Yes	☑ No
If yes, could you please provide the HREC Reference number for all sub-studies? **Note:** A separate FHS016 must be submitted for each sub-study.	N/A		
Principal Investigator	Sudesh Sivarasu		
Department / Office Internal Mail Address	Human biology, Anatomy building room 7.17, Faculty of Health Science, Anzio Rd Observatory 7925		

(Note: Please complete the Closure form (FHS010) if the study is completed within the approval period)

UNIVERSITY OF CAPE TOWN
Faculty of Health Sciences
Human Research Ethics Committee

E52-Room 45 Old Main Building
Groote Schuur Hospital
Observatory 7925
Telephone [021] 406 6492
Email: hrec-enquiries@uct.ac.za
Website: https://health.uct.ac.za/home/human-research-ethics

21 June 2024

HREC REF: 588/2022

Prof S Sivarasu
Division of Biomedical Engineering
Office 7.17 Floor 7, Anatomy Building-
Email: sudesh.sivarasu@uct.ac.za

Dear Prof Sivarasu

PROJECT TITLE: EVALUATION AND DESIGN OF AN IMPROVED PLATE FIXATION SYSTEM USED IN CONJUNCTION WITH SUTURE AND ENDOBUTTON TECHNIQUES FOR THE TREATMENT OF CORONOID PROCESS FRACTURES-
(MPHIL CANDIDATE-MISS NICOLA MASON)

Thank you for submitting the protocol amendment received 11 June 2024 to the Faculty of Health Sciences Human Research Ethics Committee (HREC) for review.

1. This MPHIL be submitted in addition as a stand-alone substudy of HREC.REF 588/2022. Each master's study requires its own protocol, application form (FHS013) and study number. Title of MSc should be different to main study protocol. This also requires a study staff amendment.

Please quote the HREC REF 588/2022 in all your correspondence.

Yours sincerely

PROFESSOR MARC BLOCKMAN
CHAIRPERSON, FACULTY OF HEALTH SCIENCES HUMAN RESEARCH ETHICS COMMITTEE

Appendix B – Fracture Mapping Data Collection Sheet

Patient Number	Scan File Name	Left or Right	Age	Sex	Excluded (Yes/No)	Comminuted Fracture	Additional Fractures	Dislocation
1	SER_0000	Left	61	F	Yes	Yes	None	Potential dislocation
2	SER_0001	Left	44	M	No	No	Radial head fracture	None
3	SER_0004	Left	38	F	Yes	Yes	Radial head fracture + ulna shaft fracture	Yes - partial dislocation
4	SER_0000	Right	55	M	No	Yes	Radial head fracture	None
5	SER_0002	Right	25	M	No	Yes	Radial head fracture	Yes - partial dislocation
6	SER_0002	Right	23	F	No	No	Radial head fracture	None
7	SER_0002	Left	25	M	Yes	Yes	None	None
8	SER_0002	Left	59	M	No	Yes	None	None
9	SER_0003	Right	34	M	No	Yes	None	Yes - partial dislocation
10	SER_0006	Left	59	M	Yes	No	None	None
11	SER_0003	Right	58	F	No	Yes	Radial head fracture	Yes - partial dislocation
12	SER_0003	Left	34	F	No	No	Radial head fracture	None
13	SER_0002	Right	41	M	No	Yes	Radial head fracture	None
14	SER_0005	Right	36	M	No	Yes	Radial head fracture	None
15	SER_0002	Left	34	F	Yes	No	None	None
16	SER_0005	Left	34	M	No	Yes	Radial head fracture	None
17	SER_0004	Right	38	M	No	Yes	Radial head fracture	None
18	SER_0002	Right	78	F	No	No	Distal humerus fracture (medial epicondyle fracture)	Yes - partial dislocation
19	SER_0003	Left	65	M	No	Yes	None	None
20	SER_0004	Right	30	F	No	No	Radial head fracture	Yes - partial dislocation
21	SER_0001	Left	34	M	No	No	Radial head fracture	None
22	SER_0001	Left	55	F	Yes	Yes	Radial head fracture	Yes - fully dislocated
23	SER_0002	Left	59	M	Yes	Yes	Other additional fractures	None
24	SER_0003	Left	33	M	No	Yes	Other additional fractures	None
25	SER_0001	Left	29	M	Yes	No	Radial head fracture, olecranon process fracture, midline ulna fracture and ulna shaft fracture	Potential dislocation
26					Yes			
27	SER_0002	Right	29	M	No	Yes	None	None
28	SER_0000	Right	30	M	Yes	No	Radial head fracture	None
29	SER_0003	Left	57	M	Yes	Yes	Radial head fracture	None
30	SER_0003	Left	54	M	No	Yes	Radial head fracture	Yes - fully dislocated
31	SER_0002	Right	62	F	Yes	No	Radial head fracture	None
32	SER_0003	Left	36	M	Yes	No	Radial head fracture, Olecranon process fracture, Ulna shaft fracture	Potential dislocation
33	SER_0001	Left	44	M	No	Yes	None	None
34	SER_0005	Left	26	M	No	Yes	None	None
35	SER_0002	Left	41	F	Yes	No	Distal humerus fracture (entire distal head and lateral epicondyle)	Potential dislocation
36	SER_0001	Left	44	M	No	No	Radial head fracture	None
37	SER_0001	Left	35	M	Yes	Yes	None	None
38	SER_0002	Left	13	M	Yes	Yes	Separate fractures to the medial and lateral epicondyle of the distal humerus. Fracture to the posterior surface of the olecranon process. Possible fracture to the radial head.	Yes - partial dislocation
39	SER_0002	Left	62	F	Yes	?	*UNKNOWN*	*UNKNOWN*
40	SER_0004	Left	29	M	No	Yes	None	Yes - fully dislocated
41	SER_0001	Left	38	F	No	Yes	Radial head fracture	None
42	SER_0003	Left	38	M	No	Yes	Radial head fracture + Distal humerus fracture (Lateral epicondyle fracture)	None
43	SER_0000	Left	26	M	Yes	No	Radial head fracture + Distal humerus fracture (Separate comminuted fractures to the medial and lateral epicondyle. Possibly more fractures to the distal humerus)	None
44	SER_0005	Left	32	M	No	No	Radial head fracture	None
45	SER_0002	Left	14	M	No	No	None	None

Basic Stats

	Range	Average	Std Dev
Age	13-78	38,75	13,97
	Left	Right	Unknown
	44	16	3
Sides	69,8%	25,4%	4,8%
	Male	Female	Unknown
	42	18	3
Sex	66,7%	28,6%	4,8%
	Included	Excluded	
	33	30	
Used Scans	52,4%	47,6%	
Associated Fractures	44	73%	
Comminuted	34	57%	
Dislocation	22	37%	

Patient Number	Scan File Name	Left or Right	Age	Sex	Excluded (Yes/No)	Comminuted Fracture	Additional Fractures	Dislocation
1	SER_0000	Left	61	F	Yes	Yes	None	Potential dislocation
2	SER_0001	Left	44	M	No	No	Radial head fracture	None
3	SER_0004	Left	38	F	Yes	Yes	Radial head fracture + ulna shaft fracture	Yes - partial dislocation
4	SER_0000	Right	55	M	No	Yes	Radial head fracture	None
5	SER_0002	Right	25	M	No	Yes	Radial head fracture	Yes - partial dislocation
6	SER_0002	Right	23	F	No	No	Radial head fracture	None
7	SER_0002	Left	25	M	Yes	Yes	None	None
8	SER_0002	Left	59	M	No	Yes	None	None
9	SER_0003	Right	34	M	No	Yes	None	Yes - partial dislocation
10	SER_0006	Left	59	M	Yes	No	None	None
11	SER_0003	Right	58	F	No	Yes	Radial head fracture	Yes - partial dislocation
12	SER_0003	Left	34	F	No	No	Radial head fracture	None
13	SER_0002	Right	41	M	No	Yes	Radial head fracture	None
14	SER_0005	Right	36	M	No	Yes	Radial head fracture	None
15	SER_0002	Left	34	F	Yes	No	None	None
16	SER_0005	Left	34	M	No	Yes	Radial head fracture	None
17	SER_0004	Right	38	M	No	Yes	Radial head fracture	None
18	SER_0002	Right	78	F	No	No	Distal humerus fracture (medial epicondyle fracture)	Yes - partial dislocation
19	SER_0003	Left	65	M	No	Yes	None	None
20	SER_0004	Right	30	F	No	No	Radial head fracture	Yes - partial dislocation
21	SER_0001	Left	34	M	No	No	Radial head fracture	None
22	SER_0001	Left	55	F	Yes	Yes	Radial head fracture	Yes - fully dislocated
23	SER_0002	Left	59	M	Yes	Yes	Other additional fractures	None
24	SER_0003	Left	33	M	No	Yes	Other additional fractures	None
25	SER_0001	Left	29	M	Yes	No	Radial head fracture, olecranon process fracture, midline ulna fracture and ulna shaft fracture	Potential dislocation
26					Yes			
27	SER_0002	Right	29	M	No	Yes	None	None
28	SER_0000	Right	30	M	Yes	No	Radial head fracture	None
29	SER_0003	Left	57	M	Yes	Yes	Radial head fracture	None
30	SER_0003	Left	54	M	No	Yes	Radial head fracture	Yes - fully dislocated
31	SER_0002	Right	62	F	Yes	No	Radial head fracture	None
32	SER_0003	Left	36	M	Yes	No	Radial head fracture, Olecranon process fracture, Ulna shaft fracture	Potential dislocation
33	SER_0001	Left	44	M	No	Yes	None	None
34	SER_0005	Left	26	M	No	Yes	None	None
35	SER_0002	Left	41	F	Yes	No	Distal humerus fracture (entire distal head and lateral epicondyle)	Potential dislocation
36	SER_0001	Left	44	M	No	No	Radial head fracture	None
37	SER_0001	Left	35	M	Yes	Yes	None	None
38	SER_0002	Left	13	M	Yes	Yes	Separate fractures to the medial and lateral epicondyle of the distal humerus. Fracture to the posterior surface of the olecranon process. Possible fracture to the radial head.	Yes - partial dislocation
39	SER_0002	Left	62	F	Yes	?	*UNKNOWN*	*UNKNOWN*
40	SER_0004	Left	29	M	No	Yes	None	Yes - fully dislocated
41	SER_0001	Left	38	F	No	Yes	Radial head fracture	None
42	SER_0003	Left	38	M	No	Yes	Radial head fracture + Distal humerus fracture (Lateral epicondyle fracture)	None
43	SER_0000	Left	26	M	Yes	No	Radial head fracture + Distal humerus fracture (Separate comminuted fractures to the medial and lateral epicondyle. Possibly more fractures to the distal humerus)	None
44	SER_0005	Left	32	M	No	No	Radial head fracture	None
45	SER_0002	Left	14	M	No	No	None	None

Basic Stats

	Range	Average	Std Dev
Age	13-78	38,75	13,97
	Left	Right	Unknown
	44	16	3
Sides	69,8%	25,4%	4,8%
	Male	Female	Unknown
	42	18	3
Sex	66,7%	28,6%	4,8%
	Included	Excluded	
	33	30	
Used Scans	52,4%	47,6%	
Associated Fractures	44	73%	
Comminuted	34	57%	
Dislocation	22	37%	

46	SER_0001	Right	51	F	Yes	No	Radial head fracture, shaft of the ulna (separating the olecranon, coronoid and shaft of the bone)	Potential dislocation
47	SER_0002	Left	37	M	Yes	No	None	Yes - fully dislocated
48					Yes			
49	SER_0004	Left	33	M	Yes	Yes	Radial head fracture	None
50	SER_0006	Left	29	M	No	Yes	None	None
51	SER_0003	Left	20	M	Yes	No	Possible lateral epicondyle fracture	None
52	SER_0008	Left	23	M	No	No	Radial head fracture	Yes - fully dislocated
53	SER_0002	Left	27	M	Yes	No	Radial head fracture	None
54					Yes			
55	SER_0004	Left	28	M	Yes	Yes	Radial head fracture, possible lateral epicondyle and olecranon process fracture	Yes - fully dislocated
56	SER_0002	Left	27	M	No	Yes	Radial head fracture	None
57	SER_0001	Right	30	F	No	Yes	Potential radial head fracture, potential medial epicondyle fracture	None
58	SER_0003	Left	47	M	Yes	Yes	Potential fracture to the radial head	Yes - fully dislocated
59	SER_0001	Right	24	F	Yes	Unknown	None (Previous ORIF procedure of radial head)	None
60	SER_0002	Left	37	F	Yes	Yes	Possible radial head fracture	Yes - fully dislocated
61	SER_0006	Left	44	F	No	Yes	None	None
62	SER_0004	Left	52	M	No	Yes	Radial head fracture	None
63	SER_0001	Left	25	M	Yes	Unknown	Possible additional fractures	None, but potential

Patient Number	Scan File Name	Left or Right	Age	Sex	Excluded (Yes/No)	Comminuted Fracture	Additional Fractures	Dislocation	Classification
2	SER_0001	Left	44	M	No	No	Radial head fracture	None	Type 2 Subtype 2
4	SER_0000	Right	55	M	No	Yes	Radial head fracture	None	Type 1 Subtype 2
5	SER_0002	Right	25	M	No	Yes	Radial head fracture	Yes - partial dislocation	Type 2 Subtype 2
6	SER_0002	Right	23	F	No	No	Radial head fracture	None	Type 2 Subtype 2
8	SER_0002	Left	59	M	No	Yes	None	None	Type 2 Subtype 3
9	SER_0003	Right	34	M	No	Yes	None	Yes - partial dislocation	Type 2 Subtype 2
11	SER_0003	Right	58	F	No	Yes	Radial head fracture	Yes - partial dislocation	Type 1 Subtype 2
12	SER_0003	Left	34	F	No	No	Radial head fracture	None	Type 2 Subtype 2
13	SER_0002	Right	41	M	No	Yes	Radial head fracture	None	Type 2 Subtype 3
14	SER_0005	Right	36	M	No	Yes	Radial head fracture	None	Type 2 Subtype 3
16	SER_0005	Left	34	M	No	Yes	Radial head fracture	None	Type 2 Subtype 2
17	SER_0004	Right	38	M	No	Yes	Radial head fracture	None	Type 2 Subtype 2
18	SER_0002	Right	78	F	No	No	Distal humerus fracture (medial epicondyle fracture)	Yes - partial dislocation	Type 1 Subtype 2
19	SER_0003	Left	65	M	No	Yes	None	None	Type 2 Subtype 3
20	SER_0004	Right	30	F	No	No	Radial head fracture	Yes - partial dislocation	Type 1 Subtype 1
21	SER_0001	Left	34	M	No	No	Radial head fracture	None	Type 1 Subtype 2
24	SER_0003	Left	33	M	No	Yes	Other additional fractures	None	Type 1 Subtype 2
27	SER_0002	Right	29	M	No	Yes	None	None	Type 2 Subtype 1
30	SER_0003	Left	54	M	No	Yes	Radial head fracture	Yes - fully dislocated	Type 1 Subtype 2
33	SER_0001	Left	44	M	No	Yes	None	None	Type 2 Subtype 2
34	SER_0005	Left	26	M	No	Yes	None	None	Type 2 Subtype 2
36	SER_0001	Left	44	M	No	No	Radial head fracture	None	Type 2 Subtype 2
40	SER_0004	Left	29	M	No	Yes	None	Yes - fully dislocated	Type 2 Subtype 3
41	SER_0001	Left	38	F	No	Yes	Radial head fracture	None	Type 2 Subtype 3
42	SER_0003	Left	38	M	No	Yes	Radial head fracture + Distal humerus fracture (Lateral epicondyle fracture)	None	Type 2 Subtype 2
44	SER_0005	Left	32	M	No	No	Radial head fracture	None	Type 1 Subtype 2
45	SER_0002	Left	14	M	No	No	None	None	Type 2 Subtype 1
50	SER_0006	Left	29	M	No	Yes	None	None	Type 2 Subtype 2
52	SER_0008	Left	23	M	No	No	Radial head fracture	Yes - fully dislocated	Type 2 Subtype 2
56	SER_0002	Left	27	M	No	Yes	Radial head fracture	None	Type 1 Subtype 1
57	SER_0001	Right	30	F	No	Yes	Potential radial head fracture, potential medial epicondyle fracture	None	Type 2 Subtype 2
61	SER_0006	Left	44	F	No	Yes	None	None	Type 1 Subtype 2
62	SER_0004	Left	52	M	No	Yes	Radial head fracture	None	Type 2 Subtype 2

Patient Number	Scan File Name	Classification	Column1	Column2
2	SER_0001	2b+c	Type 2 Subtype 2	Same
4	SER_0000	1b	Type 1 Subtype 2	Same
5	SER_0002	2b+c	Type 2 Subtype 2	Same
6	SER_0002	2b+c	Type 2 Subtype 2	Same
8	SER_0002	2a-c	Type 2 Subtype 3	Same
9	SER_0003	2b+c	Type 2 Subtype 2	Same
11	SER_0003	1b	Type 1 Subtype 2	Same
12	SER_0003	2b+c	Type 2 Subtype 2	Same
13	SER_0002	2a-c	Type 2 Subtype 3	Same
14	SER_0005	2a-c	Type 2 Subtype 3	Same
16	SER_0005	2b+c	Type 2 Subtype 2	Same
17	SER_0004	2b+c	Type 2 Subtype 2	Same
18	SER_0002	1b	Type 1 Subtype 2	Same
19	SER_0003	2a-c	Type 2 Subtype 3	Same
20	SER_0004	1b	Type 1 Subtype 1	Diff
21	SER_0001	1b	Type 1 Subtype 2	Same
24	SER_0003	1b	Type 1 Subtype 2	Same
27	SER_0002	1b	Type 2 Subtype 1	Diff
30	SER_0003	1b	Type 1 Subtype 2	Same
33	SER_0001	2b+c	Type 2 Subtype 2	Same
34	SER_0005	2b+c	Type 2 Subtype 2	same
36	SER_0001	2b+c	Type 2 Subtype 2	Same
40	SER_0004	2a-c	Type 2 Subtype 3	same
41	SER_0001	2a-c	Type 2 Subtype 3	Same
42	SER_0003	2b+c	Type 2 Subtype 2	same
44	SER_0005	1b	Type 1 Subtype 2	Same
45	SER_0002	1b	Type 2 Subtype 1	Diff
50	SER_0006	2b+c	Type 2 Subtype 2	Same
52	SER_0008	2b+c	Type 2 Subtype 2	Same
56	SER_0002	1a	Typ1 Subtype 1	Same
57	SER_0001	2b+c	Type 2 Subtype 2	Same
61	SER_0006	1b	Type 1 Subtype 2	Same
62	SER_0004	2b+c	Type 2 Subtype 2	Same

	n	%
Comminuted (C)	22	66,7%
Additional fractures (AF)	23	69,7%
Dislocated (D)	8	24,2%

	n	%
C+AF	14	42,4%
C+D	5	15,2%
D+AF	6	18,2%
AF+C+D	4	12,1%

	n	%
Type 1	9	27,3%
Type 2a (T2S1)	2	6%
Type 2b+c (T2S2)	13	39,4%
Type 2a-c (T2S3)	6	18,2%

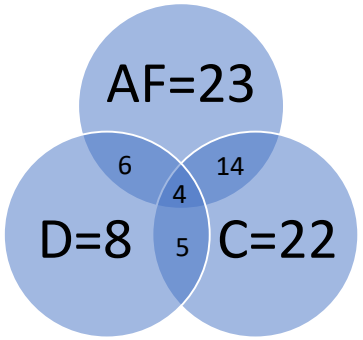

Patient Demographic Information

Patient Number	Scan File Name	Left or Right	Age	Sex
2	SER_0001	Left	44	M
4	SER_0000	Right	55	M
5	SER_0002	Right	25	M
6	SER_0002	Right	23	F
8	SER_0002	Left	59	M
9	SER_0003	Right	34	M
11	SER_0003	Right	58	F
12	SER_0003	Left	34	F
13	SER_0002	Right	41	M
14	SER_0005	Right	36	M
16	SER_0005	Left	34	M
17	SER_0004	Right	38	M
18	SER_0002	Right	78	F
19	SER_0003	Left	65	M
20	SER_0004	Right	30	F
21	SER_0001	Left	34	M
24	SER_0003	Left	33	M
27	SER_0002	Right	29	M
30	SER_0003	Left	54	M
33	SER_0001	Left	44	M
34	SER_0005	Left	26	M
36	SER_0001	Left	44	M
40	SER_0004	Left	29	M
41	SER_0001	Left	38	F
42	SER_0003	Left	38	M
44	SER_0005	Left	32	M
45	SER_0002	Left	14	M
50	SER_0006	Left	29	M
52	SER_0008	Left	23	M
56	SER_0002	Left	27	M
57	SER_0001	Right	30	F
61	SER_0006	Left	44	F

F	Female
M	Male
Age	Age at date of the scan

62	SER_0004	Left	52	M

Patient Scan Information

Patient Number	Scan File Name	Scan Date	Modality	Software Version	Manufacturer	Manufacturer Model Nar	Institution Name	Threshold Range Lower Value (OG)	Threshold Range Upper Value (OG)
2	SER_0001	30/09/2022	CT	Syngo CT VA30A	Siemens Healthineers	SOMATOM go.Top		-1023	64511
4	SER_0000	18/06/2018	CT	2,3,0	Philips	Brilliance 6	Victoria Hospital	-1023	1872
5	SER_0002	08/06/2018	CT	Syngo CT 2014A	Siemens	Emotion 16 (2007)	Groote Schuur Hospital	-1023	3071
6	SER_0002	29/04/2015	CT	Syngo CT 2007E	Siemens	Emotion 16 (2007)	Groote Schuur Hospital	-1023	1988
8	SER_0002	18/10/2018	CT	Syngo CT 2014A	Siemens	Emotion 16 (2007)	Groote Schuur Hospital	-1023	2812
9	SER_0003	22/02/2013	CT	Syngo CT 2007E	Siemens	Emotion 16 (2007)	Groote Schuur Hospital	-1023	3071
11	SER_0003	21/12/2018	CT	Syngo CT 2014A	Siemens	Emotion 16 (2010)	Mitchells Plain Hospital	-1023	1907
12	SER_0003	16/02/2015	CT	Syngo CT 2007E	Siemens	Emotion 16 (2007)	Groote Schuur Hospital	-1023	2111
13	SER_0002	19/02/2013	CT	Syngo CT 2007E	Siemens	Emotion 16 (2007)	Groote Schuur Hospital	-1023	1781
14	SER_0005	31/05/2017	CT	Syngo CT 2007E	Siemens	Emotion 16 (2007)	Groote Schuur Hospital	-1023	1750
16	SER_0005	26/03/2016	CT	Syngo CT 2007E	Siemens	Emotion 16 (2007)	Groote Schuur Hospital	-1023	3071
17	SER_0004	27/11/2019	CT	VA20A\RELEASE.VA20A	Siemens	SOMATOM go.Top	Groote Schuur Hospital	-1023	64511
18	SER_0002	23/10/2019	CT	VA20A\RELEASE.VA20A	Siemens	SOMATOM go.Top	Groote Schuur Hospital	-1023	64511
19	SER_0003	25/07/2018	CT	Syngo CT 2014A	Siemens	Emotion 16 (2007)	Groote Schuur Hospital	-1023	1878
20	SER_0004	14/06/2019	CT	VA20A\RELEASE.VA20A	Siemens	SOMATOM go.Top	Groote Schuur Hospital	-1023	64511
21	SER_0001	11/02/2021	CT	V5.00ER006	Toshiba	Aquilion PRIME	Groote Schuur Hospital	-1023	1837
24	SER_0003	16/03/2016	CT	Syngo CT 2007E	Siemens	Emotion 16 (2007)	Groote Schuur Hospital	-1023	3071
27	SER_0002	18/05/2018	CT	Syngo CT 2014A	Siemens	Emotion 16 (2007)	Groote Schuur Hospital	-1023	1846
30	SER_0003	27/07/2018	CT	Syngo CT 2014A	Siemens	Emotion 16 (2010)	Mitchells Plain Hospital	-1023	1698
33	SER_0001	26/02/2020	CT	V5.00ER006	Toshiba	Aquilion PRIME	Groote Schuur Hospital	-1023	1758
34	SER_0005	17/05/2020	CT	VA20A\RELEASE.VA20A	Siemens	SOMATOM go.Top	Groote Schuur Hospital	-1023	64511
36	SER_0001	30/09/2022	CT	Syngo CT VA30A	Siemens Healthineers	SOMATOM go.Top		-1023	64511
40	SER_0004	18/01/2016	CT	Syngo CT 2007E	Siemens	Emotion 16 (2007)	Groote Schuur Hospital	-1023	1832
41	SER_0001	13/07/2021	CT	V5.00ER006	Toshiba	Aquilion PRIME	Groote Schuur Hospital	-1023	1869
42	SER_0003	21/07/2017	CT	Syngo CT 2014A	Siemens	Emotion 16 (2010)	Mitchells Plain Hospital	-1023	1892
44	SER_0005	29/03/2018	CT	Syngo CT 2014A	Siemens	Emotion 16 (2007)	Groote Schuur Hospital	-1023	3071
45	SER_0002	13/06/2022	CT	VA20A\RELEASE.VA20A	Siemens	SOMATOM go.Top	Groote Schuur Hospital	-1023	64511
50	SER_0006	30/05/2020	CT	VA20A\RELEASE.VA20A	Siemens	SOMATOM go.Top	Groote Schuur Hospital	-1023	64511
52	SER_0008	19/12/2017	CT	Syngo CT 2014A	Siemens	Emotion 16 (2007)	Groote Schuur Hospital	-1023	1926
56	SER_0002	13/03/2017	CT	Syngo CT 2007E	Siemens	Emotion 16 (2007)	Groote Schuur Hospital	-1023	1812
57	SER_0001	28/10/2019	CT	V5.00ER006	Toshiba	Aquilion PRIME	Groote Schuur Hospital	-1023	1792
61	SER_0006	22/08/2012	CT	Syngo CT 2007E	Siemens	Emotion 16 (2007)	Groote Schuur Hospital	-1023	3071
62	SER_0004	12/06/2019	CT	VA20A\RELEASE.VA20A	Siemens	SOMATOM go.Top	Groote Schuur Hospital	-1023	64511

Patient Fracture Information

Patient Number	Fracture Classification	Presence of Multiple Fragments	Number of Fragments	Displacement of Fragment(s)	Associated Fractures	Dislocation of the Elbow
2		No	1	Fragment only had a minor degree of displacement to extent that the CT scan does not show a separation between the ulna and the fragment.	Radial head fracture	No apparent dislocation of the humerus from the trochlear notch
4		Yes	2	One main fragment displaced from the tip of the coronoid process. The smaller second fragment is displaced from the tip but not from the other fragment - looks like one fragment.	Radial head fracture	No apparent dislocation of the humerus from the trochlear notch
5		Yes	5 (possibly more)	The largest fragment is somewhat displaced. Able to differentiate it from the other fragments and from the parent bone. The second largest fragment also has a minor degree of displacement, enough to differentiate between it, the parent bone and the other fragments. The remainder of the fragments were not displaced enough to accurately separate them from the parent bone and the other fragments	Radial head fracture	Minor anterior dislocation of the humerus from the trochlear notch (the ulna has shifted slightly posterior)
6		No	1	The fragment has a visible line of displacement throught the majority of the fragment. The fragment displacement is less towards the medial side of the fragment.	Radial head fracture	No apparent dislocation of the humerus from the trochlear notch
8		Yes	4	There are two large fragments which both have visible lines of displacement from the parent bone and from each other. The largest of the fragments (Fragment 1) is significantly displaced from the parent bone. It also appears to be made up of two separate fragments (one large one and one smaller one) with no distinct line of displacement between the fragments; therefore they appear as one. The second separated fragment (Fragment 2) appears to be made up of two smaller fragments of somewhat equal size, but with distinct line of displacement between the two fragments; therefore they appear as one. The fragments were further separated into their respective smaller fragments in order to perform a more accurate reduction	None	No apparent dislocation of the humerus from the trochlear notch
9		Yes	6,8,9	There are approx 8 or 9 fragements. The largest 6 were separated out and the others were deemed too small to be included in the fracture reconstruction. The majority of the coronoid fragments are significantly displaced. There are a few fragments that only have a slight measure of displacement. These fragments had to be carefully separated. The fragments are clearly from either the ulna or the radius; therefore all of the fragments were separated from the parent bones in the hopes that the fragments from each parent bone become apparent when the reduction is underway.	Potential radial head fracture	Slight superior dislocation of the humerus from the trochlear notch. This might just be from the way the scan was taken
11		Yes	2	There is one large fragment and one small fragment that would potentially be excluded from the fixation due how small it is. There is a clear line of displacement between the fragments and the parent bone, and between the two fragments themselves; therefore all the parent bone and fragments are easily separated.	Radial head fracture	Slight superior dislocation of the humerus from the trochlear notch. This might just be from the way the scan was taken
12		No	1	There is one large fragment that is partially displaced from the parent bone. The fragment and the parent bone had to be separated carefully.	Radial head fracture	No apparent dislocation of the humerus from the trochlear notch

13	Yes	3	There are multiple fragments present. Some of them are from the radial head fracture and some of them from the ulna. There is a significant degree of displacement between all of the fragments, therefore making it easy to separate the fragments from the parent bones. The degree of displacement between the fragments themselves is not as significant. All of the fragments will be converted to STLs in order to make sure that non of the coronoid process fragments are left out. STLs labeled "Fragment 3 (R)" and "Fragment 4 (R)" are identifiabe as fragments from the radial head. This can be seen by the clear circular artciular surface that is characteristic of the radius. This identification of the fragments will be confirmed by Prof Roche.	Radial head fractures	No apparent dislocation of the humerus from the trochlear notch
14	Yes	2	There is one, potentially 2 coronoid fragments. Both fragments are signifcantly displaced from the parent bone but there is no distinguishable line of displacement between the two fragments. There are also radial head fracture fragments present; however, these are easily distinguished from the coronoid fragments. The coronoid fragments will be separated should it be necessary.	Radial head fracture	No apparent dislocation of the humerus from the trochlear notch
16	Yes	3	There is one large fragment and two smaller fragments from the coronoid process. There is a signifcant amount of displacement between the fragments and the parent bone. There is also a significant amount of displace between each of the fragments. The fragments are easily separated out and distinguishable from the fragments from the radial head fracture.	Radial head fracture	No apparent dislocation of the humerus from the trochlear notch
17	Yes	2	There is one larger (medium sized) fragment and a smaller fragment. There is clear displacement between the two fragments and the parent bone. The displacement between the two fragments isn't as significant but the two fragments can still be distinguished from each other.	Radial head fracture	No apparent dislocation of the humerus from the trochlear notch
18	No	1	There is one medium sized coronoid fragment. The fragment is only slightly displaced from it's original position on the parent bone. The line of displacement is not signifcant enough to easily separate the fragment from the parent bone but the fragment is distinguishable. The fragment has displaced upwards towards the medial epicodylar fragment.	Distal humerus fracture (medial epicondyle fracture)	Partial dislocation of the entire joint due to the nature of the distal humerus fracture. The ulna is still articulated with the medial epicondyle, and the radius is still articulated with the lateral epicondyle. The radius and ulna are still articulated at the radial notch.
19	Yes	4	There is one medium fragment and 3 smaller sized fragments. There is a clear line of displacement between all the fragments and the ulna. There is also a clear line of displacement between three of the fragments. Fragment 4 and fragment 2 don't have a clear line of displacement between them but they are easily distinguished from each other.	None	No apparent dislocation of the humerus from the trochlear notch
20	No	1	There is one small tip fracture to the coronoid process. There is minimal displacement between the fragment and the parent bone but the fragment is easily discernable.	Radial head fracture	Partial dislocation (superior and anterior) of the humerus from the trochlear notch due to the fracture the radial head.
21	No	1	There is one medium/large sized fragment that significantly displaced from the ulna. There are smaller fragments around but their small size would render them negligable.	Radial head fracture	No apparent dislocation of the humerus from the trochlear notch
24	Yes	3	There are 3 medium sized fragments that are discernable and significantly displaced from the parent bone. Only two are potentially from the coronoid but each fragment will be evaluated the reduced.	Potential radial head fracture	No apparent dislocation of the humerus from the trochlear notch

27	Yes	3	There is one comparitively larger, medium and smaller fragments. They are all discernable and significantly displaced from the ulna.	None	No apparent dislocation of the humerus from the trochlear notch.
30	Yes	2	There is one larger fragment and a smaller fragment. The larger fragment is displaced from the ulna to a significant degree. The smaller fragment is displaced distally from it's original position towards the shaft of the ulna. The smaller fragment will not be reduced due to the small size of the fragment.	Radial head fracture	The elbow joint is completely dislocated. The huermus is anteriorly dislocated from the trochlear notch of the ulna and the radial head.
33	Yes	3	There is one large fragment and two small fragments. All fragments are clearly visible and displaced from the parent bone. The two smaller fragments would not be used in the fracture reduction.	None	No apparent dislocation of the humerus from the trochlear notch
34	Yes	2 or 3	There is one medium sized fragment and two small fragments. All 3 are discernable and partially displaced from their original location. The two smaller frgaments might not be used in the reduction. The one fragment is located near the radial notch of the ulna. This fragment might not be from the coronoid process. (but there are no other fractures present)	None	No apparent dislocation of the humerus from the trochlear notch
36	No	1	There is one large fragment. There is no significant displacement of the fragment from the parent bone but the fragment is easily discernable from the rest of the ulna.	Radial head fracture	No apparent dislocation of the humerus from the trochlear notch.
40	Yes	2 or more	There are 2 large fragments that are displaced from the ulna. The large fragments are easily separated from the rest of the bones and fragments. There are additional artifacts in the scan. Some appear to be additional small fragments from the comminuted fracture to the coronoid. These small fragments can be ignored as they would be too small to surgically fixate. The rest of the artifacts on the scan do not appear to be fragments from any additional fractueres. They are probably due to some interference with the scan. These artifacts have been left visible in the "Bone" mask.	No apparent additional fractures	The elbow joint is completely dislocated. The huermus is anteriorly dislocated from the trochlear notch of the ulna and the radial head.
41	No	1	One large fragment that is displaced from the parent bone enough to clearly separate the fragment from the bone.	Radial head fracture	No apparent dislocation of the humerus from the trochlear notch
42	Yes		One large and one medium fragment that have displaced from the parent bone enough to clearly separate the fragment from the bone. There are multiple smaller fragments that are too small to be surgically fixated.	Lateral epicondyle fracture and radial head fracture	No apparent dislocation of the humerus from the trochlear notch
44	No	1	One medium-larged fragment that has partially separated from the parent bone. This line of displacement is clear and the fragment is clearly discernable.	Radial head fracture	No apparent dislocation of the humerus from the trochlear notch
45	No	1	One medium-large fragment that is completely displaced from the ulna. It is clearly discernable and separtable from the parent bone.	No apparent additional fractures	No apparent dislocation of the humerus from the trochlear notch
50	Yes	2	There is one large fragment and one very small fragment. They are both clearly discernable and displaced from the parent bone. The fragments are easily separated from the ulna. The small fragment is too small to be surgically fixated so therefore it can be ignored.	No apparent additional fractures	No apparent dislocation of the humerus from the trochlear notch
52	No	1	There is one large fragment that is completely displaced from the parent bone. It is clearly discernable from the rest of the bones and can easily be separated.	Radial head fracture	The elbow joint is completely dislocated. The huermus is anteriorly dislocated from the trochlear notch of the ulna and the radial head.
56	Yes	2	There are two medium sized fragments. One is partially displace from the parent bone and is easily discernable. The second fragment has minimal displacement and the margins of the fragment are not clearly visible.	Radial head fracture	No apparent dislocation of the humerus from the trochlear notch

57	Yes	2 (possibly more)	There is one large fragment and one small fragment that would potentially be excluded from the fixation due how small it is. There is a clear line of displacement between the fragments and the parent bone, and between the two fragments themselves.	Potential radial head fracture, potential medial epicondyle fracture	No apparent dislocation of the humerus from the trochlear notch
61	Yes	2	One medium and one small fragments. The fragments are easily discernable. They have displaced upwards towards the medial epicondyle of the humerus. The fragments can be easily separated from the humerus and the parent bone	No apparent additional fractures	No apparent dislocation of the humerus from the trochlear notch
62	Yes	3	There is one large fragment and two smaller fragments. All the fragments are discernable from the parent bone. The largest fragment is displaced from it's orignal location and the two smaller fragments aren't as displaced but they are easily separated from the ulna	Radial head fracture	No apparent dislocation of the humerus from the trochlear notch

Patient Fracture Map Images

Patient	Anterior (Fragmented)	Anterior (Merged)	Superior (Fragmented)	Superior Merged	Lateral (Fragmented)	Lateral (Merged)	Medial (Fragmented)	Medial (Merged)
2			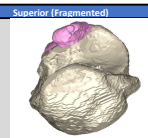	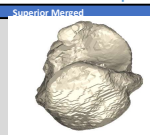	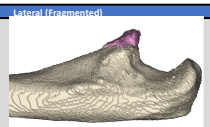	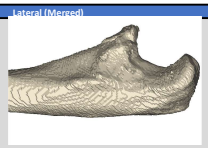	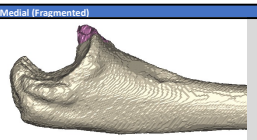	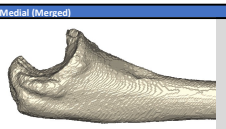
4			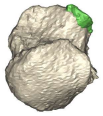	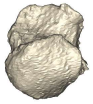			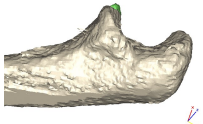	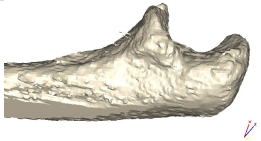
5			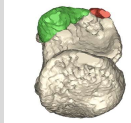	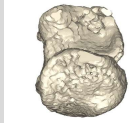	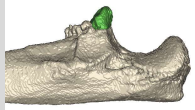	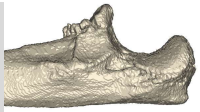	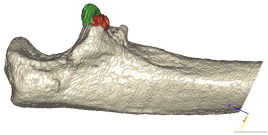	
6			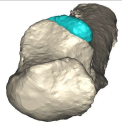	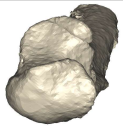	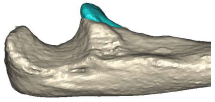		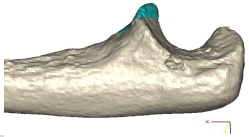	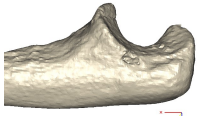
8			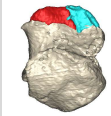	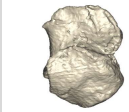	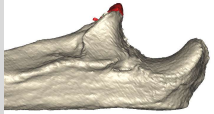	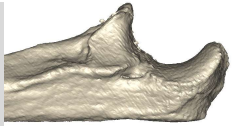	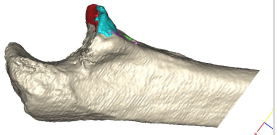	
9			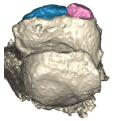	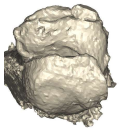		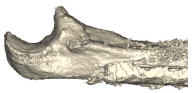		
11					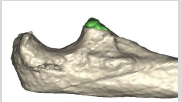	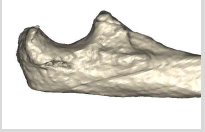	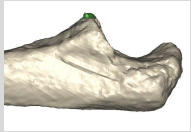	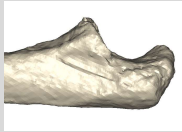
12					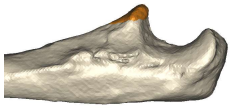	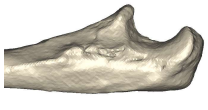		

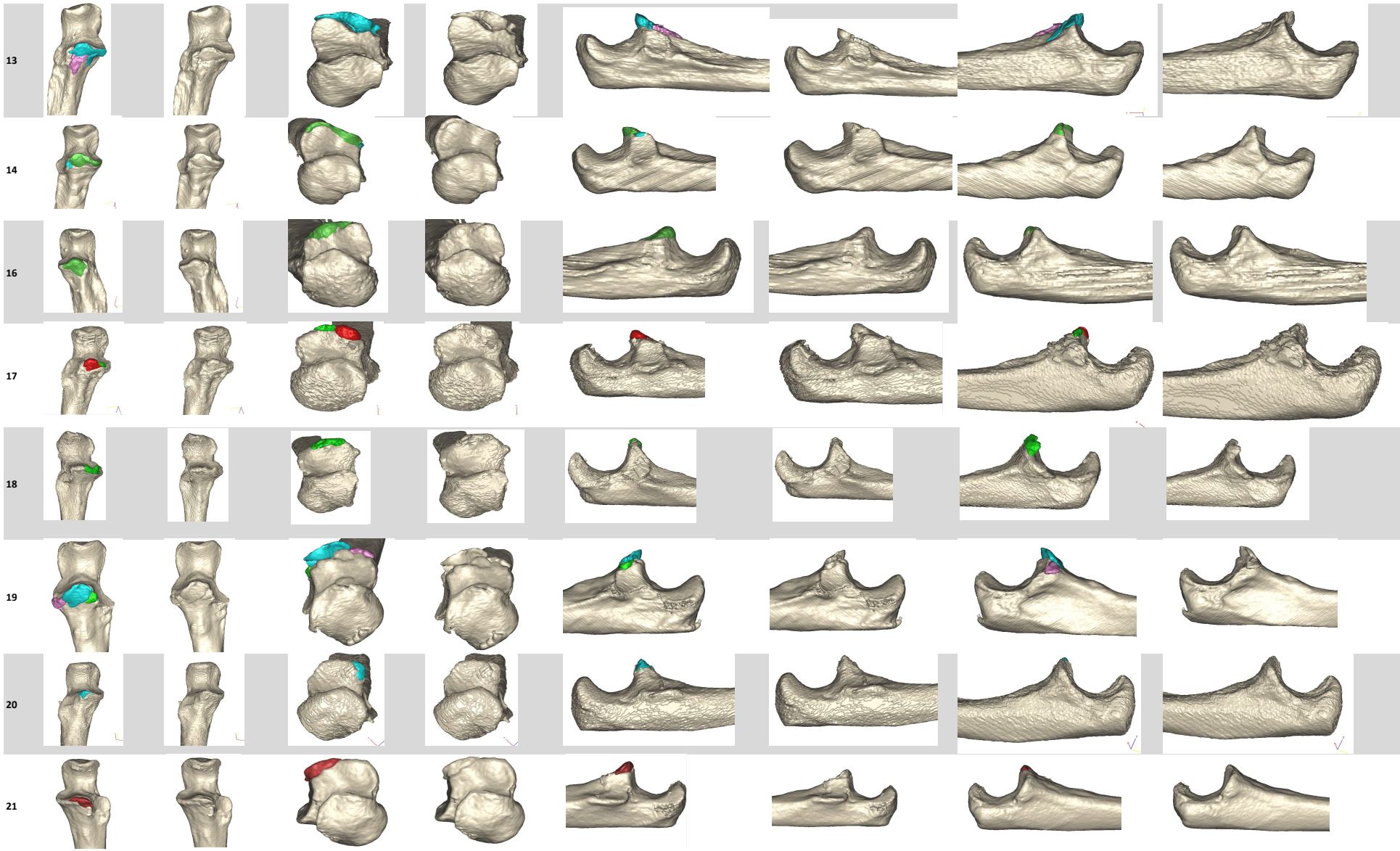
13
14
16
17
18
19
20
21

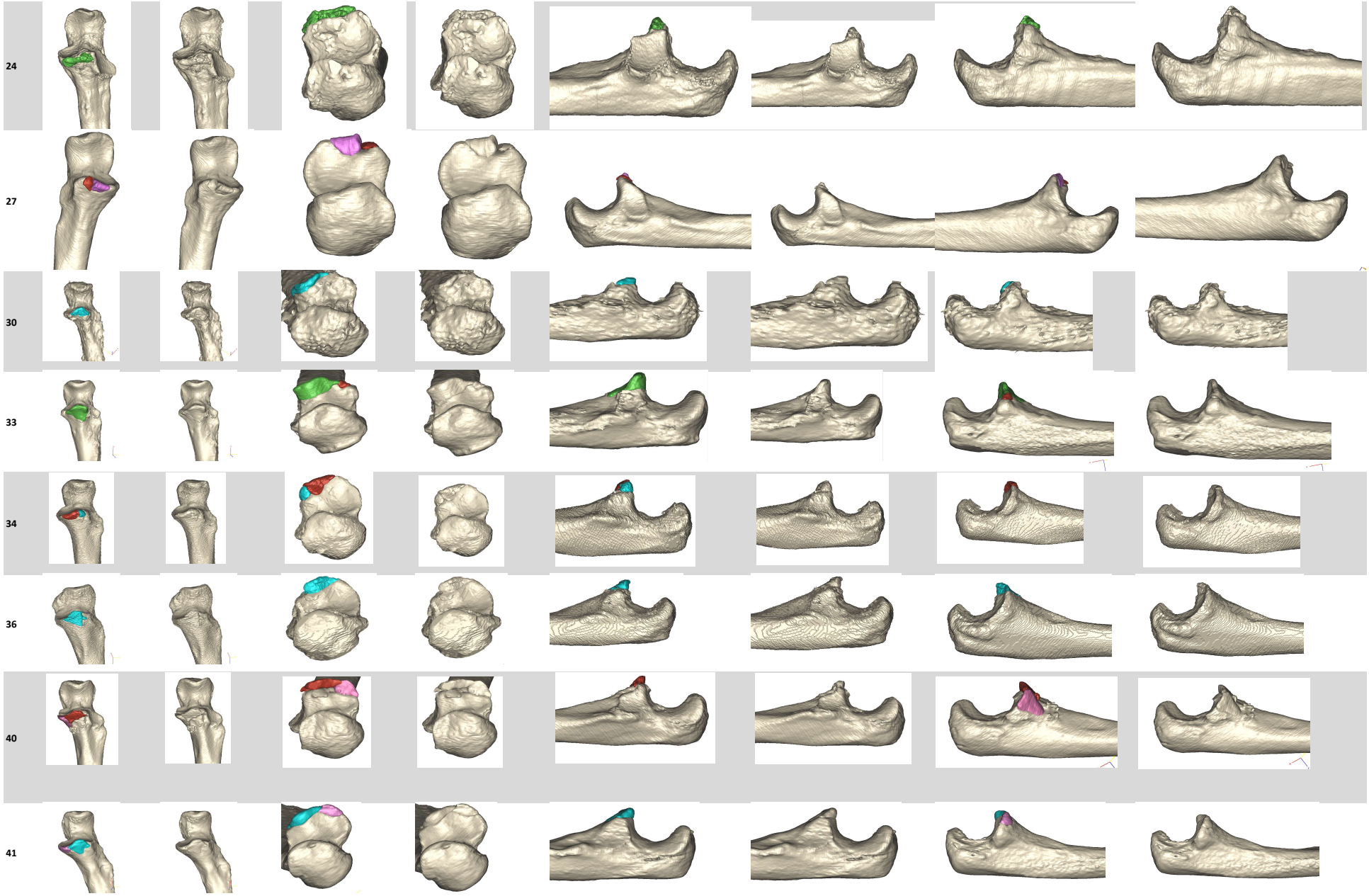
24
27
30
33
34
36
40
41

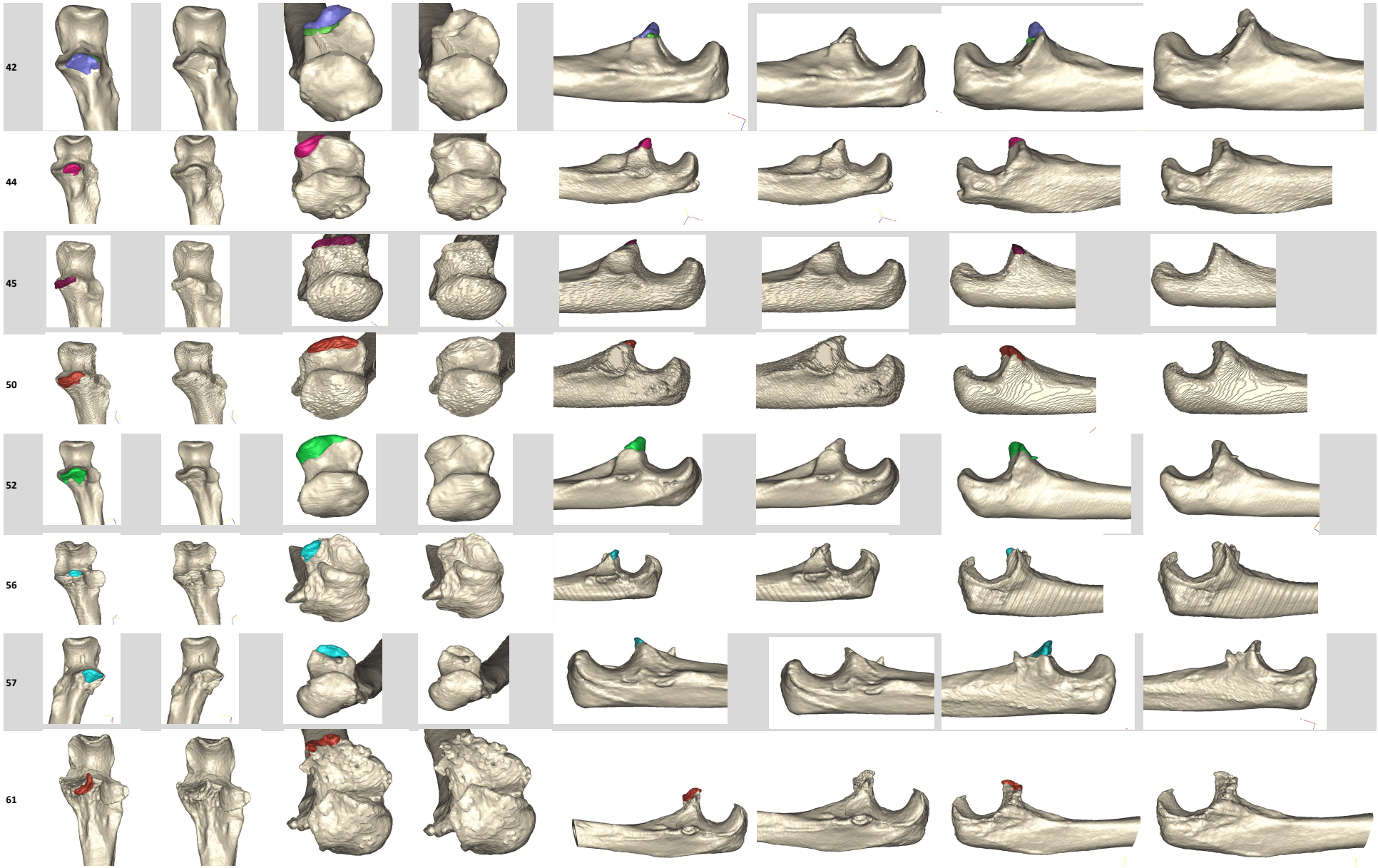
42
44
45
50
52
56
57
61

62

.

Fracture Map Images

Patient	Anterior	Superior	Lateral	Medial
2	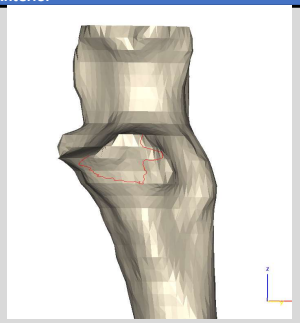	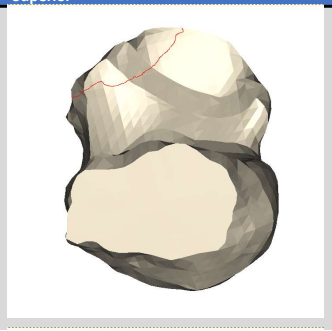	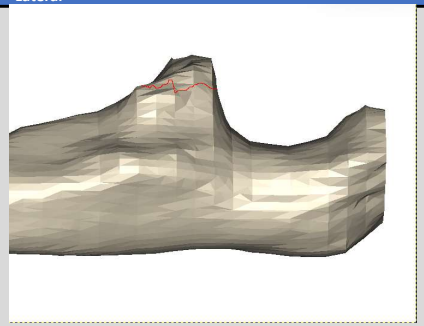	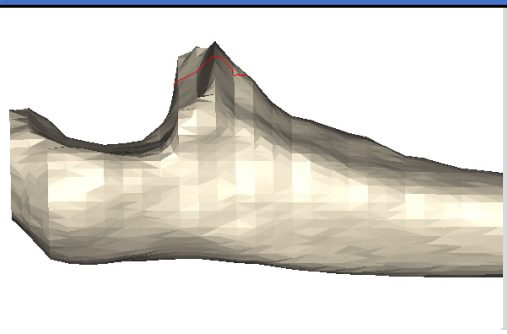
4	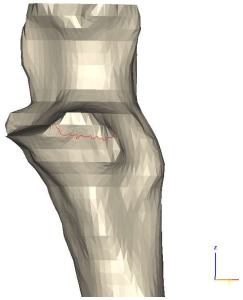		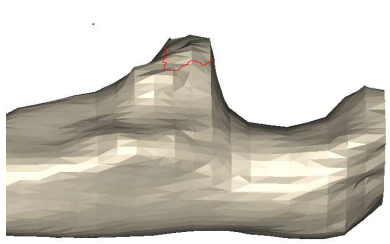	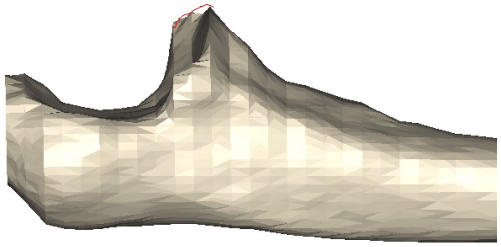
5	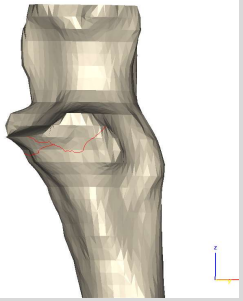		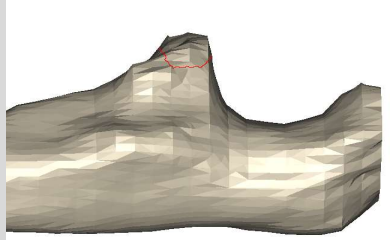	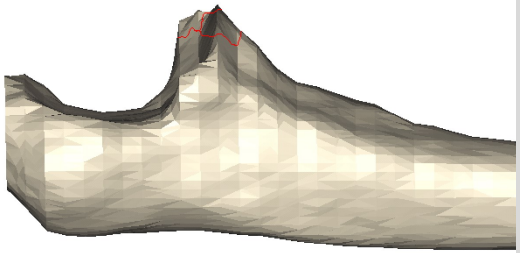

6	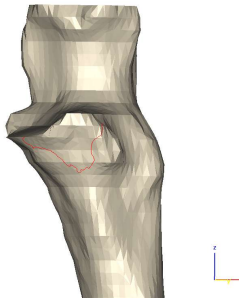	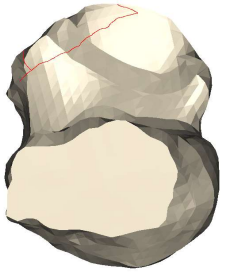	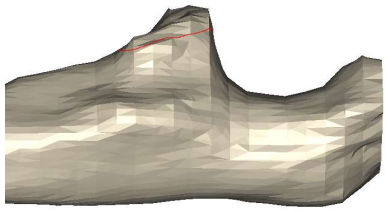	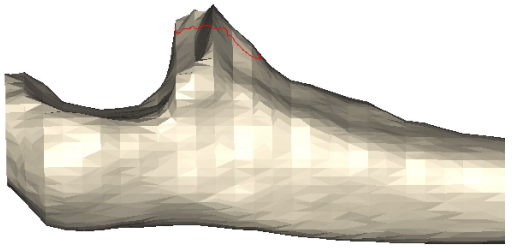
8	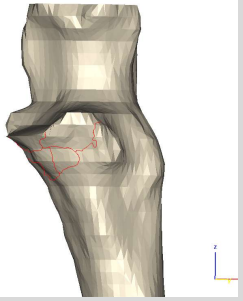		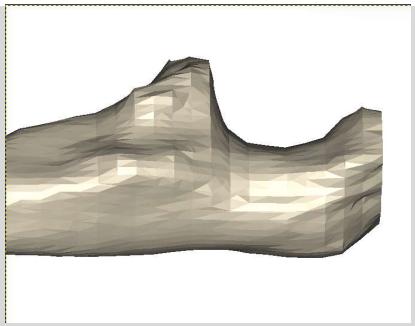	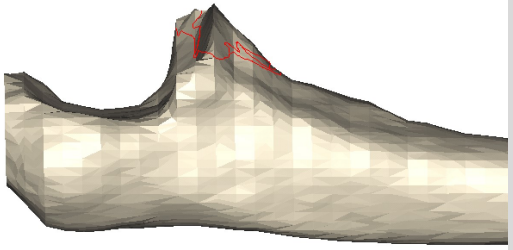
9	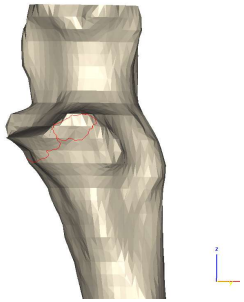	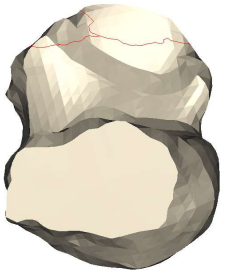	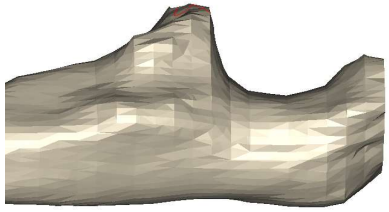	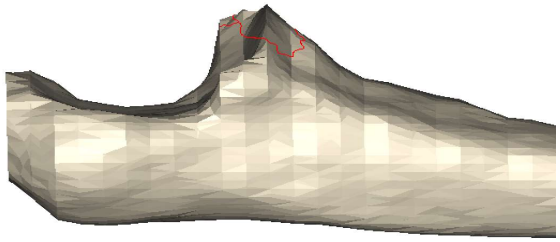

11	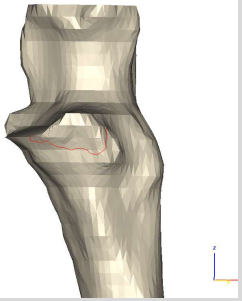	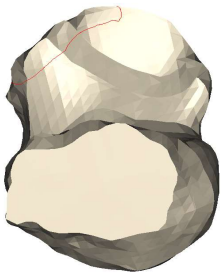	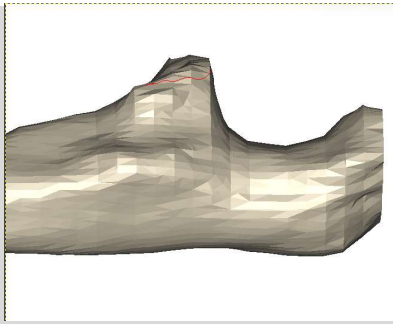	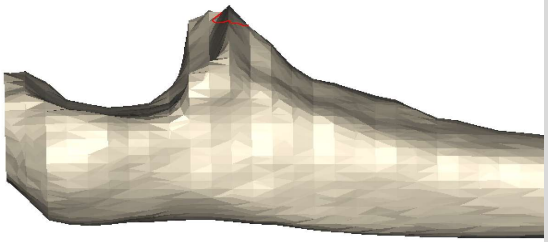
12	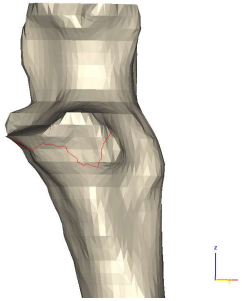	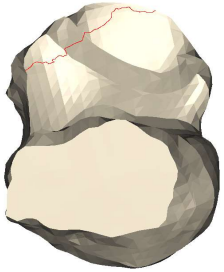	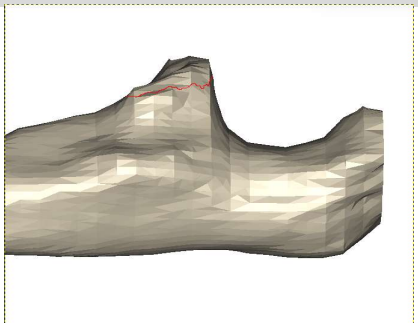	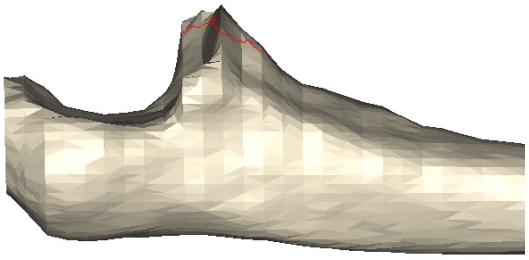
13	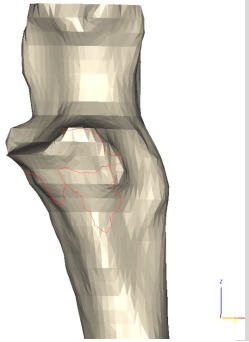	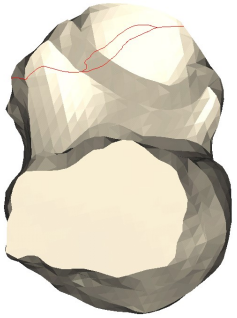	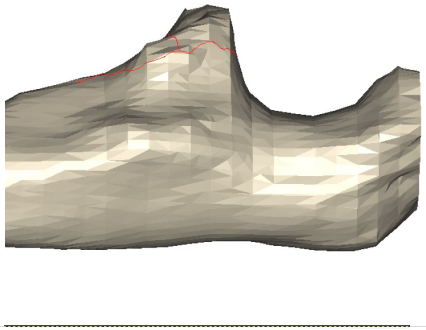	

14	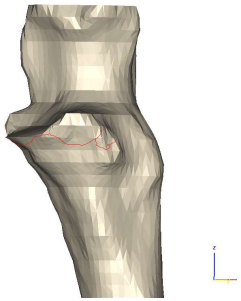		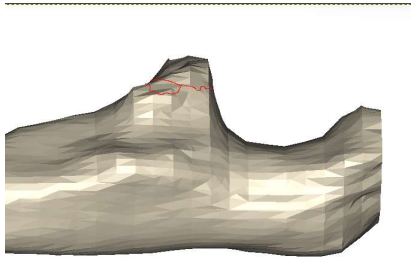	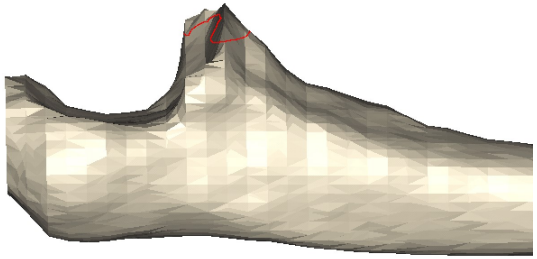
16	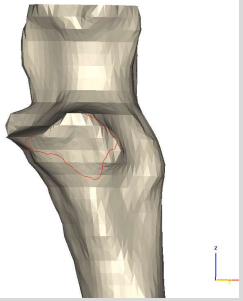		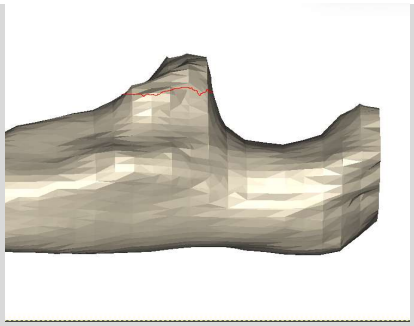	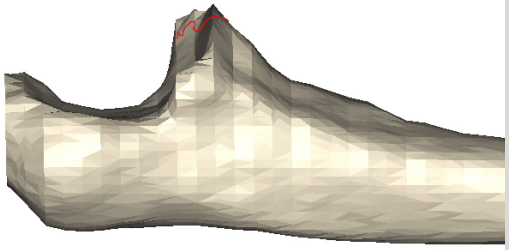
17	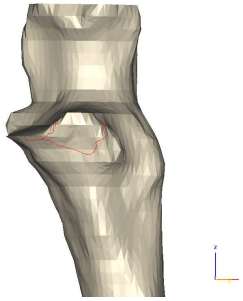		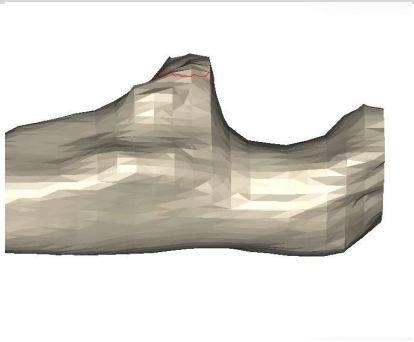	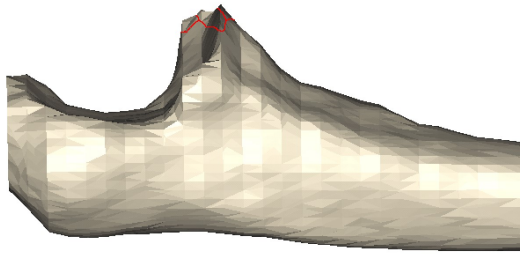

18

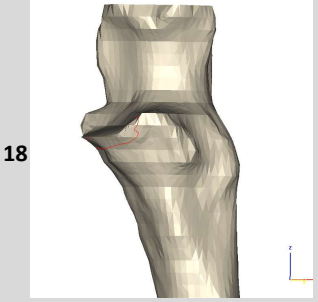

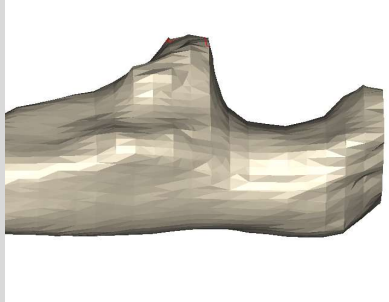

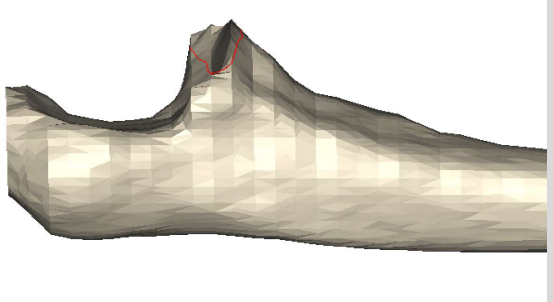

19

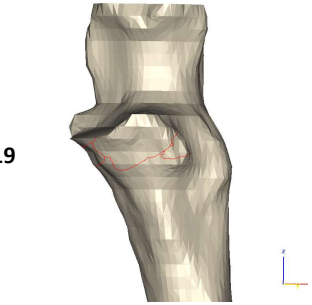

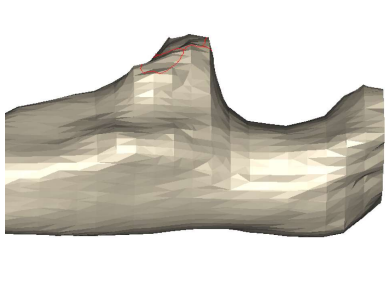

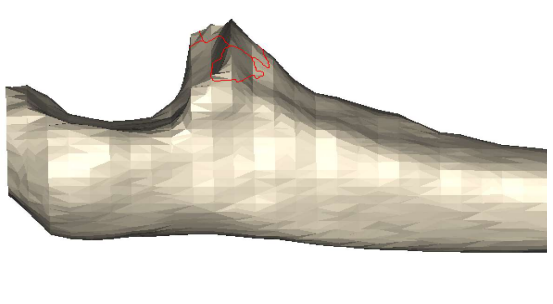

20

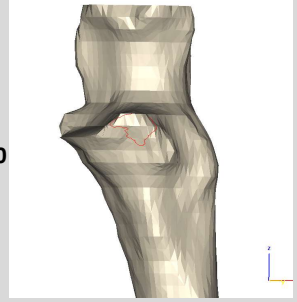

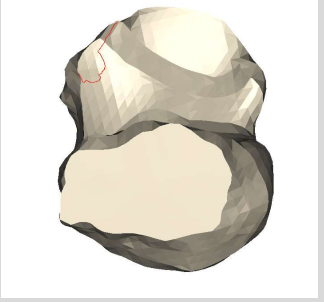

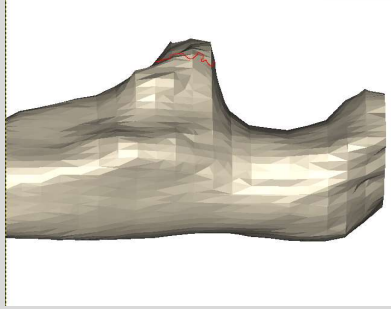

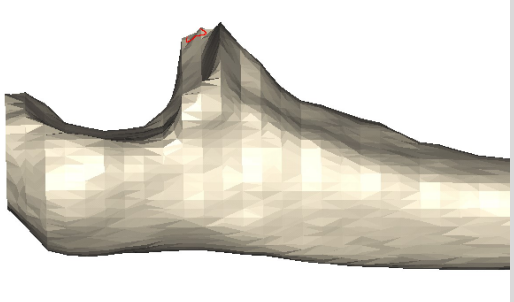

21

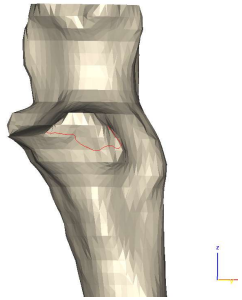

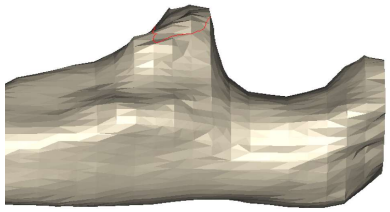

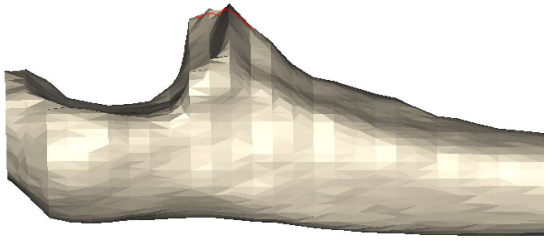

24

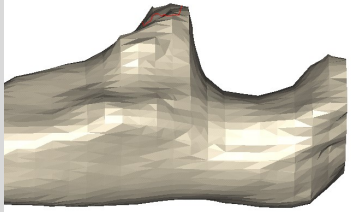

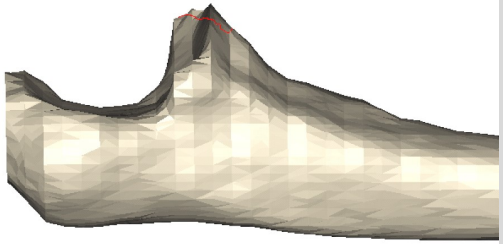

27

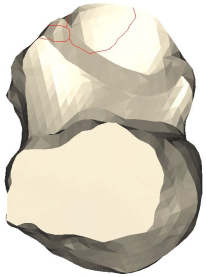

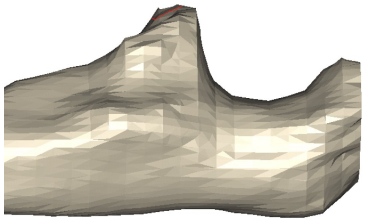

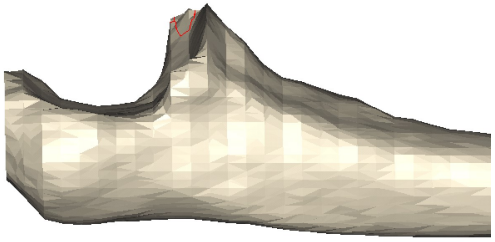

30

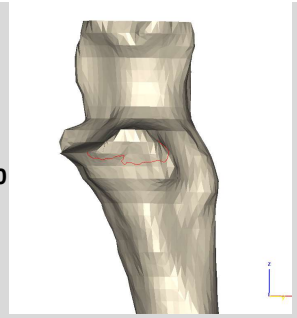

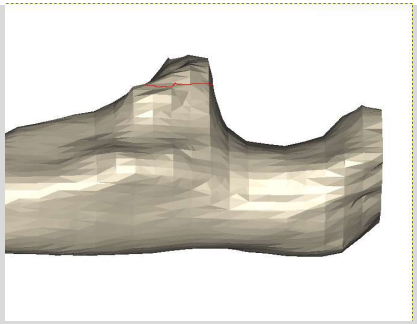

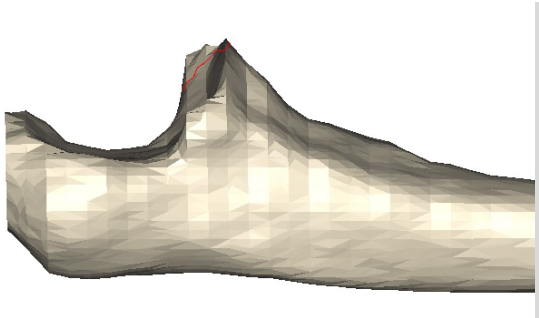

33

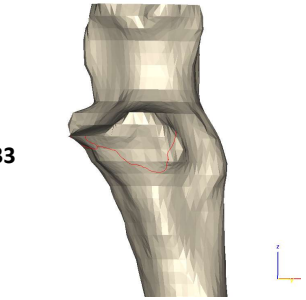

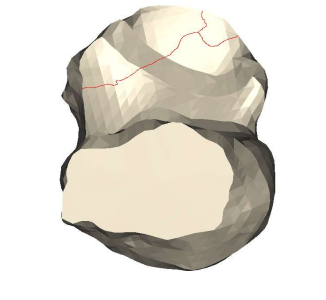

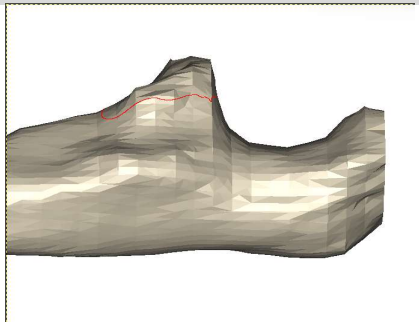

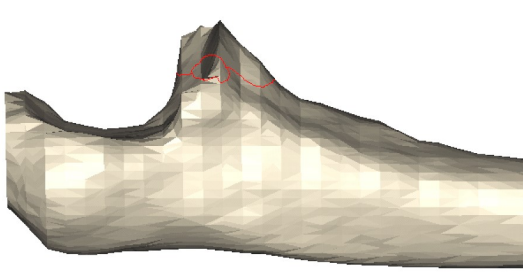

34

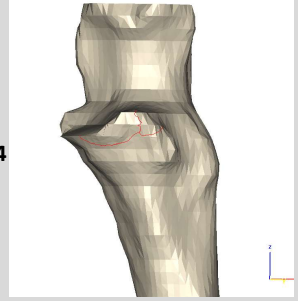

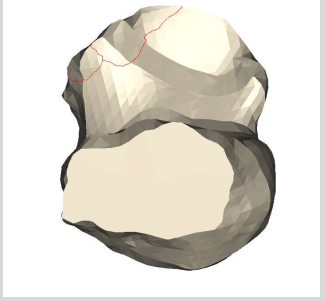

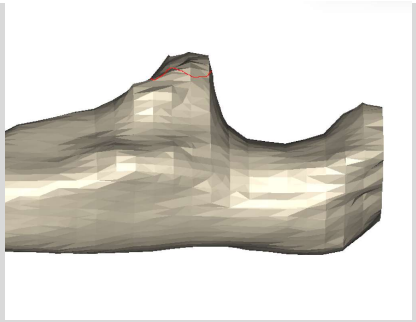

36

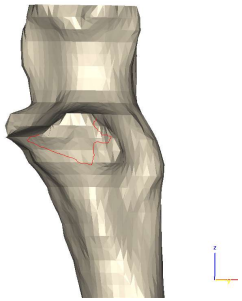
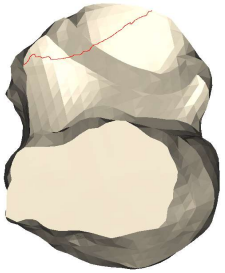
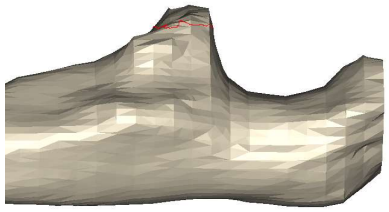
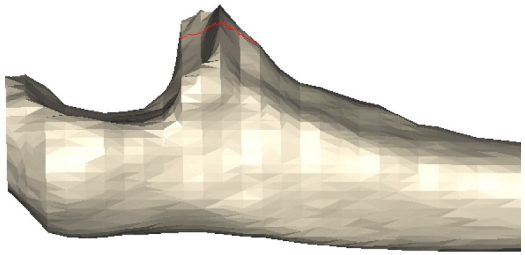

40

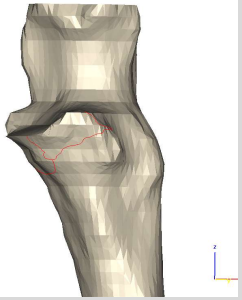

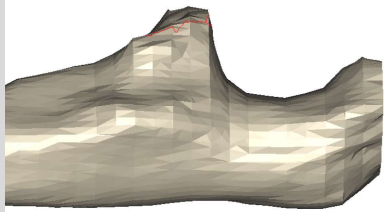
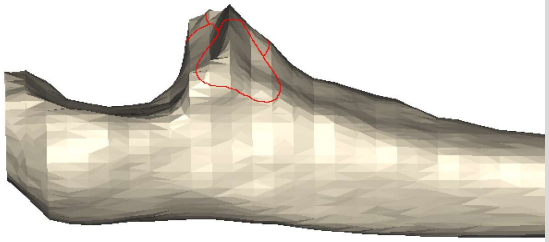

41

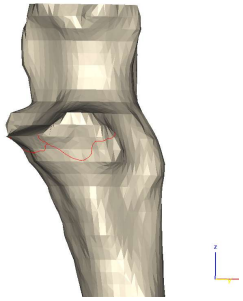
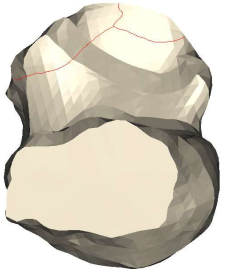
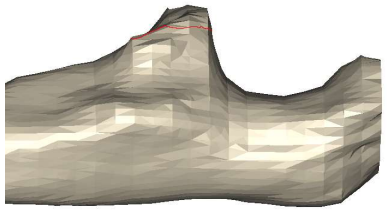
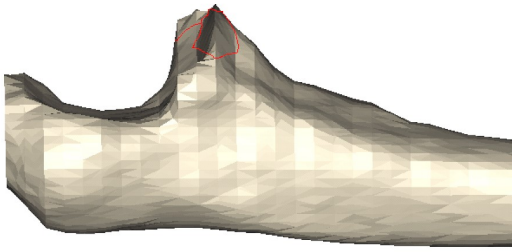

42

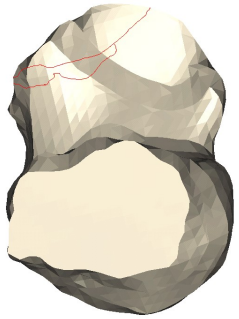

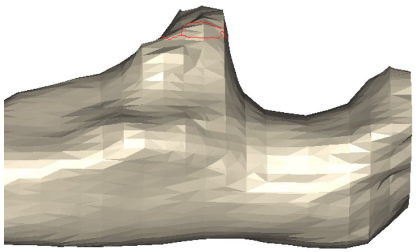

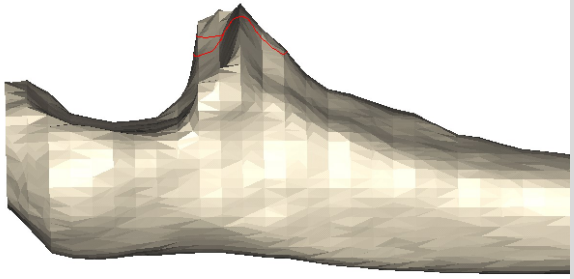

44

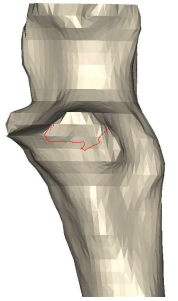

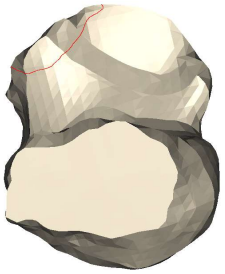

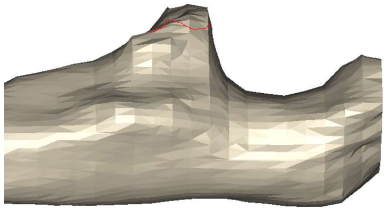

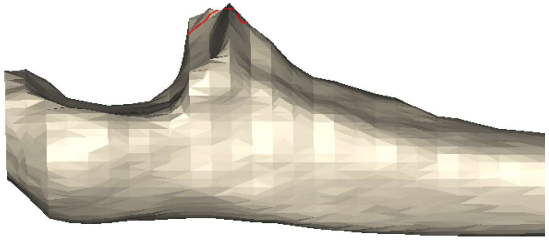

45

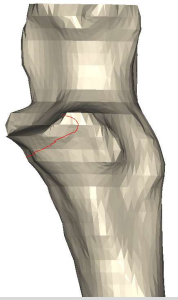

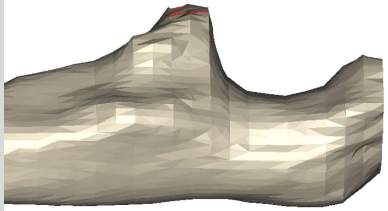

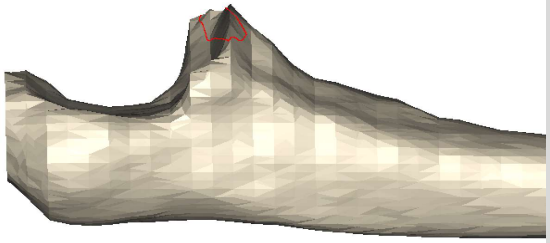

Appendix C – Fracture Maps

Fracture Maps – All Patients

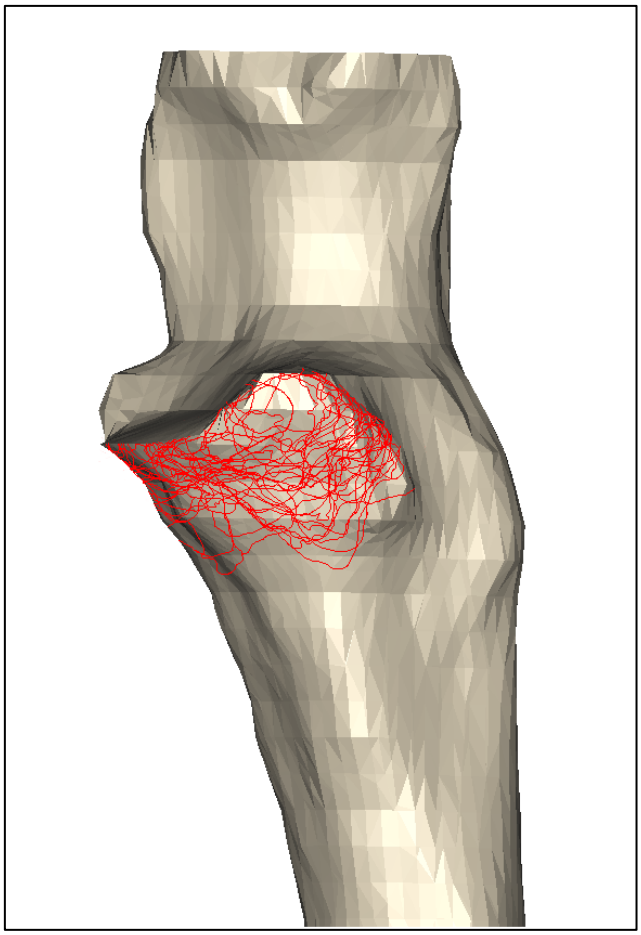

Anterior fracture maps depicting the location and distribution of all the coronoid fractures.

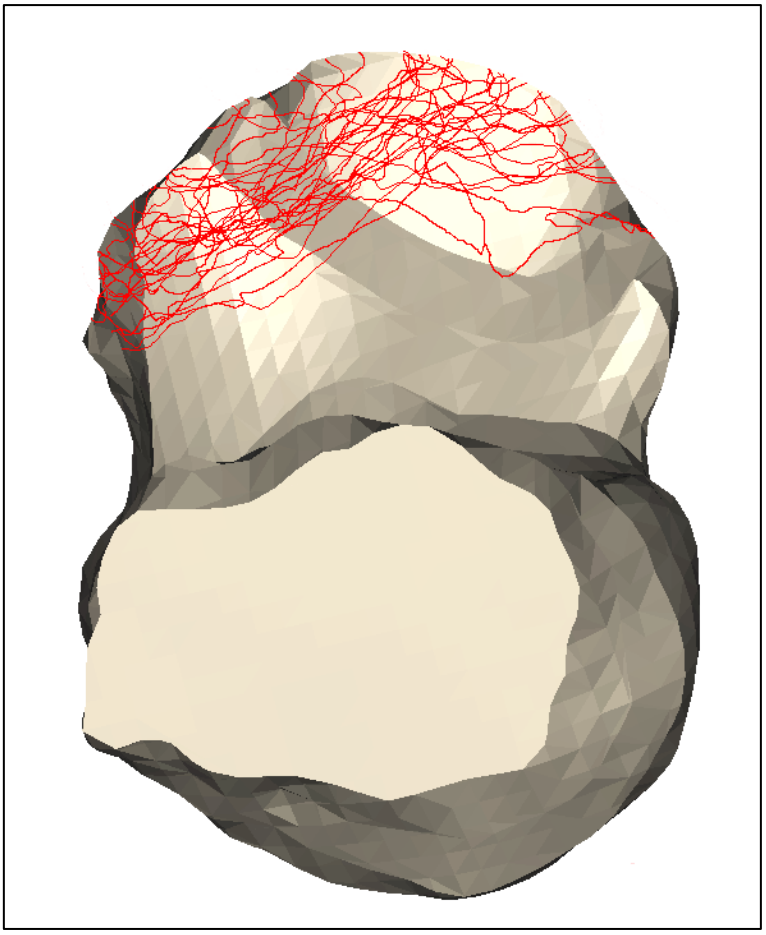

Superior fracture maps depicting the location and distribution of all the coronoid fractures.

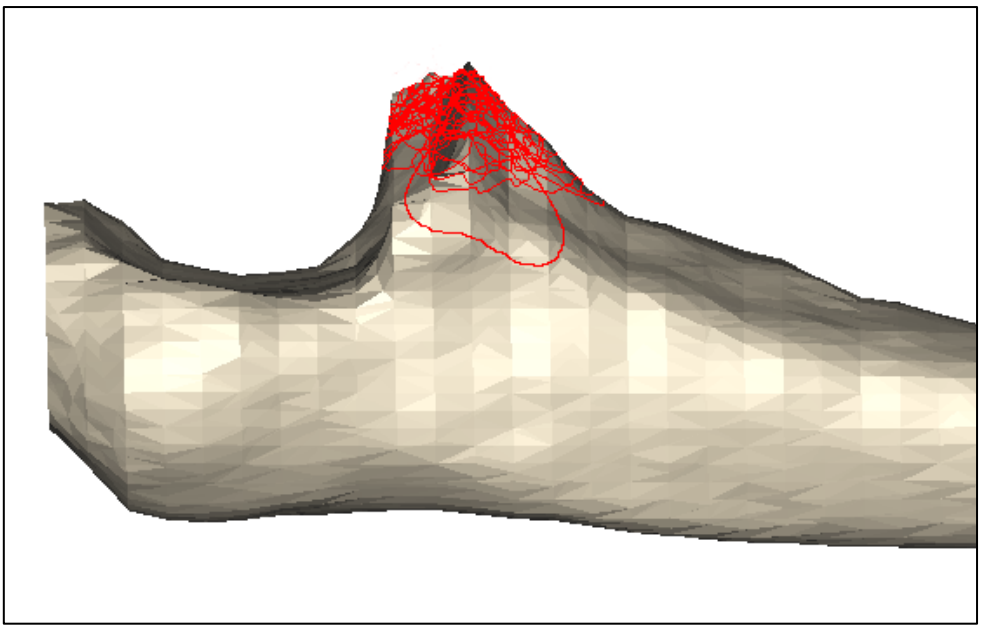

Medial fracture maps depicting the location and distribution of all the coronoid fractures.

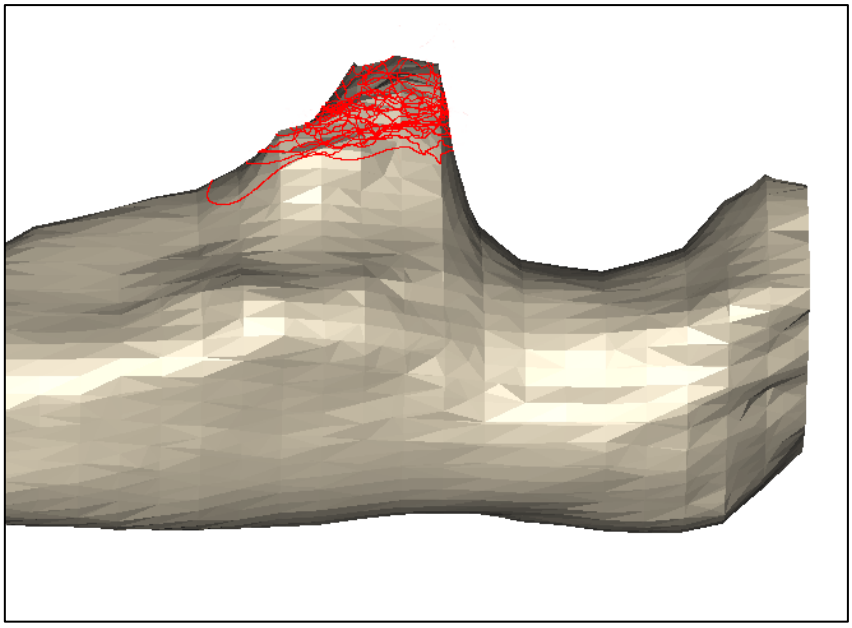

Lateral fracture maps depicting the location and distribution of all the coronoid fractures.

Type 1 & Subtypes

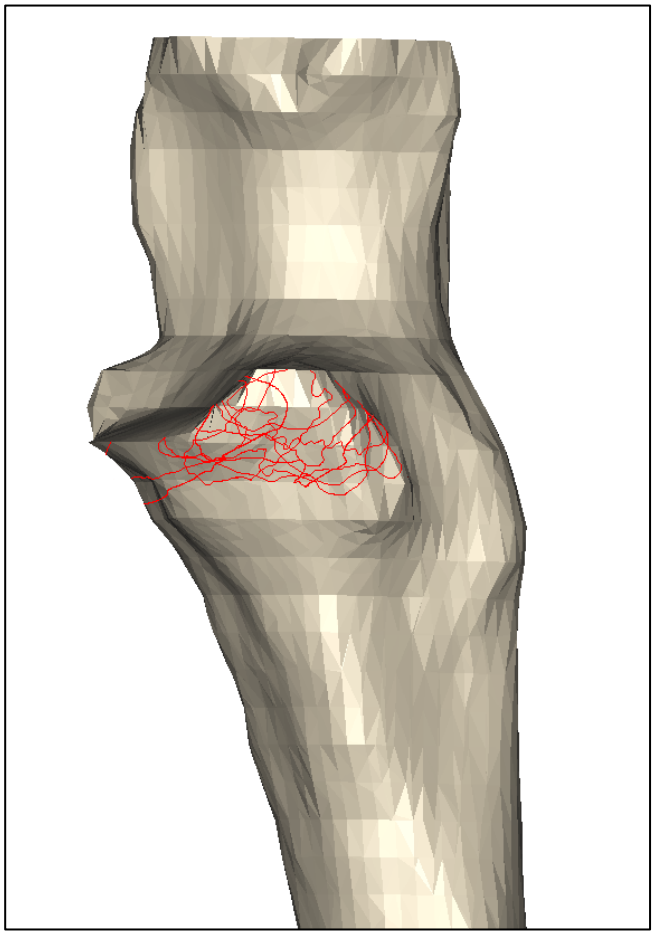

Anterior fracture maps depicting the location and distribution of the Type 1 coronoid fractures.

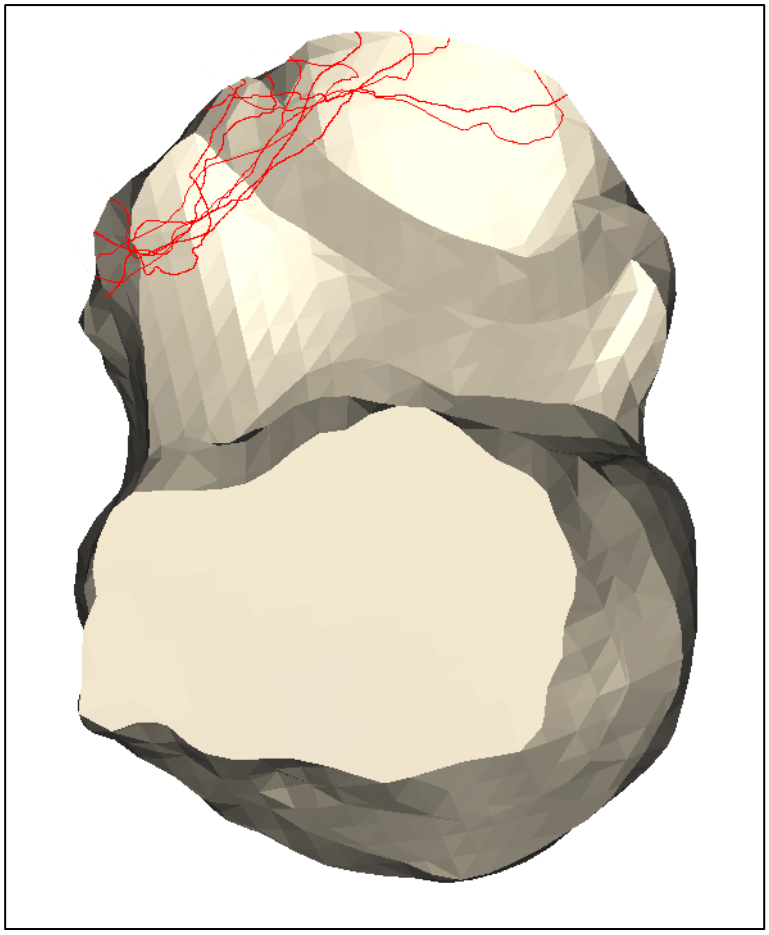

Superior fracture maps depicting the location and distribution of the Type 1 coronoid fractures.

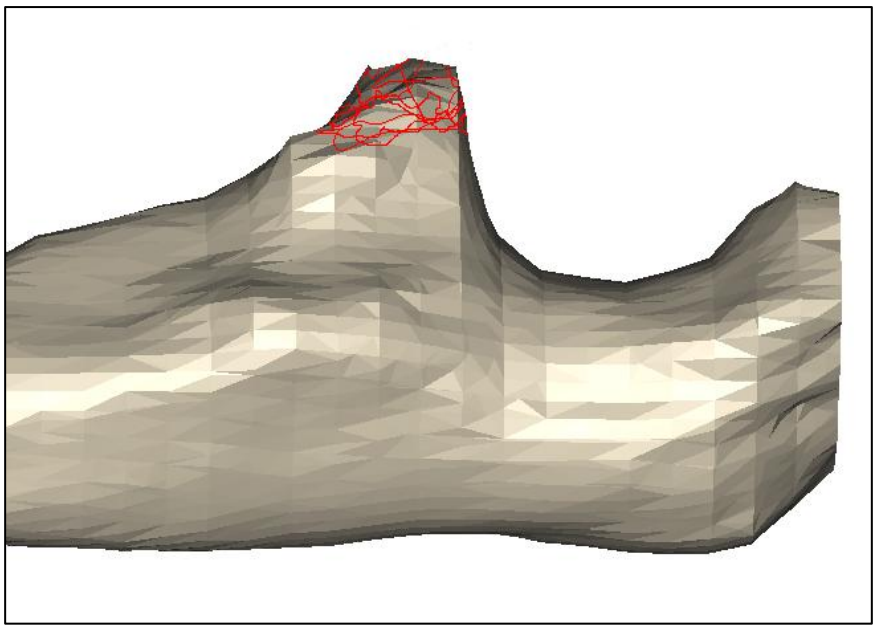

Lateral fracture maps depicting the location and distribution of the Type 1 coronoid fractures.

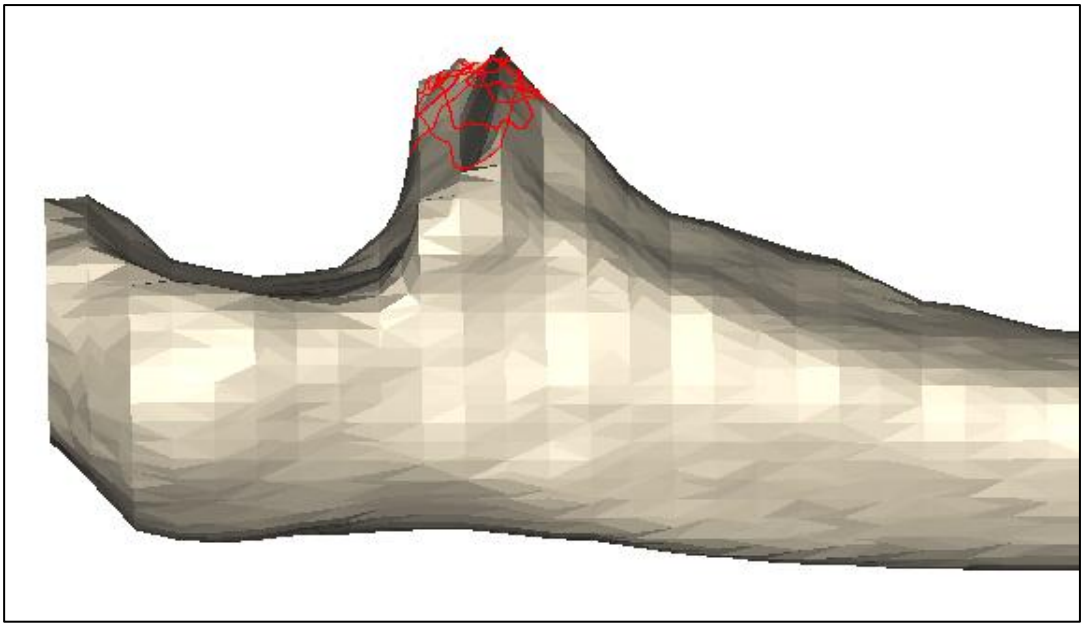

Medial fracture maps depicting the location and distribution of the Type 1 coronoid fractures.

Type 2 – Subtype 2

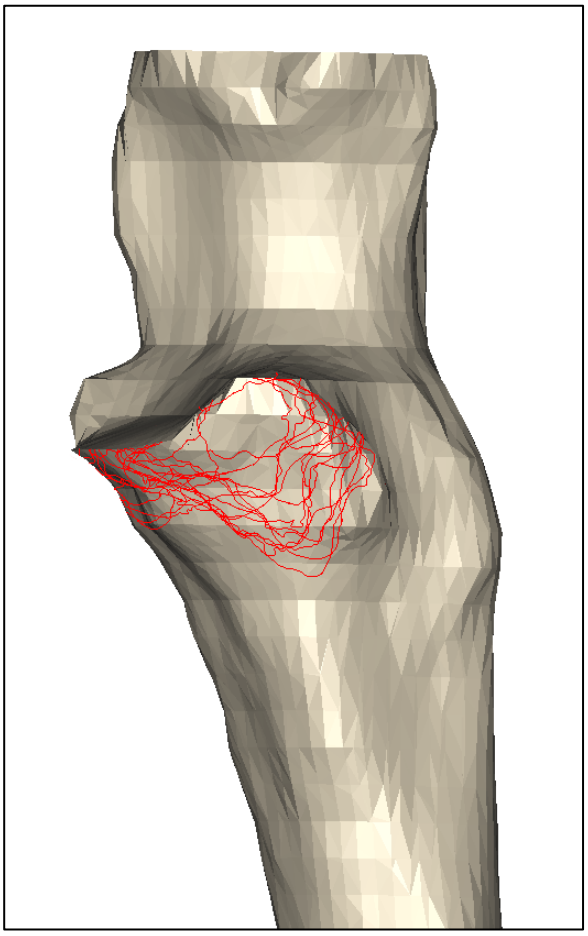

Anterior fracture maps depicting the location and distribution of the Type 2 Subtype 2 coronoid fractures.

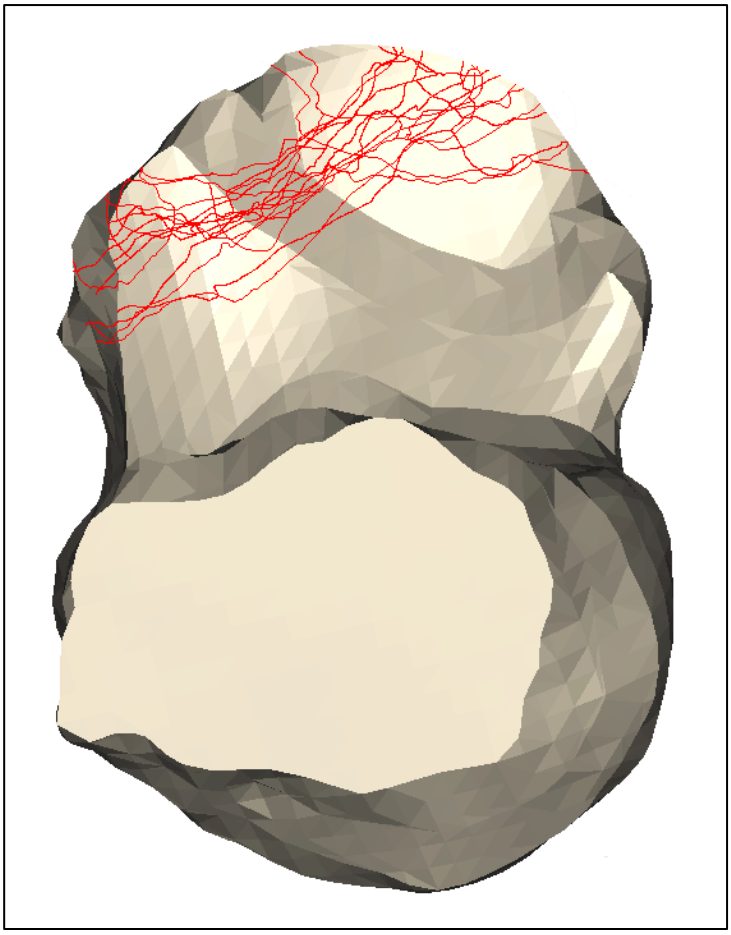

Superior fracture maps depicting the location and distribution of the Type 2 Subtype 2 coronoid fractures.

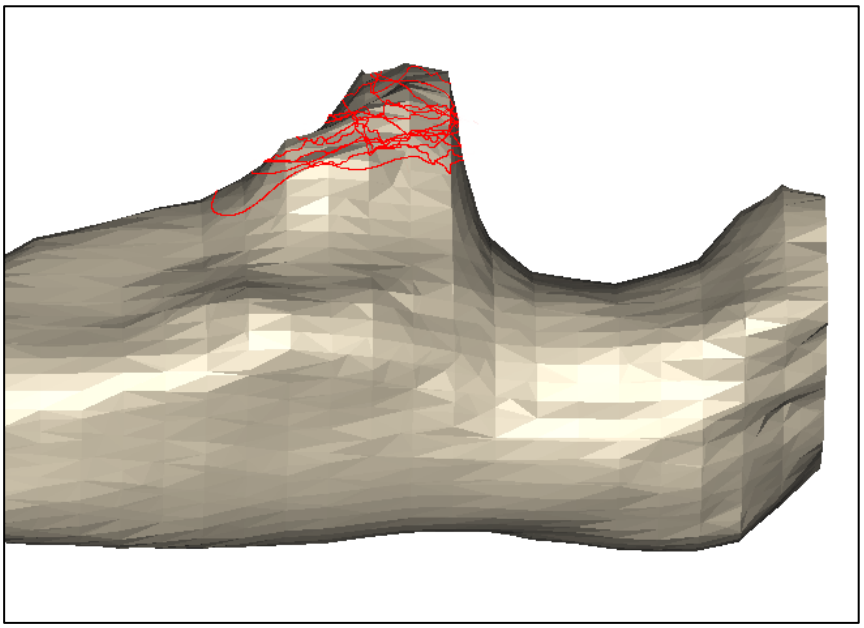

Lateral fracture maps depicting the location and distribution of the Type 2 Subtype 2 coronoid fractures.

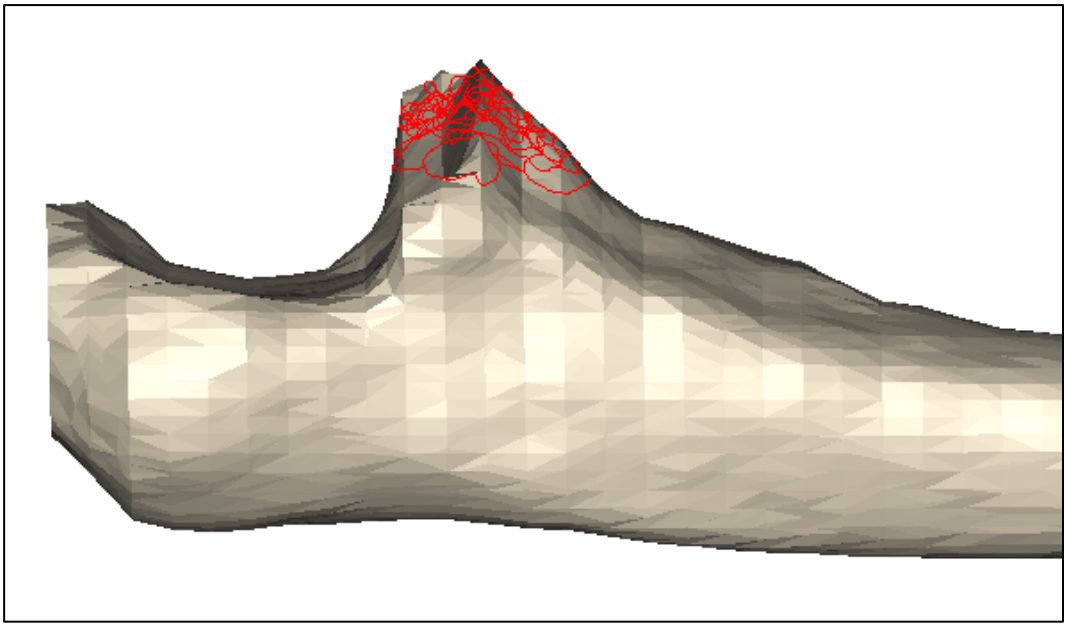

Medial fracture maps depicting the location and distribution of the Type 2 Subtype 2 coronoid fractures.

Type 2 – Subtype 3

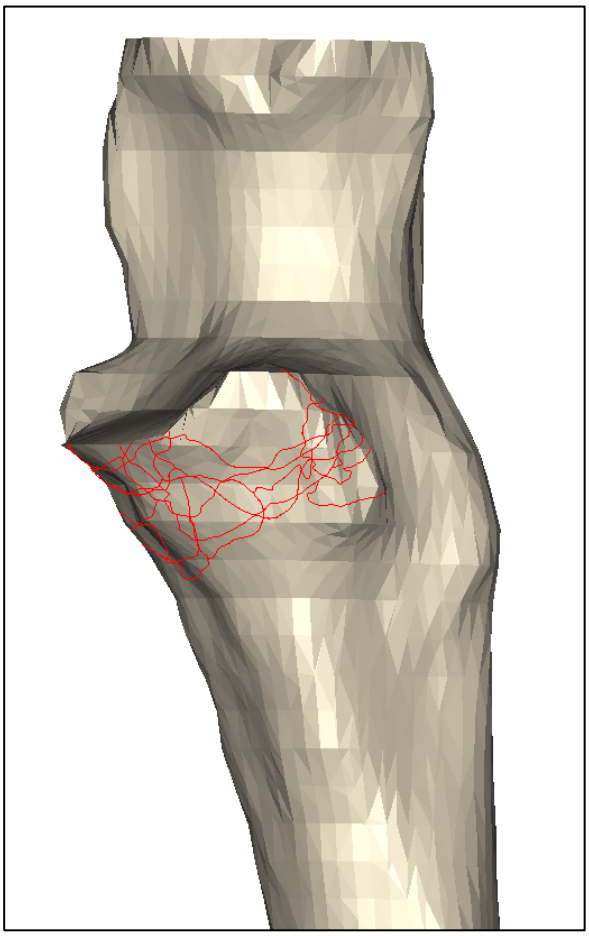

Anterior fracture maps depicting the location and distribution of the Type 2 Subtype 3 coronoid fractures.

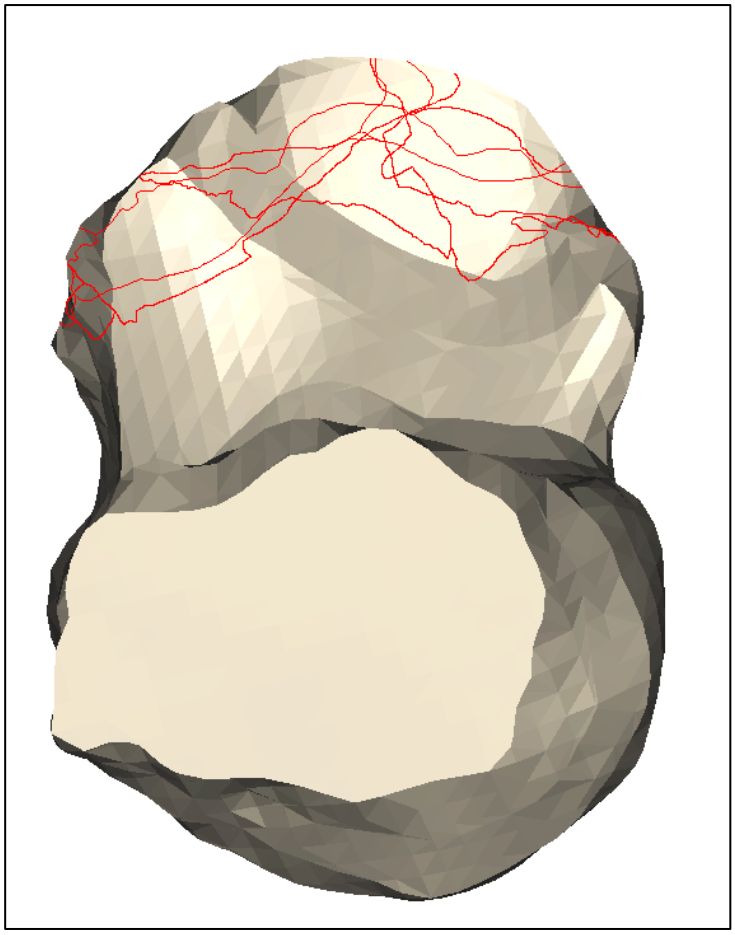

Superior fracture maps depicting the location and distribution of the Type 2 Subtype 3 coronoid fractures.

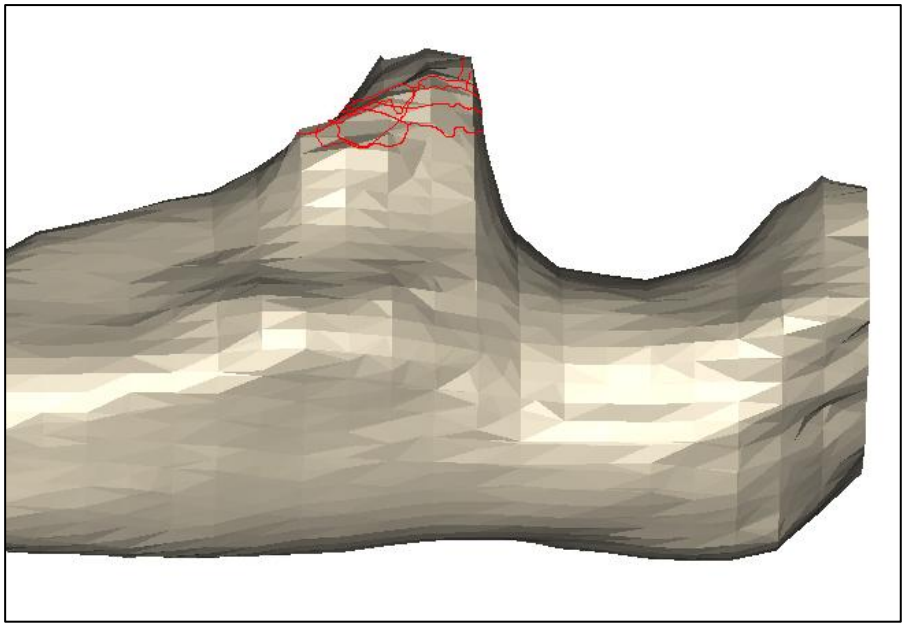

Lateral fracture maps depicting the location and distribution of the Type 2 Subtype 3 coronoid fractures.

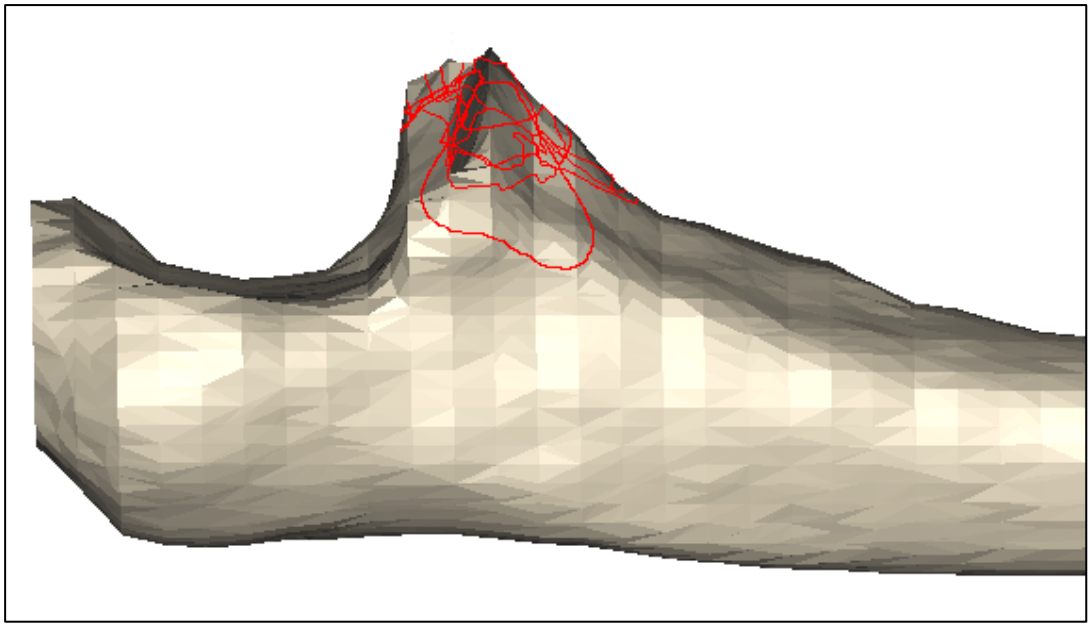

Medial fracture maps depicting the location and distribution of the Type 2 Subtype 3 coronoid fractures.

Appendix D – Heat Mapping Code

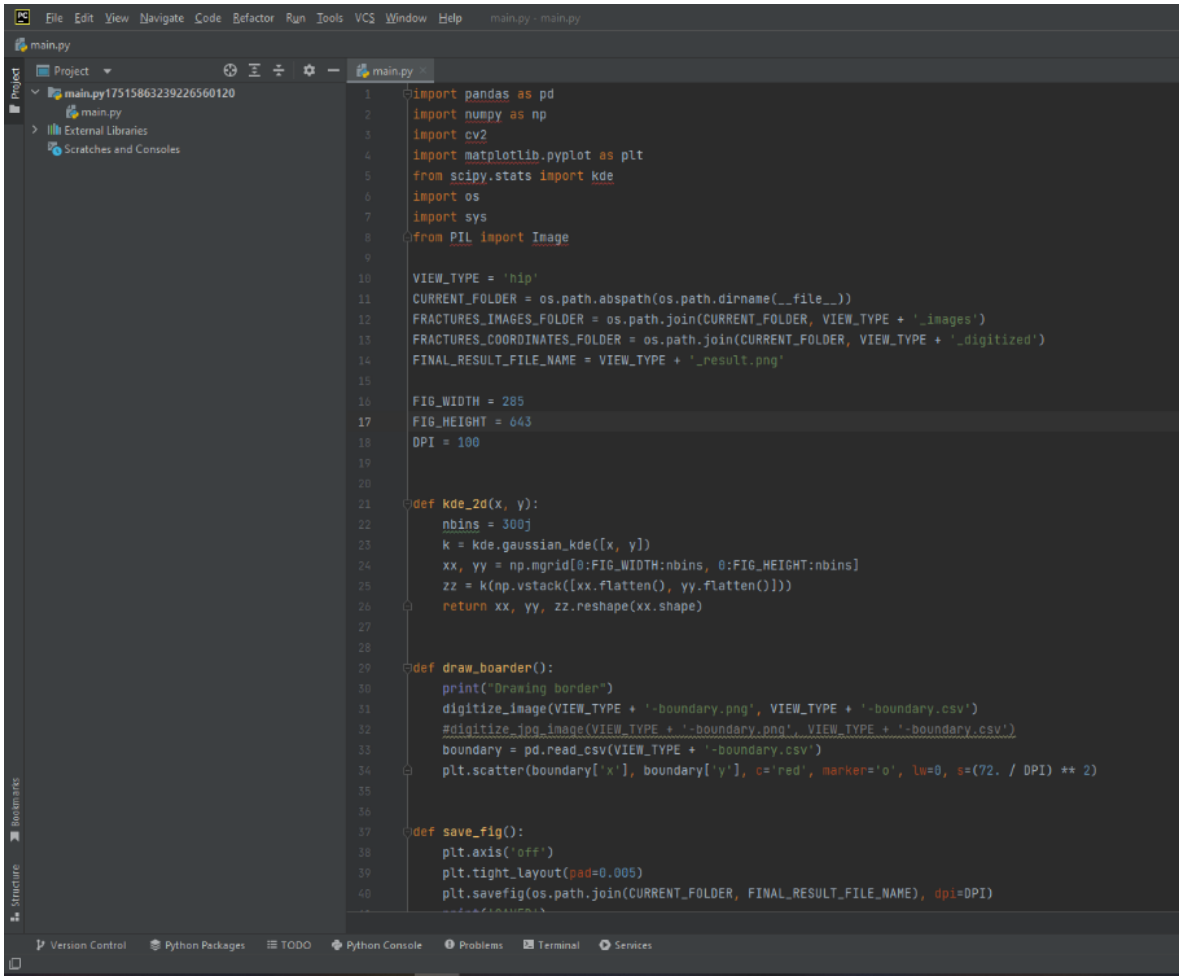

Appendix E – Heat Maps

Heat Maps - All Patients

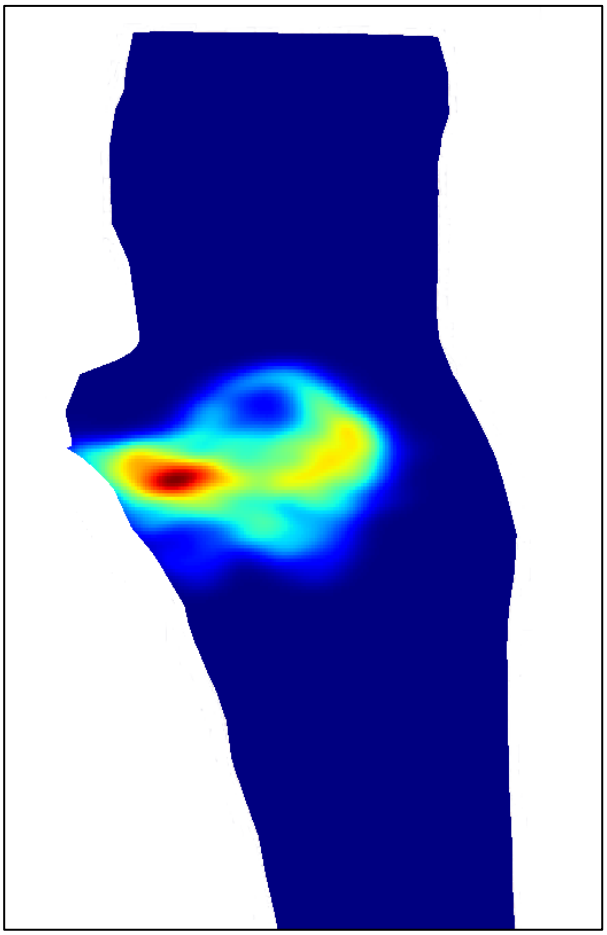

Anterior heat map of all the patient fracture lines.

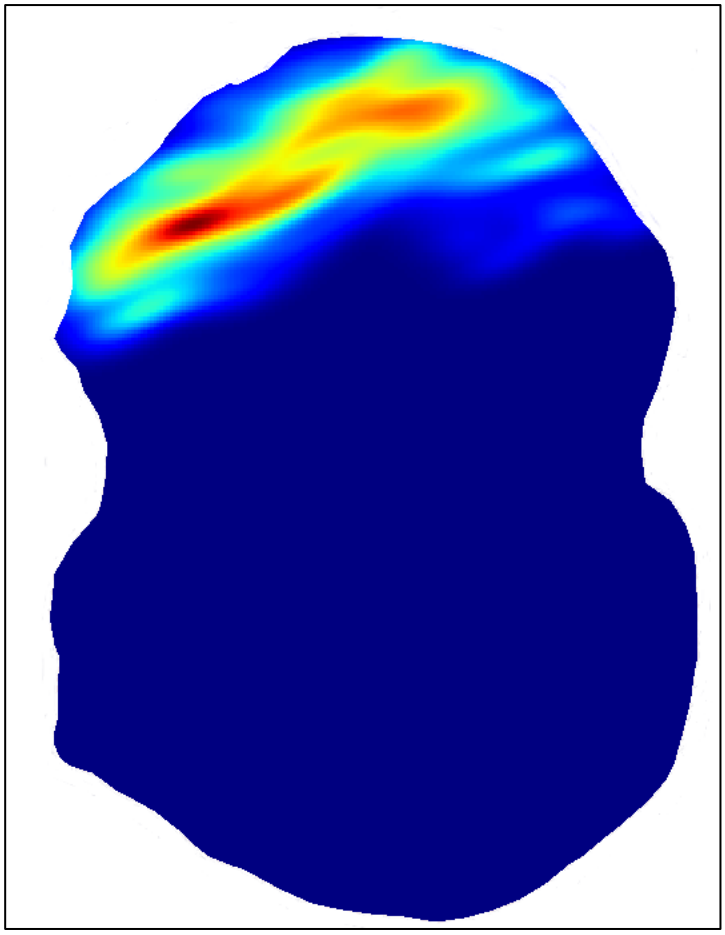

Superior heat map of all the patient fracture lines.

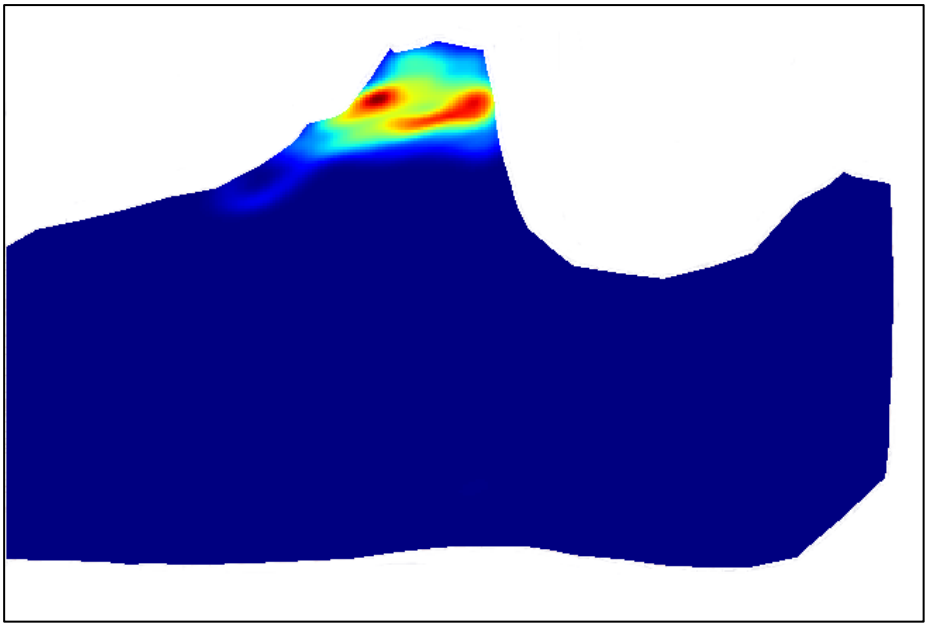

Lateral heat map of all the patient fracture lines.

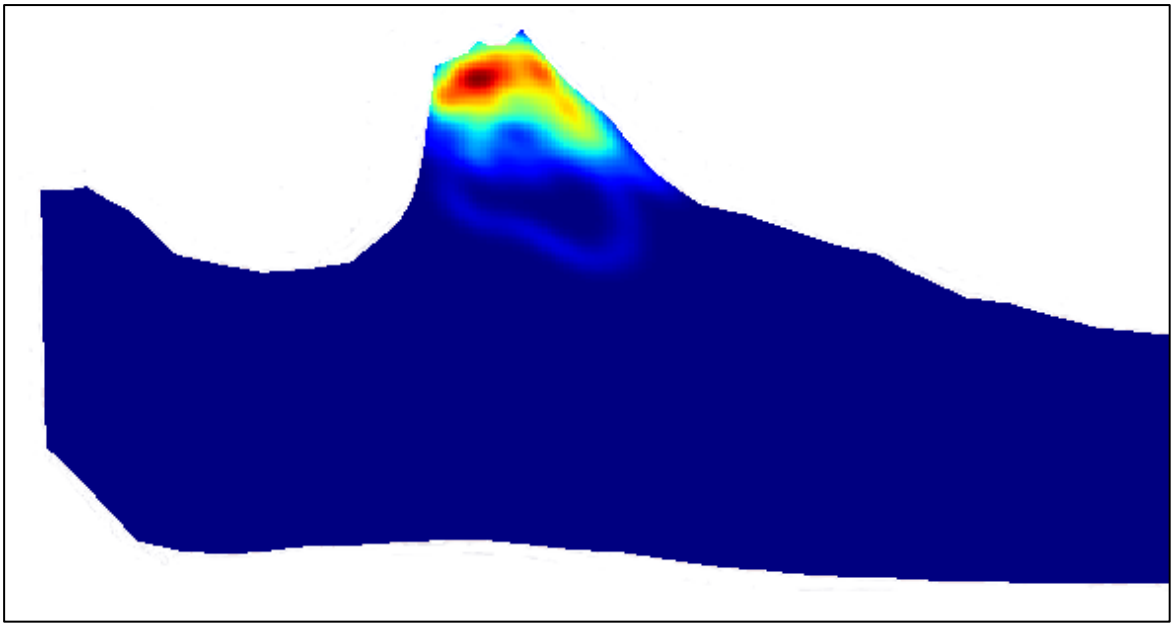

Medial heat map of all the patient fracture lines.

Type 1 & Subtypes

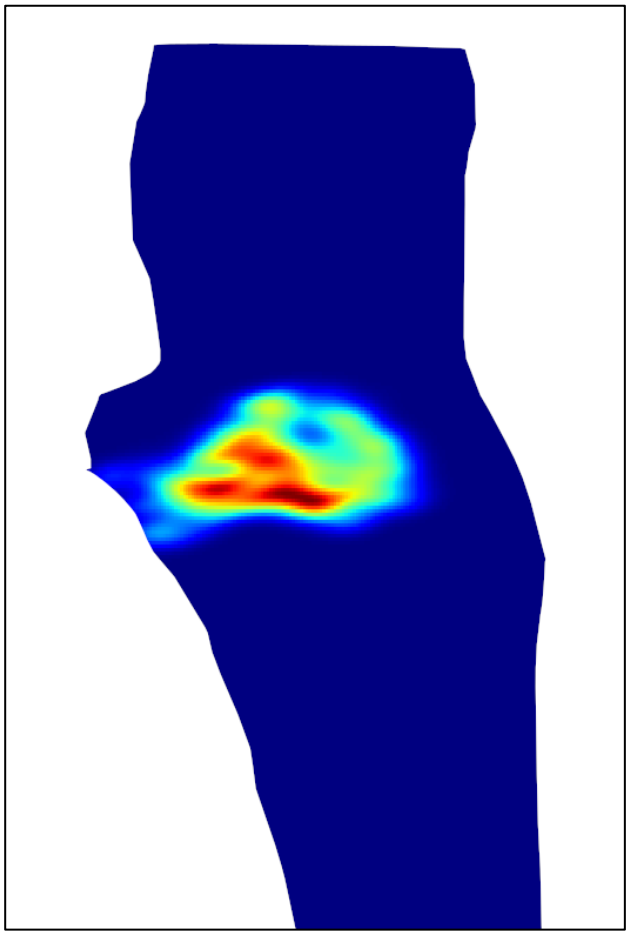

Anterior heat map of the Type 1 fracture lines.

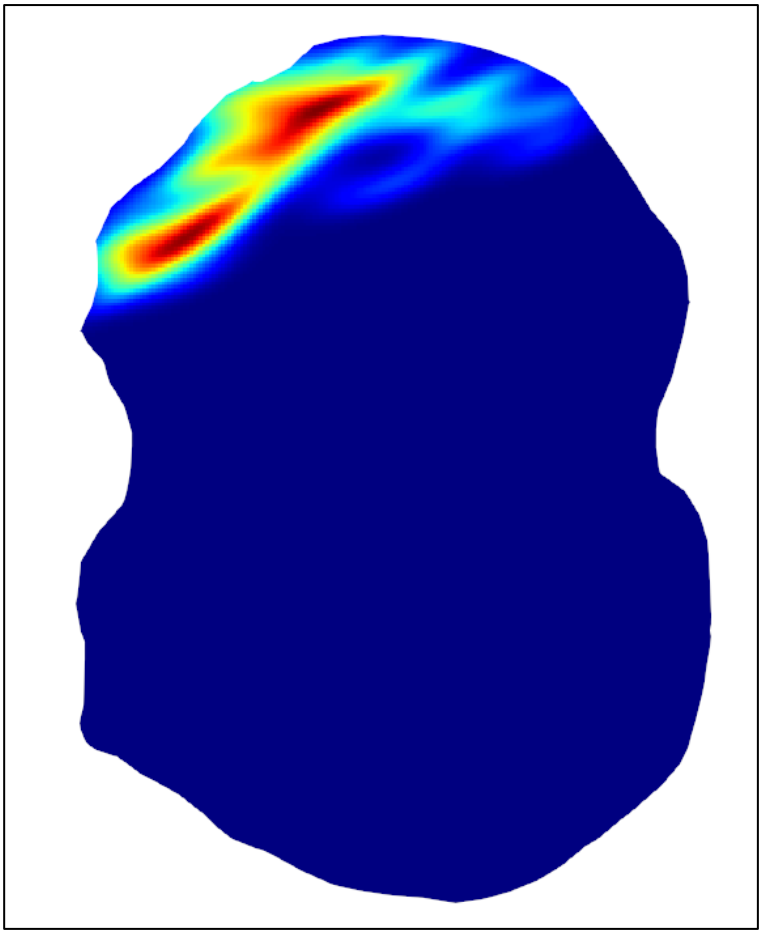

Superior heat map of the Type 1 fracture lines.

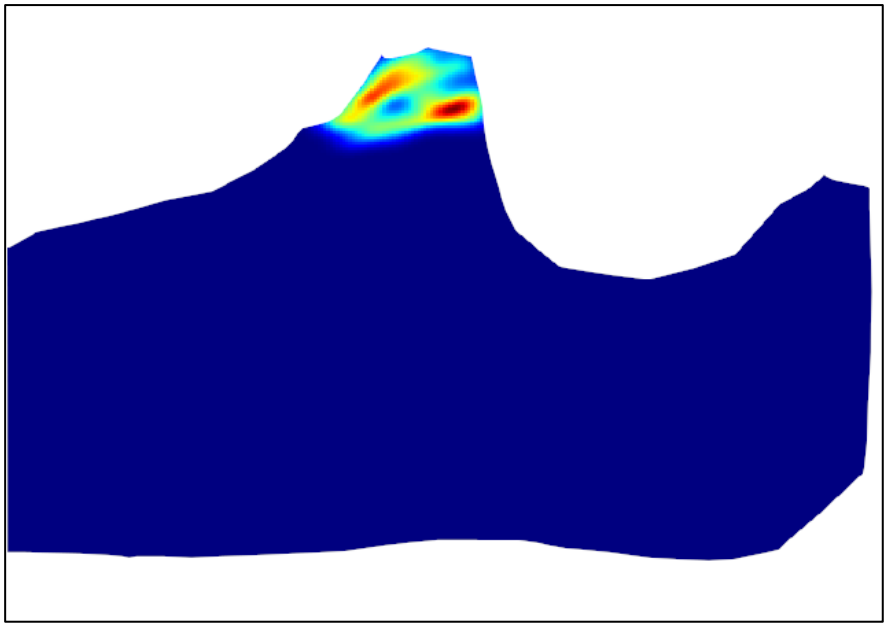

Lateral heat map of the Type 1 fracture lines.

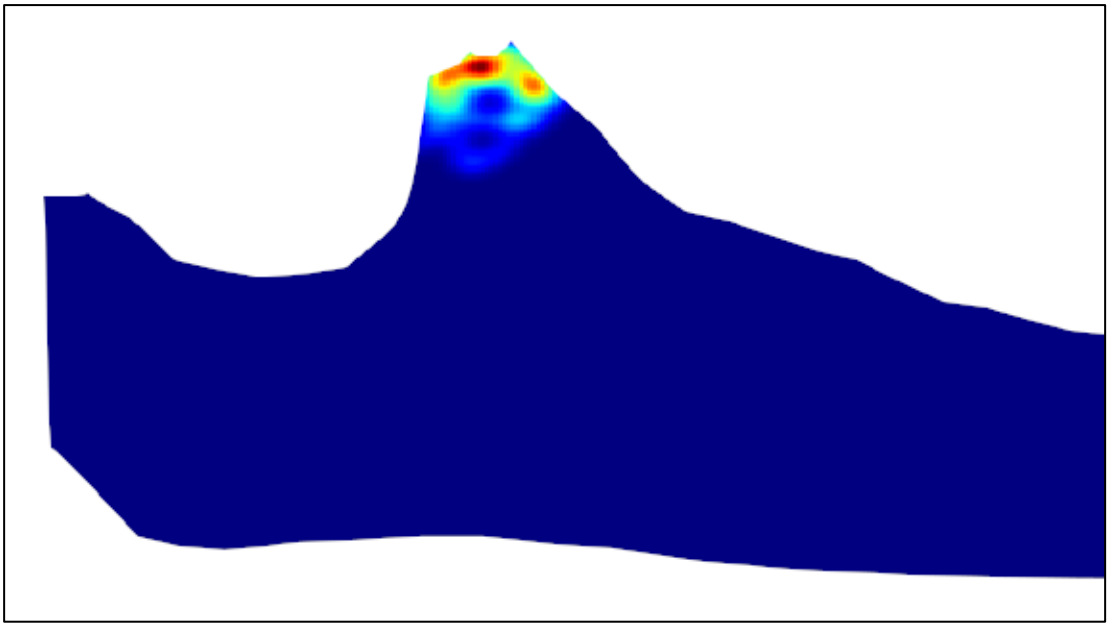

Medial heat map of the Type 1 fracture lines.

Type 2 – Subtype 2

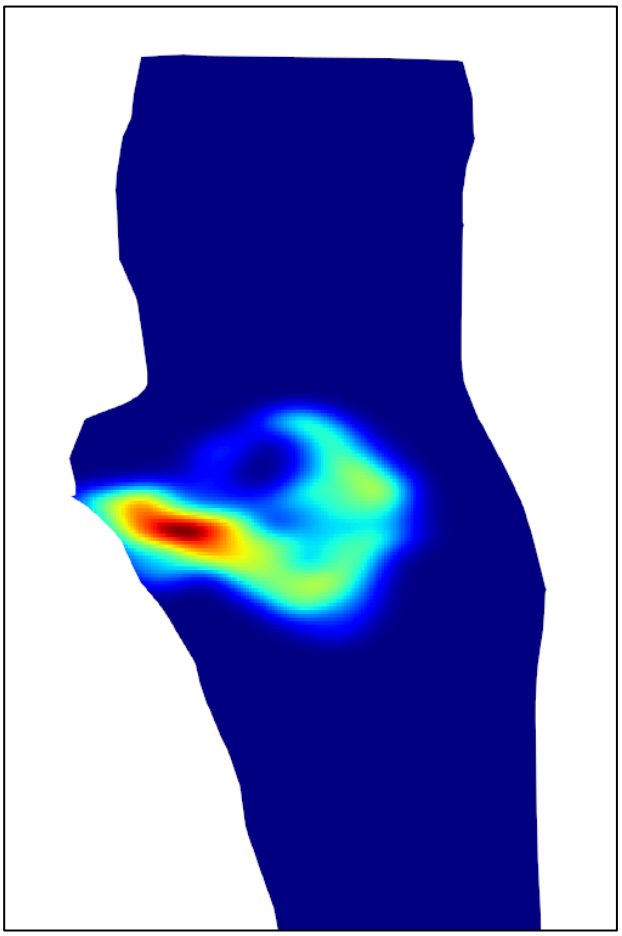

Anterior heat map of the Type 2 – Subtype 2 fracture lines.

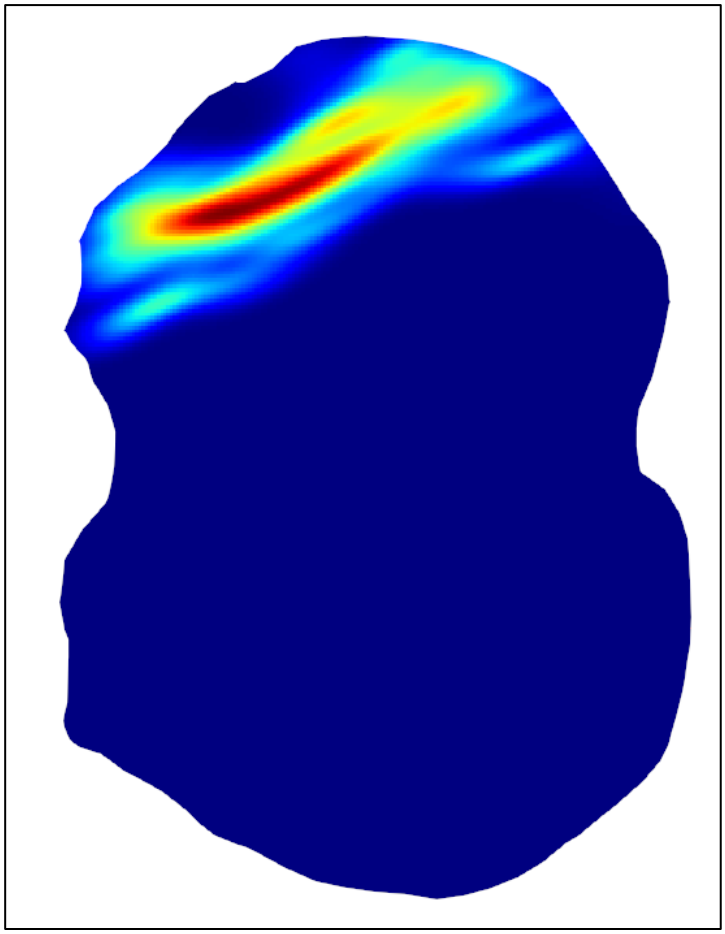

Superior heat map of the Type 2 – Subtype 2 fracture lines.

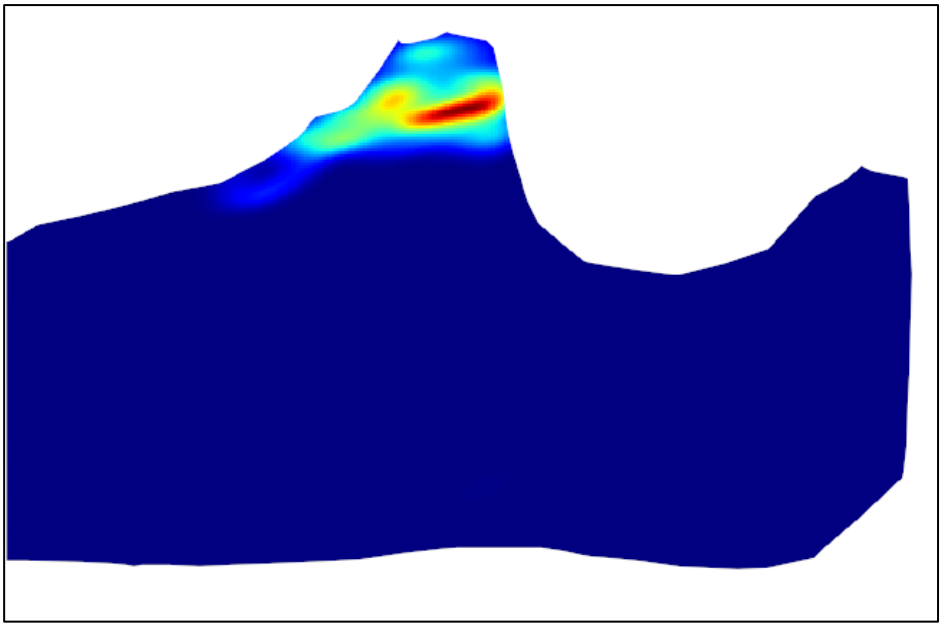

Lateral heat map of the Type 2 – Subtype 2 fracture lines.

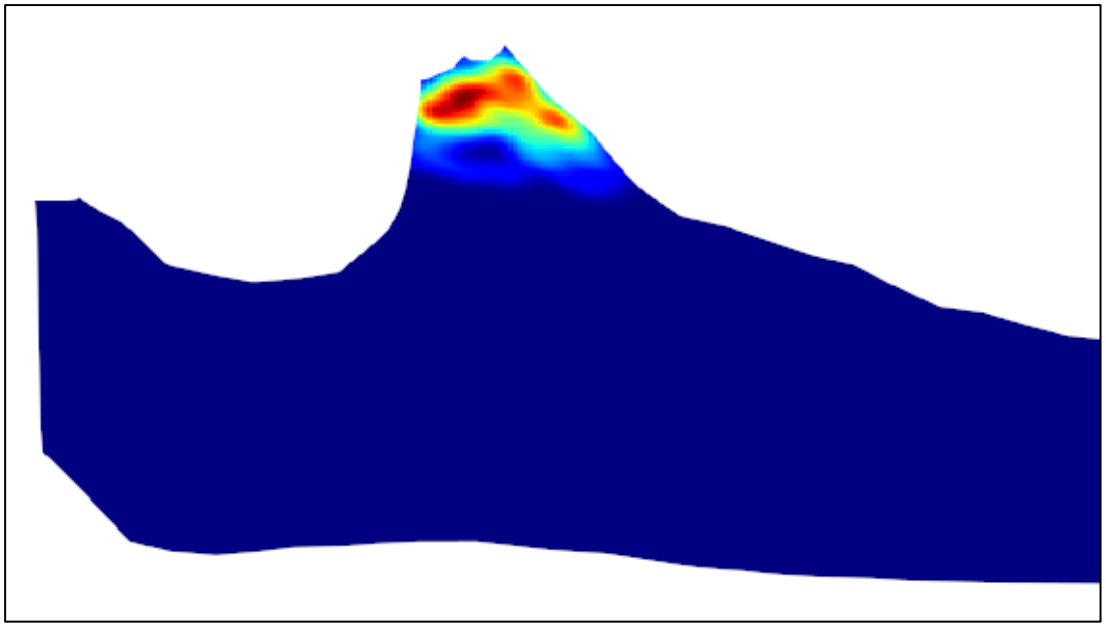

Medial heat map of the Type 2 – Subtype 2 fracture lines.

Type 2 – Subtype 3

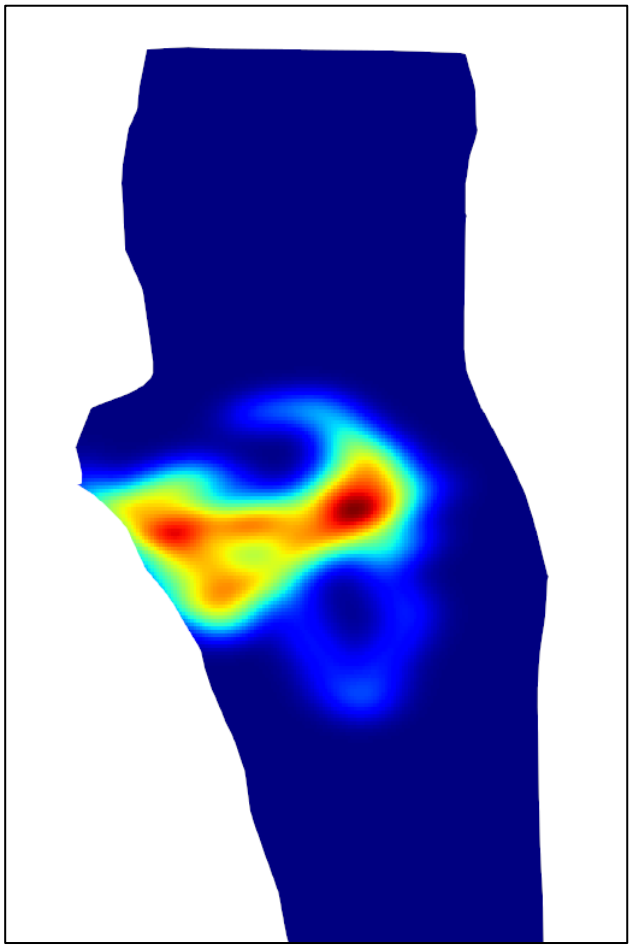

Anterior heat map of the Type 2 – Subtype 3 fracture lines.

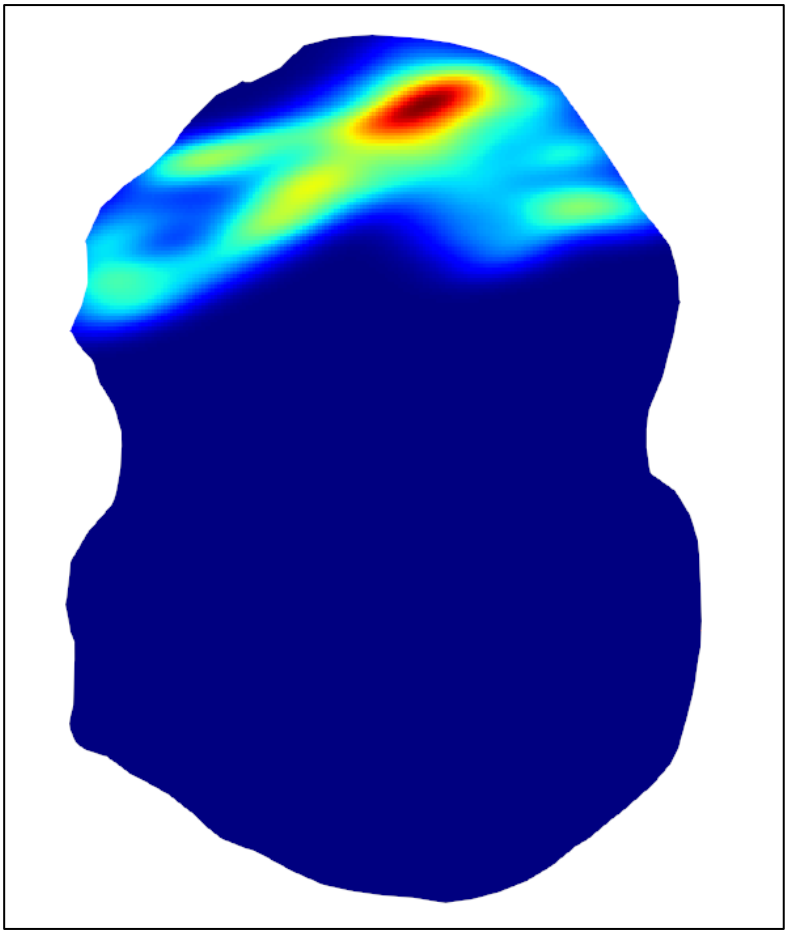

Superior heat map of the Type 2 – Subtype 3 fracture lines.

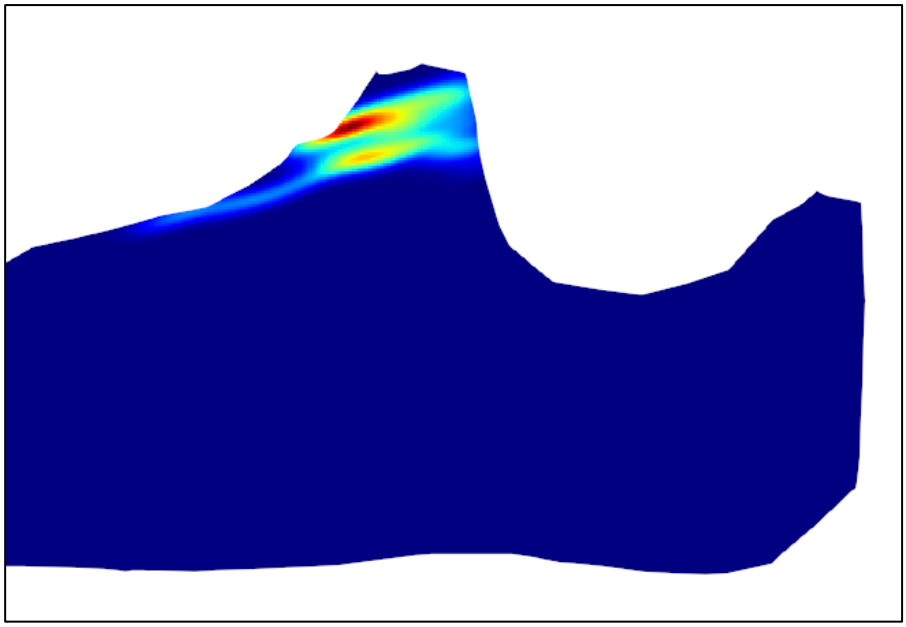

Lateral heat map of the Type 2 – Subtype 3 fracture lines.

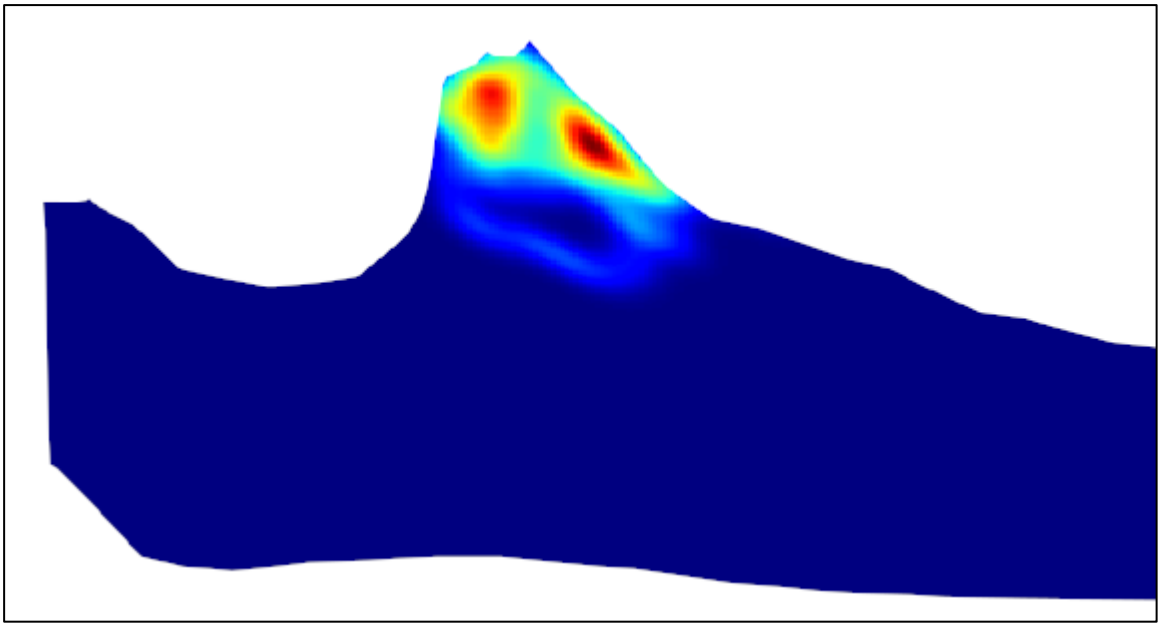

Medial heat map of the Type 2 – Subtype 3 fracture lines.

Appendix F – Endobutton Drawing

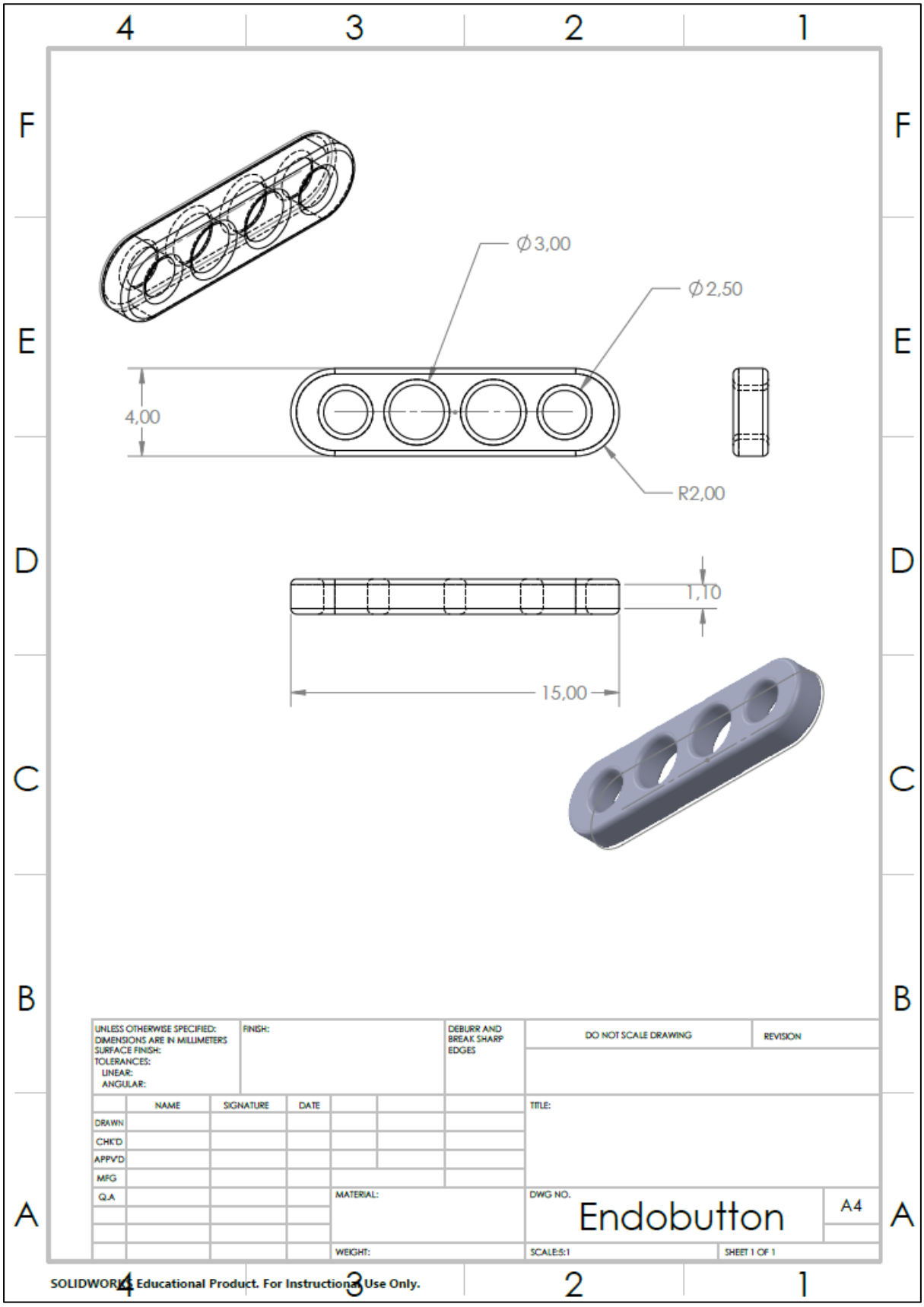

Appendix G – Qualitative Assessment Questionnaire

Qualitative Analysis of Endobutton in the Fixation of Coronoid Process Fractures

Participant Details	
Participant Name	
Profession & Qualifications	
Upper limb/elbow ORIF Experience (Years)	

1 – Very Poor, 2 – Poor, 3 – Adequate, 4 – Good, 5 - Excellent							Comments / Issues
General Usability	1	2	3	4	5	N/A	
1. Do you think this fixation device is easy to use	○	○	○	○	○	○	
2. This device is easily attached to the bone	○	○	○	○	○	○	

Fixation Process				
3. This fixation device fits on the following fractures:				
				Comments / Issues
Patient 2	Yes	No	N/A	
Patient 4	Yes	No	N/A	
Patient 6	Yes	No	N/A	
Patient 12	Yes	No	N/A	
Patient 14	Yes	No	N/A	
Patient 17	Yes	No	N/A	
Patient 20	Yes	No	N/A	
Patient 30	Yes	No	N/A	
Patient 36	Yes	No	N/A	
Patient 40	Yes	No	N/A	
Patient 41	Yes	No	N/A	
Patient 45	Yes	No	N/A	
Patient 50	Yes	No	N/A	
Patient 52	Yes	No	N/A	
Patient 62	Yes	No	N/A	

4. This fixation device would be used in the fixation of the following fractures:							
	1	2	3	4	5	N/A	Comments / Issues
Patient 2	○	○	○	○	○	○	
Patient 4	○	○	○	○	○	○	
Patient 6	○	○	○	○	○	○	
Patient 12	○	○	○	○	○	○	
Patient 14	○	○	○	○	○	○	
Patient 17	○	○	○	○	○	○	
Patient 20	○	○	○	○	○	○	
Patient 30	○	○	○	○	○	○	
Patient 36	○	○	○	○	○	○	

Patient 40	○	○	○	○	○	○	
Patient 41	○	○	○	○	○	○	
Patient 45	○	○	○	○	○	○	
Patient 50	○	○	○	○	○	○	
Patient 52	○	○	○	○	○	○	
Patient 62	○	○	○	○	○	○	

5. This fixation device would result in stable fixation of the fracture:							
	1	2	3	4	5	N/A	Comments / Issues
Patient 2	○	○	○	○	○	○	
Patient 4	○	○	○	○	○	○	
Patient 6	○	○	○	○	○	○	
Patient 12	○	○	○	○	○	○	
Patient 14	○	○	○	○	○	○	
Patient 17	○	○	○	○	○	○	
Patient 20	○	○	○	○	○	○	
Patient 30	○	○	○	○	○	○	
Patient 36	○	○	○	○	○	○	
Patient 40	○	○	○	○	○	○	
Patient 41	○	○	○	○	○	○	
Patient 45	○	○	○	○	○	○	
Patient 50	○	○	○	○	○	○	
Patient 52	○	○	○	○	○	○	
Patient 62	○	○	○	○	○	○	

6. The use of this fixation device would result in adequate reduction of the following fractures:							
	1	2	3	4	5	N/A	Comments / Issues
Patient 2	○	○	○	○	○	○	
Patient 4	○	○	○	○	○	○	
Patient 6	○	○	○	○	○	○	
Patient 12	○	○	○	○	○	○	
Patient 14	○	○	○	○	○	○	
Patient 17	○	○	○	○	○	○	
Patient 20	○	○	○	○	○	○	
Patient 30	○	○	○	○	○	○	
Patient 36	○	○	○	○	○	○	
Patient 40	○	○	○	○	○	○	
Patient 41	○	○	○	○	○	○	
Patient 45	○	○	○	○	○	○	
Patient 50	○	○	○	○	○	○	
Patient 52	○	○	○	○	○	○	
Patient 62	○	○	○	○	○	○	

(1 – Very Poor, 2 – Poor, 3 – Adequate, 4 – Good, 5 – Excellent)

Overall Impressions & Additional Comments

Appendix H - Detailed Design Drawing

ITEM NO.	PART NUMBER	DESCRIPTION	QTY.
1	Design 3 Asym - Original		1

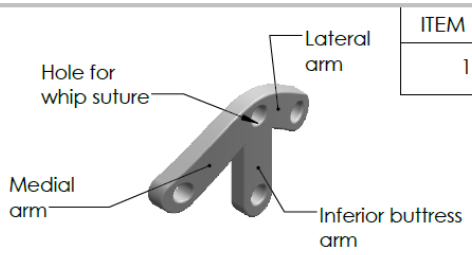

Top (Superior)

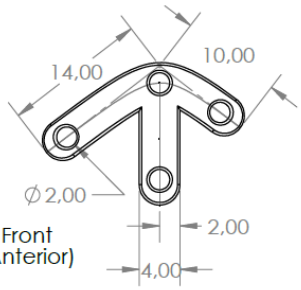

Front (Anterior)

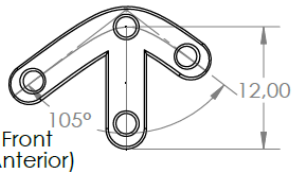

Front (Anterior)

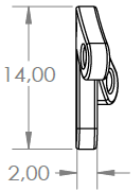

Right(Lateral)

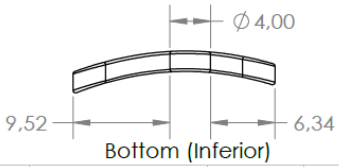

Bottom (Inferior)

		UNLESS OTHERWISE SPECIFIED:		NAME	DATE
		DIMENSIONS ARE IN INCHES TOLERANCES: FRACTIONAL ± ANGULAR: MACH ± BEND ± TWO PLACE DECIMAL ± THREE PLACE DECIMAL ±	DRAWN		
			CHECKED		
			ENG APPR.		
			MFG APPR.		
		INTERPRET GEOMETRIC TOLERANCING PER:	Q.A.		
		MATERIAL	COMMENTS:		
NEXT ASSY	USED ON	FINISH			
APPLICATION		DO NOT SCALE DRAWING			

TITLE:

SIZE	DWG. NO.	REV
A	Asymm - Original	
SCALE: 2:1	WEIGHT:	SHEET 1 OF 1

PROPRIETARY AND CONFIDENTIAL
THE INFORMATION CONTAINED IN THIS DRAWING IS THE SOLE PROPERTY OF <INSERT COMPANY NAME HERE>. ANY REPRODUCTION IN PART OR AS A WHOLE WITHOUT THE WRITTEN PERMISSION OF <INSERT COMPANY NAME HERE> IS PROHIBITED.

SOLIDWORKS Educational Product. For Instructional Use Only.

Appendix I – Design Prototype Images

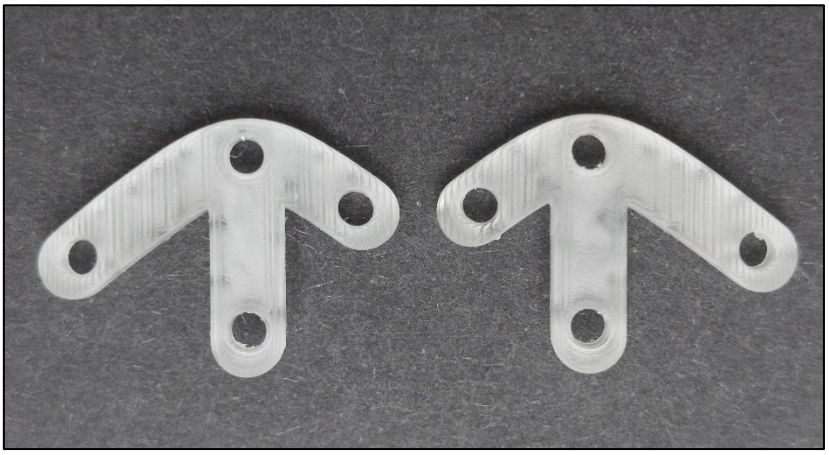

Right and left versions of designed adapted Endobutton.

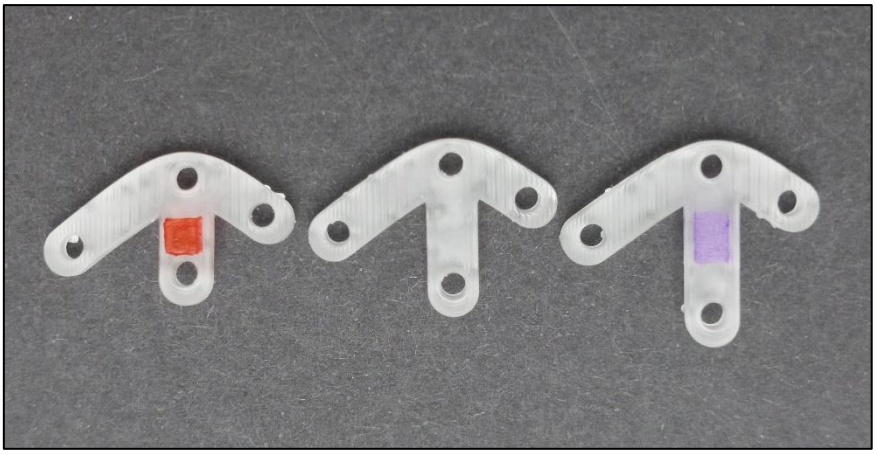

Short, original, and long version of adapted Endobutton design.

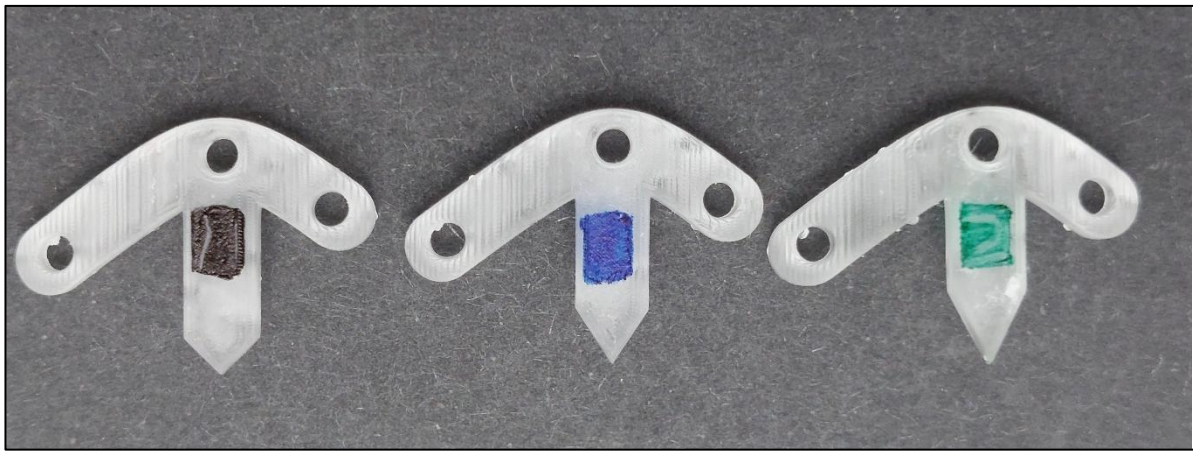

Close up of spiked version of adapted Endobutton (Black – 2mm, Blue – 3mm and Green – 4mm).

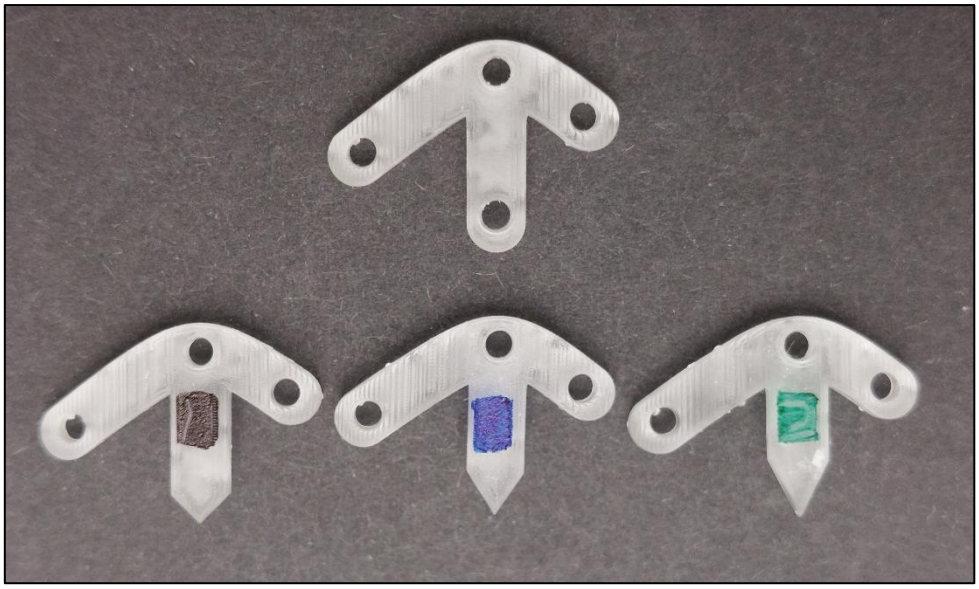

Spiked version of adapted Endobutton in relation to original design.

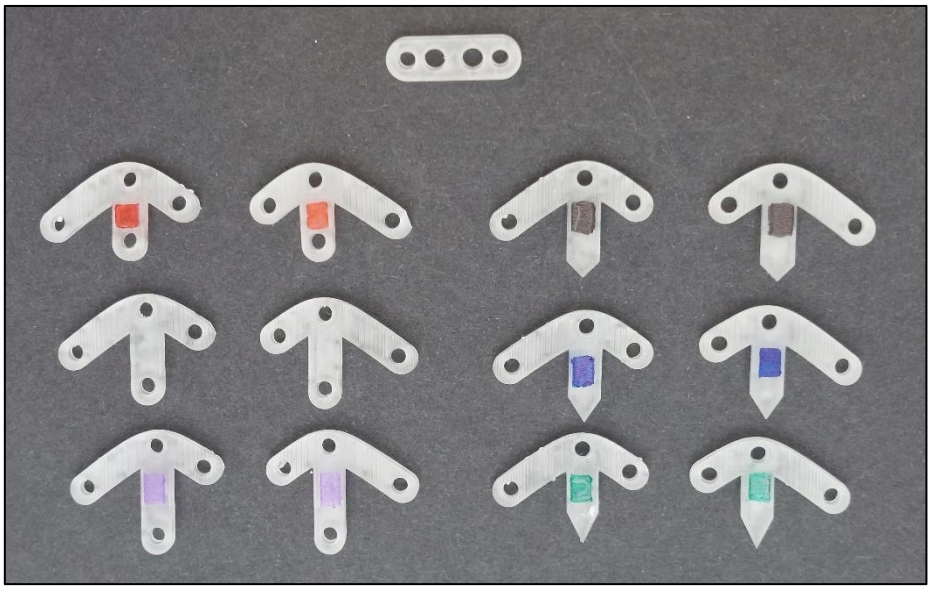

All versions of adapted Endobutton design in relation to commercially available Endobutton.